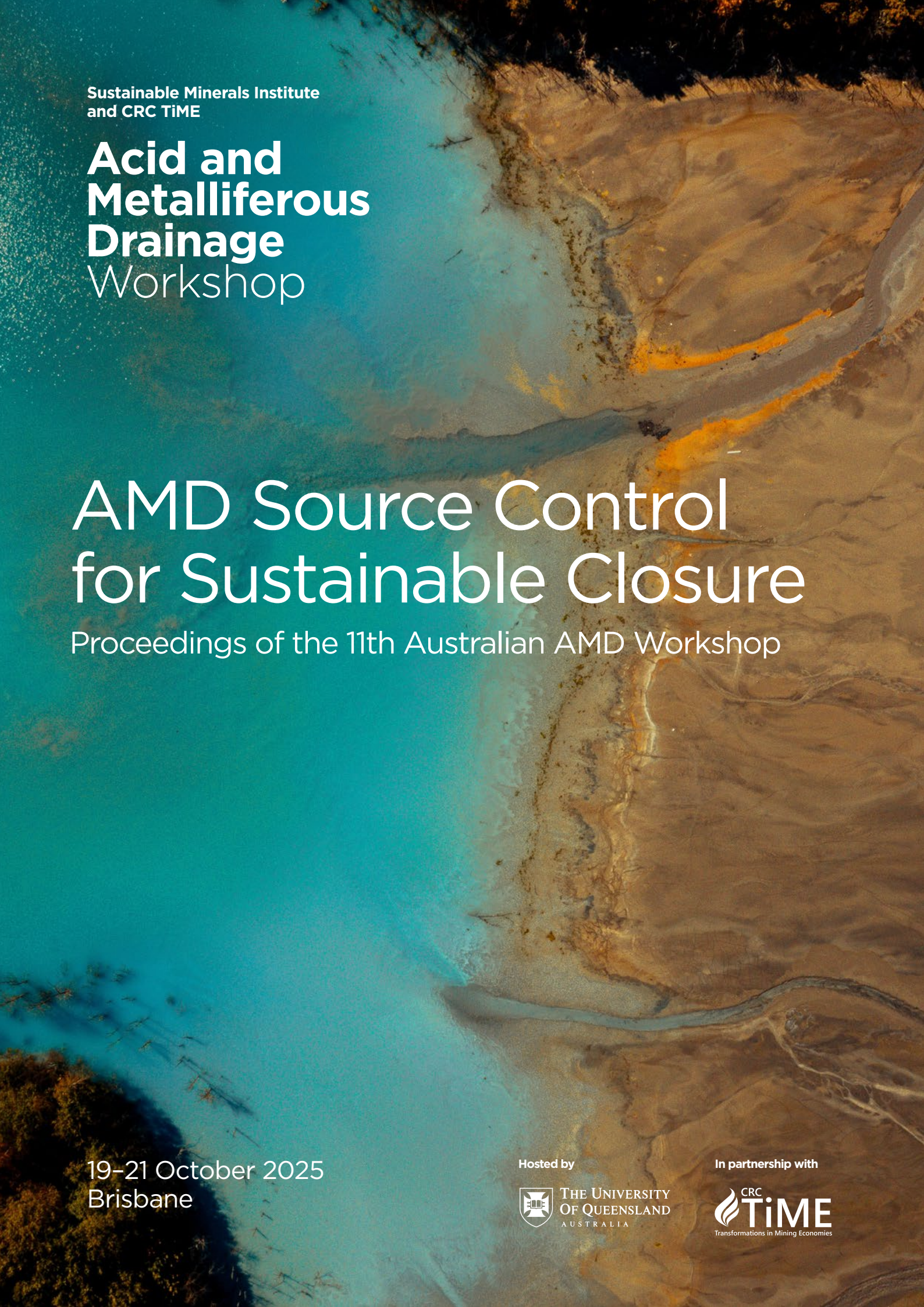

Sustainable Minerals Institute
and CRC TiME

Acid and Metalliferous Drainage Workshop

AMD Source Control for Sustainable Closure

Proceedings of the 11th Australian AMD Workshop

19–21 October 2025
Brisbane

Hosted by

The University Of Queensland
AUSTRALIA

In partnership with

CRC TiME
Transformations in Mining Economies

Enquiries and requests for copies should be directed to:

Sustainable Minerals Institute
The University of Queensland
Brisbane QLD 4072
Telephone: +61 7 3346 4003
Fax: +61 7 3346 4045

Citations of this publication should take the form:

Jennings, E. and Edraki, M, Jones, D (Eds)(2025) Proceedings of the Eleventh Australian Workshop on Acid and Metalliferous Drainage, Brisbane, 19-21 October 2025. (The University of Queensland: Brisbane)

Individual papers should be cited as:

Author(s) Name(s) Title of paper. In “Proceedings of the Eleventh Australian Workshop on Acid and Metalliferous Drainage, Brisbane, 19-21 October 2025. (Eds. Jennings, E. and Edraki, M, Jones, D) pp. 00-00 (The University of Queensland: Brisbane)

ISBN: 978-1-74272-515-4

Welcome

Welcome to the 11th Australian Acid and Metalliferous Drainage Workshop.

Acid and Metalliferous Drainage (AMD), also known as Acid Rock Drainage (ARD), remains one of the most significant environmental challenges facing the global mining industry. The University of Queensland (UQ) has been involved in designing and delivering the Australian AMD Workshops for more than three decades, since the first event in 1992. This forum brings together mine planners, mining engineers, environmental specialists from mining companies, government regulators, geochemical and geotechnical consultants and researchers, and graduate students. It has been run as a "Workshop" to promote collaborative learning, engagement, and the exchange of ideas, and has been tightly focused on the relevant technical issues.

Over the years, AMD management in Australia has evolved from reactive treatment based on the results from static geochemical testing methods in the 1990s to proactive, engineered, prevention-first strategies informed by improved kinetic testing, field verification, and best practice guidance developed by Australian and International contributors. Current best practice focuses on scaling up source-control engineering and embedding AMD prevention into closure planning, governance, and ESG frameworks. Controlling the oxidation of sulfidic materials as soon as they are exposed to air and water is the most logical, practical, and cost-effective approach to managing and preventing AMD. Hence, the overarching theme of the 2025 Workshop is AMD Source Control for Sustainable Closure. For the 2025 Workshop, the Sustainable Minerals Institute (SMI) at UQ has partnered with CRC TiME (the CRC for Transformations in Mining Economies) to emphasise the critical importance of effective prevention of AMD to successful mine closure and post-mining land use.

For this workshop, the Committee decided on the format of extended abstracts rather than full papers as for previous workshops, to encourage greater participation from industry personnel, being mindful of their time constraints and approval processes. This year we also welcomed the participation of representatives from a number of the INAP (International network for Acid Prevention) member companies who will be presenting case studies and contributing to panel discussions.

We sincerely thank everyone for their ongoing support of the AMD Workshop, and we hope these proceedings capture the continued progress and collective efforts to address this key challenge.

Mansour Edraki on behalf of the Organising Committee

Table of Contents

Acknowledgements

The organising committee reviewed suggested case studies and submitted abstracts and developed the program for this workshop with support from a reference group.

2025 Organising Committee

Professor Mansour Edraki, (Chair)
Centre for Environmental Responsibility in Mining
Sustainable Minerals Institute

Dr Agnes Samper
CRCTiME and Sustainable Minerals Institute

Dr David Jones
DR Jones Environmental Excellence
Industry Fellow, Sustainable Minerals Institute

Dr Bruce Kelly
Chair CRCTiME

Dr Jeff Taylor
Earth Systems

Gilles Tremblay
International Network for Acid Prevention (INAP)

Reference Group 2025

Dr Bill Price
Natural Resources Canada

Dr Russell Staines
BHP

Dr Ros Green
Rio Tinto

Dr Marilena Stimpfl
BHP

Associate Professor Anita Parbhakar-Fox
WH Bryan Mining Geology Research Centre (BRC)
Sustainable Minerals Institute

Hugh Davies
Newmont

Dr Alan Robertson
RGS Environmental

We also gratefully acknowledge the following individuals who contributed to the abstract review process.

Dr Warwick Stuart
Environmental Geochemistry International

Dr Claire Linklater
SRK

Workshop sponsors

Thank you to our sponsors for their support of this important event

Gold sponsors

Silver sponsors

Bronze sponsors

Abstracts

AMD (source) through mine planning and selective material handling

M. Stimpfl, L. Terrusi and C. van der Merwe
BHP, Level 30, 125 Stg Georges Terrace, Perth WA 6000 Australia.
marilena.stimpfl@bhp.com

Effective management of Acid and Metalliferous Drainage (AMD) is a critical challenge in mining operations, requiring proactive strategies to prevent environmental impacts and reduce closure liabilities. This presentation outlines an integrated approach to AMD source management through mine planning and selective material handling, emphasizing the importance of early characterization, classification, and operational execution across the life of asset (LOA).

The foundation of AMD management lies in accurate source characterization, which begins during exploration. Leveraging assay data and targeted geochemical test work enables validation of AMD classification algorithms embedded within geological and mining models. These classifications—ranging from inert (AMD0) to problematic (AMD1–3)—inform material handling decisions and underpin mine planning processes. By incorporating AMD attributes into block models, operators can predict the spatial distribution of reactive and benign materials, supporting precise material balance assessments and scheduling.

Mine planning horizons—long-term, medium-term, and short-term—provide a structured framework for implementing AMD management strategies. At the strategic level, long-term planning establishes the overall framework for material balance, dump design, and closure objectives. Medium-term planning refines these strategies into executable schedules, integrating AMD considerations into operational workflows. Short-term planning translates these strategies into daily actions, ensuring that waste classification drives destination planning and landform construction. This granular approach enables the safe encapsulation of reactive materials and the effective use of inert waste for engineered cover systems.

Closure design guidelines further reinforce the importance of selective handling. For example, AMD1 materials require containment within engineered landforms, with inert waste layers encapsulating pyritic waste to ensure geochemical stability. These design principles mitigate long-term risks and align with regulatory and corporate standards.

The presentation also highlights practical tools for operational execution, including classification algorithms, block model attributes, and daily scheduling templates. These tools enable real-time decision-making, ensuring that AMD management objectives are met without compromising production efficiency. By integrating geochemical data into mine planning systems, operators can transform AMD from a reactive problem into a manageable challenge.

Ultimately, selective waste handling is not merely a best practice—it is a strategic imperative. Accurate classification and proactive planning reduce the need for costly downstream treatment, enhance compliance, and build stakeholder confidence. Furthermore, this approach minimizes closure costs and legacy risks, supporting sustainable mining operations. WAIO's ability to leverage detailed geochemical datasets exemplifies the benefits of data-driven AMD management, though the principles outlined are broadly applicable across the industry.

In conclusion, AMD source management through mine planning and selective material handling empowers operations to achieve environmental stewardship while maintaining operational efficiency. By embedding AMD considerations into every stage of planning and execution, mining companies can deliver landforms that are stable, safe, and aligned with long-term closure objectives.

Why Metal Leaching and Acid Rock Drainage Remains an Intractable Issue and Suggested Solutions. Australian Acid and Metalliferous Drainage Workshop, Brisbane, October 20-21.

W. Price
nrcprice@telus.net

Abstract

ML/ARD work remains the most technically challenging environmental issue facing the mining industry and an onerous undertaking. While ML/ARD practices have improved and present guidance is sound, a more methodical and well-informed approach supported by a number of practice improvements, and additional actions, tools, and information are required to prevent practice deficiencies, sustain present successes, and enable the increased mining required to move to a more computerized, lower carbon economy.

Challenges to be addressed include failure to follow existing guidance, well-informed proactive prevention of problems, sustained long-term mitigation performance, increasing work requirements, understanding site-specific and changing conditions, taking a logical scientific approach, and needs of personnel. Additional tools and actions to enable practitioners and organizations to properly understand, follow ML/ARD requirements and Improve performance include the following: detect missing info with checklists, incorporate measures that decrease risks and costs, create mine site databases and reviews, withstand future climate events, need more staff and more efficient processes, evaluate variability, recognizing changing conditions, need professional accountability and professional of record, recognition that the objective is successful not best performance, and create standard well-defined terminology.

Gaps in Knowledge and Methods that are Obstacles to Successful Management of Metal Leaching and Acid Rock Drainage. Australian Acid and Metalliferous Drainage Workshop, Brisbane, October 20-21.

W. Price
nrcprice@telus.net

Abstract

The objectives of this presentation are to identify and suggest solutions to gaps in knowledge and methodology that are obstacles to successful metal leaching and acid rock drainage management. Gaps in ML/ARD knowledge and methodology are an outcome of the nature of mines and mine materials, past practice deficiencies, parameters that are difficult to accurately measure or predict, lack of information about future, drainage chemistry and mitigation needs and performance, and deficiencies of methods for analysis, data evaluation, and future governance.

Information is needed from existing mines about drainage chemistry, the performance, durability and maintenance requirements of different forms of mitigation, settling of mine materials, and contaminant bioavailability, bioaccumulation and release after biological invasion of water covers. Plans needed for future governance include how to deal with organizational constraints, increasing work requirements and changing conditions, and how to provide long-term governance and financial security. Actions suggested to enable future governance include audits of practices, inventories of ML/ARD conditions and mitigation, plans for future governance, and recognition of deficiencies in future cost projections.

Managing Mine Wastes – what should be the focus?

P. Brown
Chief Geochemist, General Manager, Water, Waste and Tailings, Rio Tinto
Board Chair, International Network for Acid Prevention. paul.l.brown@riotinto.com

Reactive mineral wastes and their effective management are a significant liability facing the global mining industry. Mineral waste is material composed of rock or unconsolidated sediments that is disturbed or exposed by mining, or a waste composed of mineral residue that is generated by the processing of ore. Reactive mineral wastes are those wastes whose innate physical, chemical or biological properties could now, or in the future, create an environmental exposure hazard. By far, the largest issue associated with reactive mineral waste is acid and metalliferous drainage (AMD) that has been reported as having a liability in the billions of dollars globally. AMD can result from waste derived from the mining of the vast majority of commodities including coal, base metals, precious metals, iron ore, uranium, diamonds and many other minerals. The risk from AMD and its associated liability can be significantly diminished by effective management of the wastes from mining of these commodities.

Acid and metalliferous drainage issues can develop from both waste rock and tailings. Moreover, issues can also derive from other sources such as overburden and interburden, spent heap leach residues, underground workings, dredged materials, open pits (and subsequently, possibly pit lakes), and acid sulfate soils. An individual operating site will often need to effectively manage many of these different material types concurrently. In addition, effective management strategies need to extend beyond mine life into closure and the post-closure period. Often, water contacting the wastes will also need to be effectively managed during operation, but possibly also at closure and beyond.

Focal areas on managing wastes and water that may have AMD issues must be related to the risk each potential issue poses to a mining site (whether operational or in closure). Risks will likely vary substantially from site to site, depending upon such factors, for example, as climate (rainfall to evaporation), proximity to sensitive receiving environments, availability of transport pathways and proximity to communities. Effective management strategies may also depend on where in the mining life cycle a particular operation is. Risk identification is key to determination of focal areas enabling effective management strategies to be implemented.

Implementing Leading Practice Geochemical Design and Construction – Observations from McArthur River Mine, NT, Australia

P. Marianelli[A], B. Usher[B], and J. Fourie[B]
[A]Glencore Zinc Australia. pyramo.marianelli@glencore.com.au
[B]KCB Australia, Level 3, 150 Mary Street, Brisbane, Australia

1.0 INTRODUCTION

The McArthur River Mine (the Mine) is a zinc-lead mine located in the monsoonal tropics of Northern Australia, approximately midway between Darwin and Mount Isa in the Gulf Region of the Northern Territory (NT). The Mine is the world's largest producer of zinc in bulk concentrate form, with specific zinc and lead concentrates also produced. Underground mining at McArthur River commenced in 1995 and continued through to 2006, with open-cut mining commencing in 2005. The current mine life extends to approximately 2040. The economic mineralization is associated with finely laminated to thinly bedded dolomitic and pyritic siltstones, massive dolomitic breccias, and pyritic carbonaceous shales. The waste rock is characterised by the simultaneous presence of high levels of carbonates and pyrite, with minor sphalerite and galena. Most of the waste rock contains a significant amount of carbonate, with a high acid neutralisation capacity. The overall acid base properties are therefore largely determined by differences in pyrite content, which can vary from 0.1% to over 40%. Waste rock exits the pit at temperatures exceeding 60°C.

The initial waste rock classification was based on a simple binary system using acid base accounting as well as NAG pH. Waste rock was either classified as Non-Acid Forming (NAF) and considered environmentally benign, or as Potentially-Acid Forming (PAF), requiring encapsulation. While broadly correct on acid/base properties, that classification did not adequately account for the high reactivity of some of the sulphides or for the risk of neutral metalliferous drainage from the NAF material. The main waste rock storage facility (the Northern Overburden Emplacement Facility, or NOEF) used a conventional design based on high lifts constructed by end tipping, resulting in high porosity within the stockpile. This led to higher than anticipated rates of sulphide oxidation and the progressive development of high temperature zones in the batters of the NOEF, which allowed sporadic episodes of spontaneous combustion to occur. The mine recognised that in order to control sulphide oxidation rates effectively, a fundamentally different approach to the design and construction of the NOEF would be required. This involved additional mineralogical, petrographic and geochemical studies, improved understanding of internal sulphide oxidation processes, revision of the architecture and construction methodology, and implementation of a monitoring program for internal temperatures, gas exchanges and moisture.

2.0 APROACH AND DESIGN PHILOSOPHY

A comprehensive review of the site geochemistry resulted in a new classification of the waste according to reactivity and AMD potential. This was based on over 4,000 static testing samples, more than 300 of which had leaching, acid buffering characteristics curves and kinetic tests completed. Multiple types of kinetic testing (18 humidity cells, 9 AMIRA-style columns (AMIRA 2002), 18 oxygen consumption tests and 15 field barrels) were used to obtain a comprehensive evaluation of geochemical reactivity and potential water quality risks. The original binary NAF/PAF classification was replaced by a six-class system with three classes of NAF and three classes of PAF. The most significant changes were the management of the potential neutral metalliferous and saline drainage risk from the

NAF, and the identification and segregation of the most reactive PAF, based on its propensity to self-heat.

Several measures were immediately implemented to stabilise the existing NOEF including excavation, transport, cooling, compaction, and re-encapsulation of high-temperature material. The outer geometry was modified by removing the existing batter and berm configurations and shallowing the slopes. The existing PAF cell was covered with a reduced air permeability alluvial (sand-silt-clay) cover, which also acted as a temporary store and release cover for the wet season.

The waste rock facility was completely redesigned based on multiphase (transient air/water/temperature modelling linked to geochemistry; Figure 1 shows an example) reactive geochemical modelling. The impact of paddock dumping with small lifts was simulated to assess the benefits compared to end-tipped waste where large scale segregation can be expected, with the expectation from literature (e.g. Wels et al, 2003) and leading practice that lower lift heights would reduce segregation and lengths of air flow paths. A radically different approach based on managing sulphide oxidation during the construction phase was taken. The geometry was changed to remove batter and berm configurations (as far as possible) and construction amended to rapidly batter down exposed faces to shallower angles. A low lift construction methodology was implemented with a combination of paddock dumping and 5 m tip heads to limit particle segregation and reduce porosity. Perhaps more significantly, multiple internal low air permeability barriers, built out of alluvial clayey sandy silts were introduced into the design to reduce advective oxygen transport both laterally and vertically ("advection barriers"). The most reactive PAF waste is segregated and placed in specific internal cells (PAF(RE) cells) with thin horizontal advection barriers between each lift and thicker ones on the batters. The effectiveness of the design was evaluated using two dimensional multiphase geochemical models with a focus on the performance of the advection barriers. Modelling results showed a significant reduction in advective air flux and a reduction in expected temperatures.

The PAF(RE) cells also benefit from the use of interim wet season covers to reduce water infiltration. They are in turn encapsulated within the less reactive PAF cells. The lower reactivity and non-acid forming material is placed around the PAF core, forming a protective "halo" above the advection barrier and providing a buffer between the cover system and the PAF cell. The facility is progressively covered, with the final cover system consisting of a geosynthetic liner and 1.5 m of benign NAF and topsoil progressively placed as each section reaches ultimate design height.

An in-situ gas and temperature monitoring network was installed in 2016 and has been progressively expanded and updated since. There are currently 20 monitoring locations active in 2025 consisting of 18 vertical bores instrumented with thermocouples, as well as two horizontal instrument arrays (70 and 90 m long respectively) installed into batters with multiple sensors for temperature, oxygen and moisture. This is supplemented by weekly drone surveys using thermal cameras for the early detection of abnormal temperature patterns.

3.0 IMPLEMENTATION AND RESULTS

The stabilisation measures for the existing NOEF yielded very positive results with the successful remediation of spontaneous combustion. While the risk of self-heating can probably not be completely eliminated due to the challenge of placing in these types of materials (high temperature from the pit with significant sulphide) in the tropical climate and the scale of the operation, minor localised zones of elevated temperature are identified early through regular surveys and action is taken before these

become problematic. Internal temperatures in the PAF cell have significantly reduced over time. As an example, the two vertical temperature profiles in Figure 2 show a rapid reduction in temperatures from 2017 to 2019 from 110 and 130°C to 70°C and 80°C respectively, followed by subsequent stabilisation in the 60 to 80°C range. These values are consistent with the average "background" temperature of ~65°C. For context, maximum air temperatures at the site are in the range 35 to 45°C, which corresponds well to measured surface temperatures on the NOEF batters.

The new design has been implemented since 2018. The reactive PAF cells are built in 2 m lifts by paddock dumping with ~0.1–0.2 m advection barrier placed before the next lift. Batters for these cells have ~0.5 m advection barriers with ~1.5 m MS-NAF protection cover. To date, monitoring results from a horizontal array in one of the PAF(RE) cells over the last two years provide validation for this approach with maximum measured temperatures of 44°C in the batters. The reactive PAF cells are encapsulated with 7.5 m lifts of PAF (2.5 m paddock dump overlain by a 5 m tip head) with 0.1–0.2 m alluvium layers placed progressively over each lift and a thicker 0.5 m on the batters to limit lateral advection. Surrounding the PAF and above the advection barrier is the minimum 5 m thick "halo" built of metalliferous/saline NAF which insulates the cover system from the underlying PAF cell. Figure 3 shows a PAF cell under construction in a new stage of the NOEF.

The effectiveness of the method in controlling oxygen ingress is supported by the monitoring results from a temperature moisture and oxygen instrument array extending 70 m horizontally through the halo, advection barrier and PAF material in one of the newer sections of the NOEF. Oxygen concentrations show a progressive decrease with depth in the profile from 0.10 atm in the outer halo, decreasing from 0.05 to 0.02 atm in the advection barrier, and values in the 0.01 atm range in the PAF cell.

4.0 CONCLUSION

Monitoring results and field observations to date indicate that the remediation measures and changes in design philosophy are effective in reducing sulphide reactivity during the operational phase of the facility. It is important to stress that the measures are not designed to completely eliminate sulphide oxidation or achieve the long-term environmental performance of the facility on their own. These construction changes are supported by progressive placement of the cover system, as detailed in the progressive rehabilitation plan for the facility. While these measures contribute significantly to the overall environmental performance by reducing sulphide reactivity and generation of soluble contaminant loads and reducing reliance on the cover system, their primary aim is to limit self-heating and control spontaneous combustion, and as such have been very successful. Results have shown that temperatures in the older core of the facility have significantly reduced, spontaneous combustion is now uncommon and is limited to episodic small-scale outbreaks which can be quickly and effectively remediated. The monitoring network is critical in validating the approach and forms an important control measure, and results since the implementation of more rigorous design and construction methods show encouraging improvements in the performance of this facility

REFERENCES

AMIRA (2002) ARD Test Handbook; Prediction & Kinetic Control of Acid Mine Drainage; AMIRA International.

Klohn Crippen Berger (2019) NOEF Heat and Gas Modelling: Phase 1. January 2019.

Wels, C., Lefebvre, R., and A. Robertson, 2003. "An Overview of Prediction and Control of Air Flow in Acid-Generating Waste Rock Dumps", In proceedings of the Sixth International Conference on Acid Rock Drainage, Cairns, Queensland, Australia, 14-17 July, 2003, pp. 639-650

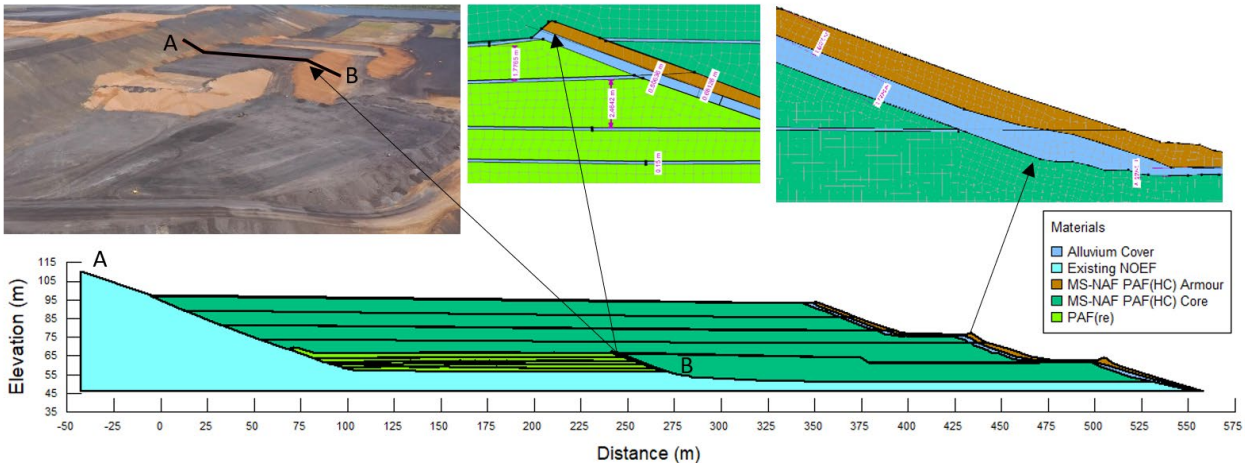

Fig 1. **Example of model including PAF(re) cell with future MS-NAF encapsulation with covers. (KCB, 2019).**

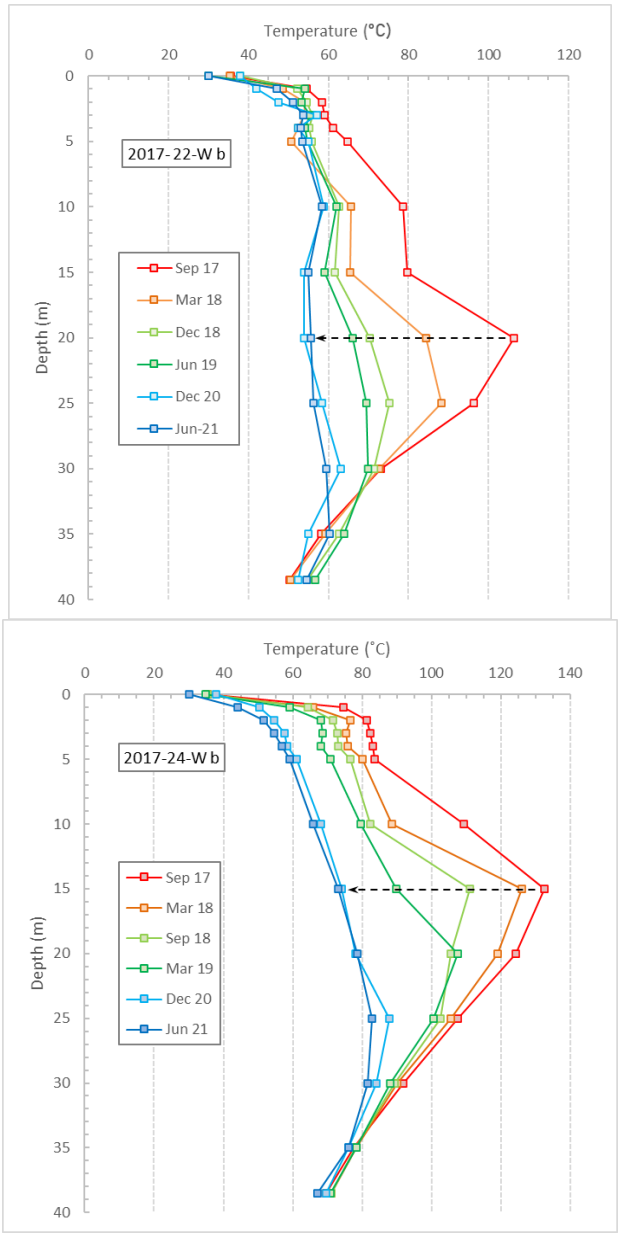

Fig 2. **The temperature in a covered part of the older waste rock dump (significant decrease in temperature about 50 m from the sides after placement of cover)**

Fig 3. **Paddock dumped PAF, outer NAF shell, and horizontal advection barriers (water trucks in foreground for scale)**

Clearing the hurdles of mine waste management for greenfield sites

R. Green
Rio Tinto, Rosalind.Green@riotinto.com

Increases in renewable energy, population and economic development are expected to double the 2020 demand for copper to 50 million tonnes worldwide by 2050, driving the exploration and development of additional copper reserves and extraction facilities. Demand for many other commodities is similarly expected to grow. Contrary to this demand, the permitting timeframes for new mines has also grown in recent years across multiple jurisdictions, meaning it is taking longer to source new minerals, once discovered. Environmental stewardship and the management of mineral waste to reduce offsite water quality risks are an intrinsic component of any environmental approval for a new mine.

Two case studies will be presented, where obstacles in mine waste management have been overcome or proactive approaches to reduce permitting delays have been taken:

1. Changing the tailings storage facility design to reduce long term AMD risks
2. The importance of geochemical characterisation, including acid sulfate soils, in construction areas of a new mine

In isolation, the benefits of technical excellence, and comprehensive planning, and mine waste prediction and management methods are limited. Indeed, continual consultation from the conceptual stage has been found to be a proactive measure to increase host community support, and trust, reducing the subsequent public opposition and critique during the technical planning and proposal stages of large projects.

Source Control for AMD risk management using cover system and landform design – Lessons from a quarter century of practice -

M. O'Kane[A]

[A]O'kane Consultants, 1000 7th Ave. SW Calgary, AB, Canada T2P 5L5. mokane@okaneconsultants.com

1.0 INTRODUCTION

Acid and metalliferous drainage (AMD) continues to pose significant environmental and financial challenges for the mining industry. The past 25 years have demonstrated that proactive source control through integrated cover system and landform design is essential for effective AMD risk management. This extended abstract synthesizes a quarter century of field-based experience, drawing on recent advances in conceptual 22odelling, regulatory practice, and design implementation to outline a practical framework for source control when constructing mine rock stockpiles. Key to this framework is integration of unsaturated soil mechanics, conceptual landform design, and risk-informed performance assessment to limit water and oxygen ingress to reactive mine rock material.

1.1 Conceptual Model Approach

The conceptual model approach provides a structured methodology for aligning design objectives with site-specific climatic, hydrogeologic, and geochemical conditions. This allows for early identification of thermodynamic and gravitational imbalances created when subsurface reactive materials are exposed on the surface. By managing these imbalances through engineered controls and progressive closure strategies, the likelihood and magnitude of AMD generation can be substantially reduced. Particular emphasis is placed on the application of these principles during project development, when influence over long-term costs and liabilities is greatest.

1.2 Focus for the Extended Abstract

This extended abstract outlines key technical and governance lessons learned over 25 years of practice, including:

- The importance of beginning landform design at the project description and preliminary economic assessment stage;
- A robust, yet simple, conceptual model to support landform design;
- Use of climate, and site informed binning systems to guide conceptual model development;
- Functional, rather than prescriptive, classification of cover systems;
- Advantages of source control-based construction for mine rock stockpiles; and
- Integration of closure vision into corporate governance and investment frameworks.

Ultimately, the goal is to embed source control and land stewardship as core business within mine planning, enabling sustainable closure and measurable reduction in AMD-related liabilities. The result is a simpler definition for integrated mine closure in respect of managing AMD risk, which is more applicable compared to relatively complex definitions offered in guidance documents. For example: *"…integrated mine closure is the process of considering both the extraction plan and the closure plan concurrently, such that on an annual basis, a change to one plan should directly affect the other..."*

would sufficiently capture the goal of closure plan and operation plan integration for AMD risk management.

2.0 PROBLEM DEFINITION

AMD, or metal leaching and acid rock drainage (ML/ARD), results from exposure of sulphide-bearing rock to water and oxygen. Without mitigation, AMD can require perpetual collection, conveyance, storage and treatment, which has led to billions in liabilities globally. Traditional reliance on cover systems and water treatment at cessation of mine operations is insufficient. Instead, a robust, yet simple, conceptual model to inform on landform design, and use of source control strategies, must be embedded into mine planning and landform construction.

A lack of alignment between mine planning and closure planning is common; the result is unrecognised and underfunded liabilities: most critically, lack of executable closure plans resulting in unforeseen liabilities, often manifesting as water quality issues requiring long-term seepage water collection, conveyance, and storage, and subsequent water treatment, and/or the requirement to move large volumes of material long distances to achieve required rehabilitation outcomes.

3.0 LANDFORM AND COVER SYSTEM DESIGN

Cover systems and landforms function together. Cover systems must be designed in the context of landform material, geometry, and hydrogeology. Thermodynamic and gravitational imbalances inherent to mine rock placement are best mitigated through early design that addresses:

- The geologic system;
- Site-specific climate conditions;
- Construction practices that influence landform internal airflow capacity;
- Net surface water infiltration and net percolation (the latter for cover systems); and
- Geochemical characteristics inherent to the geologic system, which are influenced by construction practices and landform water balance.

A key principle is beginning landform design during the planning phase; specifically, the project description (PD) or preliminary economic assessment (PEA) stage to maximize ability to influence cost and performance outcomes.

4.0 CONCEPTUAL MODELS AND BINNING FRAMEWORKS

The INAP Global Cover System Design guidance promotes use of site-specific conceptual models, built around climate and hydrogeologic setting, to guide early cover system design. These models apply hierarchical frameworks that categorize site characteristics (e.g., climate classification, material texture, etc.) to inform likely performance.

Cover system performance is best expressed probabilistically. For instance, the probability of exceeding a net percolation threshold under a defined climatic regime provides more useful risk insight than binary design outcomes.

This binning framework can be applied to all aspects of the simple, yet robust, conceptual model framework shown in Figure 1.

5.0 MINE ROCK STOCKPILE CONSTRUCTION FOR SOURCE CONTROL

Traditional mine rock stockpile construction (high tip heads, segregated placement) allows extensive oxygen ingress, indeed, continuous re-supply of oxygen via advection. Reducing lift heights, layering with finer-textured material, and constructing engineered internal layers can reduce internal airflow capacity, and thus re-supply of oxygen, and therefore sulphide oxidation.

These construction practices lessen dependence on cover systems, as well as collection, conveyance, and storage of seepage waters and subsequent water treatment, while also enhancing predictability and lowering closure risk.

6.0 CONCLUSIONS

Effective AMD source control requires early, integrated design of cover systems and landforms, guided by robust conceptual models and implemented through source-control oriented landform construction. A shift in mindset, where mine closure, land stewardship, and water stewardship are seen as core business, is essential. Lessons learned over the past 25 years provide a clear roadmap for embedding this mindset into practice. The robust, yet simple, conceptual model provides the tool to apply this new mindset at all stages of the mine life cycle, particularly early in a project well before pre-feasibility and feasibility.

The approach allows for integrated thinking, breaking down design ‘silos’, and a focus on developing “and” questions, rather than on asking “or” questions; because “or” questions result in efficient and compliant solutions, whereas “and” questions result in effective and sustainable solutions. The latter solutions are strongly aligned with the application of an integrated mine closure approach and defining mine closure as a continuous journey of improvement, rather than as a destination.

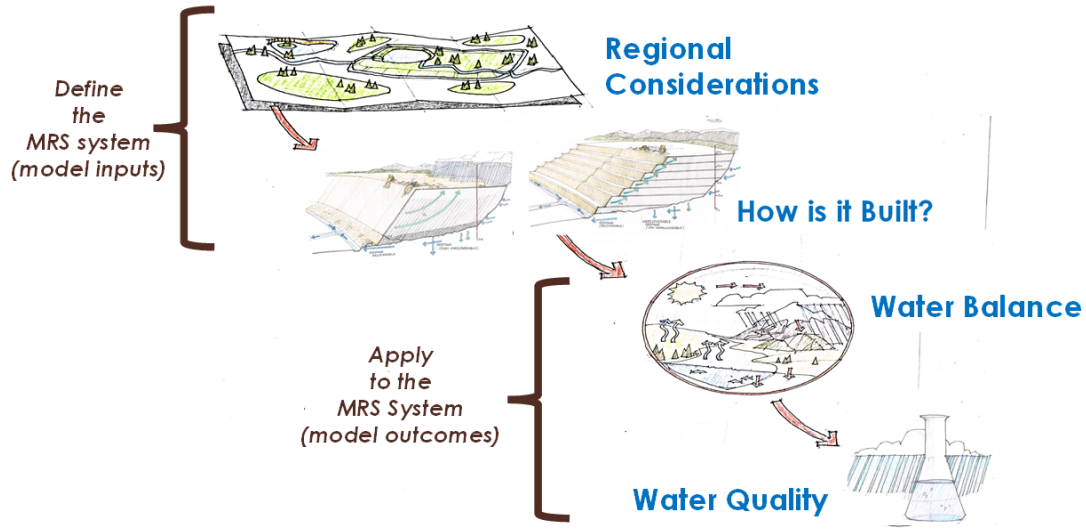

Fig. 1. **Summary of the conceptual model, or tool, for predicting the evolution of metal mobility of mine rock placed into a mine rock stockpile, illustration by D Shuttleworth**

Design of Engineered Landforms to Improve Closure Outcomes

P. Weber[A], L. Navarro[B], C. Hillman[C], and S. Hoodhills[D]
[A]Principal Environmental Geochemist, Mine Waste Management, Christchurch, New Zealand.
paul.weber@minewaste.com.au
[B]Senior Environmental Research Scientist, Mine Waste Management, Christchurch, New Zealand.
[C]Environmental Geochemist, Mine Closure Management, Calgary, Canada.
[D]Environmental geoscientist, Mine Waste Management, Christchurch, New Zealand.

The availability of empirical data (water quality, flow rate, geochemical data) for waste rock storage facilities can support the development of geochemical models for a project and/or serve as analogue models for other sites having the same material properties (lithologies, sulfur content, acid neutralisation capacity, potential constituents of concern [PCOC]) and geographic conditions (e.g., rainfall, evaporation, temperature, seasonal effects). This paper assesses several empirical datasets to aid in the development of predictive models to consider source control opportunities for improved closure outcomes.

Case Study #1: Empirical datasets were used to determine water quality (sulfate concentration in toe seepage) as a function of the average height of a waste rock storage facility. The sulfate versus height relationship was then used to develop predictive models and water quality estimates for other PCOC in waste rock storage facilities with no designed oxygen control. Models were developed to assess the benefits of engineering controls where oxygen was excluded.

Case Study #2: Empirical datasets were available to assess the benefits of source control (low lift height (2 m high), geochemical controls (limestone addition), water control, and cover systems) for an Engineered Landform. Data demonstrated that three phases were identified including an operational phase of increasing PCOC concentrations with increasing material placement; a stabilisation phase and then a decay phase where concentrations decrease at ~7-10% per year. Almost 10 years of data support the trends and the benefits of source control. Results are used to forecast water quality for other engineered landforms.

Empirical data from a project or from a comparable analogue site is a tremendous opportunity to develop models to understand effects and opportunities for source control. This paper explains two models that were developed and the estimated benefits from source control.

The Rum Jungle Rehabilitation Project – implementing Source Control for a Legacy Site and Current Status

F. Egerton[A], D. Jones[B], P. Ferguson[C], D. O'Toole[D]
[A]Mines Division, Department of Industry, Tourism, and Trade, Darwin, NT, Australia.
forrest.egerton@nt.gov.au
[B]DR Jones Environmental Excellence, Atherton, QLD, Australia
[C]SLR Consulting Ltd., Vancouver, BC, Canada
[D]SLR Consulting Ltd., Townsville, Australia

1.0 INTRODUCTION

The Rum Jungle legacy site is located approximately 100 km south of Darwin in Australia's Northern Territory (NT). Groundwater and surface water quality at the site is severely impacted by Acidic and Metalliferous Drainage (AMD) generated mainly by waste rock in the historic Waste Rock Dumps (WRDs).

The mine operated between 1952 and 1971 and produced uranium oxide, copper concentrate, and lesser amounts of cobalt and lead concentrate (Davy, 1975). The East Branch of the Finnis River (EBFR) was realigned around the Main Pit and Intermediate Pit to allow for mining operations to be undertaken. Sulfide-bearing waste rock was deposited via high lift end dumping in the Main WRD, Intermediate WRD, and Dyson's WRD where it was exposed to oxygen and water ingress. Tailings were discharged into a poorly constrained surface tailings dam or to Dyson's Open Pit from 1953 to 1965, then discharged sub-aqueously into the Main Pit. The site was essentially abandoned at the end of mining operations (Figure 1).

The water quality in the EBFR and further downstream was substantially degraded due to AMD inputs (largely copper and acidity) from the oxidising waste rock. Severe downstream impacts of AMD occurred until the completion of large-scale rehabilitation works, funded by the Commonwealth Government of Australia (Commonwealth) and undertaken by the Northern Territory Government (NTG) between 1982 and 1986 (Figure 2). Arguably this rehabilitation saw the start of application of source control in several aspects.

(1) Treatment of the acidic pit water to largely remove this as a source to the established through-flow of the pit.
(2) The containment of the surface sulfidic tailings below the water table level in Dyson's Pit.
(3) The covering of the Main and Intermediate WRDs with a multilayer cover system to reduce oxygen penetration and water infiltration. This was one of the first applications of a multilayer cover system to reduce the rate of oxidation and limit infiltration of water to waste rock.

The target for the initial rehabilitation works was a minimum of a 70% reduction in the loads of copper (Cu), zinc (Zn) and manganese (Mn) in the EBFR downstream of the site. The target reductions were achieved for these metals - 95%, 80% and 70%, respectively (Allen and Verhoeven 1986). However, given that substantial oxidation of waste rock had already occurred prior to cover placement, the WRDs remain an ongoing source of AMD to groundwater and the EBFR. The dramatic improvements in downstream water quality post 1986 are shown in Figure 3, which shows yearly time series concentration data for Cu, which is the contaminant of most toxicological concern.

Whilst the 1980s rehabilitation met its technical objectives, the planning and implementation of the works did not address the cultural health and concerns of the Traditional Owners. In particular, the site

remained a highly engineered and visually disturbed landscape with above-grade WRDs with rock batters, and gabion-lined drainage channels to manage surface runoff. Moreover, while the load reduction in metals resulted in a major improvement to aquatic ecosystem health several kilometres downstream, metal concentrations (especially Cu) at the site boundary remained much higher than contemporary standards, with only 1% ecosystem protection.

2.0 NEW REHABILITATION STRATEGY

2.1 Background

The combination of progressive failure of the cover system coupled with the recognition that any future works needed to also address the Traditional Owner's cultural values, led to the Commonwealth and NTG entering in 2009 into a four-year National Partnership Agreement (NPA) for the management of the site. The NT Department of Mines and Energy (DME) selected a rehabilitation strategy from a series of five alternatives after extensive consultation and technical workshopping with various government departments and Traditional Owner representatives. The preferred strategy included:

- Backfilling the permanently flooded portion of the Main Pit with the Potentially Acid Forming (PAF) waste rock with the highest sulfide content to inhibit future AMD generation, and
- Building and capping new Waste Storage Facilities (WSF) for the remaining PAF material in locations suitable to the Traditional Owners.

The results of this initial assessment were used to develop an improved rehabilitation strategy that is consistent with the views and interests of Traditional Owners and that meets contemporary mined land rehabilitation standards. In particular, and in contrast to many mine rehabilitation projects, the works needed to be designed to improve site conditions to restore cultural values. This includes:

- Restoration of the flow of the EBFR to its original course as far as possible, and
- Removing culturally insensitive landforms such as the WRDs, from adjacent to sacred sites and relocating, ensuring a culturally safe distance from the sacred sites.

In 2016 the Commonwealth and NTG determined that the proposal required assessment under their respective environmental protection legislation at the level of an Environmental Impact Statement (EIS). The draft EIS was submitted in 2020 (DPIR, 2020) and the final version approved in 2023.

One of the key conditions for the project's performance during construction and post closure relates to initially maintaining, and subsequently improving post closure, the downstream water quality. This is to be ensured by adherence (both in terms of concentration values and frequency of compliance) to locally derived water quality objectives (LDWQOs) for discharges from the site's water treatment plants (WTPs). The process for derivation of the LDWQOs and their application is described in a companion paper (Jones et al. 2025) (this proceedings).

2.2 Source Control Design Philosophy

The plan to totally rework the legacy WRDs on site has provided a unique opportunity to implement source control practices for all components of the project. These are described below.

(1) Backfilling the Main Pit with the highest sulfide containing waste rock such that this material will remain submerged below the recovered ground water table.
(2) Relocating the remaining waste rock to new purpose built WSFs. These will be built from the ground up in thin lifts with interlayer compaction, with a final cover system overlaying the waste, aimed at minimising both water and oxygen ingress.

(3) Amending the waste rock placed in the pit and in the new WSFs with limestone to neutralise the existing acidity contained within this material. If this was not done the load of metals and acidity would comprise a future source to groundwater (backfilled pit) and surface and groundwater (new WSFs).

A seepage interception system (SIS) will also be installed to remove the existing contaminated groundwater that underlies the footprints of the WRDs and a previous heap leach area. Although not a source control method, if the contaminated groundwater is not removed it would continue to be a source of seepage to the EFBR downgradient and delay the trajectory for final recovery of the EFBR.

2.3 Main Pit Backfill

The cross section of the Pit is shown in Figure 4, with several features of note. There is approximately 40m of relatively good quality (compared to LDWQOs) water overlying a highly contaminated 2m thickness of water below the chemocline. This contaminated water is the combined result of legacy process water remaining after the pit profile was partially treated in the 1980s and the upwards diffusion of pore water from the underlying tailings.

Dewatering will be done using floating pontoon-mounted pumps with the water reporting, if required to meet discharge criteria, to a high-rate WTP to remove Mn (the main contaminant of concern down to the chemocline). Dewatering the pit has the potential to induce geotechnical instability in the pit walls. This will require close monitoring of wall movements/integrity with the rate of dewatering potentially needing to be reduced below the maximum proposed rate of 100L/s if instability occurs.

Once dewatering is complete the current plan is to develop a new access ramp to the tailings level, at which point geofabric layers will be laid out to provide loading support for the initial bridging layers of rock to be placed, after which the pit will be backfilled with neutralant amended waste rock.

The waste rock materials at Rum Jungle have been well characterised over time (Robertson GeoConsultants and DR Jones Environmental Excellence, 2019) with approximately 85% of the volume of being classified as PAF. PAF-I has the highest acid forming potential whilst PAF-III has the lowest. Figure 5 shows the distribution of classification types across site by current storage location. A high proportion of all waste rock stored at the site is classified as PAF-I and only a small portion is classified as Non-Acid Forming (NAF).

There is limited storage available in the Main Pit so priority for this needs to be given to the material with the highest residual reactive sulfide content (PAF-I and PAF-II). This material is most concentrated in the Intermediate WRD and in the surface rockfill of the Dysons Pit. Thus, the waste rock from these two locations will be placed in the pit first. The tailings in Dysons Pit will be left in situ and re-covered with benign NAF material and soil. The Main Pit will be filled with waste to below the minimum seasonal groundwater elevation, before being covered with a layer of benign fill. The final configuration of the Main Pit will be as a shallow flow-through pit lake that discharges into the existing Intermediate Pit lake and thence into the EFBR along the existing flow line.

2.4 Water Treatment and Management

Two WTPs will be required for the project. The first will be a high-rate treatment plant designed to polish the bulk of the water to be removed from the Main Pit, down to the level of the chemocline. The main contaminant in this water is Mn, so the pit WTP will incorporate a catalytic Mn removal process. A conventional high density sludge treatment plant will be installed to treat high grade AMD water from the highly contaminated lens of water at the bottom of the Main Pit, contaminated water

that may accumulate in the pit as it is being backfilled; water being produced by the groundwater SIS, and seasonal runoff and infiltration water captured during the relocation of the waste rock.

2.5 New Waste Storage Facilities (WSFs)

The construction methodology for the new WSFs has been developed with the primary focus on long-term risk mitigation associated with future AMD, consistent with guidance provided in the Australian Leading Practice Sustainable Development in Mining Series AMD Handbook (DIIS, 2016) and the recommendations in a recent INAP coordinated report (INAP, 2020) on construction methods for WSFs to minimise AMD risk. Key elements of the risk mitigation measures are detailed below.

- Bottom-up (paddock dumping) construction methodology to avoid internal particle size segregation and settlement issues associated with a top-down or end-dumped approach.
- Upon placement, waste rock will be treated with agricultural lime and then compacted in controlled layers (each nominally 0.5 m and 90% standard maximum dry density) to increase density, water residence time and saturation, and create a net alkaline environment.
- The WSF will be built up vertically over a number of cells to allow part, or all, of the cover system to be constructed prior to the wet season for each cell.
- Constructing outer surfaces to final geometry within the placement cycle to expedite final surfaces available for revegetation covers.
- Construction of cover systems progressively alongside the waste rock lifts and progressive revegetation of cells and cover system surfaces to reduce rainfall infiltration during construction and to stabilise the outer surfaces as rapidly as possible.

The purpose of the WSF cover system is two-fold: to limit oxygen and water ingress into the waste rock mass, and to develop a viable substrate for vegetation establishment. Modelling has been undertaken and the resulting design specifies a 0.5 m low permeability barrier layer beneath a 2.0 m store and release layer (growth material) with internal capillary breaks/drainage layers (DPIR, 2020).

3.0 CURRENT PROJECT STATUS

The project is preparing to implement the program of works with key attention focussed on finalising remaining approvals; and delivering key project pillars of maximising Traditional Owner and local participation pathways, so that maximum value can be returned to community through works execution.

The 2024-25 period has been crucial as key contractors are procured, the project delivery team is recruited and final approvals are settled. Early works will start in 2025 with commencement of site access, public road safety works, the contaminated groundwater capture (SIS) drilling program and starting general site revegetation. Dewatering of the Mail Pit will commence in Q2 2025.

4.0 SUMMARY

This paper has summarised the history of the site and the social challenges and key AMD-related technical issues (solute load reduction, pit backfill, method of WSF construction etc) that have had to be addressed to develop a fully costed rehabilitation plan to bring the site to a condition so that it can both be returned to its traditional owners and meet contemporary environmental performance objectives. Following rehabilitation, it is predicted that the load of copper will reduce from 2.5 t/year to 0.24 t/year, a ten-fold reduction (Robertson Geoconsultants 2019). This extent of reduction translates to an increase from less than 1% aquatic species protection to 70% on site.

ACKNOWLEDGEMENTS

The authors thank the NT Government's Environmental Monitoring Unit and Rum Jungle Project team for their assistance in sample collection and field work and the various personnel from Hydrobiology, Robertson Geoconsultants, DR Jones Environmental Excellence and their subconsultants who assisted with data collection and analysis. Particular thanks are given to the traditional owners of the lands that this work was conducted on, the Warai, Kungarakan and Maranunggu peoples, and the Commonwealth and Territory government staff who assisted with the rehabilitation planning and approvals.

REFERENCES

Allen CG and Verhoeven (1986) The Rum Jungle rehabilitation project - final project report. Northern Territory Dept of Mines & Energy, Darwin, NT, June 1986.

Davy (1975) Rum Jungle Environmental Studies. Australian Atomic Energy Commission, AAEC/E365. Lucas Heights, NSW, September 1975, pp. 322.

DIIS (2016) Preventing Acid and Metalliferous Drainage, Leading Practice Sustainable Development Program for the Mining Industry, Australian Government Department of Industry Innovation and Science, September 2016, pp. 221. www.industry.gov.au/resource/Programs/LPSD/Pages/LPSDhandbooks.aspx#

DPIR (2020) Draft Environmental Impact Statement for the former Rum Jungle mine site, Department of Primary Industry and Resources, Northern Territory Government, January 2020. https://nt.gov.au/_media/docs/business-and-industry/mining/rum-jungle/environmental-impact-assessment-and-statement/eis-executive-summary.pdf

INAP (2020) Rock Placement Strategies to Enhance Operational and Closure Performance of Mine Rock Stockpiles Phase 1 Work Program – Review, Assessment & Summary of Improved Construction Methods, prepared by Earth Systems and O'Kane, pp. 105. https://www.inap.com.au/wp-content/uploads/2020-Jan-INAP-Improving-Stockpile-Construction-Phase-1-Final-Report.pdf.

Robertson Geoconsultants (2019) Groundwater and Surface Water Modelling Report, Rum Jungle Stage 2a, Report 183008/1, Prepared for Northern Territory Government, November 2019, pp. 173. https://nt.gov.au/_media/docs/business-and-industry/mining/rum-jungle/environmental-impact-assessment-and-statement/appendices-to-the-eis/robertson-geoconsultants-2019-groundwater-and-surface-water-modelling-report-rum-jungle-stage-2a-part-1.pdf

Robertson Geoconsultants and DR Jones Environmental Excellence (2019) Rum Jungle mine site. Physical and geochemical characteristics of waste rock and contaminated materials (rev2), REPORT NO. 183008/2 by Robertson Geoconsultants Inc and DR Jones Environmental Excellence for Northern Territory Department of Primary Industry and Resources, November 2019, pp. 379. https://nt.gov.au/_media/docs/business-and-industry/mining/rum-jungle/environmental-impact-assessment-and-statement/appendices-to-the-eis/robertson-geoconsultants-and-jones-d-2019-rum-jungle-physical-and-geochemical-characteristics-of-waste-rock-and-contaminated-materials-part-1.pdf

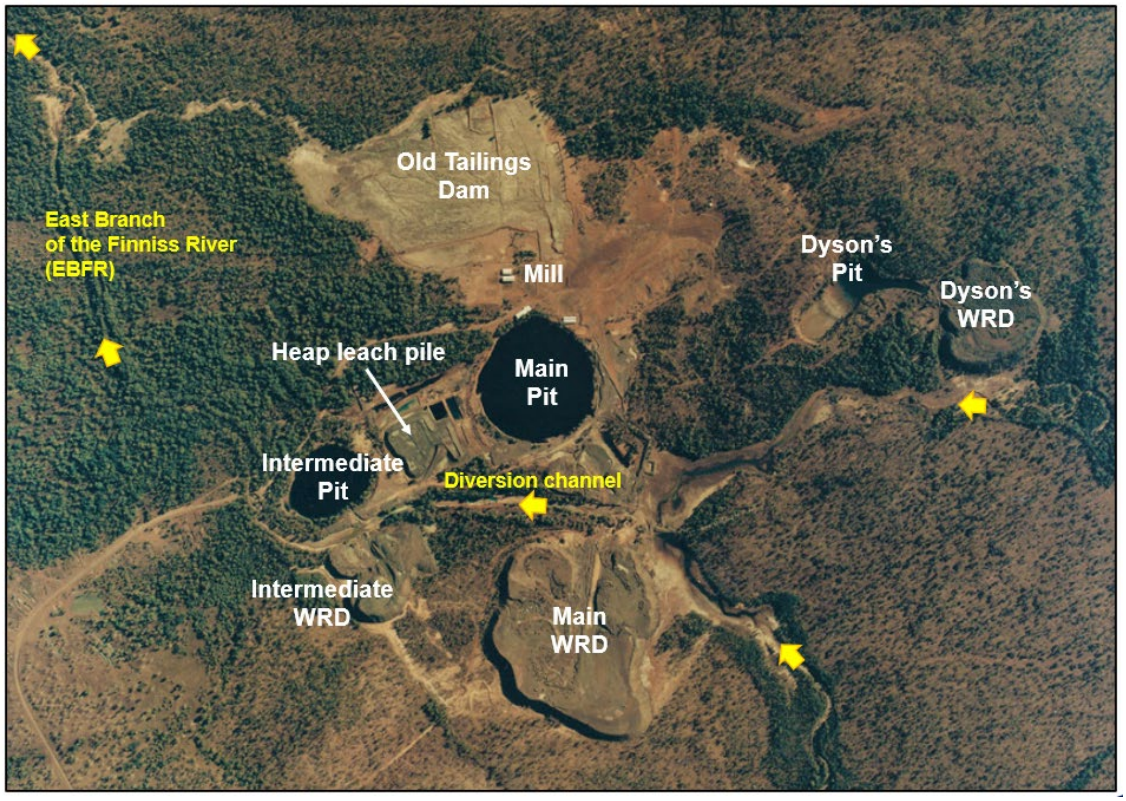

Fig. 1. **Site in the 1970s prior to the 1980s rehabilitation. Yellow arrows show stream flow lines.**

Fig. 2. **Appearance of main site features after 1980s rehabilitation**

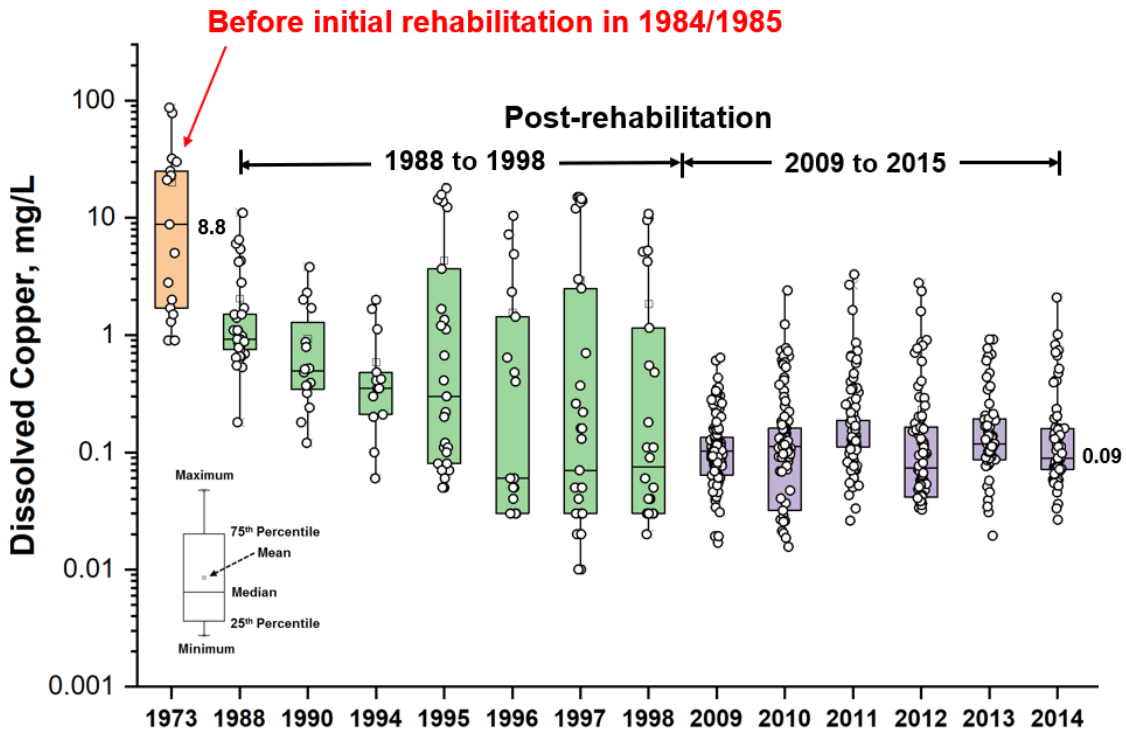

Fig. 3. **Time series data for Cu before and after 1980s rehabilitation (Robertson Geoconsultants 2019)**

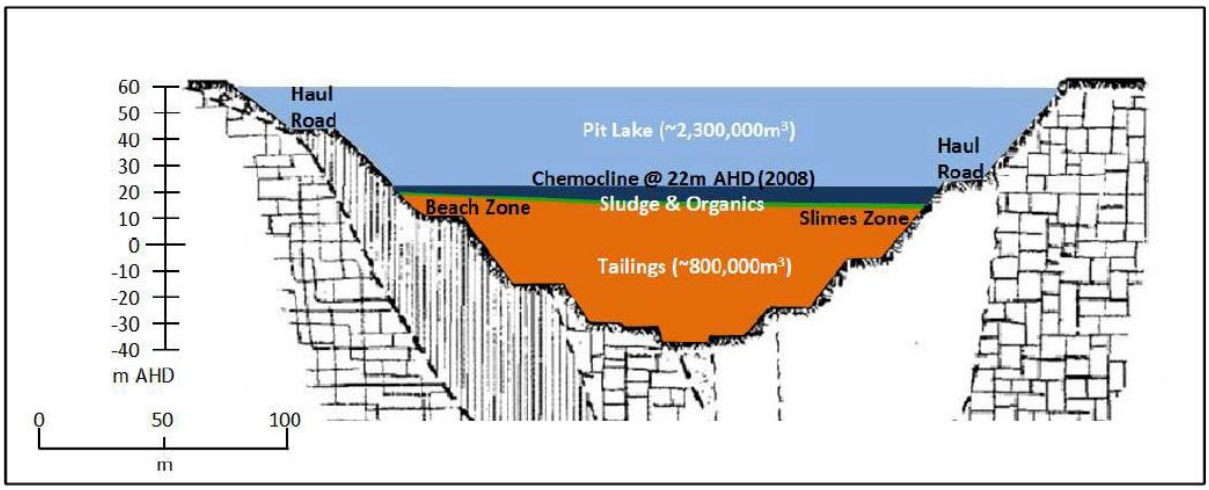

Fig.4. **Cross-section profile of Main Pit**

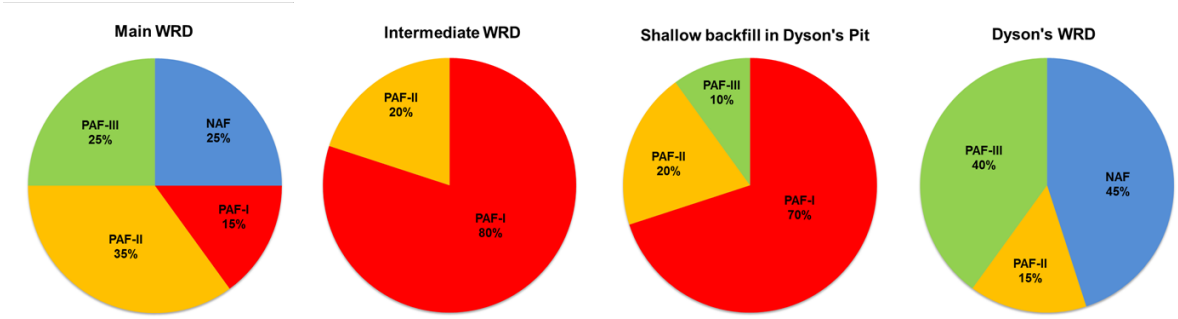

Fig. 5. **Distribution of PAF materials by current waste storage location. The highest sulfide containing material is PAF-I (red), with PAF-II (orange) and PAF-III (green) containing progressively lower residual sulfide. Non-Acid forming material is shown in blue.**

Water Quality Performance Objectives and Geochemical Characterisation for the Rum Jungle Legacy Site, Northern Territory (NT), Australia

D.R. Jones[A], P. Ferguson[B], and R. Smith[C]
[A]DR Jones Environmental Excellence, Atherton, QLD, Australia, drdrjjones@gmail.com
[B]Robertson GeoConsultants Inc., Vancouver, BC, Canada
[C]Hydrobiology, Milton, QLD, Australia

1.0 INTRODUCTION

Rum Jungle is one of the world's iconic legacy sites in the history of acid rock drainage (ARD) assessment and management. A major program of rehabilitation works was implemented in the mid-1980s, resulting in a greater than 70% reduction of metal loads, and substantial improvement in aquatic ecosystem health downstream. However, this improvement was not sufficient to meet contemporary environment protection standards. This issue amongst others prompted the Australian and Northern Territory Governments to set up a National Partnership Agreement to develop and implement a rehabilitation plan to bring the site to current standards. The development of locally derived water quality objectives (LDWQOs) for ecosystem protection (performance objectives) and the geochemical characterisation program underpinning the scoping of the works needed to meet these objectives are summarised here.

The current layout and status of the site, and full details of the proposed rehabilitation strategy, are provided in the Environmental Impact Statement (EIS) and supporting technical documentation (DPIR, 2020). A summary overview is given in Hartnett et al 2024.

Central to the planning for the rehabilitation works was the establishment of agreed water quality performance objectives for both the construction and post rehabilitation phases. Such objectives provide the performance metrics for water treatment that may be needed during construction as well as for long term performance of the newly constructed waste containment facilities. The starting premise for performance during the construction phase was that the downstream load of contaminants would be no worse, and ideally much better, than currently. Copper is the major toxicant (Jeffrey et al. 2001) in water from the Rum Jungle site, reflecting the reactive sulfide content in the waste rock contained in the three waste rock dumps (WRDs).

In parallel with development of the water quality objectives was the geochemical characterisation required to establish the containment and treatment that would be needed to ensure that the post rehabilitation load of metals would comply with the proposed LDWQOs. This in turn facilitated an assessment of the likelihood of meeting the water quality performance objectives that are now approved by the regulator.

2.0 DERIVATION OF LDWQOS

Importantly in this case a community consultation process was incorporated from the start. This approach established upfront agreed levels of aquatic biodiversity protection for each zone of the Finniss River (Figure 1), including accounting for the indigenous cultural and spiritual values appropriate for each zone.
The process for developing the LDWQOs is described in detail in Hydrobiology (2022b) and Jones et al. (2024). In summary, taxonomic richness across fishes, invertebrates and periphyton at sites

downstream of the mine and in control sites in other parts of the Finniss River system were fitted to measured concentrations of parameters of concern, and the concentrations that would protect the agreed proportion of resident species for each river zone were derived from those curves. Where adequate curve fits were not achieved, the highest observed concentration associated with the appropriate level of protection or the national default guideline value was used, whichever was the highest. Examples of the derived curve fits are provided in Figure 2. The final LDWQOs are provided in Table 1. The zone numbers (See Fig 1 for location) in Table 1 refer to increasing distance downstream with Zone 2 being the most contaminated reach of the river, currently receiving discharges from the legacy site.

Table 2 compares the LDWQOs for Cu and Zn with the default water quality guidelines and with the current 95th percentile concentrations on the minesite, which correspond to an ecosystem protection of less than 1% for zone 2. This shows not only the extent to which the aquatic ecosystem health will be improved, but also how the application of locally-derived criteria mean that the performance targets aren't nearly as restrictive as would be the case by applying the default ANZG criteria, but still provide a similar level of aquatic ecosystem protection.

Both total and dissolved concentrations of metals and metalloids will be measured as part of the environmental compliance monitoring for the project, but importantly in this case it is the dissolved concentrations that will be used to assess compliance with the LDWQOs.

This outcome resulted in environmental management of the mine rehabilitation being founded on stakeholder consultation-derived environmental values and levels of protection for each reach, which expressly included both ecosystem and cultural and spiritual value protection to a level acceptable to the communities downstream of the mine. However, it was not reached quickly. Rather, there were extensive discussions with the Territory and Federal regulators about this approach over a decade. The primary regulator concerns were, in essence, that this was an unusual approach that potentially set precedents for other sites. In particular, that it incorporated levels of protection that differed from the default levels, and that the LDWQOs differed from the national DGVs.

It was evident that the paradigm shift required for a legacy site, aimed at a net environmental improvement, was very unlike the aims of most green- or brown-field assessments, they were more familiar with. Acceptance of a LDWQO approach challenged assessment processes even further as it required an acceptance of atypical (non-default) water quality targets. While the financial and technical constraints on a publicly funded rehabilitation of a legacy site were understood, there remained a reluctance to providing a permit for an outcome that did not comply with familiar norms. These issues were able to be worked through via extensive consultations. This experience highlights that when designing for pragmatic limits to environmental benefits for legacy site rehabilitation, it is critical to start dialogue with the regulators as soon as practicable, because permitting the rehabilitation is an essential part of the journey of feasibility assessment and design.

3.0 GEOCHEMICAL CHARACTERISATION

The rehabilitation of legacy sites can be more challenging than for operating mine sites that are mining and managing fresh material since sulfidic waste at legacy sites is often broadly distributed across the landscape, is often poorly characterised and is already at least partly oxidised. This oxidised material can contain substantial immediately leachable acidity and metals as well as poorly soluble acidic secondary minerals such as potassium jarosite - $KFe_3(SO_4)_2(OH)_6$. Thus, achieving protection of the receiving environment from this partly oxidised material can be more complex than for fresh waste rock where protection from oxidation alone can be an effective management strategy. The

rehabilitation strategy at Rum Jungle will involve a combination of in-pit containment for the highest residual sulfide material and new purpose-built surface waste storage facilities (WSFs) for the remainder of the waste rock (DPIR 2020).

Waste rock samples were initially characterized by a suite of static tests to estimate acid and metalliferous drainage potential (Shaw et al. 2002; Price 2009; Jones et al. 2016). Additional tests (Jones et al. 2024) were done to quantify the total existing acidity content of waste rock to develop a neutralization strategy appropriate for previously partially oxidized waste rock. A batch contact procedure was used to assess the effect of adding neutralant to waste rock.

The acidity distribution (incipient and existing) characteristics for the three assigned classes of potentially acid forming (PAF) materials are summarised in Table 3, noting that there is very little acid neutralising capacity (ANC) in these materials (ANC/MPA << 1 for PAF-I and PAF-II), and that PAF material comprises 85% of the total amount of waste. The existing acidity which comprises a substantial proportion of the total acidity, needs to be neutralised prior to final placement to ensure that this source is not able to leach out and contaminate groundwater (for in pit disposal) and surface water (from WSFs). Extensive test work has shown that finely ground calcium carbonate (ag lime) is the most appropriate neutralant for this application.

The neutralant demand for each type of PAF waste rock was determined by calculating the 80th percentile of the existing acidity contents of the PAF waste rock samples that have a rinse pH less than 5. These are the most acidic samples within each PAF category, so this is a conservative approach that would lead to over-liming the majority of waste rock and under-liming only a small proportion (less than 20%). An additional degree of conservatism was provided by initially using the existing acidity content of the less than 2 cm particle size range in the WRDs (as opposed to the much coarser particle size distribution of a WRD as a whole). This is because the mg/kg acidity content decreases as the particle size increases. Adjusting the conservative values in Table 3 to account for the particle size dependence of material in the existing waste rock dumps on site will substantially reduce by about one-third the amount of neutralant required by the project.

The target pH for neutralization is estimated to be around pH 7 based on the concentrations of soluble metals remaining in suspensions of acidic waste titrated to higher pH values by the addition of sodium hydroxide solution. The amendment of waste rock with limestone consistently achieved a pH of 6.5 to 7.0. Extract concentrations of most metals were reduced by at least 95%. Mn is an exception, as it was only reduced by an average of 87%.

4.0 WATER QUALITY PREDICTIONS

Based on the multiple lines of evidence produced from the testwork described above it was inferred that the concentrations of Fe, Al, Co, Cu, Mn, Ni and Zn in seepage from the new WSF and in porewater in the backfilled pit (assuming neutralization of existing acidity with limestone) will each be less than 1 mg/L. There is a high degree of confidence that for Fe, Al, Cu and Zn the concentrations will be less than 0.2 mg/L. The concentration of Ca will be limited by the solubility of gypsum and could be around 500 to 600 mg/L.

Predictive water quality modelling, using the inputs from the geochemical characterisation program, a site wide hydrological model, a regional groundwater model and a surface flow model was used to infer the solute loads that will leave site during the construction period and post rehabilitation. (Robertson Geoconsultants 2019). The model was run assuming the same rainfall pattern observed from 2010 to 2017 and using predicted SO_4 and Cu loads from the groundwater model. SO_4

concentrations in the East Branch of the Finnis River (EBFR) downstream of the minesite are predicted to be much lower than for current conditions, and future Cu concentrations in the EBFR are predicted to be generally much lower than Cu concentrations for current conditions. In particular, the load of copper, the toxicant of most concern, reporting to the river system downstream of the site will decrease from 2.5 t/year to 0.24 t/year, a ten-fold reduction.

5.0 CONCLUSIONS

The process used to derive LDWQOs has been summarised in this paper. It has been shown in this case that the effort involved in developing such objectives for an historically impacted river system can result in substantially less restrictive water quality compliance criteria than would be the case for application of default national (ANZG, 2018) water quality criteria. Nevertheless, a major reduction in annual loads will still be required by the rehabilitation works at Rum Jungle if these LDWQOs are to be met. The geochemical testwork that was used to develop input source terms for the post rehabilitation water quality predictive model has been described. The outputs from this model indicate that the 80th percentile post rehabilitation ecosystem protection criteria required by the regulator will be able to be met.

6.0 ACKNOWLEDGEMENTS

The authors thank the NT Government's Environmental Monitoring Unit and Rum Jungle Project team for their assistance in sample collection and field work and the various personnel from Hydrobiology, Robertson Geoconsultants, DR Jones Environmental Excellence and their subconsultants who assisted with data collection and analysis. Particular thanks are given to the traditional owners of the lands that this study was conducted on, the Warai, Kungarakan and Maranunggu peoples, and the Commonwealth and Territory government staff who assisted with the rehabilitation planning and approvals.

7.0 REFERENCES

ANZG (2018) Water Quality Guidelines Home. http://www.waterquality.gov.au/anz-guidelines. Accessed 17 Oct 2018.

DPIR (2020) Draft Environmental Impact Statement for the former Rum Jungle mine site, Department of Primary Industry and Resources, Northern Territory Government, January 2020. https://ntepa.nt.gov.au/environmental-assessments/register/rum-jungle-former-mine-site/draft-environmental-impact-statement

Harnett J, Jones D and Ferguson F (2024) The Rum Jungle legacy rehabilitation project, NT, Australia: history and current status, a case study to inform industry practice, In: Proceedings of ICARD 2024. Canadian Institute of Mining, Metallurgy and Petroleum, Halifax, Canada, September 16-20, 2024.

https://nt.gov.au/industry/mining/legacy-mines-remediation/remediation-projects/rum-jungle-rehabilitation/rum-jungle-rehabilitation-plan

Hydrobiology (2022b) Rum Jungle Locally Derived Water Quality Objectives Update. Hydrobiology, Brisbane, Australia.

Jeffree RA, Twining JR, Thomson J (2001) Recovery of fish communities in the Finniss River, Northern Australia, following remediation of the Rum Jungle uranium/copper mine site Environmental Science and Technology, Vol. 35, 2932-2941. https://doi.org/10.1021/es001719

Jones D, Ferguson P, Smith R (2024) Geochemical Characterization and Water Quality Performance Objectives for the Rum Jungle Legacy Site, Northern Territory, Australia. In: Proceedings of ICARD 2024. Canadian Institute of Mining, Metallurgy and Petroleum, Halifax, Canada, September 16-20, 2024.

Robertson GeoConsultants (2019). Groundwater and Surface Water Modelling Report, Rum Jungle Stage 2A

Robertson Geoconsultants and DR Jones Environmental Excellence (2019) Rum Jungle mine site. Physical and geochemical characteristics of waste rock and contaminated materials (rev2), REPORT NO. 183008/2 by Robertson Geoconsultants Inc and DR Jones Environmental Excellence for Northern Territory Department of Primary Industry and Resources, November 2019, pp. 379. https://dpir.nt.gov.au/mining-and-energy/mine-rehabilitation-projects/rum-jungle-mine/completed-studies

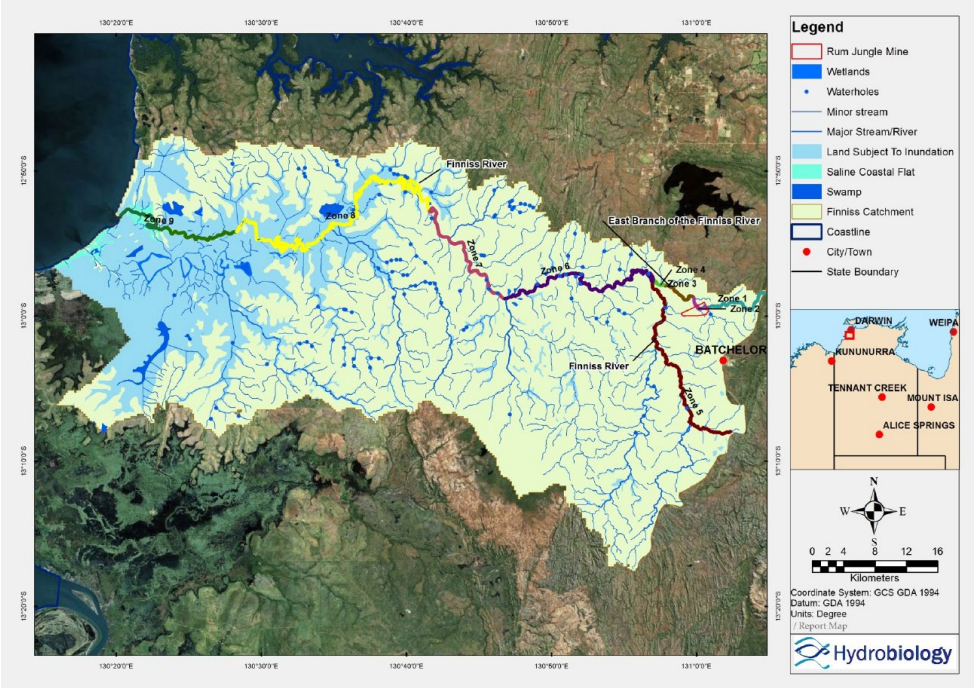

Fig. 1. **The Finnis River system showing the zones used to assess the gradient of exposure to develop the water quality objectives. The mine site is defined by the triangular red boundary at centre-right is Zone2.**

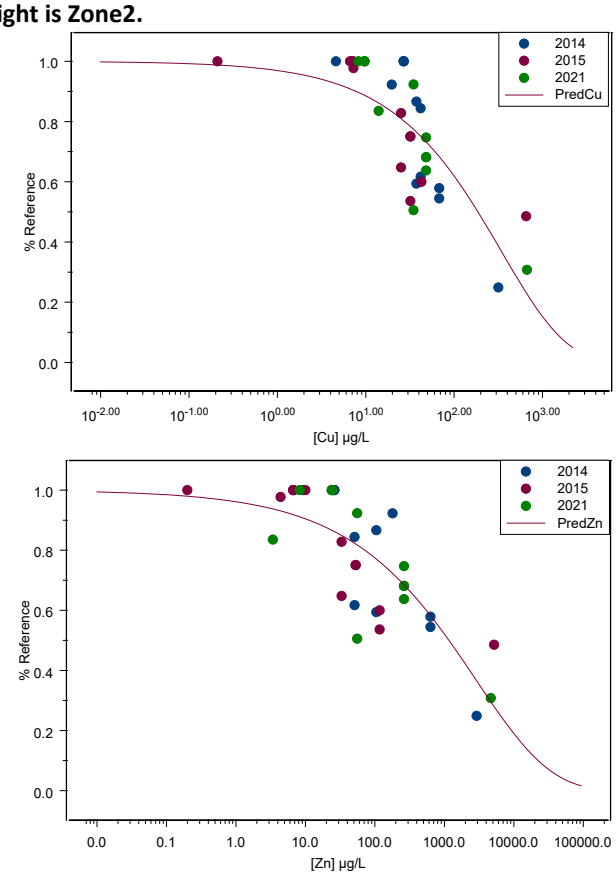

Fig. 2. **Examples of Weibull four parameter cumulative distribution fits for parameter concentration (Cu and Zn) versus percent of average control site number of taxa for all taxonomic groups.**

Table 1. Revised LDWQOs in comparison with the 2016 values for each parameter [A]

			Parameter																					
	River		Cu (µg/L)		Zn (µg/L)		Ni (µg/L)		Co (µg/L)		Al (µg/L)		Fe (µg/L)		Mn (µg/L)		U (µg/L)	Se (µg/L)	EC (µS/cm)		SO_4 (mg/L)		Mg (mg/L)	
%PC	Zone	Site	Current	Revised	Current	Revised	Current	Revised	Current	Revised	Current	Revised	Current	Revised	Current	Revised	Current	Current	Current	Revised	Current	Revised	Current	Revised
70	2	EB@G_Dys	60.2	60.8	210.5	227	130.4	135.1	89	106.5	236	142	300	300	759	503	31	2	2985	687	1192	230	86.6	86.6
70	2	EB@GS200	60.2	60.8	210.5	227	130.4	135.1	89	106.5	236	142	300	300	795	503	31	2	2985	687	1192	230	86.6	86.6
80	3	EB@GS327	27.5	27.6	180	71.6	43.1	48.3	25.9	33.2	150	142	300	300	443	225	22.5	2	2985	464	997	98.4	86.6	86.6
80	3	EBdsRB	27.5	27.6	180	71.6	43.1	48.3	25.9	33.2	150	142	300	300	443	225	22.5	2	2985	464	997	98.4	86.6	86.6
80	3	EB@GS097	27.5	27.6	180	71.6	43.1	48.3	25.9	33.2	150	142	300	300	443	225	22.5	2	2985	464	997	98.4	86.6	86.6
80	3	EBusHS	27.5	27.6	180	71.6	43.1	48.3	25.9	33.2	150	142	300	300	443	225	22.5	2	2985	464	997	98.4	86.6	86.6
90	4	EBdsHS	7.86	7.9 (7.80)	180	26.1 (11.3)	32.5	20 (9.3)	3.6	5.1	117	121	300	300	228	62.2	13.2	2	427	354 (242)	761	25.3	33.2	44.3
90	4	EBusFR	7.86	7.9 (7.80)	180	26.1 (11.3)	32.5	20 (9.3)	3.6	5.1	117	121	300	300	228	62.2	13.2	2	427	354 (242)	761	25.3	33.2	44.3
95	6	FR@GS204	3.4	14*/7.9	26.1	26.1	20	20	2.8	2.8	117	142*/121	300	300	140	140	2.9	2	190.7	354*/438	594	594	33.2	41.1*/39.9
95	6	FR3	3.4	14/7.9	26.1	26.1	20	20	2.8	2.8	117	142/121	300	300	140	140	2.9	2	190.7	354/438	594	594	33.2	41.1/39.9
95	6	FRusFC	3.4	14/7.9	26.1	26.1	20	20	2.8	2.8	117	142/121	300	300	140	140	2.9	2	190.7	354/438	594	594	33.2	41.1/39.9
95	7	FRdsFC	3.4	14/7.9	26.1	26.1	20	20	2.8	2.8	117	142/121	300	300	140	140	2.7	2	190.7	354/438	594	594	33.2	41.1/39.9
95	7	FR0	3.4	14/7.9	26.1	26.1	20	20	2.8	2.8	117	142/121	300	300	140	140	2.7	2	190.7	354/438	594	594	33.2	41.1/39.9

*=wet season

[A] For zones 2 to 4, **Black** text indicates LDWQO derived from a statistical curve fit (Weibull function), **Red** text indicates derived from the maximum concentration recorded with at least the desired taxonomic richness, Green text indicates values derived from the default water quality objectives.

Table 2. Comparison of LDWQOs for Cu and Zn with current Zone 2 water quality conditions and ANZG default guidelines. Concentration units - µg/L

Analyte	ANZG 2018 80%	LDWQO 80%	LDWQO 70%	Zone 2 WQ 95th ile
Cu	2.5	28	60	668
Zn	31	180	210	4671
		Post Rehab	Construction	Current

Table 3. Distribution (80th percentile) of acidity types in waste rock (Robertson Geoconsultants and DR Jones Environmental Excellence 2019)

Type	AMD Potential	Rinse pH	Jarosite Acidity, kg H_2SO_4/t	Titratable Acidity, kg H_2SO_4/t	Incipient Acidity, kg H_2SO_4/t	Total Acidity, kg H_2SO_4/t
Potentially Acid Forming (PAF) Waste Rock						
PAF-I	High	4.8	14.8	2.8	142.6	157.2
PAF-II	Medium	4.8	13.1	1.5	37.0	42.8
PAF-III	Low	6.1	3.2	1.2	14.2	18.5
Non Acid Forming (NAF) Waste Rock						
NAF	Minimal*	7.2	0.2	0.1	2.2	2.1

Assessing large static geochemical datasets for AMD risk

J. Waters, S. Pape, and N. Murphy
Earth Systems, Suite 4, 290 Salmon Street, Port Melbourne 3207 Australia.
john.waters@earthysystems.com.au

Increasing amounts of static geochemical data are being collected as part of Acid and Metalliferous Drainage (AMD) risk management and routine regulatory environmental reporting at mine sites. These large datasets are often under-utilised and poorly understood. The diversity of static geochemical testwork procedures can often produce conflicting and uncertain results that are difficult to interpret.

To avoid the requirement for specialist geochemical knowledge, increase the efficiency of data use, minimise classification uncertainties, and standardise outputs for ease of data comparison, an Excel-based AMD Assessment and Classification Tool (*AMDact*) has been developed. *AMDact* can assess multi-parameter static geochemical datasets including total sulfur / chromium reducible sulfur, net acid producing potential (NAPP), maximum potential acidity (MPA), acid neutralising capacity (ANC) and net acid generation data (NAG_{pH}, $NAG_{4.5}$ and $NAG_{7.0}$). Additional secondary acidity, sulfur, and carbon speciation data can also be incorporated to calculate the relative proportions of acid and non-acid storing sulfate species and provide an independent check on measured MPA and ANC. The tool produces rapid, industry standard, conservative, and unbiased risk assessments and materials classifications. It also has the ability to deal with the significant geochemical complexity arising from multi-parameter materials characterisation and assessment of AMD risk.

Applied to large, complex static geochemical data sets, *AMDact* produces uniform standard tabulated, graphical and statistical outputs based on lithology or other user-defined groupings (e.g. ore/waste, location). Using data in Excel format, the tool can assess several thousand samples in a few minutes. Outputs can either be in Southern Hemisphere (e.g. NAPP / MPA / ANC) or North American (NNP / AP / NP) format. As the outputs are inserted into separate spreadsheets into the original Excel data file, the classification data is capable of being formatted for incorporating into mine block models to assist with regulatory approvals, mine planning, waste scheduling and closure planning.

In addition to the simple potentially acid forming (PAF) or non-acid forming (NAF) classification, the tool provides a more detailed classification scheme including (i) High Potential for Acid Generation, (ii) Moderate / High Potential for Acid Generation, (iii) Moderate Potential for Acid Generation, (iv) Low Potential for Acid Generation, (v) Unlikely to be Acid Generating, and (vi) Likely to be Acid Consuming. In addition, the potential for neutral metalliferous drainage (NMD) and saline drainage (SD) impacts are assessed. This sophisticated classification scheme is documented in the Australian Government Leading Practice Handbook on Preventing Acid and Metalliferous Drainage (DIIS, 2016).

Static geochemical testwork procedures based on whole rock chemistry aim to clarify the mineralogy of a sample to predict long term geochemical behaviour. Interpreting this static geochemical data often results in varying numbers of uncertain classifications. These occur largely due to conflicting results arising from limitations in these test procedures. For example:

- Using Total Sulfur for MPA calculations assumes that all the sulfur present is contained within pyrite. This assumes that there is no non-acid generating sulfur present in the sample and can result in overestimation of MPA and NAPP.

- Standard ANC test procedures overestimate ANC where siderite ($FeCO_3$) and rhodochrosite ($MnCO_3$) are present, due to delayed acid production from the oxidation of Fe(II) and Mn(II). This has led to a modified version of the ANC test, although this test is not routinely conducted. Overestimation of ANC can lead to an underestimation of NAPP.
- NAG testwork suite results assume that all the sulfur present within the sample has reacted following chemical oxidation with hydrogen peroxide (H_2O_2), and all acid produced has been subsequently fully neutralised. Results can be impacted where insufficient hydrogen peroxide is added, or hydrogen peroxide is consumed on organic matter. This can result in NAG values being underestimated.

Key outputs of the tool include:

- General PAF/NAF classification for each sample.
- Detailed AMD risk classification for each sample.
- Summary statistics for key geochemical parameters both for the entire dataset and lithological groupings.
- Static geochemical and sulfur speciation graphical outputs to facilitate visual interpretation / data assessment.
- Recommendations for additional testwork.

Tables 1 and 2 show part of AMDact's output from a small sample set.

The tool accommodates the strengths and limitations of each of these methods in developing an AMD risk classification for each sample. Recommendations for follow-up test work (i.e.. kinetic tests on strategic samples), to confirm assessments and classifications can also be provided to better understand the geochemical behaviour of these materials.

Assessing large datasets using AMDact enables non-geochemists to rapidly produce uniform, unbiased, industry standard AMD risk assessments, minimising uncertain classifications and producing the data in a format that has the potential to be directly incorporated into specialised mine modelling software for waste scheduling / management, impact assessment and mine closure planning.

REFERENCES

DIIS (Department of Industry, Innovation and Science) (2016) Preventing Acid and Metalliferous Drainage: Leading Practice Sustainable Development Program for the Mining Industry. May 2016.

Table 1. **Extract from an AMDact report showing one of the tables providing a breakdown of AMD potential across the various sampled lithologies.**

Sample Details		AMD Risk Classification - No. of Samples											
		General Classification			Detailed Classification							Totals	
					Potential Acid Forming (PAF)				Non-Acid Forming (NAF)		Not Classified		
Sample Type	Sample Sub-Type	Potential Acid Forming (PAF)	Non-Acid Forming (NAF)	Not Classified	High Potential for Acid Generation	Moderate / High Potential for Acid Generation	Moderate Potential for Acid Generation	Low Potential for Acid Generation	Unlikely to be Acid Generating	Likely to be Acid Consuming	Insufficient, Inconsistent, Ambiguous Data	Sub-total (lithology)	Sub-total (mine material type)
Ore	Altered Volcanic	71	2	1	9	35	19	8	2	0	1	**74**	**91**
	Sulfides	15	0	2	14	1	0	0	0	0	2	**17**	
Waste Rock	Altered Volcanic	32	19	4	2	5	10	15	17	2	4	**55**	**99**
	Metasediments	16	20	0	0	5	6	5	12	8	0	**36**	
	Regolith	0	6	0	0	0	0	0	1	5	0	**6**	
	Carbonate Rock	0	2	0	0	0	0	0	0	2	0	**2**	
Tailings	Tailings	4	6	0	4	0	0	0	6	0	0	**10**	**10**
Sub-Total		138	55	7	29	46	35	28	38	17	7	**200**	**200**

Table 2. Extract from an AMDact report extract showing the acid and metalliferous drainage / neutral metalliferous drainage / saline drainage classification of individual samples.

Sample Details			Geochemical Risk Classification			
Sample ID	Sample Type	Sample Sub-Type	AMD / ARD Risk Classification		Additional Risk Classification	
			General Classification	Detailed Classification	Neutral Metalliferous Drainage (NMD/ML)	Saline Drainage (SD)
1	Waste Rock	Altered Volcanic	NAF	Unlikely to be Acid Generating	Potential for NMD	Moderate SD Potential
2	Waste Rock	Altered Volcanic	NAF	Unlikely to be Acid Generating	Potential for NMD	Low SD Potential
3	Waste Rock	Altered Volcanic	NAF	Unlikely to be Acid Generating	Potential for NMD	Moderate SD Potential
4	Ore	Altered Volcanic	PAF	Moderate / High Potential for Acid Generation	-	Moderate SD Potential
5	Waste Rock	Altered Volcanic	PAF	Moderate Potential for Acid Generation	-	Moderate SD Potential
6	Waste Rock	Altered Volcanic	PAF	Moderate Potential for Acid Generation	-	Low SD Potential
7	Waste Rock	Altered Volcanic	Not assessed	WARNING: NAPP is greater than the MPA.	Not assessed	Not assessed
8	Waste Rock	Altered Volcanic	PAF	Low Potential for Acid Generation	-	Low SD Potential
9	Waste Rock	Metasediments	NAF	Unlikely to be Acid Generating	Unlikely to Generate NMD	Low SD Potential
10	Waste Rock	Metasediments	NAF	Unlikely to be Acid Generating	Unlikely to Generate NMD	Low SD Potential
11	Ore	Sulfides	PAF	High Potential for Acid Generation	-	High SD Potential
12	Ore	Sulfides	PAF	Moderate / High Potential for Acid Generation	-	High SD Potential
13	Ore	Altered Volcanic	PAF	Low Potential for Acid Generation	-	Low SD Potential
14	Ore	Altered Volcanic	PAF	Moderate / High Potential for Acid Generation	-	Moderate SD Potential
15	Ore	Altered Volcanic	PAF	High Potential for Acid Generation	-	High SD Potential
16	Ore	Altered Volcanic	Not assessed	Inconsistent Data	Not assessed	Not assessed
17	Waste Rock	Regolith	NAF	Unlikely to be Acid Generating	Potential for NMD	Low SD Potential
18	Waste Rock	Regolith	NAF	Likely to be Acid Consuming	Potential for NMD	Low SD Potential
19	Waste Rock	Regolith	NAF	Likely to be Acid Consuming	Unlikely to Generate NMD	Low SD Potential
20	Waste Rock	Altered Volcanic	Not assessed	WARNING: The NAG 7.0 is too low for the NAG pH.	Not assessed	Not assessed
21	Waste Rock	Altered Volcanic	PAF	Low Potential for Acid Generation	-	Low SD Potential
22	Waste Rock	Altered Volcanic	PAF	Low Potential for Acid Generation	-	Low SD Potential
23	Tailings	Tailings	NAF	Unlikely to be Acid Generating	Unlikely to Generate NMD	Low SD Potential
24	Tailings	Tailings	NAF	Unlikely to be Acid Generating	Unlikely to Generate NMD	Low SD Potential
25	Tailings	Tailings	PAF	High Potential for Acid Generation	-	High SD Potential

Assessing large mineralogical datasets for potential geochemical hazards

J.R. Taylor[A], A. Fitzpayne[B], and J. Waters[A]
[A]Earth Systems, Suite 4, 290 Salmon Street, Port Melbourne VIC 3207 Australia.
jeff.taylor@earthsystems.com.au
[B]Earth Systems Europe, Suite 2:02, Generator Building, Finzels Reach, Counterslip, Bristol BS1 6BX, UK.

The mining sector encounters a broad range of geochemical hazards that have the potential to impact both human health and the environment during operations. Assessing these hazards generally requires specialist expertise and multiple time consuming geochemical testwork procedures. One aim of these procedures is to classify the potential AMD hazard of geological materials as either potentially acid forming (PAF) or non-acid forming (NAF).

Most of the current industry-standard testwork procedures for AMD classification are designed to infer the presence of specific minerals. For example, conventional static geochemical testwork procedures use total sulfur as a proxy for the concentration of pyrite in a sample when used for acid and metalliferous drainage (AMD) risk assessments. Similarly, chromium reducible sulfur (SCr) measurements assume that all of the sulfidic sulfur is also pyrite. ANC measurements assume that only carbonate minerals are present, and that all are neutralising. Not uncommonly, these assumptions are incorrect, requiring additional chemical tests for verification (e.g. the NAG suite or ABCC). These chemical tests have been vital because the resolution of early mineralogical techniques, such as X-Ray diffraction (XRD) was insufficient to identify low concentrations of minerals. However, advances in the limits of detection, cost, and speed of mineralogical techniques, including quantitative XRD (QXRD) and hyperspectral scanning, now provide more accurate and unambiguous assessments of mineralogy, and hence the AMD hazard posed by geological materials.

Mining companies seeking to secure geological data that does not rely on human interpretation are increasingly turning to automated scanning techniques. Such techniques enable very large mineralogical datasets to be generated rapidly, leading to challenges in converting the data into usable information. An Excel-based software tool, *Impact*Scan, has been developed to rapidly and unambiguously clarify the potential physical and chemical behaviour of various geological materials based on their mineralogy. This screening tool overcomes the requirement for specialised geochemical knowledge during preliminary AMD and broader materials assessments.

With appropriate mineralogical inputs, the software has the ability to resolve potential impacts as well as resources associated with the following topics:

- Geochemistry & Water Quality:
    - AMD Classification;
    - NMD (Neutral Metalliferous Drainage) Classification;
    - Acid Neutralisation Capacity / Maximum Potential Acidity (ANC/MPA) ratio;
    - Excess ANC calculation;
    - Likely leachate pH;
    - Potential salinity impacts.
- Occupational Health & Safety:
    - Presence of potentially fibrous minerals;
    - Presence of naturally occurring radioactive minerals (NORM);
    - Potential for dust emissions;
    - Potential for silica dust.

- Greenhouse gas (CO_2) issues:
    - Potential for CO_2 emissions from mine wastes;
    - Potential for CO_2 absorption by mine wastes.
- Landform Design:
    - Clay sodicity / dispersivity;
    - Erosional stability;
    - Degree of weathering.

In addition to these potential hazards, *Impact*Scan also suggests additional industry standard testwork procedures that could assist with the further definition of the nature and extent of a hazard. Over 520 minerals are currently in the database, covering a wide range of deposit types and host rock environments. Table 1 provides an indicative extract from an *Impact*Scan report dealing with a small number of samples.

Table 1. **Indicative extract from an *Impact*Scan report showing some of the potential hazards capable of being assessed from mineralogical data.**

Sample Details			Classification of Mineral Characteristics / Potential Hazards / Resources *															Supplementary Testwork Procedures
			Water / Rock									Air			Civil / Mechanical			
Sample ID	Sample Type	Sample Sub-Type	AMD/ARD Classification	NMD Potential	ANC/MPA Ratio	Excess ANC kg $CaCO_3$ equivalent per Tonne	Naturally Occurring Radioactive Minerals (NORM)	Organic Matter	Salinity	Likely Drainage pH	Erodibility by Water	Turbidity	Erodibility by Air	Minerals with Potential Fibrous Habit	Max potential CO_2 emission kg CO_2 per Tonne sample	Sodicity / Dispersivity	Low Permeability Materials	Milling Resistance	
A-1	Waste	Siltstone	PAF	-	<1	-	-	-	Low	< 4.5	High	Mod.	Low	-	-	Mod.	Mod.	-	Static, Kinetic, NAG-Leach, GeoChem+, EC, TDS, ASLP, TSS, Turb, Rill, Pinhole, CEC, SAR, Emerson, CHPT/FHPT, Mineral, OM, PSD, SEM, XRD
A-2	Waste	Siltstone	PAF	-	<1	-	-	-	-	< 4.5	High	Mod.	Low	-	-	Mod.	Mod.	-	Static, Kinetic, NAG-Leach, GeoChem+, TSS, Turb, Rill, Pinhole, CEC, SAR, Emerson, CHPT/FHPT, Mineral, OM, PSD, SEM, XRD
A-3	Waste	Sandstone	NAF	-	-	-	-	-	Low	> 4.5	High	Mod.	Low	-	-	Mod.	Mod.	-	Static, GeoChem+, NAG-Leach, EC, TDS, ASLP, TSS, Turb, Rill, Pinhole, CEC, SAR, Emerson, CHPT/FHPT, Mineral, OM, PSD, SEM, XRD
A-4	Waste	Sandstone	NAF	-	>3	6.2	-	-	-	> 4.5	Mod.	Mod.	Low	-	< 0.1	Mod.	Mod.	-	GeoChem+, NAG-Leach, TSS, Turb, Rill, Pinhole, CEC, SAR, Emerson, CHPT/FHPT, Mineral, OM, PSD, SEM, XRD
A-5	Waste	Sandstone	NAF	-	-	4.1	-	-	-	> 4.5	Mod.	Mod.	Low	-	-	Mod.	Mod.	-	Static, GeoChem+, NAG-Leach, TSS, Turb, Rill, Pinhole, CEC, SAR, Emerson, CHPT/FHPT, Mineral, OM, PSD, SEM, XRD
A-6	Waste	Sandstone	NAF	-	-	8.4	-	-	-	> 4.5	High	High	Low	-	-	High	High	-	Static, GeoChem+, NAG-Leach, TSS, Turb, Rill, Pinhole, CEC, SAR, Emerson, CHPT/FHPT, Mineral, OM, PSD, SEM, XRD
A-7	Ore	Sulfide	PAF	-	<1	-	-	-	-	< 4.5	-	-	-	-	0.2	-	-	-	Static, Kinetic, NAG-Leach, GeoChem+, TSS, Turb, CEC, SAR, Emerson, CHPT/FHPT, Mineral, OM, PSD, SEM, XRD
A-8	Waste	Siltstone	NAF	-	>3	<1	-	-	-	> 4.5	Mod.	Mod.	Low	-	< 0.1	Mod.	Mod.	-	GeoChem+, NAG-Leach, TSS, Turb, Rill, Pinhole, CEC, SAR, Emerson, CHPT/FHPT, Mineral, OM, PSD, SEM, XRD
A-9	Waste	Siltstone	NAF	-	>3	<1	-	-	-	> 4.5	-	-	-	-	< 0.1	-	-	-	GeoChem+, NAG-Leach, TSS, Turb, CEC, SAR, Emerson, CHPT/FHPT, Mineral, OM, PSD, SEM, XRD

Improved predictions of Acid and Metalliferous Drainage for Greenfield projects

W. Zhang[A], M. Edraki[B], and R. Green[C]
[A]Research fellow, The University of Queensland, Brisbane, QLD, 4072. wenqiang.zhang@uq.edu.au
[B]Professor, The University of Queensland, Brisbane, QLD, 4072.
[C]Principal Environmental Geochemist, Rio Tinto, Brisbane, QLD, 4000.

1.0 INTRODUCTION

Extrapolating predictions of acid and metalliferous drainage (AMD) from laboratory to the field face significant challenges due to the heterogeneity of waste rock dumps (WRDs), encompassing variations in particle size distribution, geochemical and hydrological properties of rock fragments, control of experimental conditions and duration, and lack of input parameters reference for numerical models. For greenfield mine sites where the design of WRDs is not finalised, these challenges are further compounded beyond the shortcomings of industry-standard procedures for AMD predictions. Therefore, it is necessary to develop appropriate methods for systematic AMD predictions for greenfield sites. This study investigates how closely the hydrological conditions of waste rock dumps, such as intrinsic permeability, liquid-to-solid ratio, and residence time, can be simulated in the laboratory to derive WRD design parameters.

2.0 MATERIALS AND METHODS

The case study focuses on a greenfield copper-gold deposit in a semi-arid region. Around 50 kg of drilled core samples from the mafic and metasediment rock units at the greenfield site were packed in trays and transported to The University of Queensland (UQ) with a cooling system. Given that the waste rock dump (WRD) has not been built yet, the drilled rock cores are the only available samples from the site to assess the AMD potential of the prospective dump materials. 10 kg of the core samples were selected for mineralogical analysis and geochemical static tests. The rest of the core samples were crushed to < 15 mm using a Boyd crusher for the standard compaction and the column leaching tests. The quantitative X-ray diffraction (QXRD) analysis result of the mixed drill core sample is summarised in Table 1. The main lithologies consist of metasediments (sandstone, siltstone) and mafic rocks with varying mineralogy. Sulfide content of the sample is about 2.16 %. Silicates, such as muscovite, the biotite group, hornblende, and chlorite, provide some neutralising capacity at low reaction rates, while carbonates (e.g. calcite) mainly offer neutralising capacity. The acid-base accounting (ABA) test shows that the maximum potential acidity (MPA) of the mixed sample is 63 kg H_2SO_4/t and the acid neutralising capacity (ANC) is 25.2 kg H_2SO_4/t. So the net acid production potential (NAPP) of the mixed sample is 37.8 kg H_2SO_4/t. Given that the net acid generation (NAG) pH is 2.6 and a positive NAPP value, the mixed sample can be classified as a potentially acid-forming (PAF) material (AMIRA, 2002).

The particle size distribution (PSD) of the crushed sample is shown in Fig. 1. From the PSD curve, D_{10}, D_{30} and D_{60} were 0.85 mm, 4mm and 6.5 mm, respectively, suggesting that the uniformity coefficient was 7.6 and the coefficient of gradation was 2.9. Based on the Unified Soil Classification System (USCS), the crushed rock can be regarded as well-graded gravel (GW), indicating a coarse-sized material and poor water-holding capacity. The standard compaction results suggest the maximum dry density and optimum moisture content were 2.21 t/m^3 and 5.1%, respectively. This provides references to the compaction rates that can be achieved for the specific PSD. It is noted that the PSD of waste rock in the

field would be significantly larger than that in the laboratory, and it is unlikely to reproduce the compaction rate applied in the WRD construction due to scale limitations in the lab. However, downscaling the field PSD and compaction rate by using finer particles but with the same distributions would be an alternative method.

Conventional kinetic testing methods, such as humidity cell and AMIRA funnel leaching, are often too simplified with respect to experimental conditions. They typically lack the capability to monitor for gas (e.g. oxygen) variations, provide limited temperature control and particle sizes, and do not account for density changes of materials. To address those limitations, this study introduces newly designed kinetic leaching columns that integrate direct oxygen consumption measurements with leachate chemistry analysis and can evaluate AMD risk of the samples at different compaction rates. The column leaching apparatus was improved to withstand compaction energy, allowing the target dry density to be directly achieved within the column rather than transferring the compacted samples from other devices. The dimensions of the column are 150 mm in diameter and 200 mm in height, which is suitable for the crushed sample with a maximum particle size of 15 mm to minimise edge effects.

Oxygen consumption is always a key parameter to assess the oxidation of pyrite, which is a dominant reaction in AMD generation. While previous studies also indicated the importance of carbonates and silicates in providing acid-buffering/neutralising capacity within waste materials (Schoen et al., 2023), which can be evaluated by the release of CO_2 in the waste products (for carbonates) and leachate solution chemistry (for silicates such as biotite, chlorite and muscovite). So, in addition to leachate collection, the improved column leaching apparatus was equipped with a sensor case that contained an O2-A3 oxygen sensor and an IRC-A1-CO2-A-NDIR sensor from Alphasense® to monitor variations in both O_2 and CO_2 concentrations in the well-sealed column. The two types of sensors were calibrated using sealed bottles containing known concentrations of O_2 and CO_2, and temperature compensation was applied to the readings when the experimental temperature changed. The two sensors were installed in a case above the top of the column and connected to a 3-way ball valve, which was integrated with a timer. Gas concentrations in the column were measured at four-time intervals over a 24-hour period: 3 AM, 9 AM, 3 PM, and 9 PM, with each measurement lasting 45 minutes. During the measurements, the channel between the sensor case and the column was connected, allowing gas from the column to diffuse into the sensor case. After each measurement, the ball valve rotated to release the moist gas in the sensor case to the atmosphere. This process ensures that the sensors are effectively protected from humidity in the column.

According to the standard proctor compaction curve, three levels of compaction (i.e. max compaction, medium compaction and less compaction) were achieved by compacting the crushed samples with different initial moisture contents of 3%, 4% and 5.1 % (AS 1289.5.2.1: 2017). For each column, the pre-prepared sample was compacted in five equal layers using a hammer, with 25 blows applied for every 20 mm height. Once the compaction of the final layer was completed, the instrumented lid was screwed onto the top of the column to ensure it is water- and air-tight. Once all the samples were packed into the columns, silicone heat pads were applied around the column wall to control the experimental temperature, which was set to be constant at 35 °C to accelerate the chemical reaction inside the column and mitigate the impact of temperature fluctuations on sensor readings. The dry densities of the compacted samples in three columns are summarised in Table 2. Fig. 2 shows the schematic diagram of the improved kinetic leaching column.

At the beginning of each leaching cycle, half a pore volume of deionised water was pumped into the column through the inside nozzle. Additional deionized water was added to achieve one pore volume after a 14-day reaction time, and leachates were collected one day after to provide enough time for solute dissolution. Then the leachates were sampled 100 mL for filtering (45 μm) and analysed for electrical conductivity, pH, alkalinity/acidity, major cations and anions and metal concentrations.

3.0 RESULTS

The experiment has been running for over 16 leaching cycles. The gas monitoring results indicated that all three samples had significant changes in oxygen consumption, with the maximum compacted sample keeping the lowest oxygen concentration for the most leaching cycles. At the beginning of the experiment, the less compacted samples consumed more oxygen than the other two samples. After two leaching cycles, the most compacted samples started to have higher oxygen consumption than the less and medium compacted samples (Fig. 3a). Similar to the variations in oxygen concentrations, in the first two leaching cycles, the less compacted sample generated the highest amounts of CO_2, and the CO_2 sensor reading reached the upper threshold of the measurement (5000 ppm) in a short time. On the contrary, the most compacted sample had the lowest CO_2 generation (~3000 ppm) during the same period. From leaching cycles 3 to 7, CO_2 generation rates from the three samples remained high all the time with similar trends (Fig. 3b). Then, the most and medium compacted samples tend to have lower CO_2 generation rates than the less compacted sample. To evaluate the sensor measurements, direct gas sampling was conducted using syringes at the leaching cycles 12-15, and the samples were sent for gas chromatography (GC) analysis. The O_2 and CO_2 concentrations measured from GC are shown in Table 3. The oxygen results from both sensor and GC measurements matched well, while the CO_2 results from GC showed that the CO_2 concentration of the most compacted sample measured from GC was two times more than the sensor measurement. This is mainly due to the measurement capacity of the CO2 sensor is only 5000 ppm. From the leachate chemistry in Fig. 4, we found that higher compaction resulted in higher electrical conductivity in leachates, but pH fluctuated in a similar manner for the three samples. It is noted that the sample with maximum compaction had the highest sulfate release in leachates, and its Fe^{2+} concentration was 5~6 times higher than the other two samples after three leaching cycles, particularly between leaching cycles 6 and 13.

4.0 CONCLUSIONS

The new kinetic column leaching test demonstrates the capacity of the apparatus for both capturing variations in gas concentrations and tracing the release of metals and acid. It also highlights the significant impact of compaction rates on oxygen consumption and CO_2 generation. Given that the leachate valve remained closed during each leaching cycle, the experiment is considered an undrained condition. Both the gas measurements and leachate chemistry indicate that the most compacted sample had higher reaction rates than the less and medium compacted samples. This is mainly because the higher compaction results in higher water holding capacity and closer contact between solid samples, water and air in a well-sealed column. Comparison of the results helps enhance understanding of particle size and mineral liberation effects on reaction rates, and distinguish the roles of carbonates versus silicates in the neutralisation of acidity through CO_2 monitoring and leachate chemistry analysis. Although the experiment does not fully represent complex field conditions (e.g. PSD and variable ambient weather conditions), the results are still able to provide reliable reference values regarding input parameters for numerical models, e.g. hydraulic properties of the material and reaction rates under different compaction levels, unlike using estimations solely based on empirical parameters or mineralogical data. The findings contribute to not only identifying key parameters that affect the geochemical and hydrogeological performance of WRDs but also aiming to providing optimum dump designs prior to mining activities.

REFERENCES

AMIRA International (2002) ARD Test Handbook: Prediction & Kinetic Control of Acid Mine Drainage, AMIRA P387A. Ian Wark Research Institute and Environmental Geochemistry International Ltd., Melbourne. http://www.amira.com.au/documents/downloads/P387AProtocolBooklet.pdf

AS 1289.5.2.1. (2017) Methods of testing soils for engineering purposes Soil compaction and density tests - Determination of the dry density/moisture content relation of a soil using modified compactive effort. Methods of Testing Soils for Engineering Purposes, Australian Standard.

Schoen, D., Savage, R., Pearce, S., Shiimi, R., Gersten, B., Roberts, M., & Barnes, A. (2023). A novel empirical approach to measuring pore gas compositional change in mine waste storage facilities: A case study from northern Europe. In Mine Closure 2023: Proceedings of the 16th International Conference on Mine Closure. Australian Centre for Geomechanics.

Table 1. Mineralogical results of the mixed drilled core sample for column tests

Minerals	Mixed drill core (wt.%)[A]
Quartz/ SiO_2	21.34
Magnesio-ferri-hornblende	15.78
Anatase/ TiO_2	0.46
Antigorite/ $(Mg,Fe^{2+})_3Si_2O_5(OH)_4$	4.11
Pyrite/ FeS_2	2.01
Marcasite/ FeS_2	0.15
Calcite/ $CaCO_3$	0.25
Titanite/ $CaTiSiO_5$	4.06
Albite/ $NaAlSi_3O_8$	3.75
Microcline / $KAlSi_3O_8$	6.34
Clinozoisite/ $Ca_2Al_3(Si_2O_7)(SiO_4)O(OH)$	4.58
Chlorite IIb/ $(Mg,Fe)_3(Si,Al)_4O_{10}(OH)_2{\cdot}(Mg,Fe)_3(OH)_6$	4.42
Illite/Muscovite/ $KAl_2(Si_3Al)O_{10}(OH)_2$	6.5
Phengite/ $K(Al,Mg)_2(OH)_2(Si,Al)_4O_{10}$	1.8
Phlogopite/ $KMg_3AlSi_3O_{10}(F,OH)_2$	9.18
Illite-smectite mixed layer	0.51
Boehmite/ $AlO(OH)$	0.52
Amorphous phase	14.24

[A]wt.% refers to weight percentage.

Table 2. Sample mass and dry densities in three columns

Column ID	Sample height (mm)	Mass of dry sample (kg)	Dry density (kg/m^3)
Column 1 (less compaction)	100	3.42	2070.85
Column 2 (max compaction)	100	3.55	2151.88
Column 3 (medium compaction)	100	3.48	2107.90

Table 3. O_2 and CO_2 concentrations measured by gas chromatography for the direct gas samples

Leaching cycle	Column ID	CO_2 (ppm)	O_2 (mol.%)
NO.12	Column 1 (less compaction)	6123	21.105
	Column 2 (max compaction)	12643	19.97
	Column 3 (medium compaction)	7741	21.04
NO.13	Column 1 (less compaction)	2913	21.37
	Column 2 (max compaction)	9187	20.25
	Column 3 (medium compaction)	5667	21.08
NO.14	Column 1 (less compaction)	5218	21.10
	Column 2 (max compaction)	11210	20.31
	Column 3 (medium compaction)	5901	20.96
NO.15	Column 1 (less compaction)	4387	20.96
	Column 2 (max compaction)	12149	19.79
	Column 3 (medium compaction)	5809	20.86

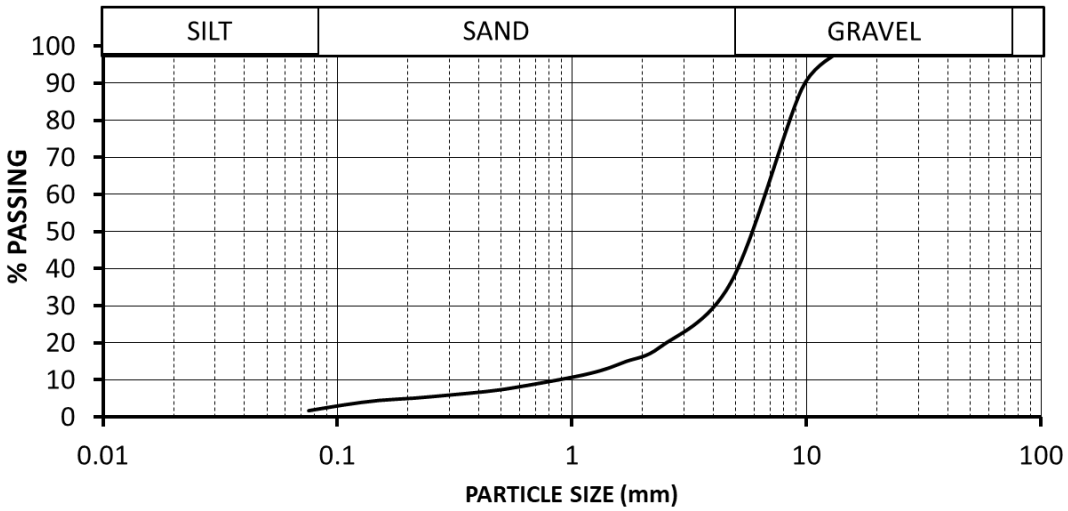

Fig.1. **Particle size distribution of the crushed drill core sample**

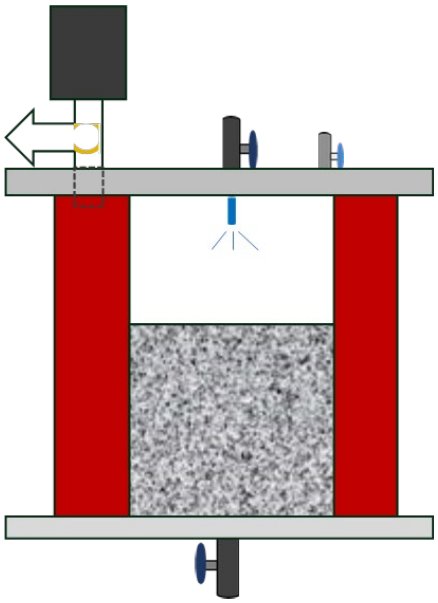

Fig.2. **Schematic diagram of the improved kinetic column leaching apparatus for different compaction rates with oxygen and carbon dioxide concentrations monitoring**

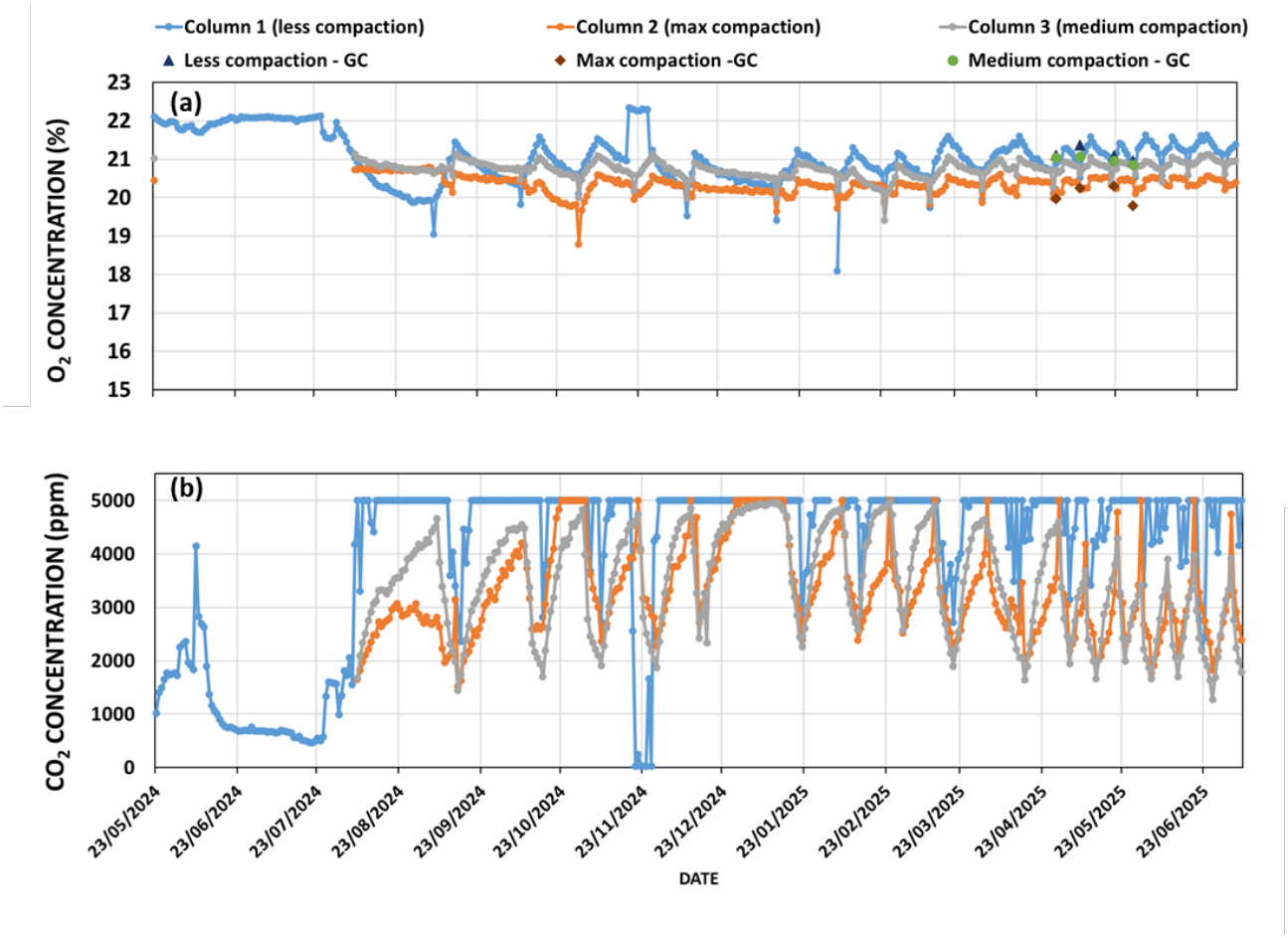

Fig.3. **Temporal changes in oxygen and carbon dioxide concentrations in three columns with different compaction rates**

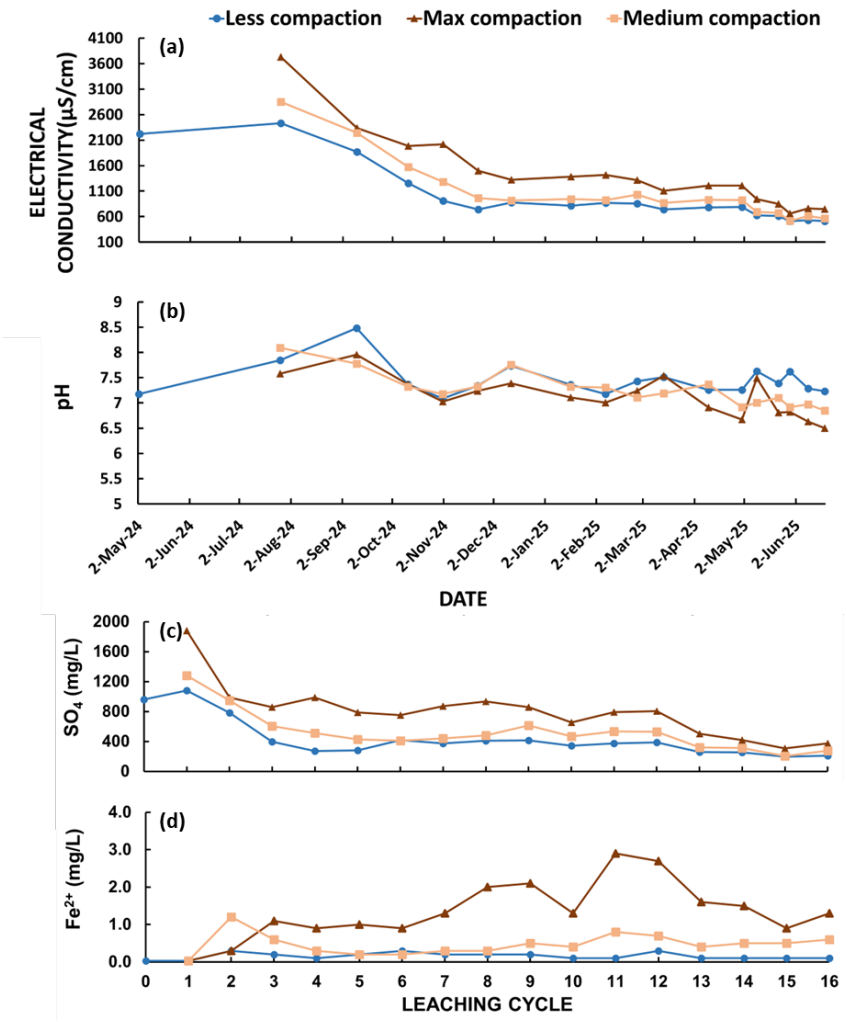

Fig.4. **Leachate chemistry data of three columns**

Turning the tide: Advanced monitoring of AMD creek at closed mine using CSIRO'S VESI™ technology

D. Caruso[A], D.S. Macedo[A], D.C. Marley[A], G. Cordery[B] , and K. Murugappan[A]
[A]CSIRO, Mineral Resources, Private Bag 10, Clayton South, Victoria, 3169, Australia.
daniella.caruso@csiro.au
[B]Sibanye Stillwater, Penghana Road, Queenstown, Tasmania, 7467, Australia

ABSTRACT

1.0 INTRODUCTION

Monitoring acid mine drainage is essential for protecting ecosystems, human health, and water resources while also supporting regulatory compliance and sustainable mining.[1] Many current techniques are labour intensive and rely on devices that require frequent maintenance, resulting in significant operational costs.

CSIRO researchers have developed Vesi™, an automated water monitoring technology featuring a robust solid-state electrochemical sensor system. It enables in-situ continuous real time parameters such as, pH, Eh/oxidation reduction potential (ORP), temperature and conductivity. At its core, Vesi™ uses CSIRO's patented solid state reference electrode (SSRE) technology, developed for durability in harsh environments. Unlike conventional liquid-filled or gel-type reference electrodes, which require regular maintenance and are prone to poisoning by high levels of sulphate/sulphide species. CSIRO's SSRE is formulated to be durable and more resistant in these conditions offering long term stability and functionality. This enables minimal upkeep and ongoing recalibration (months) in-situ continuous measuring campaigns. An infographic of the Vesi™ system is shown in Figure 1.

This paper presents a case study of Vesi™ at Sibanye Stillwater's Mt Lyell closed mine site in Tasmania. The collaborative field trial between CSIRO and Sibanye Stillwater evaluated the technology's efficacy for in-situ continuous monitoring of pH, ORP, conductivity and temperature over a 12-month period, alongside manual sampling. The purpose of the trial was to evaluate its performance and commercial suitability for monitoring AMD surface and ground water applications to make data-based decisions to mitigate impacts whilst decreasing operational costs. The system's cloud-based data management platform facilitated real-time graphical visualisation and trend analysis, contributing to the advancement of 'smart mine' technologies and sustainable mining practices.

2.0 CASE STUDY: TRIAL IN AMD CREEK AT A CLOSED MINE SITE

A Vesi™ sensor pack and system were installed at Sibanye Stillwater's Mt Lyell, closed mine site to evaluate its performance and expand its potential applications, thereby de-risking it for commercial readiness. This activity was part of a larger project funded by the Science Industry Endowment Fund (SIEF), CSIRO and three industry partners where Sibanye Stillwater (formerly Copper Mines of Tasmania) was one of the industry partners.

During the 12-month trial the Vesi™ system measured pH, ORP, conductivity and temperature continuously, while weekly manual sampling was taken to ensure data comparability. In Figure 2, an image of the location is shown.

Vesi™ data was logged at a frequency of every 10 minutes, and the measurements were stored in a cloud database and accessed via the system's software interface, where both CSIRO project team members and the client could access and visualise the graphical data remotely in real time 24/7.

Weekly comparisons between Vesi™ data and manually sampled data validated the accuracy of the automated measurements. Mine staff performed intermittent checks (monthly to quarterly) to assess the sensor pack's condition. Despite exposure to particulates and acidic conditions—where many online sensors struggle—Vesi™ showed no visible degradation or significant particulate buildup that could affect measurement accuracy. The pH calibration slope was also reviewed quarterly, and a drift was only observed at the 9-month mark, prompting recalibration. The Vesi™ data was plotted against the sampled data, and it showed good correlation. Figure 3 shows a plot of the Vesi™ pH data vs the sampled data including the rainfall during that period. The vertical line in the graph marks the initial calibration event of the pH electrode at the start of the trial. The Vesi™ pH sensor also showed sensitivity to detecting changes in pH after rainfall. This detection sensitivity gave mining staff a better understanding of real time environmental conditions of their monitoring sites assisting them to streamline their operations between sampling campaigns. Although the trial concluded after 12 months due to contractual agreements, Vesi™ showed potential for continued operation in AMD conditions beyond this period.

3.0 BENEFITS OF VESI ™ AS AUTOMATED MONITORING FOR AMD APPLICATIONS

The trial successfully demonstrated CSIRO's Vesi™ system as a proof-of-concept multi-sensor platform for in-situ, continuous monitoring of an AMD creek. It showed adequate robustness and integrated all essential components of a comprehensive monitoring solution for AMD creeks. The performance of the Vesi™ system in these conditions showed the following advantages:

Streamlined operations - less maintenance and caretaking needs.

Decreased calibration frequency - particularly valuable in challenging and remote environments.

Providing early warning alerts for issues of poor water quality – online monitoring rather than waiting for the next manual sample.

Proactive sensor management - Early detection of any sensor issues requiring intervention.

REFERENCES

CSIRO MarketPlace (2025), Vesi™ - A reliable, real time pH redox monitoring system for harsh environments, CSIRO, www.csiro.au/en/work-with-us/ip-commercialisation/Marketplace/VesiJane Nicholls (2022), Tapping into water monitoring with Vesi™ sensor technology, CSIRO, www.csiro.au/en/news/All/Articles/2022/October/water- monitoring-with-vesi-sensor-technology

Tengzhuo Zhang et al (2023) A review: The formation, prevention, and remediation of acid mine drainage. *Environmental Science and Pollution Research,* **30**, pages 111871-111890.

LIST OF FIGURES

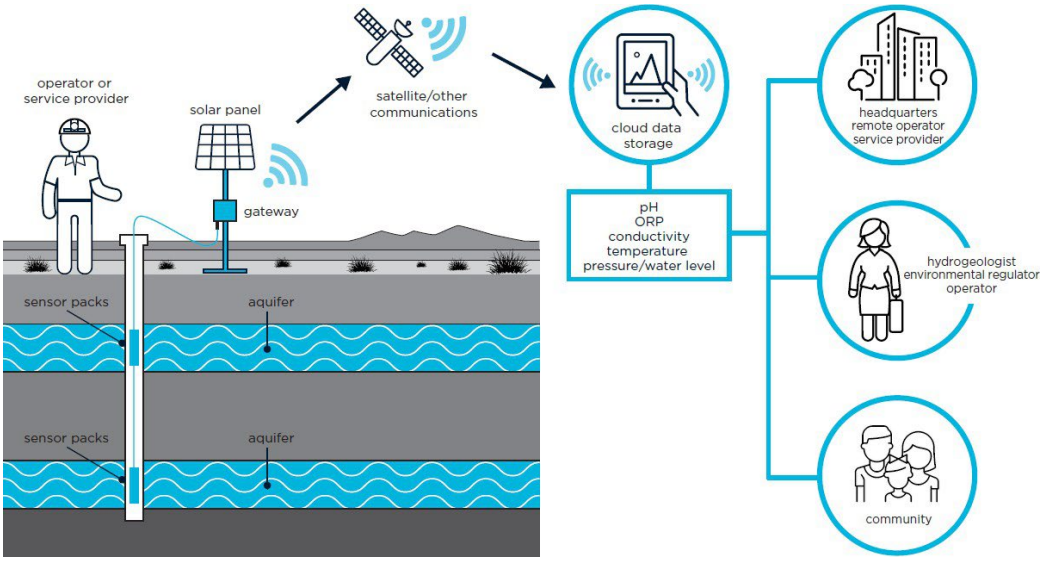

Fig.1. **Infographic of CSIRO's Vesi™ automated water quality monitoring technology**

Fig.2. **Image of Vesi™ sensor technology installed in AMD creek during the trial**

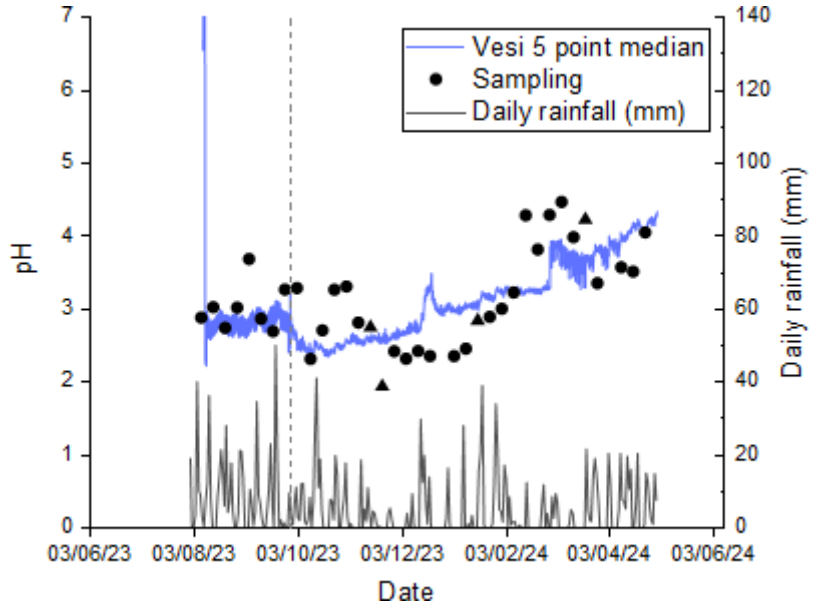

Fig.3. **Plot of Vesi pH data (blue line) vs pH sampled data (black dots). Black line is daily rainfall**

From microstructure to macroimpact: The critical role of permeability-tortuosity-porosity model in predicting Acid Mine Drainage from Mine Waste

W. Cao[A], M. Edraki[B], H. Hofmann[C], and A. Scheuermann[D]
[A]Sustainable Minerals Institute, The University of Queensland, Brisbane QLD 4072.
wenran.cao@uq.edu.au
[B]Sustainable Minerals Institute, The University of Queensland, Brisbane QLD 4072
[C]Environment, Commonwealth Scientific and Industrial Research Organisation (CSIRO), Brisbane QLD 4102
[D]School of Civil Engineering, The University of Queensland, Brisbane QLD 4072

ABSTRACT

This study presents a reactive transport model that dynamically integrates the interdependent relationships between permeability (k), tortuosity (τ), and porosity (ϕ) in response to mineral dissolution, precipitation, and structural reconfiguration. The model captures critical feedback mechanisms between geochemical processes—such as mineral dissolution and precipitation—and evolving transport properties. This approach is essential for identifying when and where permeability reductions trigger pore clogging, oxygen depletion, or the development of preferential flow paths, all of which govern the initiation and persistence of acid mine drainage.

2.0 INTRODUCTION

Mining activities, while economically essential (Onifade et al., 2023), often result in significant environmental impacts—most notably through the accumulation of mine waste, including waste rock and tailings (Nassar et al., 2022; Ódri et al., 2020). These by-products are not chemically inert; rather, they undergo complex physical and geochemical changes over time (Davies et al., 2011; Kusi et al., 2024). One of the most persistent consequences is acid mine drainage (AMD), a phenomenon characterised by the release of acidic, metal-rich waters into surrounding environments (Bussière and Guittonny, 2020; Lim et al., 2024). The generation of AMD is driven by the exposure of sulfide-bearing minerals to atmospheric oxygen and water, triggering a series of oxidation reactions that mobilise contaminant metals (Muniruzzaman et al., 2021; Welivitiya and Hancock, 2024).

The challenge In managing AMD lies not only In Its chemical aggressiveness but also In Its longevity (Bao et al., 2020; Kusi et al., 2024). Once initiated, AMD can continue for decades or even centuries, posing long-term risks to water quality and ecosystems (Vriens et al., 2020). This makes AMD a critical issue in mine closure planning and post-mining land use. Traditional prediction methods have largely relied on empirical models or simplified conceptual frameworks, which often fail to represent the complex interactions among fluid flow, solute transport, and geochemical reactions within the heterogeneous structure of mine waste (Baqer and Chen, 2022; Cao et al., 2024c). Consequently, there is increasing recognition of the need for mechanistic, process-based models that better reflect the dynamic and evolving nature of mine waste environments.

A particularly important aspect of this evolution is the dynamic relationship between permeability (k), tortuosity (τ), and porosity (ϕ)—three interdependent properties that control fluid flow and solute transport in porous media such as tailings storage facilities. These properties evolve in response to physical compaction and geochemical reactions, such as mineral dissolution and precipitation.

Accurately capturing how k, τ, and ϕ change over time is critical for improving predictions of AMD initiation, propagation, and potential mitigation strategies. To address this gap, the study proposes a novel k–τ–ϕ model developed through an integrated approach that combines theoretical formulation, laboratory experiment, and microstructural imaging. By upscaling the k–τ–ϕ relationships into field-scale reactive transport models, the framework enables more accurate predictions of long-term contaminant release and supports robust decision-making in mine hydrogeochemical management.

2.0 INTERDEPENDENCE OF k, τ, AND ϕ IN REACTIVE SYSTEMS

The hydraulic and diffusive behaviour of granular materials is fundamentally controlled by the k–τ–ϕ relationship (Seigneur et al., 2021). In non-reactive systems, these parameters are often treated as relatively stable (Sabo and Beckingham, 2021). However, in reactive environments such as mine waste repositories, they are subject to continuous alteration due to mineral dissolution and precipitation, as well as physical restructuring of the pore network (Seigneur et al., 2019). For example, an increase in porosity due to mineral dissolution does not necessarily result in higher permeability if the resulting pore structure becomes more tortuous or disconnected. In contrast, the precipitation of secondary minerals such as ferric hydroxides can clog pore throats, reducing permeability and increasing tortuosity, even if total porosity remains relatively unchanged (Cao et al., 2024b).

Porosity (ϕ) represents the volume fraction of void space, which evolves through the competing effects of mineral dissolution and precipitation. Dissolution processes contribute positively to porosity, whereas precipitation processes contribute negatively by depositing solids into the pore space. Hence, the net porosity evolution driven by geochemical reactions can be expressed as (Steefel et al., 2015):

$$\frac{d\emptyset}{dt} = \sum_i V_i \cdot R_i \qquad [1]$$

where i is the index over reacting minerals, V_i is the molar volume of mineral i (L mol^{-1}), and R_i is the reaction rate of mineral i (mol L^{-1} s^{-1}).

The rate of a mineral reaction—either dissolution or precipitation—per unit volume of porous media is commonly expressed as (Seigneur et al., 2019):

$$R_i = A_i \cdot k_i \cdot f_i\left(c_j, T, pH\right) \qquad [2]$$

where A_i is the effective reactive surface area per unit volume of porous media (m^2 L^{-1}), k_i is the intrinsic rate constant for mineral i (mol m^{-2} s^{-1}), and $f_i(c_j, T, Ph)$ is the reaction rate modifier function dependent on solute concentrations c_j (mol L^{-1}), temperature (T), Ph, and the degree of saturation.

Microstructural imaging analysis shows that reactive surface area can evolve dynamically during mineral reactions: it tends to increase during precipitation (Zhao et al., 2023), but decrease during dissolution or when primary minerals become coated with secondary precipitates (Emmanuel, 2022). A widely used empirical relationship to describe this evolution is (Pavuluri et al., 2022):

$$A_i = A_{i,0} \cdot \left(\frac{\varphi_i}{\varphi_{i,0}}\right)^w \qquad [3]$$

where $A_{i,0}$ is the initial reactive surface area (m^2 L^{-1}), φ_i and $\varphi_{i,0}$ are the current and initial volume fractions of mineral I, respectively, and w is an empirical fitting exponent.

The term f_i follows a saturation-dependent kinetic expression of the form (Appelo and Postma, 2010):

$$f_i = \left(\prod_j c_j^{n_j} \right) \cdot \left(1 - \frac{Q_i}{K_{eq,i}} \right) \quad [4]$$

where n_j is the reaction order with respect to species *j*, Q_i is the ion activity product of the reaction (mol^n L^{-n} depends on reaction), $K_{eq,i}$ is the equilibrium constant for the mineral reaction (mol^n L^{-n}).

By integrating these equations over time and space, it is possible to simulate the dynamic pore network, which in turn influences both tortuosity (τ) and permeability (k). τ describes the complexity of flow paths, while k reflects the medium's ability to transmit fluids. Based on a conceptual model of spherical particles, the τ–ϕ relationship can be derived using Archie's Law, while the corresponding k can be achieved by upscaling the Hagen–Poiseuille equation (Cao et al., 2024b):

$$\tau = \emptyset F = \emptyset^{1-m} \quad [5]$$

$$k = \frac{d^2}{72\tau^2} \frac{\emptyset^3}{(1-\emptyset)^2} \quad [6]$$

where F is the formation factor, m is the cementation exponent obtained experimentally or numerically, and d is the mean diameter of solid particles (m).

Capturing the interactive mechanism among these parameters is essential for understanding how AMD evolves over time and space. It also offers insight into the formation of preferential flow paths, and the potential for self-regulating behaviour in certain mine waste materials.

3.0 COUPLED MODELLING: BRIDGING GEOCHEMISTRY AND HYDRODYNAMICS

In natural environments with strong redox gradients and iron-rich groundwater, Fe(II) is oxidised by dissolved oxygen and then precipitates as iron oxides beneath the soil surface (Wang et al., 2024). This oxidative precipitation forms a geochemical barrier that can lead to complete pore-clogging within the porous media (Cao et al., 2024a), presenting significant challenges for numerical modelling. Recent advances in computational tools—such as *porousMedia4Foam*—have facilitated the integration of reactive transport processes with evolving k–τ–ϕ relationships. This coupled modelling framework offers a more realistic representation of porous media behaviour over time. Validation of the model was conducted through a combination of column experiments (Cao et al., 2024b), laboratory-scale observations (Cao et al., 2025b), and microstructural imaging techniques (Cao et al., 2025a), including scanning electron microscope (SEM) and micro-computed tomography (micro-CT).

As evidenced by the spatiotemporal variations in porosity and permeability linked to changes in mineral volume fractions and outflow rates (see Fig. 1), the proposed model offers a robust method for quantifying the early stages of geochemical barriers associated with iron precipitation. It also provides critical insights into the temporal evolution of pore structure, thereby enhancing our understanding of complex fluid–pore–solid interactions. These findings deliver practical implications for managing diverse hydrogeological systems, including those associated with AMD. Moreover, the integration of experimental observations with model simulations enables the identification of key thresholds that govern system transitions, such as the preferential flow paths due to physical heterogeneity.

4.0 APPLICATIONS IN AMD PREDICTION AND REMEDIATION DESIGN

The integration of k–τ–ϕ dynamics into reactive transport models has opened promising avenues for both predictive analysis and practical remediation strategies in mine waste management. By capturing the temporal evolution of hydraulic and diffusive properties in porous media, these models improve the accuracy of forecasts concerning contaminant release over time. Beyond predictive capabilities, this modelling approach offers actionable insights for the design and optimisation of engineered systems. In particular, a deeper understanding of evolving flow paths and reactive zones supports the strategic design of cover systems or surface compacted layers that are aimed at reducing oxygen ingress and water infiltration—two principal drivers of sulfide oxidation.

Additionally, coupled k–τ–ϕ models provide a solid foundation for environmental risk assessment. An example of this approach is demonstrated through field-scale simulations using TOUGHREACT, which capture the spatiotemporal evolution of key geochemical indicators such as Ph, oxygen, sulfate, Fe(II), and Fe(III) concentrations (see Fig. 2). These simulations illustrate the progressive development of AMD as reactive sulfide minerals interact with oxygen and water, thereby quantifying both the mechanistic pathways and environmental risks involved. The findings highlight the persistent nature of AMD, which is increasingly recognised as one of the most pressing global environmental challenges after climate change in terms of its longevity and ecological impact.

5.0 SUMMARY AND PROSPECT

The environmental risks associated with AMD are fundamentally tied to the complex interplay between geochemical reactions and the evolving physical structure of mine waste materials. Effectively addressing these risks requires more than empirical observation—it demands a mechanistic understanding of how permeability, tortuosity, and porosity interact and evolve under reactive conditions. Coupled reactive transport models that incorporate the interactive mechanisms represent a significant advance to simulate and manage AMD generation and migration. As the mining sector transitions toward more sustainable and accountable practices, such models will become increasingly vital for guiding remediation strategies, supporting regulatory decisions, and protecting ecosystems and communities from the long-term impacts of mine waste.

One of the major challenges in this field is scaling up insights from laboratory experiments and pilot-scale studies to real-world, full-scale mine waste facilities. The inherent heterogeneity of waste materials, site-specific climatic conditions, and extended timescales of hydrogeological regimes complicate such efforts (Opitz et al., 2016). Nevertheless, several promising research directions are emerging: (1) Multiscale modelling approaches to link pore-scale geochemical processes with field-scale hydrogeological behaviour; (2) Machine learning and data assimilation techniques to improve model calibration, parameter optimisation, and uncertainty quantification; (3) Integration with geophysical monitoring and remote sensing tools to detect and interpret in situ changes in structural properties, moisture content, heat anomalies, and geochemical signatures.

A particularly promising frontier lies in understanding the role of microbial activity in modulating k–τ–ϕ relationships. By embracing the interconnected nature of physical, chemical, and biological interactions, we can better anticipate long-term environmental responses and develop more robust, adaptive strategies for sustainable mine waste and groundwater management.

ACKNOWLEDGEMENTS

This research was funded by the Australian Research Council through a Future Fellowship (FT180100692) awarded to Professor A. Scheuermann, and supported by the Australian Coal Association Research Program Project (C35021) under the leadership of Professor M. Edraki.

REFERENCES

Appelo, C.A.J., Postma, D., 2010. Geochemistry, groundwater and pollution, 2nd ed., 5th corr. repr. ed. CRC Press, Boca Raton.

Bao, Z., Bain, J., Holland, S.P., Wilson, D., MacKenzie, P., Ptacek, C.J., Blowes, D.W., 2020. Faro Waste Rock Project: Characterizing geochemical heterogeneity in sulfide- and carbonate-rich waste rock. Applied Geochemistry 121, 104691. https://doi.org/10.1016/j.apgeochem.2020.104691

Baqer, Y., Chen, X., 2022. A review on reactive transport model and porosity evolution in the porous media. Environ Sci Pollut Res 29, 47873–47901. https://doi.org/10.1007/s11356-022-20466-w

Bussière, B., Guittonny, M., 2020. Hard Rock Mine Reclamation: From Prediction to Management of Acid Mine Drainage, 1st Edition. ed. CRC Press, Boca Raton.

Cao, W., Hofmann, H., Yan, G., Scheuermann, A., 2024a. Porewater exchange and iron transformation in a coastal groundwater system: a field investigation, driving mechanisms analysis, and conceptual model. Front. Mar. Sci. 11. https://doi.org/10.3389/fmars.2024.1385517

Cao, W., Hu, N., Yan, G., Hofmann, H., Scheuermann, A., 2024b. Permeability–porosity model considering oxidative precipitation of Fe(II) in granular porous media. Journal of Hydrology 636, 131346. https://doi.org/10.1016/j.jhydrol.2024.131346

Cao, W., Strounina, E., Hofmann, H., Scheuermann, A., 2025a. Discernible Orientation for Tortuosity During Oxidative Precipitation of Fe(II) in Porous Media: Laboratory Experiment and Micro-CT Imaging. Minerals 15, 91. https://doi.org/10.3390/min15010091

Cao, W., Yan, G., Hofmann, H., Scheuermann, A., 2025b. A Novel Permeability–Tortuosity–Porosity Model for Evolving Pore Space and Mineral-Induced Clogging in Porous Medium. Geotechnics 5, 2. https://doi.org/10.3390/geotechnics5010002

Cao, W., Yan, G., Hofmann, H., Scheuermann, A., 2024c. State of the Art on Fe Precipitation in Porous Media: Hydrogeochemical Processes and Evolving Parameters. JMSE 12, 690. https://doi.org/10.3390/jmse12040690

Davies, H., Weber, P., Lindsay, P., Craw, D., Peake, B., Pope, J., 2011. Geochemical changes during neutralisation of acid mine drainage in a dynamic mountain stream, New Zealand. Applied Geochemistry 26, 2121–2133. https://doi.org/10.1016/j.apgeochem.2011.07.010

Emmanuel, S., 2022. Modeling the effect of mineral armoring on the rates of coupled dissolution-precipitation reactions: Implications for chemical weathering. Chemical Geology 601, 120868. https://doi.org/10.1016/j.chemgeo.2022.120868

Kusi, J.K., Foli, G., Peasah, M.Y., Akoto, O., 2024. Geochemical characterization of waste rock dump and its potential to predict acid mine drainage. Scientific African 26, e02350. https://doi.org/10.1016/j.sciaf.2024.e02350

Lim, J., Sylvain, K., Pabst, T., Chung, E., 2024. Effect of waste rock particle size on acid mine drainage generation: Practical implications for reactive transport modeling. Journal of Contaminant Hydrology 267, 104427. https://doi.org/10.1016/j.jconhyd.2024.104427

Muniruzzaman, M., Karlsson, T., Ahmadi, N., Kauppila, P.M., Kauppila, T., Rolle, M., 2021. Weathering of unsaturated waste rocks from Kevitsa and Hitura mines: Pilot-scale lysimeter experiments

and reactive transport modeling. Applied Geochemistry 130, 104984. https://doi.org/10.1016/j.apgeochem.2021.104984

Nassar, N.T., Lederer, G.W., Brainard, J.L., Padilla, A.J., Lessard, J.D., 2022. Rock-to-Metal Ratio: A Foundational Metric for Understanding Mine Wastes. Environ. Sci. Technol. 56, 6710–6721. https://doi.org/10.1021/acs.est.1c07875

Ódri, Á., Becker, M., Broadhurst, J., Harrison, S., Edraki, M., 2020. Stable Isotope Imprints during Pyrite Leaching: Implications for Acid Rock Drainage Characterization. Minerals 10, 982. https://doi.org/10.3390/min10110982

Onifade, M., Said, K.O., Shivute, A.P., 2023. Safe mining operations through technological advancement. Process Safety and Environmental Protection 175, 251–258. https://doi.org/10.1016/j.psep.2023.05.052

Opitz, J., Edraki, M., Baumgartl, T., 2016. The Effect of Particle Size and Mineral Liberation on the Acid Generating Potential of Sulphidic Waste Rock. GEEA 16, 245–252. https://doi.org/10.1144/geochem2015-385

Pavuluri, S., Tournassat, C., Claret, F., Soulaine, C., 2022. Reactive Transport Modeling with a Coupled OpenFOAM®-PHREEQC Platform. Transp Porous Med 145, 475–504. https://doi.org/10.1007/s11242-022-01860-x

Sabo, M.S., Beckingham, L.E., 2021. Porosity-Permeability Evolution During Simultaneous Mineral Dissolution and Precipitation. Water Resources Research 57. https://doi.org/10.1029/2020wr029072

Seigneur, N., Mayer, K.U., Steefel, C.I., 2019. Reactive Transport in Evolving Porous Media. Reviews in Mineralogy and Geochemistry 85, 197–238. https://doi.org/10.2138/rmg.2019.85.7

Seigneur, N., Vriens, B., Beckie, R.D., Mayer, K.U., 2021. Reactive transport modelling to investigate multi-scale waste rock weathering processes. Journal of Contaminant Hydrology 236, 103752. https://doi.org/10.1016/j.jconhyd.2020.103752

Steefel, C.I., Appelo, C.A.J., Arora, B., Jacques, D., Kalbacher, T., Kolditz, O., Lagneau, V., Lichtner, P.C., Mayer, K.U., Meeussen, J.C.L., Molins, S., Moulton, D., Shao, H., Šimůnek, J., Spycher, N., Yabusaki, S.B., Yeh, G.T., 2015. Reactive transport codes for subsurface environmental simulation. Comput Geosci 19, 445–478. https://doi.org/10.1007/s10596-014-9443-x

Vriens, B., Plante, B., Seigneur, N., Jamieson, H., 2020. Mine Waste Rock: Insights for Sustainable Hydrogeochemical Management. Minerals 10, 728. https://doi.org/10.3390/min10090728

Wang, T., Zhang, C., Ma, Y., Hofmann, H., Li, C., Zhao, Z., 2024. Numerical analysis of the abiotic formation and distribution of the “iron curtain” in subterranean estuaries. Environmental Modelling & Software 171, 105894. https://doi.org/10.1016/j.envsoft.2023.105894

Welivitiya, W.D.D.P., Hancock, G.R., 2024. Quantifying mine waste rock physical weathering rate and processes for improved geomorphic post-mining landforms. Geomorphology 463, 109357. https://doi.org/10.1016/j.geomorph.2024.109357

Zhao, Z., Zhang, C., Cao, W., Hofmann, H., Wang, T., Li, L., 2023. Oxidative Precipitation of Fe(II) in Porous Media: Laboratory Experiment and Numerical Simulation. ACS EST Water 3, 963–973. https://doi.org/10.1021/acsestwater.2c00458

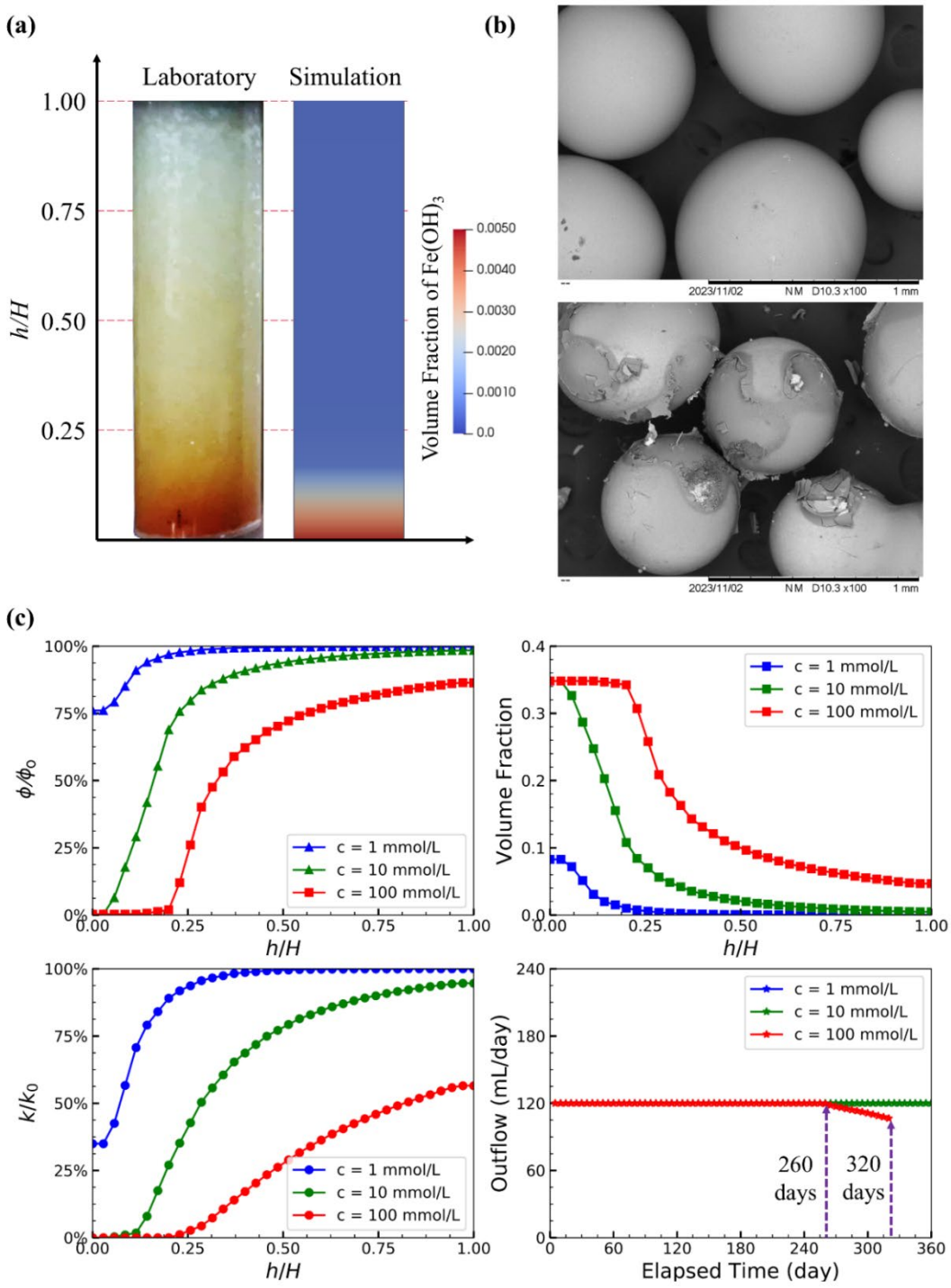

Fig. 1. **Spatial and temporal changes associated with iron precipitation processes: (a) Comparison of laboratory observations and simulation results for $Fe(OH)_3$ distribution over a 15-day period. (b) SEM images showing iron precipitates coating particle surfaces (bottom) compared to the original particles (top). (c) Temporal evolution of key parameters under multiple iron precipitation scenarios, including the relative porosity (Φ/Φ_0), $Fe(OH)_3$ volume fraction, relative permeability (k/k_0), and outflow rate over 365 days. Notes: (1) *h/H* denotes the relative height, with h measured from the column base and H being the total column height. (2) The maximum $Fe(OH)_3$ volume fraction is capped at 0.35, representing complete pore clogging.**

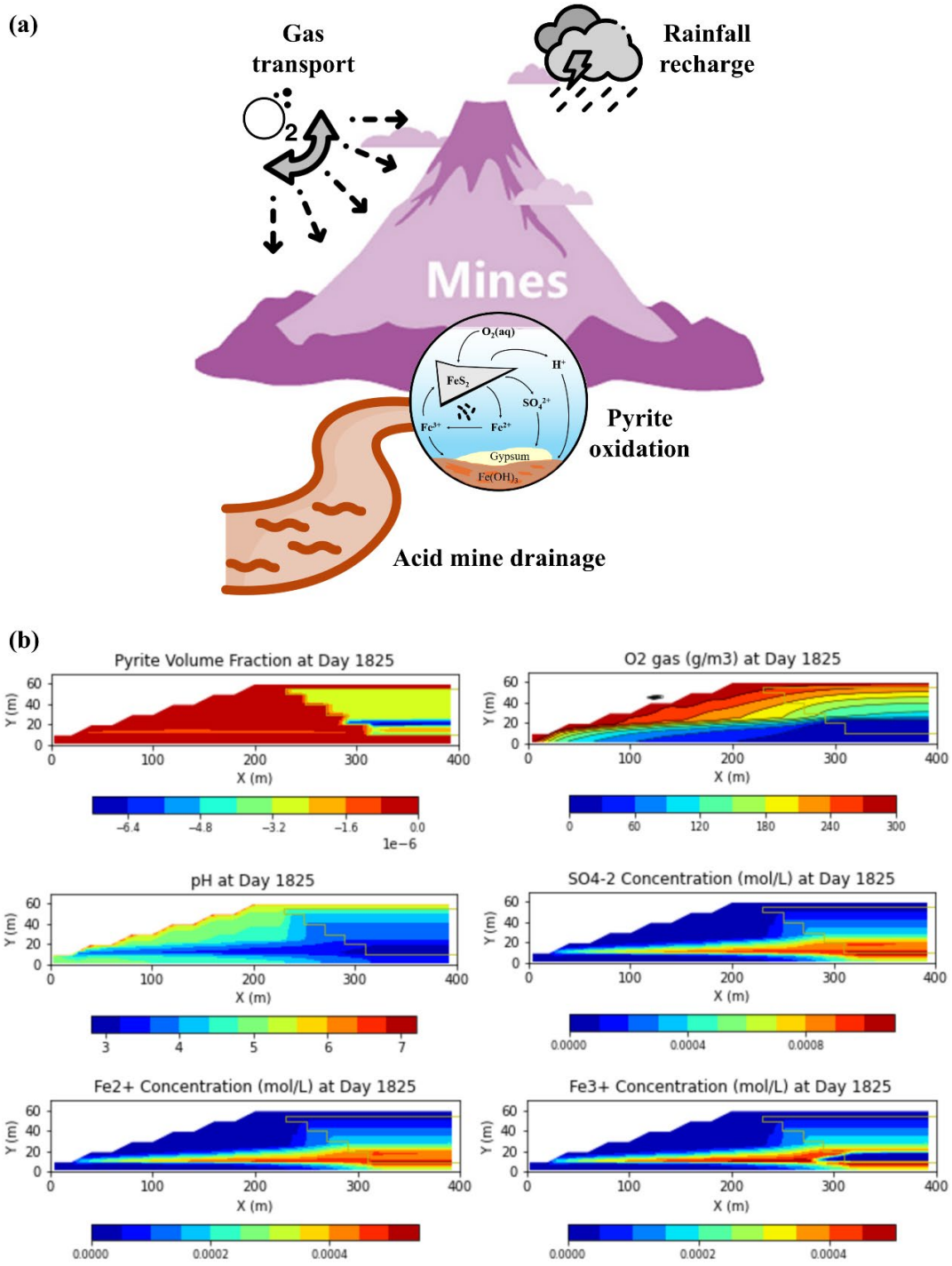

Fig. 2. **AMD generation and its spatial impacts in reactive mine waste: (a) Conceptual diagram illustrating AMD formation, highlighting the interplay between physical and geochemical processes. (b) Simulated spatial distributions of key physicochemical parameters under pyrite oxidation scenarios, including pyrite volume fraction, oxygen concentration, pH, sulfate, Fe(II), and Fe(III) concentrations throughout the waste profile.**

Electrochemical treatment of acid mine drainage to manage rehabilitation and recover resources

L.D. Berry
Clean&Recover, 791 Maleny-Stanley River Rd, Wootha Qld 4552.
luke.berry@cleanandrecover.com.au

1.0 CHALLENGES OF AMD

Mining companies face significant challenges in managing and treating acid mine drainage (AMD) and other mine-influenced water. The level of contaminants in AMD far exceeds safe standards for discharge according to world and domestic water quality guidelines. AMD commonly has highly toxic contaminants such as mercury, arsenic, cadmium, cobalt, lead, and uranium.

Current AMD treatment methods include the use of lime or caustic soda to remove contaminants. These methods of treatment are costly and operationally difficult, leaving large volumes of sludge that have the potential to clog pipework and contaminate sites beyond mine closure.

Treatments with lime and caustic soda face the following challenges:

- Adding lime or caustic soda to AMD generates large volumes of sludge. The sludge carries significant water. The AMD lime treatment plant at Mt Morgan in Queensland Australia only returns 52 per cent water from its processes, with the remainder of the water trapped in the sludge or lost as part of the process, compared with over 95 per cent water return for the ElectroClear™ AMD technology.
- Lime or caustic soda treatments lock the metals present in AMD into the sludge, making them unrecoverable.
- Lime or caustic soda present risks to human health and safety during transport, storage, and handling.
- Buying and transporting lime or caustic soda to remote mine sites is costly.
- Adding lime or caustic soda to AMD has operational challenges, such as constant clogging of pipework through sludge due to poor solubility of lime and lower treated water cleanliness. This is compounded by the fact that the purity of lime is variable, making it difficult to determine how much lime to add to AMD to neutralise the AMD.
- Making hydrated lime from quick lime to add to AMD uses high volumes of fresh water.
- Making lime to treat AMD generates high volumes of CO_2.

AMD represents not just a waste and a remediation issue during mining but also an even longer-term environmental cost. AMD contains valuable elements that can be potentially reused to offset the costs of rehabilitating and treating the mine water ahead.

2.0 WORK TO TACKLE AMD

Clean&Recover partnered with Boliden, a Nordic mining company based in Sweden, to demonstrate the techno-economic feasibility of using ElectroClear™ AMD treatment technology to deal with AMD at its closed and open mine sites. The ElectroClear™ AMD technology uses electrodialysis to remove sulphates from AMD. ElectroClear™ AMD technology precipitates metals from the drainage for

commercialisation and cleans AMD water so that it can be used on-site or discharged to the environment. The key to the process is that it uses electricity rather than alkaline chemicals (such as lime or caustic soda) to neutralise the acidity in AMD and it processes the drainage with reduced residues and at lower cost to mine operators.

Boliden currently uses traditional lime treatment of AMD and other mine-influenced water to treat AMD. Boliden's goal in partnering with Clean&Recover was to lower the operational cost of water treatment and return more and cleaner water to the environment compared to current AMD treatments. Other goals include reducing carbon dioxide (CO_2) emissions generated from water treatment, reducing power costs, and improving sustainability performance.

3.0 ELECTROCLEAR™ AMD TECHNOLOGY: PILOT PLANT

Clean&Recover and Boliden partnered to test the ElectroClear™ AMD technology on the AMD impacted water at two Boliden mine-sites. Clean&Recover built and installed a pilot plant in Sweden in the second quarter of 2024 to demonstrate the technology's performance.

In the second quarter of 2024, Clean&Recover built a demonstration plant at Boliden's workshop (Figure 1).

Clean&Recover worked with Boliden's staff to demonstrate the plant on two types of AMD, conducting eight tests on AMD #1 and three tests on AMD #2 in May 2024. Data on energy use, treated water quality, amount of sludge generated, and rate of settling of the sludge were collected from all tests. The plant processed an average of 56 L hr^{-1}or 165 L hr^{-1} of AMD depending on the type of AMD.

In processing the AMD from the two Boliden sites, the ElectroClear™ AMD technology was demonstrated, compared to lime treatment across:

- Energy use
- Water cleaning and metal removal
- Reduced sludge generation and faster sludge settling
- Cost

Comments were also made on the sustainability performance of the technology.

3.1 Energy Use

Energy use is the principal operating cost of the ElectroClear™ technology. The energy use varied due to the different water chemistries in the AMD processed from AMD #1 and AMD #2. AMD #1 has more dissolved metals and sulphate than AMD #2 which affected energy use.

AMD #1 used an average of 8.9 kWh 1,000L^{-1} and as little as 7.5 kWh 1,000L^{-1}. AMD #2 used an average of 2.6 kWh 1,000L^{-1} and as little as 2.1 kWh 1,000L^{-1} in the 11 tests for the two types of AMD (Figure 2).

3.2 Water Cleaning And Metal Removal

The average percentage of metals removed over eight demonstrations for AMD #1 showed that ElectroClear™ AMD technology removed a very high percentage (between 90 per cent and 100 per cent) of most metals present in the AMD from AMD #1 (Figure 3).

Significantly, this included removal of 100 per cent of uranium (U) and over 69 per cent of sulphate (SO_4). The resulting water was suitable for discharge into the environment under local laws.

The average percentage of metals removed over three demonstrations at AMD #2 (Figure 4) also showed the removal of a very high percentage of contaminants, including close to 100 per cent uranium (U). Again, the resulting water was suitable for discharge to the environment under local laws.

3.3 Reduced Sludge Generation, Faster Sludge Settling, And Improved Sludge Characterisation

Sludge management is a major cost of lime treatment of AMD. These costs arise from the high volumes of sludge generated and its slow settling time, for example Skousen et al. (2000).

Sludge generation was significantly reduced in AMD #1 samples treated with ElectroClear™ AMD technology compared with sludge from conventional lime treatment. AMD #1 treatment generated an average of 2.79 g L^{-1} sludge, which is 20.0 per cent of the 13.9 g L^{-1} sludge generation from lime treatment (Figure 5). When considering the millions of litres of water treated daily at all of Boliden's sites, the lower sludge volume from ElectroClear™ AMD technology treatment over time, has the potential to deliver significant savings in sludge management.

Furthermore, the sludge produced from ElectroClear™ AMD technology settled much more quickly than the lime treatment sludge, leading to a much lower water holding cost (Figure 6). The ElectroClear™-treated sludge mostly settled within 20 minutes, while the lime sludge took 90 to 100 minutes to settle. The benefit of faster settling is increased throughput, less clogging from sludge, and a lower footprint and capital costs of settling infrastructure.

After lime treatment, calcium oxide and sulphur amount to 32.5 per cent of the lime sludge for AMD #1, but only around 6.4 per cent of the AMD #1 sludge and 5.0 per cent of the AMD #2 sludge from ElectroClear™ treatment. This means that the sludges from the ElectroClear™ process are higher than lime sludge in more valuable metal content, such as Al, Cu, Mg, and Zn.

Additionally, the ElectroClear™ process offers the opportunity to use pH control to separate and concentrate target metals. It can do this by controlling the rate at which the pH of the AMD is increased and separating metals that precipitate at low pHs (for example, Al, Fe) from those that precipitate at medium pHs (for example Cu, Zn, rare earths), or high pHs (for example, Mg, Mn).

3.4 Cost

The direct operating costs of the ElectroClear™ AMD technology are low, consisting mainly of the per kWh charge associated with treating the water. A comparison with the local cost of lime treatment is being undertaken with Boliden's mines.

Savings compared to lime can arise from lower chemical reagent costs, lower sludge handling costs, less clogging from gypsum generated by lime treatment, and lower labour costs.

3.5 General sustainability performance

The ElectroClear™ AMD technology prompts a more sustainable approach to AMD treatment. This is because it avoids the carbon emissions associated with the use of lime. Lime generates carbon emissions because the process of making lime from limestone involves calcinating (roasting) the

limestone, which drives off CO_2 as a byproduct. In addition, the limestone calcination process may be powered by fossil fuels, which generate additional carbon emissions.

To illustrate the size of the potential savings in carbon dioxide emissions, a 70,000 L hr^{-1} flow of acid mine drainage treated with ElectroClear™ AMD technology could, depending on the acidity of the AMD, prevent the release of 2,118 tonnes of carbon dioxide every year compared to lime treatment.

The ElectroClear™ AMD technology is suitable to be powered by solar power. Power interruptions do not damage the equipment, unlike other water treatment processes such as reverse osmosis. This further reduces the carbon footprint of the technology.

Additionally, the lime product made from roasting limestone must be hydrated, requiring high volumes of clean fresh water as input.

The ElectroClear™ AMD technology process produces water of suitable quality for either reuse on site, agricultural use, or for discharge to the environment. If the water is reused on the mine site, it can be delivered at the preferred pH of the mine site, including up to pH 10 or potentially even pH 12 depending on the case.

In addition to this, ElectroClear™ AMD technology allows for the capture of valuable resources such as metals, water, sulphuric acid, and hydrogen gas from AMD waste. In lime treatment, these resources are trapped in the sludge generated by the process and cannot be used (Table 1).

REFERENCES

Skousen, JG, Sexstone, AJ, Ziemkiewicz, PF (2000) Acid Mine Drainage Control and Treatment. In 'Reclamation of Drastically Disturbed Lands'. (ed RI Barnhisel et al.) pp. 131–168. (Agronomy Monograph No. 41, American Society of Agronomy/American Society for Surface Mining and Reclamation, Madison, WI).

Fig. 1. **Site pilot plant installed in Boliden (May 2024)**

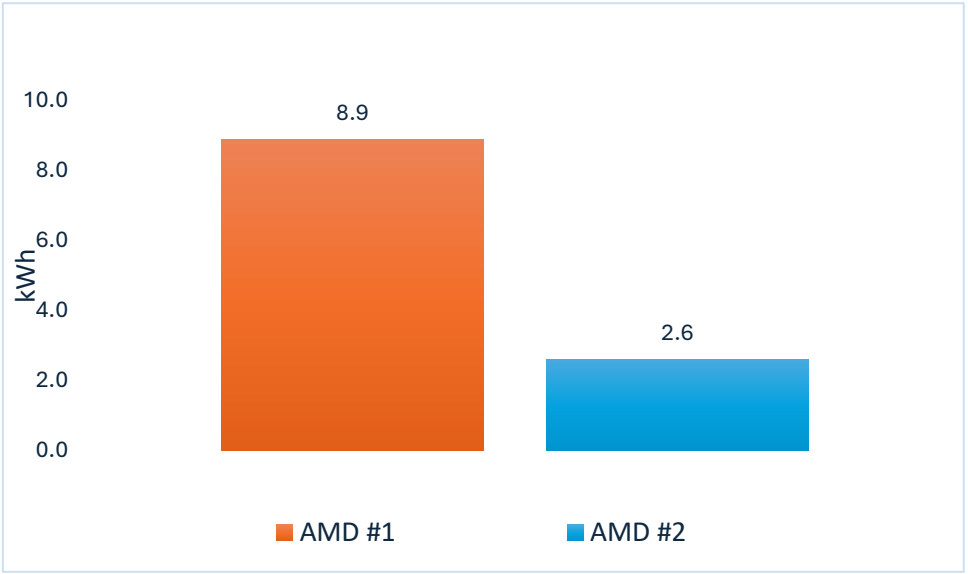

Fig. 2. **Average kWh 1,000L^{-1} for two AMD types**

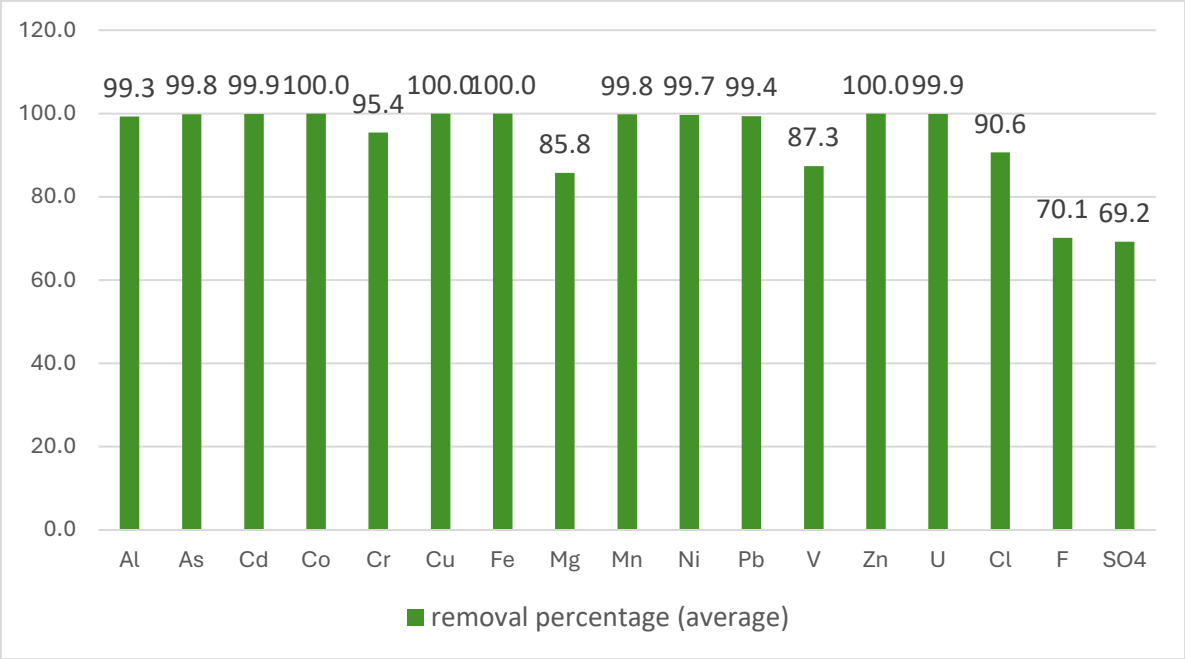

Fig. 3. **Average percentage removal over three demonstrations for AMD #1**

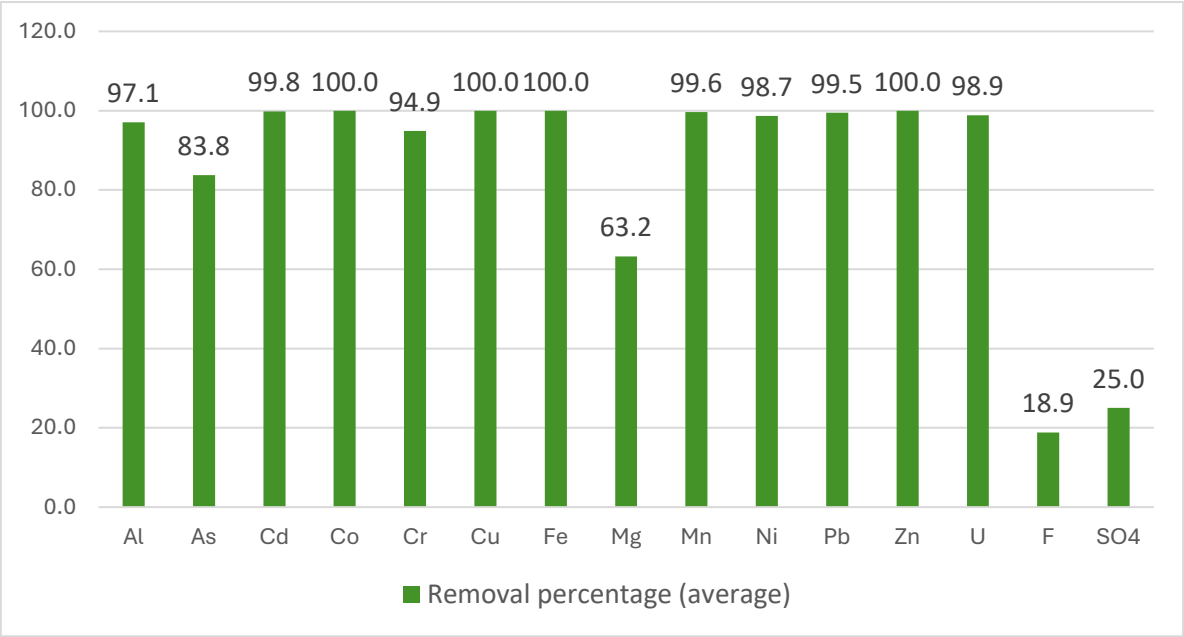

Fig. 4. **Average percentage removal over three demonstrations for AMD #2**

Fig. 5. **Sludge generation from lime treatment and ElectroClear™ processes from AMD #1**

	Lime	C&R #4-1	C&R #4-2	C&R #4-3	C&R #4-4	C&R #4-5	C&R #4-6	C&R #4-7	C&R #4-8
Dry sludge, g	13.9	2.18	2.72	2.95	3.04	3.3	2.39	2.92	NR

2L cylinder

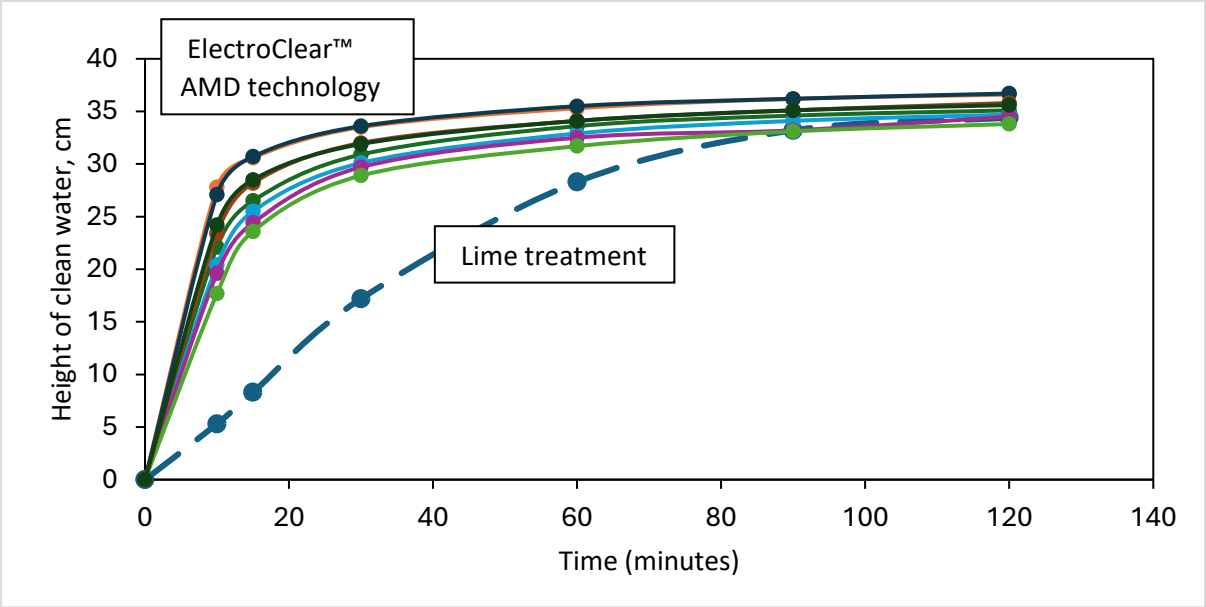

Fig. 6. **Settling rate of sludge from treatment processes**

Table 1. **Environmental benefits using ElectroClear™ AMD technology compared with lime – general case**

Environmental Benefit	Typical impact year^{-1}	Note
Carbon emissions avoided by not roasting limestone to make lime	2,118 t of CO_2	At 785 g kg^{-1} CaO
Energy saved by not making quicklime	2,379 MWh	At 3,174kj kg^{-1} CaO
Water saved by not hydrating lime	866 ML	321 g kg^{-1} CaO
Captured Metals	293 t	At 478 ppm excluding Ca, K, Na
Additional water release from ECR AMD treatment	552 ML	At 90 per cent release
Hydrogen gas from ECR AMD technology treatment	104 t	At 0.17g L^{-1}

Notes: This assumes perfect conditions for hydrating lime from quicklime and making quicklime from limestone.

Key parameters for assessing the chemical stability of coal tailings storage facilities using laboratory kinetic tests

A.O. Anumah[A], W. Zhang[A], M. Shaygan[A], G. Southam[B], M. Edraki[B]
[A]Sustainable Mineral Institute, The University of Queensland, Australia. a.anumah@uq.edu.au
[B]School of Environment, The University of Queensland, Australia

Key Words: oxygen consumption, coal tailings, acid mine drainage, microbial oxidation, particle size, carbonate buffering

1.0 INTRODUCTION

The long-term management of coal mine tailings (CMT) presents a significant challenge through the life of mine due to their potential to release AMD, including neutral and saline drainage, over extended periods of time (Baker et al., 2020; Blowes et al., 2014). While physical stability of coal tailings storage facilities (TSFs) has been widely studied (Shokouhi & Williams, 2015; Williams, 2018; Williams, 2023), chemical stability, defined as the resistance of tailings to biogeochemical transformations that mobilise contaminants, is increasingly recognised as a critical factor in environmental risk assessment. Upon deposition in the TSFS, coal tailings are subjected to complex physical/hydrological, geochemical and biological processes. These processes are influenced by intrinsic factors such as mineralogy and particle size distribution and extrinsic factors including moisture, oxygen availability, microbial activity, and temperature (Amos et al., 2015; Elghali et al., 2023; Lindsay et al., 2015; Orcutt, 2023). These parameters collectively govern solute and gas release and must be considered under realistic hydro-bio-geochemical conditions to more accurately predict long- term tailings behaviour.

Current industry-standard laboratory kinetic tests, such as the Humidity Cell Test (ASTM D5744-18), Column Test (EPA 1627/2011), British Columbia Research Confirmation Test, and Advanced Leach Columns, offer practical benefits in terms of control and cost-effectiveness (MEND, 2000; Smart et al., 2002). However, these tests often fail to replicate the synergistic effects of key environmental parameters and may misrepresent field-scale behaviour, for example, by assuming complete sulfide oxidation and neglecting buffering processes. These limitations reduce their reliability for accurately predicting acid generation rates and neutralisation potential over operational and post-closure timelines. Laboratory methods based on oxygen consumption measurements have shown promise in quantifying sulfide oxidation (Anderson et al., 1999; Bourgeot et al., 2011; Elberling et al., 1994; Hollings et al., 2001), but their application to coal tailings has been limited. Existing studies typically focus on oxygen consumption alone and rarely consider CO_2 release or microbial contributions, despite coal tailings containing carbonate minerals, macerals, and organics that can release CO_2 during oxidation. In carbonate-rich tailings, interpreting acid neutralisation potential becomes complex due to overlapping CO_2 sources and pH-buffering reactions. Furthermore, mineral associations and hydrological properties may influence gas diffusion and reactivity, particularly in low-sulfide systems where oxygen consumption does not correlate linearly with sulfide content.

This study applies a short-term, closed-system kinetic testing method to assess oxygen consumption and CO_2 release as concurrent indicators of oxidative processes in coal tailings. The aim is to improve the understanding of reaction kinetics in coal TSFs, and the results are intended to support more realistic predictions of chemical stability for mine closure planning and to promote cost-effective, holistic characterisation of reactive coal tailings.

2.0 METHODOLOGY

Fifty-four core tailings samples from Bowen Basin tailings storage facilities (TSFs) were screened based on mineralogical composition and acid-base accounting parameters. Twenty-four samples underwent detailed geochemical and hydrological characterisation. From these, eight representative samples were selected for kinetic testing to capture variations in mineralogy, moisture content, and particle size distribution. Each sample (50 g) was incubated at 10% gravimetric water content in 250 mL serum bottles at 35 °C; a range of samples was incubated at 0%, 10% and saturated Moisture content (MC). For quality control and repeatability, the samples were measured in triplicate. Gas-phase O_2 and CO_2 concentrations were analysed periodically using gas chromatography. Selected treatments included inoculation with acidophilic bacteria sourced from field samples. The mixed acidophilic bacterial culture was enumerated in the laboratory using Basal Salts [$(NH_4)_2SO_4$: 0.4 g, K_2HPO_4: 0.1 g, $MgSO_4.7H_2O$: 0.4 g, $CaCl_2.2H_2O$: 0.33 g, $FeSO_4.7H_2O$: 18 mg and dH_2O 900 ml] in acidic tailings from the study site and incubated for 21 days. The microbial density was estimated to be 1.6×10^9 cells/mL using the Most Probable Number (MPN) method (Cochran, 1950). This inoculum was introduced into selected samples to study the effect of microbial activity on oxidation kinetics. The soil water characteristic curve (SWCC) and unsaturated hydraulic conductivity (K) were evaluated through laboratory testing using desiccation and vacuum-controlled pressure methods, along with constant head permeability tests (Klute & Dirksen, 1986). SWCC parameters were derived using the van Genuchten model $\theta(\psi) = \theta_r + \frac{\theta_s - \theta_r}{(1+(\alpha\psi)^n)^m}$) (Van Genuchten, 1980; Van Genuchten et al., 1991), which relates water content to matric suction through curve-fitting parameters: residual and saturated water content (θr and θs), a scaling factor (α), and shape factors (n and m), where the air-entry value, defined as the matric suction at which air begins to enter the largest soil pores, was interpreted from the SWCC (Brooks, 1965; Fredlund & Xing, 1994).

Kinetic experiments were conducted in 250 mL serum bottles sealed with butyl rubber stoppers and submerged in a temperature-controlled water bath at 35 °C to simulate in situ conditions. For each tailings sample, 50 g of material was oven-dried to standardise initial moisture content. A calculated volume of deionised water was then added and thoroughly mixed to achieve 10% GWC, ensuring uniform distribution.

Gas concentration analysis followed a modified protocol based on Hendry et al. (1993) and Wood et al. (1993). Approximately 20 mL of gas was withdrawn regularly using a gas-tight syringe (SGE Syringe, Trajan). The extracted gas was injected into 12 mL exetainer vials and analysed at the Central Analytical Research Facility (CARF), Queensland University of Technology (QUT). Gas analysis was performed using a Shimadzu Nexus GC-2030 equipped with an AOC-6000 Plus autosampler. The GC setup included a packed ShinCarbon ST 80/100 column (2 mm inner diameter × 4 m) and a multi-detector configuration comprising a pulsed discharge detector (PDD) for O_2 and a flame ionisation detector (FID) for CO_2 and CH_4. After each sampling cycle, the serum bottles were opened briefly to re-equilibrate with atmospheric air and then resealed for the next incubation phase. Gas sampling was conducted over 14 incremental cycles: 0.00, 0.25, 0.88, 1.88, 3.88, 6.96, 11.40, 18.73, 28.77, 42.77, 63.71, 98.71, 143.71, and 198.71 days.

3.0 RESULTS AND DISCUSSION

3.1 Geochemical and Hydrophysical Properties of Coal Tailings

The selected coal tailings samples are dominated by phyllosilicate clays, primarily kaolinite, illite/mica, and illite-smectite mixed layers. Amorphous phases are most abundant in X3 (47%) and X8 (47%), and least in X4 (16.9%). Quartz is consistently present across all samples, ranging from 6% to 18%. The

major sulfide phases identified are pyrite and marcasite. Pyrite content ranges from 2.8% in X4 to 0.6% in X3 and X8, while marcasite is generally low across samples but highest in X1 (above 1%). Carbonate phases include calcite and dolomite, both present in small quantities. Siderite content ranges from above 4% in X1 and X4 to 1.3% in X8 and 2% in X3. Siderite, however, does not contribute to net neutralisation due to its tendency to oxidise and release acidity, effectively offsetting any alkalinity it may provide (Skousen et al., 1997). All samples have neutral to alkaline pH values in water extracts, ranging from 7.7 to 9.3, and moderate to saline electrical conductivity values between 272 and 1440 µS/cm. Samples are generally classified as potentially acid-forming (PAF) or uncertain. Particle size analysis indicates that the samples are predominantly silt-sized, with greater sand fractions in X3 and X8, and higher clay content in X6 and X7. Hydraulic conductivity values are moderate, near 10^{-6} m/s, typical of silty sand tailings with some fines (Woessner & Poeter, 2020). Among the samples, X3 has the highest hydraulic conductivity (5.83×10^{-6} m/s), while X7 has the lowest (8.64×10^{-7} m/s). All samples have high saturated water content ($\theta s > 0.42$ cm^3/cm^3). Air entry suction values ranged from approximately 10 to 100 are estimated at approximately 100 to 300 hPa. These values reflect differences in pore structure and compaction, which influence the onset of desaturation

3.2 Effect of Mineralogy, Particle Size, and Bacteria on Coal Tailings Oxidation (Figure 2)

Changes in oxygen and carbon dioxide concentrations over the monitoring period indicate ongoing oxidative processes within the coal tailings (Figure 2). The general trend shows that oxygen concentration consistently decreases over time for all samples (2A), while CO_2 concentration increases progressively (2C). These patterns reflect differences in chemical reactivity and gas exchange dynamics among the samples, influenced by the physical and mineralogical properties of the tailings. Sample X1, a marcasite-rich material, exhibited the steepest decline in oxygen concentration, whereas X6 and X7, which are clay-dominated with fewer sulfide minerals, maintained relatively higher oxygen levels. Marcasite, the orthorhombic polymorph of iron disulfide (FeS_2), is known to be metastable and more reactive than pyrite under oxidising conditions due to its structural defects and surface properties (Ma et al., 2025; Yao et al., 2020). Its presence at 1.1% in sample X1 suggests potential reactivity, especially in environments conducive to oxidation or phase transformation. Interestingly, samples such as X3 and X8 despite having the least amount of sulfide minerals showed faster oxygen consumption compared to more sulfide- and carbonate-rich samples. These samples were characterized by coarse textures, high hydraulic conductivity, and elevated total and organic carbon content, suggesting that oxygen consumption may be driven not only by sulfide oxidation but also by the porosity and texture of the materials. Sample X4, which contained the highest concentrations of sulfide and carbonate minerals, showed a more gradual rate of oxygen consumption and CO_2 release. This may indicate that the oxidation process is moderated by carbonate dissolution, which can buffer acidity and slow reaction rates. To better interpret reaction kinetics and standardise comparisons, oxygen and CO_2 concentrations (mol%) were converted to oxygen consumption (2B) and CO_2 release(2D) in moles using the ideal gas law. This conversion enables a more accurate assessment of acid generation potential and reaction rates based on stoichiometric and mass-balance principles, rather than relying solely on relative concentration trends.

3.3 Weight of Key parameter on OCR and CRR

The effect of key tested parameters on oxidation kinetics in coal tailings (Table 2) varies significantly in both magnitude and mechanism. Among these, moisture content is the most dominant factor influencing oxidation kinetics, regardless of mineralogical composition, organic matter, or microbial presence. In all cases, experimental results consistently showed that oxygen consumption rate (OCR)

and CO_2 release rate (CRR) were lowest under dry conditions (0% gravimetric water content, GWC), consistent with the absence of moisture required to sustain geochemical and biological oxidation. This indicates that subjecting coal tailings in TSFs to dry conditions could effectively suppress reactivity, which is a critical consideration for dry cover systems in mine closure. The 0% GWC condition used in this study represents an experimental boundary intended to isolate the influence of moisture on oxidation kinetics. While such extreme dryness is unlikely to occur under typical field conditions, especially in Australian dry covers, the results demonstrate the sensitivity of oxidation processes to moisture availability. Even minimal moisture levels (e.g., 3-5% GWC) can sustain oxidation, reinforcing the importance of moisture control in tailings management. In that dry condition, even when oxygen is physically presence in the TSF, it would remain chemically inert due to the lack of reactive aqueous pathways (Declercq & Bowell, 2019). However, moisture levels between 10-15% GWC, under both biotic and abiotic conditions, had the strongest influence on oxidation kinetics. This intermediate moisture condition represents an optimal balance where air-filled pores allow oxygen diffusion and water films enable redox exchange. Under fully saturated conditions, oxygen consumption declined due to restricted gas-phase diffusion, which becomes rate-limiting once all pore spaces are water-filled. Nevertheless, saturation had a strong effect on CRR, likely due to longer residence time for carbonate dissolution and enhanced microbial respiration.

Mineralogy ranks second in importance after moisture, with marcasite exerting a stronger influence on OCR and CRR than pyrite, and siderite contributing more significantly to CO_2 release due to its carbonate content. In samples with suitable mineralogy and moisture conditions, bacterial inoculation had the strongest effect, driving rapid oxidation and CO_2 release. This suggests that microbial mediation is dependent on favorable environmental conditions (moisture, mineralogy and PSD), and highlights its importance in mine waste risk assessments. Tailings with a 2.00 mm sieve size and optimal moisture conditions had a strong effect on OCR and CRR, likely due to improved aeration and increased reactive surface exposure. Porosity, particularly as indicated by BET surface area and pore diameter, also had a moderate to strong effect, facilitating oxygen transport and microbial colonization, thereby accelerating oxidation. For mine closure planning, this evidence reinforces the need to prioritize moisture control as the primary lever for managing tailings reactivity. Once optimal moisture conditions are established, mineralogical and microbial processes become more predictable, enabling targeted interventions to minimize long-term environmental risks.

4.0 CONCLUSIONS

A laboratory-based oxygen consumption method was used to evaluate oxidative reactivity in coal tailings from Bowen Basin TSFs. Oxidation kinetics were primarily influenced by moisture content, sulfide mineralogy, particle size, and microbial activity. Oxygen consumption peaked at 10% GWC, indicating optimal conditions for gas diffusion and aqueous-phase reactions. CO_2 release was slightly highest under saturated conditions, driven by carbonate dissolution. Marcasite-rich samples showed faster oxygen consumption, while siderite-rich samples released more CO_2 under acidic conditions. Bacterial inoculation enhanced oxidation across all samples, especially under moisture regimes that supported gas – water interactions. Physical properties such as hydraulic conductivity and air-entry value further modulated oxidation by affecting moisture retention and oxygen availability. This oxygen consumption method offers a practical tool for screening reactive materials and informing source control strategies during closure planning.

REFERENCES

Amos, R. T., Blowes, D. W., Bailey, B. L., Sego, D. C., Smith, L., & Ritchie, A. I. M. (2015). Waste-rock hydrogeology and geochemistry. *Applied Geochemistry*, *57*, 140-156.

Anderson, M., Scharer, J., & Nicholson, R. (1999). The Oxygen Consumption Method (OCM): A new technique for quantifying sulfide oxidation rates in waste rock. *Proceedings: Mining and the Environment II*.

Baker, E., Davies, M., Fourie, A., Mudd, G., & Thygesen, K. (2020). Chapter II. Mine Tailings Facilities: Overview and Industry Trends. *Towards Zero Harm: A Compendium of Papers Prepared for the Global Tailings Review*.

Blowes, D. W., Ptacek, C. J., Jambor, J. L., Weisener, C. G., Paktunc, D., Gould, W. D., & Johnson, D. B. (2014). 11.5 – The Geochemistry of Acid Mine Drainage. In H. D. Holland & K. K. Turekian (Eds.), *Treatise on Geochemistry (Second Edition)* (pp. 131-190). Elsevier. https://doi.org/https://doi.org/10.1016/B978-0-08-095975-7.00905-0

Bourgeot, N., Piccinin, R., & Taylor, J. (2011). The benefits of kinetic testwork using oxygen consumption techniques and implications for the management of sulfidic materials. Proceedings of the 7th Australian Workshop on Acid and Metalliferous Drainage (Eds. LC Bell and B. Braddock),

Cochran, W. G. (1950). Estimation of Bacterial Densities by Means of the "Most Probable Number". *Biometrics*, *6*(2), 105-116. https://doi.org/10.2307/3001491

Declercq, J., & Bowell, R. (2019). Oxygen penetration and mineral stability within the San Manuel tailings, AZ. *Geochemistry: Exploration, Environment, Analysis*, *19*(3), 255-268.

Elberling, B., Nicholson, R. V., Reardon, E. J., & Tibble, R. (1994). Evaluation of sulphide oxidation rates: a laboratory study comparing oxygen fluxes and rates of oxidation product release. *Canadian Geotechnical Journal*, *31*(3), 375-383. https://doi.org/10.1139/t94-045

Elghali, A., Benzaazoua, M., Taha, Y., Amar, H., Ait-khouia, Y., Bouzahzah, H., & Hakkou, R. (2023). Prediction of acid mine drainage: Where we are. *Earth-Science Reviews*, *241*, 104421. https://doi.org/https://doi.org/10.1016/j.earscirev.2023.104421

Hendry, M. J., Lawrence, J. R., Zanyk, B. N., & Kirkland, R. (1993). Microbial production of CO2 in unsaturated geologic media in a mesoscale model. *Water Resources Research*, *29*(4), 973-984. https://doi.org/https://doi.org/10.1029/92WR02847

Hollings, P., Hendry, M., Nicholson, R., & Kirkland, R. (2001). Quantification of oxygen consumption and sulphate release rates for waste rock piles using kinetic cells: Cluff lake uranium mine, northern Saskatchewan, Canada. *Applied Geochemistry*, *16*(9-10), 1215-1230.

Jin, Q., & Kirk, M. F. (2016). Thermodynamic and Kinetic Response of Microbial Reactions to High CO2 [Original Research]. *Frontiers in Microbiology*, *Volume 7 – 2016*. https://doi.org/10.3389/fmicb.2016.01696

Lindsay, M. B. J., Moncur, M. C., Bain, J. G., Jambor, J. L., Ptacek, C. J., & Blowes, D. W. (2015). Geochemical and mineralogical aspects of sulfide mine tailings. *Applied Geochemistry*, *57*, 157-177. https://doi.org/https://doi.org/10.1016/j.apgeochem.2015.01.009

Ma, K., Aschauer, U., & von Rohr, F. O. (2025). A combined experimental and theoretical study of the prototypical polymorphic transformation from marcasite to pyrite FeS2 [10.1039/D4DT03447C]. *Dalton Transactions*, *54*(11), 4728-4734. https://doi.org/10.1039/D4DT03447C

MEND. (2000). MEND Manual, Volume 3 - Prediction. MEND 5.4.2c, Mine Neutral Drainage Programme, Ottowa, Canada. https://mend-nedem.org/mend-report/mend-manual-volume-3-prediction/

Orcutt, H. M. (2023). *Influence of Geochemical Processes on Geotechnical Stability of Tailings Storage Facilities* (Publication Number 30566560) [M.S., Colorado State University]. ProQuest Dissertations & Theses Global. United States – Colorado.

https://www.proquest.com/dissertations-theses/influence-geochemical-processes-on-geotechnical/docview/2853762082/se-2?accountid=14723
https://resolver.library.uq.edu.au/?&genre=dissertations&sid=ProQ:&atitle=Influence+of+Geochemical+Processes+on+Geotechnical+Stability+of+Tailings+Storage+Facilities&title=Influence+of+Geochemical+Processes+on+Geotechnical+Stability+of+Tailings+Storage+Facilities&issn=&date=2023-01-01&volume=&issue=&spage=&author=Orcutt%2C+Heath+Marie
Shokouhi, A., & Williams, D. J. (2015). Settling and consolidation behaviour of coal tailings slurry under continuous loading [Text]. https://open.library.ubc.ca/collections/59368/items/1.0314307
Smart, R., Skinner, W., Levay, G., Gerson, A., Thomas, J., Sobieraj, H., Schumann, R., Weisener, C., Weber, P., Miller, S. & Stewart, W. (2002). ARD test handbook: project P387A, prediction and kinetic control of acid mine drainage. *AMIRA, Environmental Geochemistry International Ltd, Ian Wark Research Institute, Melbourne, Australia*.
Surbeck, C. Q., & Kuo, J. (2021). *Site Assessment and Remediation for Environmental Engineers*. CRC Press.
Skousen, J., Renton, J., Brown, H., Evans, P., Leavitt, B., Brady, K., Cohen, L., & Ziemkiewicz, P. (1997). *Neutralization potential of overburden samples containing siderite* (0047-2425).
Williams, D. J. (2018, 2018). *Recent advances in tailings testing methods, in Proceedings Mine Waste and Tailings Stewardship Conference* The Australasian Institute of Mining and Metallurgy: Melbourne, https://www.ausimm.com/publications/conference-proceedings/mine-waste-and-tailings-2018/recent-advances-in-tailings-testing-methods/
Williams, D. J. (2023). 17 - Management of coal tailings. In D. Osborne (Ed.), *The Coal Handbook (Second Edition)* (Vol. 1, pp. 561-589). Woodhead Publishing. https://doi.org/https://doi.org/10.1016/B978-0-12-824328-2.00008-X
Woessner, W. W., & Poeter, E. P. (2020). *Hydrogeologic properties of earth materials and principles of groundwater flow*. Groundwater Project.
Wood, B. D., Keller, C. K., & Johnstone, D. L. (1993). In situ measurement of microbial activity and controls on microbial CO2 production in the unsaturated zone. *Water Resources Research*, *29*(3), 647-659. https://doi.org/https://doi.org/10.1029/92WR02315
Yao, X., Xia, F., Deditius, A. P., Brugger, J., Etschmann, B. E., Pearce, M. A., & Pring, A. (2020). The mechanism and kinetics of the transformation from marcasite to pyrite: in situ and ex situ experiments and geological implications. *Contributions to Mineralogy and Petrology*, *175*(3), 27. https://doi.org/10.1007/s00410-020-1665-4
Zavarzina, D. G., Kochetkova, T. V., Chistyakova, N. I., Gracheva, M. A., Antonova, A. V., Merkel, A. Y., Perevalova, A. A., Chernov, M. S., Koksharov, Y. A., & Bonch-Osmolovskaya, E. A. (2020). Siderite-based anaerobic iron cycle driven by autotrophic thermophilic microbial consortium. *Scientific reports*, *10*(1), 21661.

Table 1. **Experimental Design; sample selection criterias and tested parameters**

Weight/Effect of parameters	Samples	Gravimetric Moisture Content (%)	Sieve Size	Criteria
Minerology/particle size	X1, X2, X3, X4, X5, X6, X7, X8	10	(<2mm)	Based on minerology analysis
Moisture content	X7, X6, X3,	0, 10 and full saturation	(<2mm)	Highest clay content for 3-point moisture test.
Organic content	X3, X8, X4	0 – no moisture,	<75 um	Highest total organic carbon based on SOM analysis
Microbial	X1, X3, X7	10 and 15	(<2mm)	Samples that are susceptible to bacteria activity

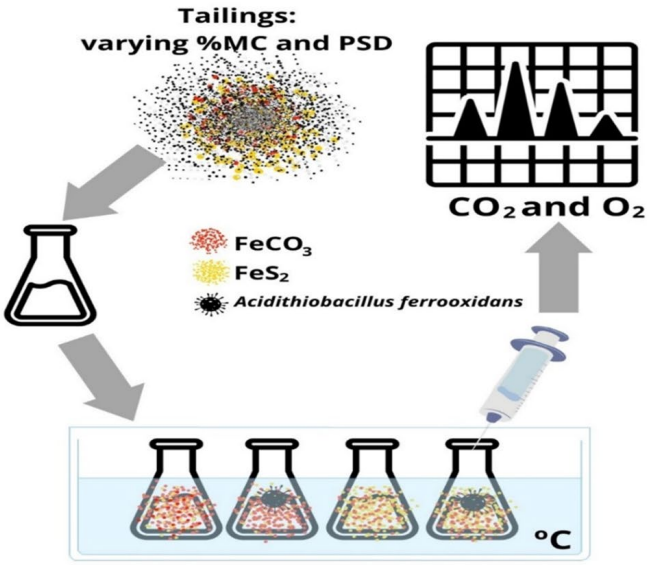

Fig. 1 **Synergistic effect of key parameters on coal tailings oxidation**

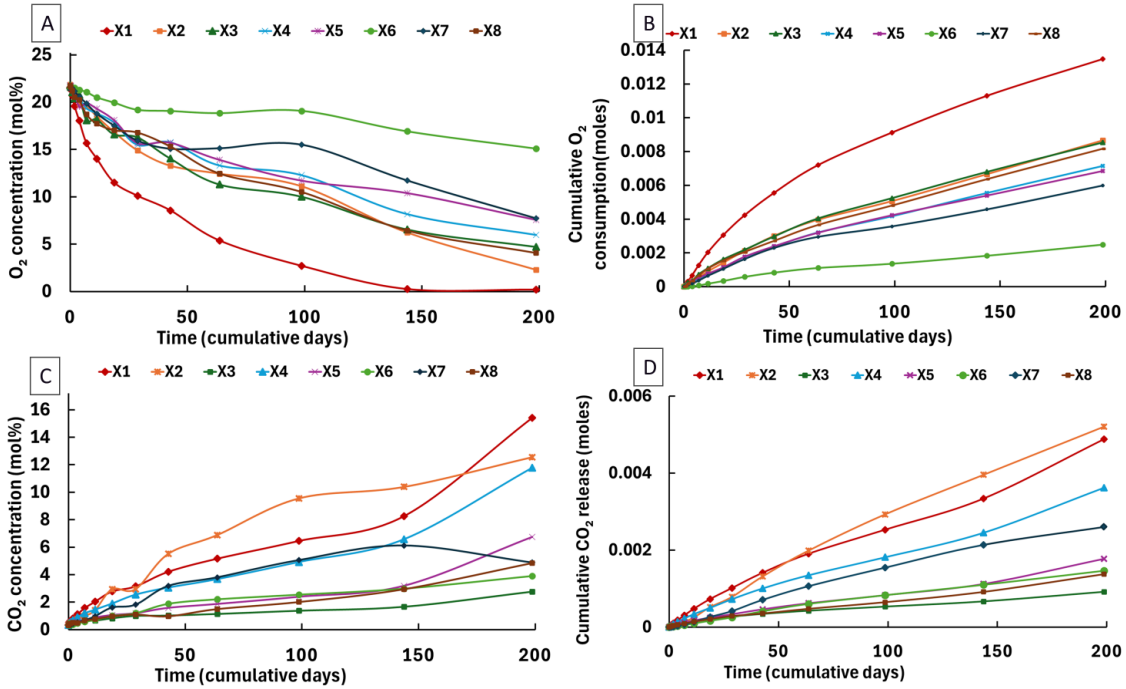

Fig. 3 A and B **Oxygen and CO_2 concentration in mol% or % (measured), C and D: Oxygen consumption and CO_2 release in moles (derived). A showed a decrease in oxygen concentration and *C showed* an increase in CO_2 concentration for different samples over the experimental duration. *All samples were tested at 10% GWC.***

Table 2. **Weight of key parameters on oxidation kinetics. 1 Minerology, 2 Organic matter(TC = Total Carbon, TOC = Total Organic Carbon, TIC = Total Inorganic Carbon), 3 Moisture Content (GWC = Gravimetric Water Content), 4 Bacteria Inoculation at 10% and 15% GWC, 5 Sieve-sized Fraction, 6 Surface Area, 7 Particle Size,**

S/N	Parameters	Oxygen Consumption Rate	Carbon dioxide Release Rate
1	Marcasite	↑	↑
	Pyrite	↑	↑
	Calcite	↓	↑
	Dolomite	n/a	n/a
	Siderite	→	↑
2	TC	→	→
	TOC	→	→
	TIC	↓	→
3	0% GWC	↓	↓
	10% GWC	↑	↑
	Full Saturation	→	↑
4	10% GWC	↑	↑
	15% GWC	↑	↑
5	2.00mm	↑	↑
	0.75mm	↓	↓
6	BET Surface Area	↑	→
	Pore Diameter	→	↓
	Pore Volume	↓	↓
7	Clay-dominated	↓	↓
	Sand-dominated	↑	↓
	Silt-dominted	↑	↑

Assessing the Sustainability of Acid and Metalliferous Drainage Treatment at Mt. Morgan Mine: Implications for Legacy Pit Lake Water Quality Management

Febriana[A], C. Smith[B], S.U. Gunathunga[C], D. Villa-Gómez[B,D], and G. Southam[C,E]

[A]Centre for Environmental Responsibility in Mining, Sustainable Minerals Institute, The University of Queensland, Brisbane QLD 4072. a.febriana@uq.edu.au

[B]School of Civil Engineering, The University of Queensland, Brisbane QLD 4072, c.smith7@student.uq.edu.au

[C]School of the Environment, The University of Queensland, Brisbane QLD 4072

[D]Australian Institute for Bioengineering and Nanotechnology, The University of Queensland, Brisbane QLD 4072

[E]W.H. Bryan Mining and Geology Research Centre, Sustainable Minerals Institute, The University of Queensland, Brisbane QLD 4068

ABSTRACT

1.0 INTRODUCTION AND BACKGROUND

Acid and Metalliferous Drainage (AMD) is one of the most persistent environmental challenges in the mining sector (Simate & Ndlovu, 2021). It forms when sulfide minerals are exposed to air, water, and iron-oxidizing bacteria (Nordstrom & Southam, 1997), producing acidic, metal-rich water that poses serious risks to ecosystems, agriculture, and human health (Naidu et al., 2019). A study by (Macklin et al., 2023) estimated that there are around 22,609 active and 159,735 abandoned mines globally. Another study by (Werner et al., 2020) estimated that there are approximately 80,000 abandoned mines in Australia, and around 2,825 of them are located in Queensland.

One of the mine sites facing AMD concerns in Queensland is the historic Mount Morgan gold and copper mine site in Central Queensland (Kaur et al., 2018). Even though mining operations at the site ceased in 1990, the environmental concerns related to AMD generated from the site persist (Vicente-Beckett et al., 2016). Remediation efforts applied at the legacy mine site including operation of a lime-dosing water treatment plant, along with the installation of 3 large industrial land-based evaporators and a bank of 5 floating evaporators to increase mine pit water level reduction, sealing of the Dam 8 upstream wall and installation of high-capacity pumps to reduce the mine pit catchment by more than 40% (Queensland Government, 2021).

Limestone or lime addition is among the most widely used AMD treatment methods (Skousen et al., 2017). While effective in neutralizing acidity and precipitating most metals, it generates chemical sludge requiring further management and contributes to greenhouse gas emissions through limestone production and CO_2 release during the acid-neutralization process (Iizuka et al., 2022). These environmental impacts are often overlooked in environmental assessments. A recent study indicated that application of passive treatment is more beneficial in reducing CO_2 emissions associated with AMD treatment compared to active treatment such as lime addition (Kim et al., 2025), albeit that passive treatment has limited capacity to deal with elevated loads of acidity and metals in AMD.

This study aims to assess the sustainability of the current AMD treatment applied to treat AMD from the Mt. Morgan mine pit lake and the potential of an alternative treatment method by leveraging indigenous microorganism found in the mine site. This sustainability assessment was based on an

analysis of the annual CO_2 emissions associated with AMD neutralization, sludge production, and water quality. In contrast, the opportunity for an alternative treatment was assessed through the identification of the microbial community in the AMD and the estimation of the same sustainability assessment parameters based on a sulfate reducing bacteria (SRB) mediated AMD treatment theoretical values.

2.0 METHODOLOGY

2.1 Study Location and Sample Collection

The Mt. Morgan site is a legacy gold and copper mine located 35 km southwest of Rockhampton, Central Queensland (Queensland Government, 2021). The Mount Morgan mine pit maximum capacity is estimated at 11,555 ML (Taylor et al., 2002) and lime dosing rate used at the mine site wastewater treatment plant was 6 ML/day (Stirloch Group, 2014). Water, sediment, and biofilm samples were collected in March 2023 and June 2024 at Mine Pit, Frog Hollow Tailing Dump, Linda Gully, and Dee River Downstream as shown in **Error! Reference source not found.**. AMD sample from Frog Hollow Tailing Dump was used for the AMD neutralization experiment in this study.

2.2 Experimental Determination of CO_2 Emissions and Sludge Generation from AMD Neutralization

In this study, 100 mL of field collected AMD samples was neutralized with 0.65 g of calcium carbonate ($CaCO_3$) from initial pH of 3.1 to 6.0. The experiment was conducted in triplicate at room temperature. The reaction involved in this neutralization process is shown in Eqn. [1] (Iizuka et al., 2022).

$$CaCO_3 + H_2SO_4 \rightarrow CaSO_4 + CO_2 + H_2O \quad [1]$$

Utilising experimental data for $CaCO_3$ consumption, the Mt. Morgan mine dosing rate, and the reaction stoichiometry the CO_2 released during the AMD treatment was determined.

This calculation involved determining $CaCO_3$ molarity, assessing CO_2 emissions per litre of AMD treated, and then scaling these emissions to daily and annual values using the dosing rate, as well as estimating the total CO_2 produced for treating the entire mine pit volume. In addition, sludge generation resulting from $CaCO_3$ neutralization was evaluated using the same reaction stoichiometry. The mass of $CaSO_4$ formed from remaining sulfate was calculated using the post-treatment sulfate concentration and lime dosing rate. The total sludge produced, including $CaSO_4$ and metal hydroxides ($Me(OH)_2$), was estimated on an hourly and annual basis by summing the relevant quantities and incorporating operational time.

2.3 Water Chemistry and Secondary Electron Microscopy (SEM) Analysis

Water pH values were measured using Eutech Instruments pH 700 pH meter. Metal concentrations in the titrated AMD solutions were filtered using 0.2 µm syringe filter, then analysed using Inductively Coupled Plasma Optical Emission Spectroscopy (ICP-OES) analysis using Thermo iCap6000. Metal concentrations at final pH were compared against guidelines for livestock drinking water, as shown in Table 1 (ANZG, 2018). Precipitated metals in the titrated AMD sediment were analysed by Secondary Electron Microscopy Energy Dispersive X-ray Spectroscopy (SEM-EDS) using a JEOLJSM – 7100F. For this analysis, 2 mL of water sample from the $CaCO_3$ neutralization experiment was filtered through 0.2 µm

filter paper, then fixed with 2.5% glutaraldehyde. Fixed filter paper subsequently dehydrated and dried according to the protocol stated by Jones et al. (2023).

2.4 Isolation of Sulfate Reducing Bacterial Consortium and Molecular Identification using Amplicon Sequencing

The water sample from Frog Hollow tailing dump at Mt. Morgan mine was mixed with LifeGuard™ soil preservation solution (Qiagen) and stored in a refrigerator at 4°C until processing. One (1) mL subsamples were inoculated into media consist of 6 mL/L lactate (60% w/w), 10 g L^{-1} tryptone, 1 g L^{-1} yeast, 2 g L^{-1} $MgSO_4.7H_2O$, 0.5 g L^{-1} $FeSO_4.7H_2O$, and 0.75 g L^{-1} ascorbic acid to isolate sulfate reducing bacterial consortium. Biomass pellets from the culture were submitted for DNA extraction and amplicon sequencing at the Australian Centre for Ecogenomics employing Polymerase Chain Reaction (PCR) amplification of 16S rRNA gene using universal primers (Jones et al., 2024). The resulting raw DNA sequences were then processed using MOTHUR software version 1.48.0 (Schloss et al., 2009) following the pipeline reported in Gagen et al. (2018).

3.0 RESULTS AND DISCUSSION

3.1 Annual CO_2 Emissions, Water Quality, and Sludge Generation from Lime Treatment

The results showed that $CaCO_3$ neutralization reaction released approximately 0.286 g CO_2 per litre AMD treated. Based on experimental CO_2 emission calculations, daily CO_2 emissions from AMD neutralization process at Mt. Morgan mine is estimated at approximately 17 tonnes CO_2 per day or 6,255 tonnes CO_2 per year. Furthermore, if this calculation is applied to the mine pit maximum capacity, this equates to approximately 32,844 tonnes of CO_2 generated to treat 11,555 ML mine impacted water with $CaCO_3$. This $CaCO_3$ emissions estimation has not considered CO_2 emissions resulted from the manufacturing or transportation of $CaCO_3$ to the mine site and pumps operation. The results demonstrate that while AMD neutralisation with $CaCO_3$ is an effective method for controlling acidity and precipitating most metals, it contributes to CO_2 emissions. This condition is an environmental trade-off that has not been sufficiently acknowledged in previous studies about the mining sector carbon footprints.

Although the estimated 33,000 tonnes CO_2 emissions resulting from AMD neutralisation at this single legacy mine may appear negligible when compared to the 99 Mt CO_2 equivalent emitted annually by Australia's entire mining sector (Australian Government Department of Climate Change; Energy; the Environment and Water, 2022) or 5,070 Mt CO_2 equivalent associated to global mining activities (McKinsey & Company, 2020), the cumulative impact is noteworthy when considering the hundreds of legacy mines worldwide that generate AMD and are treated with limestone or lime. Unlike energy-related emissions that can be mitigated via electrification or fuel switching, AMD treatment CO_2 emissions are chemically inherent to the neutralisation process. This underscores the need to consider AMD not only as a water contamination issue but also as a contributor to the sector's carbon footprint.

The results also confirm the effectiveness of limestone neutralisation in precipitating most metals as hydroxides (Nordstrom et al., 2015). The results showed that iron, aluminium, copper, and zinc concentrations are within acceptable limits when compared against applied livestock drinking water guidelines (ANZG, 2018). However, further treatment is needed to reduce cadmium and lead concentrations to meet the applied guideline values.

Sludge generation calculations also showed that the total amount of chemical sludge generated from $CaCO_3$ that needs further management is approximately 10,639 tonnes per year. SEM analysis of the resulting sludge revealed nano-sized particles (Figure 2). This result underscores that although effective

in neutralizing pH and removing metals from AMD through precipitation mechanism, conventional neutralization resulted in nano-sized chemical particles that need to be managed further as been demonstrated by the sludge generation calculations.

3.2 Potential of an Alternative Treatment Method for Mt. Morgan Mine Site

SRB mediated AMD treatment, which leverages metabolic activity of indigenous microbial communities and increase the pH of the acidic leachate to neutral or alkaline conditions, represents a promising alternative to conventional alkaline chemical neutralization methods that are associated with substantial CO_2 emissions. The 16S rRNA gene sequencing analyses of the SRB cultured from water samples collected at the Frog Hollow tailings dump revealed a predominance of acidophilic SRB bacteria (Figure 3). This result is notable as SRB more commonly thrive in pH 5.0 to 9.0 environment (Rambabu et al., 2020), but the SRB from Mt. Morgan mine was isolated from AMD with 2.5-3.0 pH. The presence of SRB under such acidic conditions suggests that Mt. Morgan mine possess acidophilic SRB strains that could influence carbon and sulfur cycling and potentially reduce metal toxicity under certain conditions. These native microbial populations offer significant potential for biologically mediated remediation by promoting sulfate reduction and metal precipitation, thereby reducing the reliance on chemical additives and potentially lowering the carbon footprint of AMD treatment.

Theoretical calculations based on the SRB-mediated process (Weijma et al., 2022) indicate a reduced sludge production rate of approximately 852 tonnes per year for the same AMD sample, which is markedly lower than sludge volumes generated through traditional lime dosing. These finding underscores SRB-based treatment options as a more sustainable and environmentally preferable alternative to active chemical treatments for AMD remediation.

In terms of treated water quality, Du et al. (2022) reviewed that SRB treatment results in improved parameters such as Cu, Fe, Cd, Zn, and Pb, compared to the outcomes observed with limestone or lime treatment, which typically results in higher residual concentrations of certain contaminants or greater alkalinity fluctuations. Additionally, metal recovery from SRB treatment is potentially enhanced, as metals precipitated as sulfides are generally easier to recover and recycle than the metal hydroxides formed during lime neutralization (Villa-Gomez et al., 2011).

Despite these advantages, a comprehensive evaluation of the CO_2 emissions associated with SRB treatment is warranted, as these emissions may vary depending on factors such as the choice of electron donor and operational conditions. Future research should therefore focus on quantifying greenhouse gas emissions for SRB processes under site-specific conditions to fully assess their environmental benefits.

4.0 IMPLICATIONS AND FUTURE DIRECTIONS

These findings highlight the hidden environmental cost of conventional AMD treatment and the potential of leveraging native microbial communities for more sustainable, biologically mediated remediation. This study introduces a novel perspective to pit lake water quality management and supports the development of lower-emission alternatives, such as biologically driven sulfate reduction, that reduce chemical use, associated CO_2 emissions from AMD treatment, and effluent sludge generation that need to be further managed, while offering opportunities for metal recovery from AMD. These efforts will be critical to transitioning toward more environmentally and economically sustainable management of legacy mine sites globally.

REFERENCES

ANZG. (2018). Australian and New Zealand Guidelines for Fresh and Marine Water Quality, Australian and New Zealand Environment Conservation Council and Agriculture and Resource Management Council of Australia and New Zealand, Canberra. Retrieved 11 August 2025 from https://www.waterquality.gov.au/guidelines/anz-fresh-marine

Australian Government Department of Climate Change; Energy; the Environment and Water. (2022). National inventory by economic sector: annual emissions. Retrieved 21 July 2025 from https://www.dcceew.gov.au/climate-change/publications/national-greenhouse-accounts-2019/national-inventory-by-economic-sector-annual-emissions

Du, T., Bogush, A., Mašek, O., Purton, S., & Campos, L. C. (2022). Algae, biochar and bacteria for acid mine drainage (AMD) remediation: A review. Chemosphere, 304, 135284-135284. https://doi.org/10.1016/j.chemosphere.2022.135284

Gagen, E. J., Levett, A., Shuster, J., Fortin, D., Vasconcelos, P. M., & Southam, G. (2018). Microbial diversity in actively forming iron oxides from weathered banded iron formation systems. Microbes and Environments, 33(4), 385-393. https://doi.org/10.1264/jsme2.ME18019

Iizuka, A., Ho, H.-J., Sasaki, T., Yoshida, H., Hayakawa, Y., & Yamasaki, A. (2022). Comparative study of acid mine drainage neutralization by calcium hydroxide and concrete sludge–derived material. Minerals Engineering, 188, 107819. https://doi.org/10.1016/j.mineng.2022.107819

Jones, T. R., Poitras, J., Gagen, E., Paterson, D. J., & Southam, G. (2023). Accelerated mineral bio-carbonation of coarse residue kimberlite material by inoculation with photosynthetic microbial mats. Geochemical Transactions GT, 24(1). https://doi.org/10.1186/s12932-023-00082-4

Jones, T. R., Poitras, J., Levett, A., da Silva, G., Gunathunga, S., Ryan, B., Vietti, A., Langendam, A., & Southam, G. (2024). Microbe-mineral interactions within kimberlitic fine residue deposits: impacts on mineral carbonation. Frontiers in Climate, 6. https://doi.org/10.3389/fclim.2024.1345085

Kaur, G., Couperthwaite, S. J., Hatton-Jones, B. W., & Millar, G. J. (2018). Alternative neutralisation materials for acid mine drainage treatment. Journal of Water Process Engineering, 22, 46-58. https://doi.org/10.1016/j.jwpe.2018.01.004

Kim, D.-M., Lee, K.-R., & Park, M.-S. (2025). Potential generation and consumption of carbon dioxide during treatment of mine drainages in South Korea. The Science of the Total Environment, 975, 179270. https://doi.org/10.1016/j.scitotenv.2025.179270

Macklin, M. G., Thomas, C. J., Mudbhatkal, A., Brewer, P. A., Hudson-Edwards, K. A., Lewin, J., Scussolini, P., Eilander, D., Lechner, A., Owen, J., Bird, G., Kemp, D., & Mangalaa, K. R. (2023). Impacts of metal mining on river systems: a global assessment. Science (American Association for the Advancement of Science), 381(6664), 1345-1350. https://doi.org/10.1126/science.adg6704

McKinsey & Company. (2020). Climate risk and decarbonization: What every mining CEO needs to know. Retrieved 21 July 2025 from https://www.mckinsey.com/capabilities/sustainability/our-insights/climate-risk-and-decarbonization-what-every-mining-ceo-needs-to-know#/

Naidu, G., Ryu, S., Thiruvenkatachari, R., Choi, Y., Jeong, S., & Vigneswaran, S. (2019). A critical review on remediation, reuse, and resource recovery from acid mine drainage. Environmental pollution (1987), 247, 1110-1124. https://doi.org/10.1016/j.envpol.2019.01.085

Nordstrom, D. K., & Southam, G. (1997). Geomicrobiology of sulfide mineral oxidation. In J. F. Banfield & K. H. Nealson (Eds.), Geomicrobiology: Interactions between microbes and minerals (Vol. 35, pp. 361-390). De Gruyter Mouton. https://doi.org/https://doi.org/https://doi.org/10.1515/9781501509247

Nordstrom, D. K., Blowes, D. W., & Ptacek, C. J. (2015). Hydrogeochemistry and microbiology of mine drainage: An update. Applied Geochemistry, 57, 3-16. https://doi.org/10.1016/j.apgeochem.2015.02.008

Queensland Government Department of Resources. (2023). Queensland Globe. Retrieved 24 December 2023 from https://qldglobe.information.qld.gov.au/qldglobe/private/proposed-sampling-points

Queensland Government. (2021). Mount Morgan remediation project. Retrieved 12 May 2025 from https://www.qld.gov.au/environment/land/management/abandoned-mines/remediation-projects/mount-morgan

Rambabu, K., Banat, F., Pham, Q. M., Ho, S.-H., Ren, N.-Q., & Show, P. L. (2020). Biological remediation of acid mine drainage: Review of past trends and current outlook. Environmental Science and Ecotechnology, 2, 100024-100024. https://doi.org/10.1016/j.ese.2020.100024

Schloss, P. D., Westcott, S. L., Ryabin, T., Hall, J. R., Hartmann, M., Hollister, E. B., Lesniewski, R. A., Oakley, B. B., Parks, D. H., Robinson, C. J., Sahl, J. W., Stres, B., Thallinger, G. G., Van Horn, D. J., & Weber, C. F. (2009). Introducing mothur: Open-source, platform-independent, community-supported software for describing and comparing microbial communities. Applied and Environmental Microbiology, 75(23), 7537-7541. https://doi.org/10.1128/AEM.01541-09

Simate, G. S., & Ndlovu, S. (2021). Acid mine drainage: Chemistry, effects and treatment (1st ed.). CRC Press.

Skousen, J., Zipper, C. E., Rose, A., Ziemkiewicz, P. F., Nairn, R., McDonald, L. M., & Kleinmann, R. L. (2017). Review of Passive Systems for Acid Mine Drainage Treatment. Mine water and the environment, 36(1), 133-153. https://doi.org/10.1007/s10230-016-0417-1

Stirloch Group. (2014). Mt Morgan WTP Lime Dosing. Retrieved 12 May 2025 from https://www.stirloch.com.au/projects/water-treatment-plants/mt-morgan-lime-dosing-water-treatment-plant/

Taylor, G., Howse, R., Duivenvoorden, L., Vicente-Beckett, V., Greenfield, P., & Ward, S. (2002). Downstream flow event sampling of acid mine drainage from the historic Mt Morgan mine. Water Science and Technology, 45(11), 29-34. https://doi.org/10.2166/wst.2002.0376

Vicente-Beckett, V. A., McCauley, G. J. T., & Duivenvoorden, L. J. (2016). Metal speciation in sediments and soils associated with acid-mine drainage in Mount Morgan (Queensland, Australia). Journal of Environmental Science and Health. Part A, Toxic/Hazardous Substances & Environmental Engineering, 51(2), 121-134. https://doi.org/10.1080/10934529.2015.1087738

Villa-Gomez, D., Ababneh, H., Papirio, S., Rousseau, D. P. L., & Lens, P. N. L. (2011). Effect of sulfide concentration on the location of the metal precipitates in inversed fluidized bed reactors. Journal of Hazardous Materials, 192(1), 200-207. https://doi.org/10.1016/j.jhazmat.2011.05.002

Weijma, J., Klok, J. B. M., Dijkman, H., Jansen, G., Sànchez-Andrea, I., Buisman, C. J. N., van Hullebusch, E. D., Hennebel, T., du Laing, G., Cruz, H., Pikaar, I., & Villa Gomez, D. K. (2022). Established technologies for metal recovery from industrial wastewater streams. In I. Pikaar, J. Guest, & R. Ganigué (Eds.), Resource recovery from water: Principles and application (pp. 295-318). IWA Publishing. https://doi.org/10.2166/9781780409566_0295

Werner, T. T., Bach, P. M., Yellishetty, M., Amirpoorsaeed, F., Walsh, S., Miller, A., Roach, M., Schnapp, A., Solly, P., Tan, Y., Lewis, C., Hudson, E., Heberling, K., Richards, T., Chia, H. C., Truong, M., Gupta, T., & Wu, X. (2020). A geospatial database for effective mine rehabilitation in Australia. Minerals (Basel), 10(9), 1-21. https://doi.org/10.3390/MIN10090745

Table 1. **Metal concentrations before and after caco3 neutralization compared to ANZG guidelines for livestock drinking water**

Metals	Before Treatment pH 3.1 (mg L^{-1})	After Treatment pH 6.0 (mg L^{-1})	ANZG Guidelines Recommended Trigger Value
Iron	213.8	0.04	Not sufficiently toxic
Magnesium	322.7	93.9	NA
Aluminium	191.7	0.3	5.0
Copper	4.9	0.1	0.4 (sheep), 1.0 (cattle), 5 (pigs and poultry)
Zinc	11.7	8.3	20.0
Cobalt	2.1	0.8	1
Nickel	0.7	0.4	1
Cadmium	0.2	0.1	0.01
Chromium	0.04	0.02	1
Lead	0.5	0.3	0.1
Arsenic	1.8	0.4	0.5-5
Sulfur	3,244.1	1,487.1	NA
Sulfate*	9,732.3	4,461.3	NA

*Sulfate concentration is calculated based on sulfur concentration

Fig 1. **Mt. Morgan gold and copper mine site sampling locations: Frog Hollow Seep, Frog Hollow Outlet, Main Pit, Linda Gully, and Dee River Downstream. Source: Mt. Morgan Ltd.; (Queensland Government Department of Resources, 2023).**

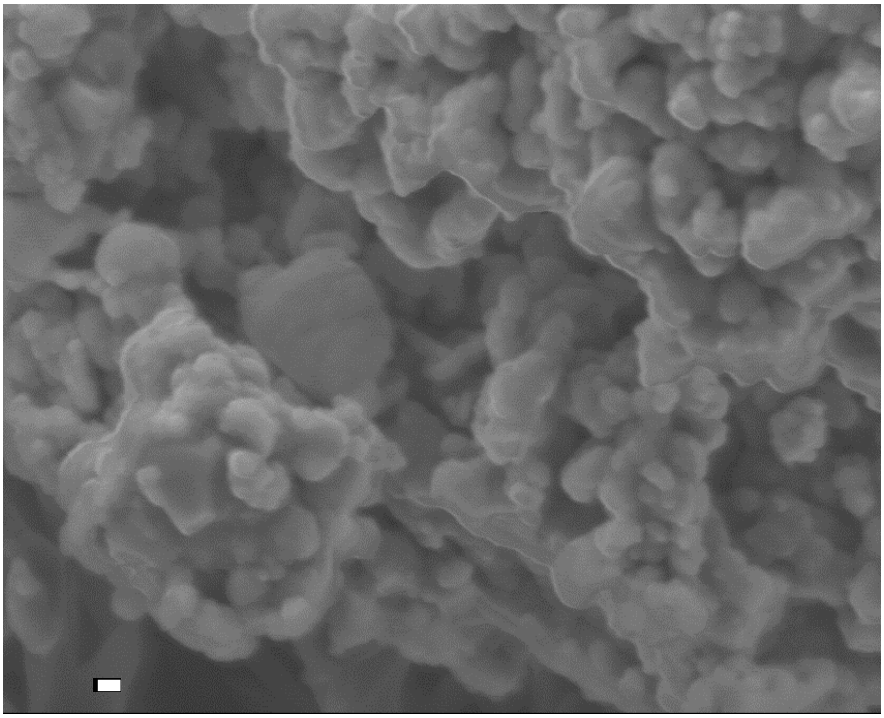

Fig 2. **Secondary Images of AMD neutralization experiment sediment sample**

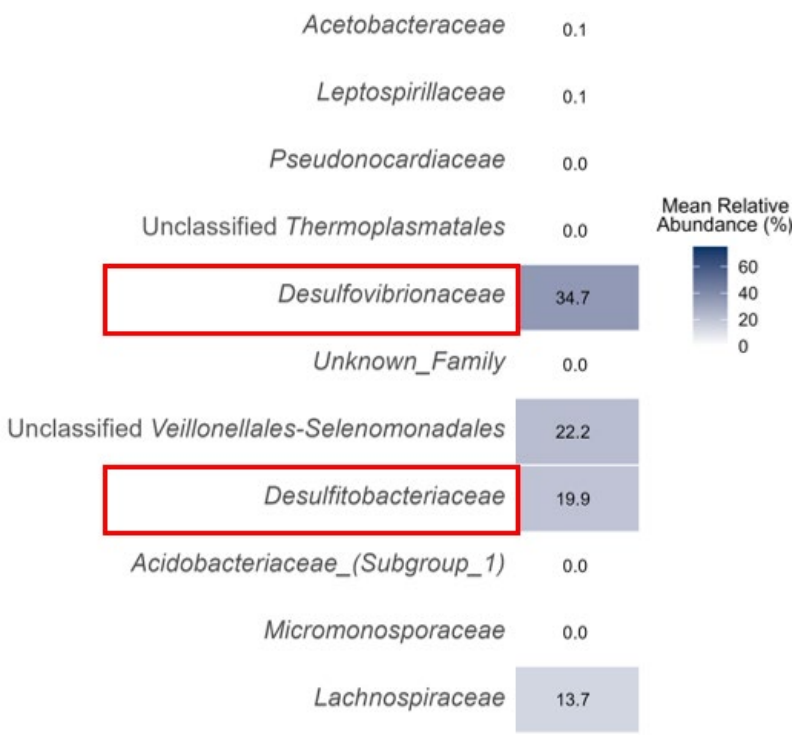

Fig 3. **Taxonomy of Bacteria Identified in Frog Hollow Tailing Dump culture**

AMD management at a legacy arsenic-tin mine in Eastern Australia

A. Soltys[A], A. Poozan[A], S. Winchester[B], B. Cork[B] and R. Davis[C]
[A]Earth Systems, Suite 4, 290 Salmon Street, Port Melbourne VIC 3207 Australia.
ashton.soltys@earthsystems.com.au
[B]GHD Ltd, Level 15 133 Castlereagh Street, Sydney NSW 2000 Australia.
[C]Legacy Mines Program, NSW Resources.

A legacy underground arsenic-tin mine is located in the highlands of Eastern Australia. Mineralisation occurs as a series of steeply dipping to vertical quartz veins containing pyrite-cassiterite-arsenopyrite hosted largely in strongly altered granitic lithologies.

Mining commenced in approximately 1880 and proceeded discontinuously until approximately 1960, sometimes focussed on arsenic, sometimes on tin, and other times on both. Tin was processed by crushing and gravity separation, while arsenic was recovered via sublimation of arsenopyrite and condensation of arsenic trioxide (As_2O_3) in a series of brick condensation chambers.

The primary mining features which remained included three adits, multiple shafts, several opencuts and numerous stopes which were occasionally backfilled to the surface with waste rock. Several sulfidic waste rock piles and discrete tailings deposits were scattered across the site. A partially disintegrating arsenic refining facility is also included amongst the site's polluting legacy features.

Post mining activities, the weathering of mine wastes, and accelerated degradation of the arsenic refinery has resulted in the discharge of acid and metalliferous drainage from the underground void (via the lowermost Level 2 Adit), as well as from discrete waste rock and tailings deposits, and the arsenic refinery. Pre-remediation, the total acidity (pollution) loads released from the site averaged approximately 42 tonnes of H_2SO_4 per year. This acidity load was comprised of low pH (2.7-3.0), high salinity (~1.8 mS cm^{-1}) water containing elevated concentrations of sulfate (~800 mg/L), and dissolved aluminium (~47 mg L^{-1}), arsenic (~1.5 mg L^{-1}), cadmium (~0.14 mg L^{-1}), copper (~2.1 mg L^{-1}), manganese (~4 mg L^{-1}), and zinc (~19 mg L^{-1}).

A Stage 1 remediation plan for the site involved expansion of the historical opencuts to receive mine waste rock and tailings in an engineered disposal cell. Following geochemical characterisation, all potentially acid forming (PAF) mine wastes were converted to non-acid forming (NAF) materials via blending with limestone aggregate prior to placement in the cell. Various geochemically disparate mine wastes were strategically placed within the cell in thin layers to optimise air entry control and arsenic immobilisation / adsorption. This included disposal of wastes by paddock dumping and dozing to optimise to formation of thin, homogenous, low air-entry lifts. Careful interlayering of coarse waste rock aggregate with thin, low permeability layers of sulfidic and non-sulfidic tailings was a key component of the cell construction design. Wastes with the highest sulfide content (i.e., the highest risk materials) were placed as low in the disposal cell as possible to minimise air entry into these materials. Several hematitic tailings layers were strategically placed throughout the layered sequence, designed to help adsorb and immobilise any soluble arsenic released from overlying waste layers. The cell was capped with inert, low permeability clay dominated material and then covered with a ~50 cm thick layer of coarse rocky mulch aggregate (20-500 mm) to retard the development of deeply rooted vegetation from enhancing air entry into the cell.

Prior to the transfer of waste rock and tailings to the containment cell (see above), the drainage from the catchment hosting these wastes had average calculated acidity values of ~1,760 mg H_2SO_4 L^{-1} and laboratory measured acidity values of ~1,390 mg H_2SO_4 L^{-1}. After the mine wastes were transferred to the containment cell within the same catchment, the average calculated acidity was lowered (by ~92%) to ~135 mg H_2SO_4 L^{-1}; and the average measured acidity was lowered (by ~88%) to ~170 mg H_2SO_4 L^{-1}. To date, there is no evidence in any of the site water quality data to suggest the discharge of AMD/NMD from the containment cell.

To lower the substantial soluble arsenic discharged from the refinery prior to Stage 2 of remediation, a temporary / short-term Permeable Reactive Barrier (PRB) was designed and installed immediately down hydraulic gradient of the arsenic refinery. Water quality monitoring of the PRB influent and effluent was conducted over ~3 years following installation, with a total of nine sampling events. Key water quality characteristics are summarised below and reported in
Table **3**.

Runoff and seepage from the arsenic refinery area (see "PRB Influent" in
Table **3**) is typified by weakly acidic pH values (~5.5), moderate sulfate concentrations (~125 mg L^{-1}), and elevated concentrations of dissolved arsenic (~29 mg L^{-1}), antimony (~0.010 mg L^{-1}), zinc (~0.3 mg L^{-1}), cadmium (~0.004 mg L^{-1}), copper (~0.07 mg L^{-1}), and manganese (0.13 mg L^{-1}).

Runoff from the refinery area first passes through ~60 tonnes of 20 mm limestone aggregate for pre-treatment / pH modification. This partially treated water then flows into the PRB, which consists of ~150 m^3 of 20 mm aggregate of reactive adsorbent substrate plumbed for vertical upflow and passive discharge to the environment (e.g.
Fig. **4**).

Treated water discharging from the PRB is typified by near neutral pH values (~6.4), moderate sulfate concentrations (~90 mg L^{-1}), and substantially lower dissolved metal(loid) concentrations compared to influent chemistry. Dissolved arsenic concentrations of the effluent average ~0.9 mg L^{-1} (between ~87% and ~99% removal efficiency), with other metal(loid)s commonly below their respective detection limits (see "PRB Effluent" in
Table **3**).

Stage 2 remediation will focus on AMD point sources that were not targeted during the Stage 1 program, with a focus on AMD discharge from the underground mine void (the largest single point source), and permanent solutions to address the poor-quality runoff and seepage from the refinery area. A remediation options assessment is currently underway to inform the Stage 2 remediation strategy.

Table 3. **Summary of PRB Influent (untreated) and Effluent (treated) water quality.**

Location	Date	pH (Laboratory)	Electrical Conductivity (Laboratory)	Laboratory Acidity (as H_2SO_4)	Calculated Acidity (as H_2SO_4)	Sulfate	Aluminium (filtered)	Antimony (filtered)	Arsenic (filtered)	Cadmium (filtered)	Copper (filtered)	Lead (filtered)	Manganese (filtered)	Zinc (filtered)
		-	µS/cm	mg/L	mg/L	mg/L	mg/L	mg/L	mg/L	mg/L	mg/L	mg/L	mg/L	mg/L
PRB Influent	13/02/2022	**6**	**250**	**5**	**72**	**85**	**0.19**	**0.019**	**21.0**	**0.0056**	**0.018**	<0.001	**0.240**	**0.500**
	8/09/2022	**4.7**	**220**	**35**	**130**	**180**	**0.83**	**0.003**	**37.0**	**0.0080**	**0.040**	**0.004**	**0.180**	**0.590**
	23/11/2022	**4.5**	**510**	**69**	**161**	**320**	**1.5**	**0.010**	**44.0**	**0.0087**	**0.086**	**0.005**	**0.200**	**0.740**
	10/05/2023	**5.8**	-	**35**	**95**	**120**	**0.07**	**0.008**	**28.0**	**0.0037**	**0.011**	<0.001	**0.130**	**0.260**
	8/11/2023	**6.5**	**120**	**5**	**23**	**37**	<0.05	**0.003**	**6.8**	**0.0007**	**0.004**	<0.001	**0.031**	**0.100**
	22/05/2024	**5.5**	**360**	**28**	**115**	**110**	**0.08**	**0.006**	**34.0**	**0.0024**	**0.011**	<0.001	**0.070**	**0.200**
	19/11/2024	**5.8**	**220**	**5**	**76**	**59**	**0.25**	**0.025**	**22.0**	**0.0010**	<0.001	**0.005**	**0.062**	**0.150**
	5/02/2025	**5.5**	**159**	**15**	**49**	**40**	**0.06**	**0.003**	**14.4**	**0.0012**	**0.003**	**0.001**	**0.037**	**0.074**
	8/04/2025	**4.9**	**452**	**49**	**182**	**183**	**0.55**	**0.017**	**52.6**	**0.0057**	**0.030**	**0.004**	**0.193**	**0.382**
PRB Effluent	13/02/2022	**6.5**	**230**	**5**	**0.3**	**42**	<0.05	<0.005	**0.004**	<0.0002	<0.001	<0.001	<0.005	<0.005
	8/09/2022	**6.6**	**98**	**5**	**0.2**	**83**	<0.05	<0.005	<0.001	<0.0002	**0.007**	<0.001	<0.005	<0.005
	23/11/2022	**6.2**	**360**	**5**	**20.3**	**190**	**0.06**	<0.005	**5.800**	<0.0002	**0.002**	<0.001	**0.016**	**0.006**
	10/05/2023	**6.7**	-	**5**	**2.7**	**110**	<0.05	<0.005	**0.740**	<0.0002	<0.001	<0.001	**0.010**	<0.005
	8/11/2023	**6.7**	**290**	**5**	**1.8**	**110**	<0.05	<0.005	**0.470**	<0.0002	<0.001	<0.001	<0.005	<0.005
	22/05/2024	**6.3**	**260**	**5**	**1.2**	**77**	<0.05	<0.005	**0.290**	<0.0002	<0.001	<0.001	<0.005	<0.005
	19/11/2024	**6.2**	**190**	**5**	**0.9**	**54**	<0.05	<0.005	**0.210**	<0.0002	**0.001**	<0.001	<0.005	<0.005
	5/02/2025	**6.1**	**179**	**7**	**0.7**	**55**	<0.01	<0.001	**0.154**	<0.0001	<0.001	<0.001	**0.001**	<0.005
	8/04/2025	**6.4**	**254**	**5**	**1.4**	**76**	<0.01	<0.001	**0.390**	<0.0001	<0.001	<0.001	**0.002**	<0.005

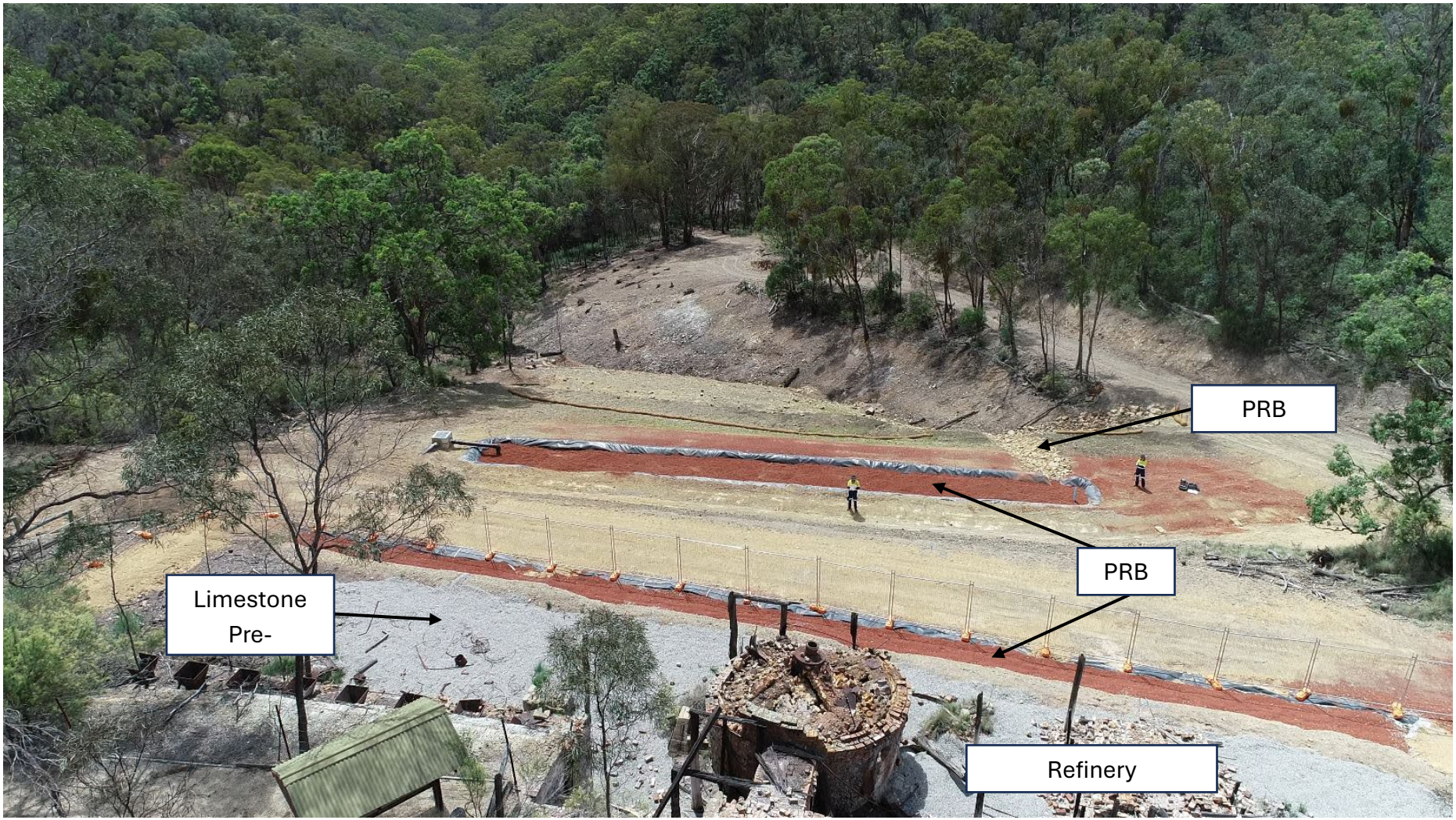

Fig. 4 **Drone photograph of the arsenic refinery area (foreground) and the PRB.**

A Standardised Method to Assess the AMD Source Hazard and Associated Geochemical Risks

M. Stimpfl[A], K.R. Jain[B], and I. Swane[C].

[A]BHP, Level 30, 125 Stg Georges Terrace, Perth WA 6000 Australia. marilena.stimpfl@bhp.com

[B]Mine Waste Management, Unit 201, Level 2, 490 Upper Edward Street, Spring Hill, QLD 4000 Australia. (Corresponding Author).

[C]Terrenus Earth Sciences, PO Box 132, Wilston, QLD 4051 Australia.

ABSTRACT

BHP is responsible for the operation, rehabilitation, and closure of several coal mines in eastern Australia. In 2019, BHP initiated a program to holistically review acid and metalliferous drainage (AMD) hazards across its coal portfolio. The first step focused on assessing the AMD risk posed by key source materials using historic environmental data and an extensive testwork program. Potential AMD sources were grouped into five material types: carbonaceous and non-carbonaceous spoil (waste rock), tailings, coarse and fine rejects, and coal, and evaluated using geochemical, geological, and coal quality data.
To ensure consistency in assessing AMD hazard, a scoring system was developed that considered the geochemical propensity (through testwork) for AMD, the capacity (75th percentile of total sulphur), and the quantity (tonnage-based) for each material type within landform domains (such as waste rock dumps and rejects dumps). The resulting landform scores defined AMD hazard and likelihood ratings, enabling targeted prioritisation of further characterisation, management strategies, and closure planning. This universal methodology allows objective comparison of AMD hazard across materials and sites and is broadly applicable to other commodities and mining operations. For it coal operations BHP has access to over 11,000 pH and EC (1:5), 9500 ABA, 2300 NAG (and a subset of NAG boil), 1500 DI leach and total metals, 200 QXRD across all material domains. This database was used to classify samples based on an AMD risk category, and to identify the most appropriate S cut-offs for the geochemical propensity as inferred from the geochemical testwork listed above.

1.0 INTRODUCTION

Effective mine operational and closure planning requires a robust understanding of geochemical risks associated with mineral waste, with acid and metalliferous drainage (AMD) representing a key long-term risk where materials are placed in landforms such as waste rock dumps (WRD), tailings storage facilities (TSF), and residual voids. To address this, BHP undertook a portfolio-wide program in 2019 to systematically review AMD hazard across its coal mines in eastern Australia, re-interpreting more than 20 years of geochemical data, identifying knowledge gaps, and implementing extensive sampling and testwork. Central to this program was the development of a structured, data-driven methodology and objective scoring system that integrates environmental geochemistry, geological and coal quality data, and testwork results to consistently assess AMD hazard and risk across multiple sites and material types. While developed for coal operations, the framework is transferable to other commodities and provides a practical basis for evaluating AMD hazard ratings, informing management strategies, and supporting operational and closure decision-making. The geochemical database included over 8000 pH and EC (1:5), 7000 ABA, 850 NAG (and a subset of NAG boil), 850 DI leach and total metals, 100 QXRD testwork results for overburden/interburden samples; and over 2900 pH and EC (1:5), 2500 ABA, 1500 NAG (and a subset of NAG boil), 800 DI leach, 690 total metals, 90 QXRD testwork results for tailings and rejects samples. This database was used to classify samples based on an AMD risk category, and to identify the most appropriate S cut-offs for the geochemical propensity as detailed below.

2.0 METHODOLOGY

2.1 OVERVIEW OF THE MULTI-STEP APPROACH

To enable consistent AMD risk assessment across sites, a structured methodology was developed, integrating source hazard characterisation, landform-scale hazard aggregation, and site-specific risk assessment that can be incorporated into source–pathway–receptor (SPR) framework. The approach is data-driven (using geological, environmental, coal quality, and geochemical datasets), transferrable (across commodities and waste types), and scalable (for site or portfolio assessments).
The steps comprise: (1) Source Hazard Assessment - quantifying AMD potential of material types based on geochemistry and volumes; and (2) Landform Hazard Scoring - aggregating source scores to evaluate AMD hazard of landforms such as WRDs or TSFs.

2.2 SOURCE HAZARD ASSESSMENT

This step quantifies the hazard of sulphide oxidation (acidity generation) in waste materials and landforms using three components.

- Propensity to generate AMD: Reflects the proportion of samples with AMD potential, determined through static geochemical tests (e.g., calculated net acid production potential [NAPP], net acid generation test [NAG]).
- AMD Capacity: represents the severity of AMD risk, based on the 75th percentile of total sulphur concentrations for potentially acid-forming (PAF) materials, including uncertain PAF [UC(PAF)], high-sulphur NAF (NAF-S), and sulphate-rich samples. Where data allow, distinctions between acid drainage (AD), saline drainage (SD), and neutral metalliferous drainage (NMD) are made.
- AMD Quantity: The volumetric or tonnage-based estimate of each material type likely to contribute to AMD generation. Greater quantities of AMD-prone material result in higher hazard scores.

The three components are scored using a matrix system (Table 1) and combined to produce an AMD source material hazard score for each material type reporting to a landform. Definitions and sulphur cut-off values were calibrated against thousands of samples from Permian coal measures in eastern Australia but can be adapted for site-specific or non-coal contexts. Conservatively, weightings of 1.0, 0.5, and 0.5 are applied to propensity, capacity, and quantity respectively, reflecting their relative influence on AMD outcomes.

2.3 LANDFORM HAZARD SCORING

Landform hazard scores (e.g., for WRDs, TSFs, and residual voids) are calculated by integrating the hazard scores of constituent materials, weighted by their proportions. Where field evidence or kinetic data are lacking, unsaturated conditions are conservatively assumed, reflecting the typically dry post-mining state of most above-ground landforms in eastern Australia. The composite score is then mapped to a likelihood ranking (Table 2), consistent with ISO 31000[1] risk management standards, providing a basis for screening AMD risks and prioritising landforms for further characterisation or management.

[1] *ISO 31000 is a family of standards relating to risk management codified by the International Organization for Standardization.*

2.4 AMD HAZARD SCORE FOR FINAL LANDFORM

Following the assessment of individual source material hazards, AMD hazard scores are aggregated at the landform scale (WRDs, TSFs, reject dumps, residual voids) by weighting material scores against their relative tonnage to estimate cumulative AMD potential. This enables consistent, quantitative assessment at closure-relevant spatial units, for example, by summing hazard scores of carbonaceous and non-carbonaceous spoil within a WRD or averaging scores of exposed lithologies in residual voids using geological and geochemical data. Risk ranking can be performed with or without considering mitigation measures, allowing identification of landforms with elevated AMD potential and prioritisation of further investigation, management strategies, or closure design. The outcome is a site-wide spatial risk model that forms the basis for subsequent SPR analysis and knowledge building.

3.0 CASE STUDY: COAL MINE IN EASTERN AUSTRALIA

In this case study, the above methodology for AMD hazard assessment was applied to a coal mine in eastern Australia, focusing on geochemical risks associated with the WRD landform. The same approach can be applied to TSF landforms and residual voids; however, the discussion here is limited to the WRD. The mine included typical open-pit facilities, with three main waste types: waste rock (97%, subdivided into carbonaceous/non-carbonaceous and fresh/weathered), tailings (0.5% from the CHPP), and rejects (2.4% from the CHPP). The key landforms relevant to waste characterisation and closure were residual voids, WRD, TSFs, and small amounts of coal within WRDs or exposed in void highwalls.

3.1 STEP 1: SOURCE HAZARD ASSESSMENT

This step evaluated each source material using historical and recent geochemical data (Table 3), with samples classified as NAF or PAF and assigned hazard scores based on AMD propensity, capacity (sulphur content), and quantity. Coal, tailings, and rejects recorded higher hazard scores, while waste rock (80% NAF) was low hazard. These scores were then aggregated across landforms to develop the initial risk profile (Step 2).

3.2 STEP 2: AMD HAZARD SCORE FOR FINAL LANDFORMS

After determining hazard scores for each source material, the overall AMD risk was assessed at the landform scale by weighting scores according to material proportions. For example, carbonaceous waste rock (6.3%) posed higher risk, while non-carbonaceous waste rock (>90%) was low risk, giving a weighted AMD hazard score for the WRD landform (Table 4). This method was applied across WRDs, TSFs, and residual voids, highlighting high-risk landforms (e.g., TSFs with sulfidic materials) and low-risk ones (e.g., WRDs with mostly NAF materials).

3.3 CONCLUSIONS AND IMPLICATIONS

A large geochemical database was used to define the assign an AMD risk classification the samples selected for testwork. This robust database supported the identification of the appropriate sulphur cut-offs and risk ranking for the AMD propensity and capacity.

The application of the methodology provided a clear assessment of AMD source hazards and associated risks across the site. Key findings included:

- Low-risk landforms, such as those dominated by non-carbonaceous waste rock, required minimal targeted management, reducing closure costs.
- High-risk landforms can be identified and prioritised for further assessment and monitoring, with mitigation measures (e.g., engineered covers) recommended to manage geochemical risks at closure.
- Next Steps: Source pathway receptor assessment for each landform that identifies and evaluates potential pathways for AMD migration from source materials to receptors.

The BHP approach allowed the closure team to objectively rank landforms across all sites, removing subjectivity and ensuring consistent outcomes. While preliminary, the method is robust, adaptable to other commodities, and useful for developing closure strategies. It also provided a clear platform for communicating geochemical risk to non-technical audiences.

In conclusion, the methodology applied in this study enabled quantitative assessment of AMD risks, prioritisation of landforms for further investigation, and the development of closure-specific mitigation strategies. This structured approach supports effective closure planning, minimises environmental impacts, and enhances transparency with regulators and stakeholders, building confidence in the overall risk assessment.

While the methodology is transferable to other sites and jurisdictions, the S-cut offs and risk ranking must be site specific, with their definitions based on robust and site specific geochemical data.

References:

ISO 31000: 2018, Risk Management Guidelines. https://www.iso.org/home.html

Table 1. AMD hazard scoring matrix.

COMPONENT	RATING	CATEGORY	DEFINITION
Propensity for AMD generation	1	Implausible	Geochemical properties suggest that the vast majority of the material has a negligible potential for AMD generation (less than 5% of the samples identified at potential for AMD in the samples set)
All material types/domains - Non-carb. - Coaly & carb. - Reject/tailings	5	Plausible	Geochemical properties suggest that significant proportion of the material may have potential for AMD generation (5-40% of the samples identified at potential for AMD in the samples set)
	7	Expected	Geochemical properties strongly suggest that the material has a high potential for AMD generation but has not yet been observed in the field (due to lag time) -(>40% of the samples identified at potential for AMD in the samples set)
Per spoil landform and TSF landform	15	Certain	Evidence of AMD from a material type or landform domain have been observed in the field
AMD **Capacity**	1	Low	Source has a negligible potential for AMD generation with 75th percentile total S less than 0.1%
All material types/domains - Non-carb. - Coaly & carb.	3	Low-Moderate (NMD)	Dominant AMD sources contain material that will likely generate NMD and/or SD (related to sulphide oxidation). Assumed to be bulk NAF but sulphide bearing, with NAF samples having 75th percentile total S greater than 1%
- Reject/tailings	5	Moderate	Dominant AMD sources with 75th percentile total S concentration ranging 0.1-1.0% and with potential to generate AD.
Per spoil landform and TSF landform	7	Moderate-High	Dominant AMD sources with 75th percentile total S ranging 1.0-1.5% and with potential to generate AD.
	10	High	Dominant potential AMD sources with 75th percentile total S >1.5% and with potential to generate AD.
AMD **Quantity**	1	Low	All material rated LOW for AMD capacity; or less than 5% of waste is rated LOW-MODERATE for AMD Capacity
All material types/domains: - Non-carb. - Coaly & carb. - Reject/tailings	3	Low-Moderate	Less than 5% of mineral waste rated as MODERATE for AMD capacity
	5	Moderate	Greater than 5% of mineral waste rated as LOW-MODERATE or MODERATE for AMD capacity
Per spoil landform and TSF landform	7	Moderate-High	Less than 5% of mineral waste rated as MODERATE-HIGH or HIGH for AMD capacity
	10	High	Greater than 5% of mineral waste rated as MODERATE-HIGH or HIGH for AMD capacity
AMD **Quantity**	1	Low	Less than 10% of drill-hole meters (or less than 10% of pit floor exposure) are classified as PAF
Residual void (pit) highwall & floor	3	Low-Moderate	Between 10% and 30% of drill-hole meters (or 10-30% of pit floor exposure) are classified as PAF

COMPONENT	RATING	CATEGORY	DEFINITION
Per residual void	7	Moderate-High	Greater than 30% of drill-hole meters (or greater than 30% of pit floor exposure) are classified as PAF
	10	High	Observed AMD on highwall or floor of pit or AMD affected water in pit

Table 2. AMD hazard ranking and landform AMD likelihood ranking.

AMD HAZARD RANKING	LANDFORM AMD LIKELIHOOD RANKING
0 - 5	Highly Unlikely: Highly unusual; may occur in extreme circumstances
5 - 10	Unlikely: Known to occur, but only rarely
10 - 15	Probable: May occur
15 - 20	Likely: Could easily occur
>20	Highly Likely: Expected to occur

Table 3. Geochemical classification of sample based on material type.

Material Type	**NAF (Non-Acid Forming)**	**UC (Uncertain)**	**PAF (Potentially Acid Forming)**	**Total Samples**
Waste Rock, weathered non-carbonaceous (n=108)	104 (96%)	0	4 (4%)	108
Waste Rock, weathered carbonaceous (n=9)	7 (88%)	1 (13%)	0	9
Waste Rock, fresh non-carbonaceous (n=716)	677 (95%)	8 (1%)	35 (4%)	716
Waste Rock, fresh carbonaceous (n=101)	90 (89%)	2 (2%)	9 (9%)	101
Waste Rock [all] (n=933)	***878 (94%)***	***11 (1%)***	***44 (5%)***	***933***
Coal (n=225)	151 (67%)	10 (~4%)	64 (28%)	225
Tailings [all] (n=369)	***188 (51%)***	***65 (18%)***	***116 (31%)***	***369***
Rejects [all] (n=150)	***113 (75%)***	***8 (5%)***	***29 (19%)***	***150***

Table 4. AMD source hazard material rating.

Landform components	Est. material proportion within landform	% of samples as PAF	% of material estimated as PAF	Estimated material quantities (Mbcm)	AMD source material hazard rating				Landform domain AMD hazard scoring#	Likelihood for AMD generation from WRD Landform
					AMD Propensity	AMD capacity	AMD quantity	AMD source hazard*		
Non-carbonaceous spoil Distributed throughout	91.4 %	*4%*	*3.7%*	*124*	1	1	1	2	1.5	Bulk spoil is overwhelmingly NAF with very low sulphur and excess neutralising capacity. The hazard for AMD generation in the final landform is based on 2.4% of the landform being rejects, of which about 19% is PAF and 6.2% of the landform being coaly and/or carbonaceous waste rock, of which about 1% is conservatively estimated to be PAF. Overall, about 4.2% of the landform is expected to be PAF material. All rejects and carbonaceous spoil are buried well within non-carbonaceous spoil. Non-carbonaceous spoil has excess ANC, making the landform bulk NAF. The hazard for AMD generation from the final landform at the mine is considered to be **LOW**. The likelihood for AMD generation from the final (waste rock) landform at the mine is rated as **HIGHLY UNLIKELY**.
Coaly and/or carbonaceous spoil Distributed throughout	6.2%	*~1%*	*0.1%*	*8*	5	3	3	8		
Rejects Distributed throughout	*2.4%*	*19%*	*0.5%*	*2*	5	7	10	12		
% of spoil landform estimated to be PAF: 4.2%										
Landform scoring (50% weighting applied to AMD capacity and quantity) = 7										

**AMD Source Hazard = AMD propensity + (0.5 x AMD capacity) + (0.5 x quantity).*

#Weighted AMD hazard score based on material quantities, PAF proportions, and hazard factors.

The geochemical evolution of mine void water chemistry over 25 years at the Mt Lyell Copper mine, Tasmania, Australia

Lois Koehnken[A] and Geoff Cordery[B]
[A]Director, Technical Advice on Water, Hobart, Tasmania. lois@worldrivers.com.au
[B]Environmental Manager, Mt Lyell, Sibanye-Stillwater

The Mt Lyell Copper mine in western Tasmania fuelled the growth of Tasmania and supported West Coast communities for 120 years before entering care and maintenance in 2014. The site is globally recognised for metallurgical advances related to pyritic smelting which was developed and implemented on site in 1902. An estimated 1.9 Mtonnes of copper, 1.9 Mounces of gold and 1,300 tonnes of silver have been extracted from the site over its long history, and Silbanye-Stillwater, the current owners project a minimum 25-year mine life based on the remaining resource and are actively working towards re-opening the site.

Mt Lyell is also renowned for its dramatic bare hills and the biologically dead Queen and King Rivers, a result of a combination of logging, sulphur dioxide gas emissions during the smelting era, high rainfall in Western Tasmania, acid drainage discharge from the site, and historic mining practices. Acid drainage is derived primarily from the oxidation of pyrite which is present at concentrations of about 10% in the ore and surrounding waste. The site contains numerous orebodies, with the near vertical Prince Lyell body a focus of activity since the 1930s (**Fig 5**). The ore body was initially developed as the West Lyell open cut and in 1978 mining extended underground using sub-level open stoping. Open stoping and sub level caving mining methods were used continuously from 1978 until the site went into care and maintenance in 2014, resulting in a cone of broken sulphide rich material with a surface catchment of ~65 ha and extending to a depth of ~1,000 m. Water percolating through the fractured cone transports sulphate and metals, generating approximately 1 ML of acid drainage for every mm of the ~2,500 mm annual rainfall. The mine water is pumped to surface and discharged to the Queen River, consistent with regulatory requirements that recognise the historic and intransigent nature of the acid drainage issue at the site.

In the early 2000s, copper concentrations from the underground were in the range of 100 – 300 mg/l with up to 2,000 kg/day of copper discharged to the local river systems. During this period there was an unsuccessful government funded project to recover copper from the discharge and implement water treatment to improve environmental outcomes. Although the project failed, the monitoring regime implemented by Copper Mines of Tasmania to support the investigations has been maintained over the past 25 years providing an opportunity to understand how changes to the mining method, the cessation of mining and flooding of the lowest levels of the mine have affected water quality on the site.

Underground water quality has changed markedly since 2000 in response to a range of events, including an increase in the draw of historic 'waste' material from the cave, the site entering care and maintenance in 2014, flooding of the lower mine due to a rock fall and blockages associated with historic sludges in 2016, and stabilisation of water levels that continue to inundate the lower ~250 m of the mine workings. From an environmental perspective, the most notable change has been the dramatic decrease in copper loads discharged from underground, with a reduction of 95% over the 2000 to 2024 period (**Fig 6**). Other metals, such as aluminium and zinc have also shown substantial though smaller reductions (**Fig 7**). In contrast indicators of sulphide oxidation have not shown large changes, with only a 10% to 20% decrease in acidity, sulphate and manganese. The observed large

increase in iron likely is attributable to changes in the underground dewatering system that no longer pumps underground sludges separately.

In this presentation, the variable decrease in metals will be discussed in the context of changing flow pathways, potential neutralisation and passivation reactions, flooding and other metal removal processes.

The interpretation of the 25-year monitoring record combined with an understanding of the hydrology of the site also allows projections to be made as to what is likely to happen if / when the water levels in the underground are reduced, and what might be expected following the permanent closure and inundation of the Prince Lyell underground mine.

References

New Century, 2023, Mt Lyell Copper Mine Prefeasibility Study, 23 January 2023. https://www.listcorp.com/asx/ncz/new-century-resources-limited/news/mt-lyell-copper-mine-prefeasibility-study-2826369.html

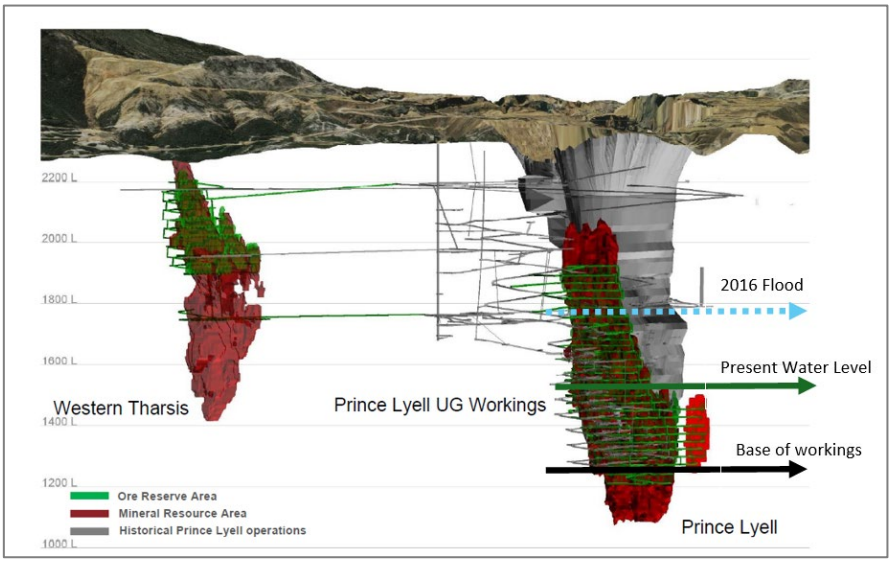

Fig 5. **Cross-section schematic of the Prince Lyell underground workings showing the extent of flooding in 2016 and level of subsequent dewatering. Modified from New Century (2023).**

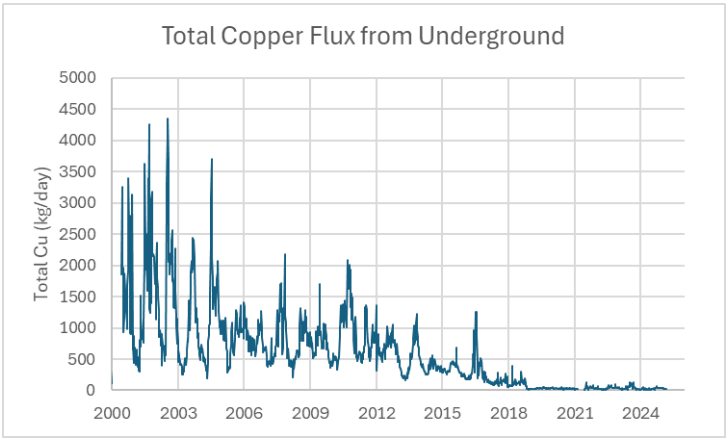

Fig 6. **Total copper loads from the underground workings at Mt Lyell, 2000 to 2024.**

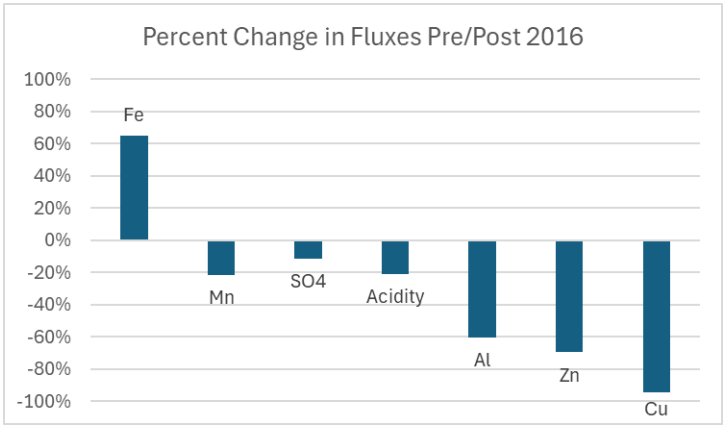

Fig 7. **Percent change in fluxes from the Mt Lyell mine pre- and post- the flooding event in 2016.**

Modern Tools, Better Predictions: Advancing from PAF/NAF to Provide Refined Water Quality Insights

H. Davies
Newmont, Englewood, Colorado 80112, United States. Hugh.Davies@newmont.com

For more than four decades, acid–base accounting (ABA) has been the pillar of mine waste characterization, providing the foundation for the PAF/NAF (or PAG/NPAG) classification systems used worldwide. These methods, initiated in the 1970s through the Sobek tests and codified in the 1997 MEND Prediction Manual, gave industry and regulators simple, accessible tools to predict acid rock drainage (ARD) potential and to design mine waste management strategies. But this acid-focused lens has also left a blind spot: many water quality impacts occur where acid never develops at all.

Mine wastes rich in carbonate minerals may delay ARD for decades or centuries, yet still contain an environmentally-significant sulfide content that oxidizes and releases metals, metalloids, oxyanions, and sulfate under neutral conditions. These neutral mine drainage processes often escape notice during planning, flying under the radar with a NAF classification, only to emerge with complex treatment challenges later in operations or after closure. Managing neutral pH discharges frequently requires membranes for sulfate and chloride, biological treatment for selenium and nitrate, or specialized methods for uranium and molybdenum, often at greater cost and complexity than conventional lime plants for acidic water.

Addressing these risks requires advancing beyond PAF/NAF designations to a more integrated approach to waste characterization. Static tests such as ABA and net acid generation (NAG) remain essential, but they cannot predict the timing or mechanisms of contaminant release. Targeted sequential extraction leach tests and mineralogical tools, ranging from bulk X-ray diffraction to grain-scale SEM-EDS and LA-ICP-MS, reveal which minerals host trace elements and how mineral phases will control reactivity in certain disposal environments.

The next step in this approach to refine water quality predictions is to link mineralogical, kinetic, and physical properties information within geochemical and reactive transport models. By mechanistically connecting detailed mineralogical data with reaction rates and transport processes, models such as MIN3P can forecast contaminant release and attenuation across the life of mine and into closure. No single test or model provides the full picture, but in combination these methods allow us to build more defensible, site-specific conceptual models that anticipate both acidic and neutral drainage risks. These insights provide a better framework for circling back to conduct targeted and confirmatory kinetic testing and field trials.

The challenge for the next generation of ARD practice in the next generation of modern mines is clear: to move beyond a narrow focus on acid potential, and to embrace mineralogy- and model-driven predictions to provide refined water quality insights.

This publication reflects the views of the author and does not necessarily represent the official position of Newmont Corporation. Any references to Newmont data, methodologies, or conceptual frameworks are made independently by the author and do not imply corporate endorsement. All such data, methodologies, and frameworks are used with permission and remain the intellectual property of Newmont Corporation. No representation is made regarding the completeness, accuracy, or applicability of the methods described to any specific project, site, or outcome.

Mitigating AMD risk from active and legacy underground mines

J.R. Taylor[A], M.T. Beilharz[A], A.J. Coward[A], S. Ruttor[A], and E. Rainey[B]
[A]Earth Systems, Suite 4, 290 Salmon Street, Port Melbourne, 3207, Australia.
jeff.taylor@earthsystems.com.au
[B]Legacy Mines Program, NSW Resources.

Acid and Metalliferous Drainage (AMD) is a common feature of both operating and legacy underground mine sites worldwide. A geochemical assessment of sulfidic mine wastes associated with underground mines clearly indicates that waste rock materials that are retained or transported underground to fulfil the requirement for ongoing mining, such as stope backfill, are the primary polluting sources in these scenarios.

As long as reactive waste rock installed in backfilled stopes remain unsaturated, AMD remains inevitable. Underground mines that drain at topographic low points to minimise the need for drilling fluid or groundwater dewatering commonly optimise the generation of AMD and ensure that it can continue in perpetuity. This style of mining was widespread in the past, making legacy mine sites particularly problematic in terms of poor-quality water discharge.

Ventilation systems in active mines and natural atmospheric pressure-temperature gradients in legacy mines provide the primary controls on air movements in mine voids. The oxygen in air is fundamental to facilitating sulfide oxidation and pollution generation. The primary reaction describing the consumption of oxygen and production of sulfuric acid during sulfide oxidation is described in Eqn. [1]:

$$FeS_2 + 3.75\ O_2 + 3.5\ H_2O = Fe(OH)_3 + 4H^+ + 2SO_4^{2-} \quad [1]$$

pyrite + oxygen + water = ferrihydrite + sulfuric acid

Underground mines offer unique and relatively simple scenarios for controlling air migration and therefore pollution generation as a result of the limited number of air entry features.

The oxidation of typical reactive wastes within a small legacy underground mine may consume approximately 1 m^3 of oxygen every 10 minutes. If the mine is unsealed, the loss of 1 m^3 of gas can be replenished many times over every few minutes via advection and/or convection from the surrounding environment via adits, shafts, or stopes to the surface. However, if key air entry passageways are effectively sealed, this restricts air entry mechanisms to the mine void to diffusion. Under such circumstances, the 1 m^3 of oxygen is more slowly replaced by 1 m^3 of air, which contains only 21 vol.% of oxygen, thereby lowering the mine void oxygen concentration and unavoidably increasing its nitrogen content.

As sulfide oxidation proceeds within an air-entry limited mine void, and the rate of sulfide oxidation exceeds the rate of oxygen re-supply, the concentration of mine void oxygen progressively and passively decreases. When oxygen concentrations fall below ~3 vol.%, sulfide oxidation rates fall toward zero, and water pollution essentially ceases. This management strategy is referred to as the Inert Atmosphere Technology (IAT) as it can passively generate an inert nitrogen atmosphere within underground mine voids. In situations where air-entry seals are unavoidably incomplete, the IAT can engage a supplementary active nitrogen gas injection system to create a subtle inert gas overpressure to actively prevent air entry into the mine void.

A large, modern, massive sulfide underground mine has the potential to consume 40-50 tonnes of oxygen per day producing the equivalent acidity of 80 tonnes of H_2SO_4/day (i.e. converting oxygen gas to soluble sulfate ions). This highlights the potential magnitude of pollution generation, as well as the load that sulfide oxidation places on a mine's ventilation system.

The IAT has been implemented at full scale at a legacy gold mine in NSW, and three further installations are either underway or planned for the coming 12 months. Two are at legacy sites and one is at an active mine site.

The Nevada Gold mine near the town of Sunny Corner in NSW was the first successful installation of the IAT. Initial air entry control engineering works commenced in January 2017 and early monitoring was terminated in July 2019. Water quality improvements over this 18-month period included a 95% decrease in acid, metals and acidity loads. Images of before, during and after the initial engineering works in Nevada No. 1 Adit are shown in Figure 1.

Routine monitoring was halted following the apparent success of the technology. Ad hoc monitoring during August 2024 identified that increases in acid and metal concentrations were measured from the No. 1 Adit discharge. It was considered possible that another nearby irregularly flooded adit was occasionally connected to the main Nevada workings and was permitting somewhat random air entry into the main mine void. Secondary air entry control works on this Nevada No. 2 Adit resulted in rapid water quality improvement once again. Images of before, during and after the second stage air entry engineering works at Nevada No. 2 Adit are shown below in Figure 2. Key field and laboratory water quality data from January 2017 to present are provided in Figures 3-5 below.

Mine void backfill at Nevada (No. 1 and 2 Adits) substantially lowered public safety risks associated with open mine voids as well as decreased infiltration into the voids, and therefore lowered adit discharge to the local creek. Recent monitoring data has confirmed that the installation of the IAT resulted in a 91% decrease in acidity concentrations and an 85% decrease in acidity load over time. The rate of change in water quality indicates that ongoing water quality improvements are expected over the coming months. Complete remediation of poor-quality drainage is predicted within the next 12-18 months. The Nevada gold mine site provides clear proof of concept for the Inert Atmosphere Technology but also highlights the importance of diligent identification of subtle air entry locations within legacy and active mine sites.

The IAT provides a substantially lower risk and lower cost alternative to AMD mitigation relative to the installation of pressure bulkheads in underground mines and can avoid the need to treat in perpetuity. It also permits installation in active mines to isolate the disused but still polluting portions of active mines, significantly decreasing pollution and simultaneously lowering ventilation cost and complexity. Re-entry into sealed sections of both active and legacy mines if re-mining is required is rapid, low cost, and low risk. Preventing sulfide oxidation until re-mining can also lower resource loss through uncontrolled dissolution.

New data on Inert Atmosphere Systems at three other mine sites will be available over the coming 12-18 months.

Fig. 1. **Three images of the Nevada No. 1 Adit. From left to right, the images show the adit pre-, during and post-air entry control engineering works. Note the post-works adit drainage pipeline (white) at the bottom left of the image on the right.**

Fig. 2. **Three images of the Nevada No.2 Adit. From left to right, the images show the adit pre-, during and post-air entry control engineering works. The post- second stage works adit drainage pipeline is buried beneath the road in the foreground of the image on the right.**

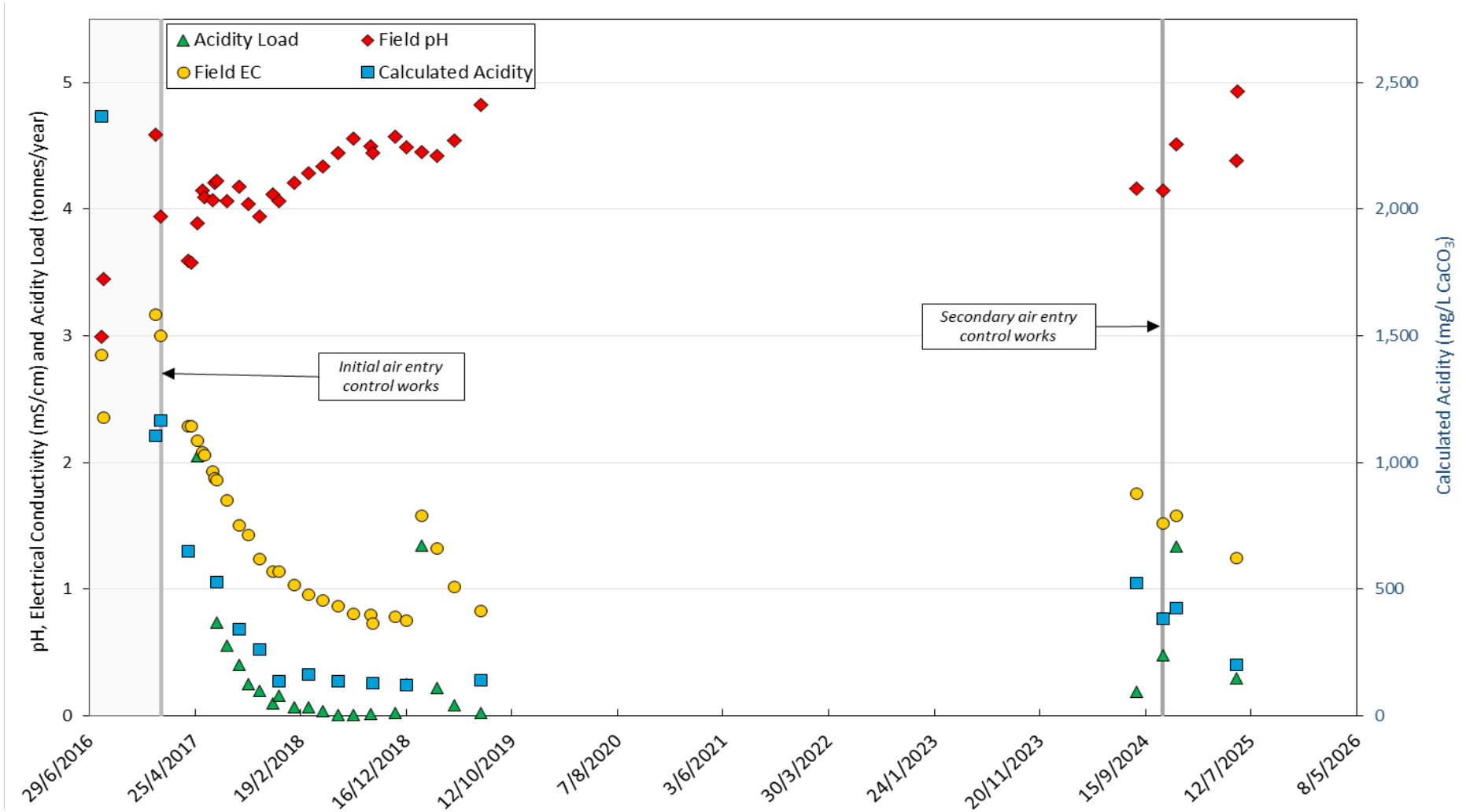

Fig. 3. **Field water quality parameters, acidity concentrations and acidity load calculations from August 2016 to June 2025 for the Nevada No. 1 Adit. The shaded area (left side of graph) indicates data collected prior to the implementation of air entry control works, while the solid grey lines mark the final day of air entry control works for each event.**

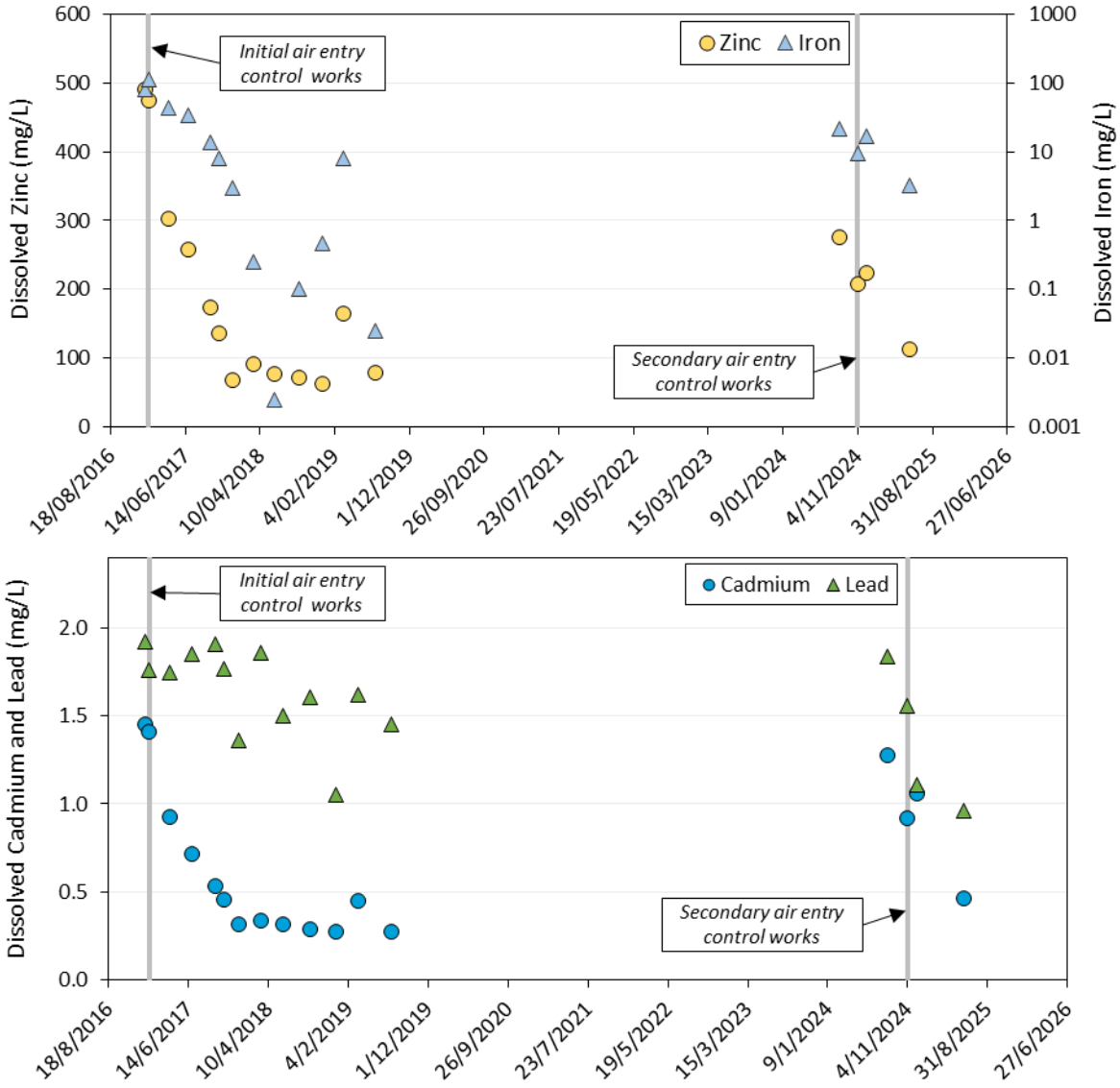

Fig. 4. **Nevada No. 1 Adit discharge laboratory results showing dissolved metal concentrations from January 2017 to June 2025. Zinc and iron are displayed in the top panel; aluminium, copper, and manganese in the middle panel; and cadmium and lead in *the bottom panel.***

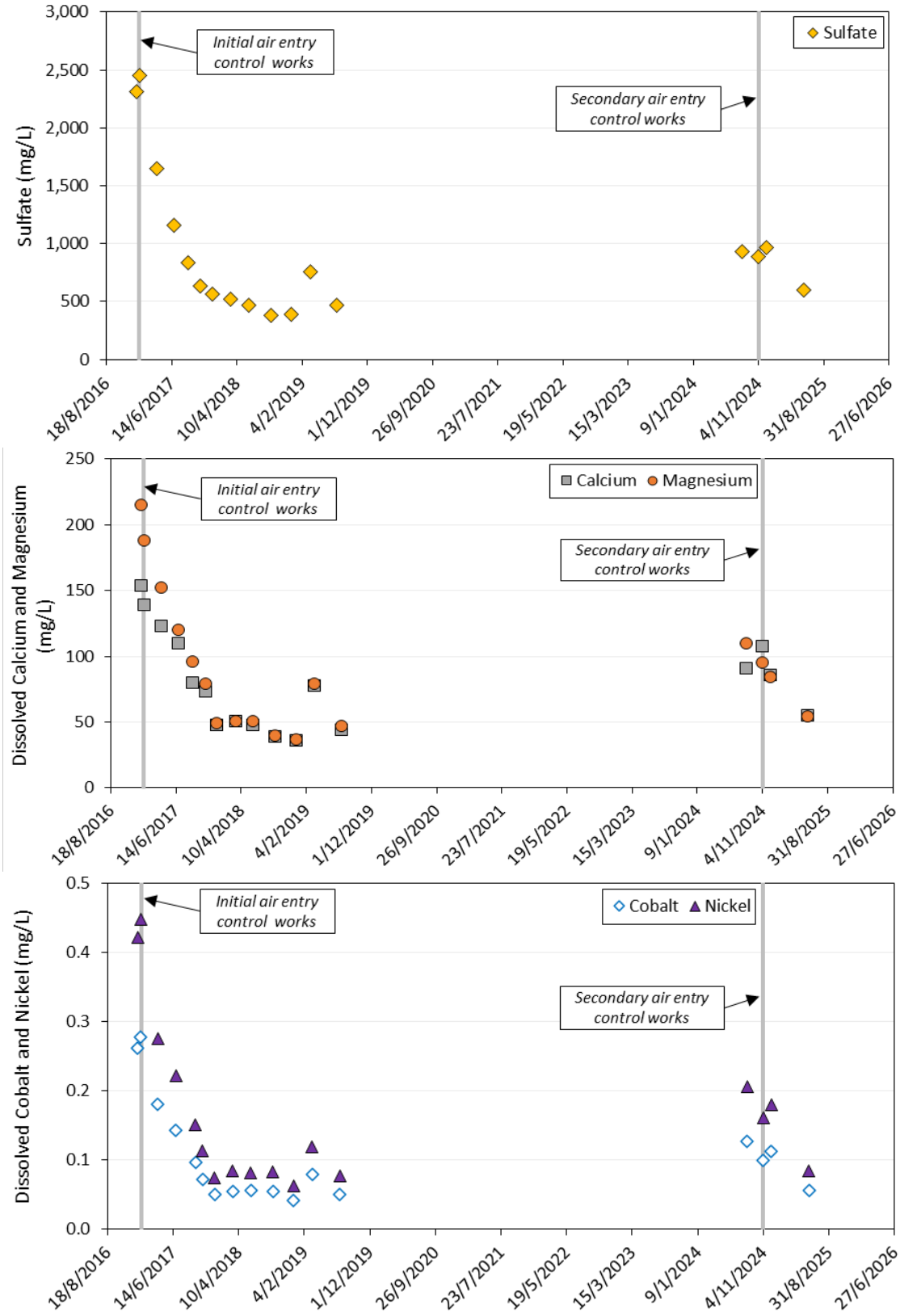

Fig. 5. **Nevada No. 1 Adit discharge laboratory results showing major ion and dissolved metal concentrations from January 2017 to June 2025. Sulfate is displayed in the top panel; calcium and magnesium in the middle panel; and cobalt and nickel in the bottom panel.**

Machine Learning Methods Applied to AMD Water Management

T. Meuzelaar
Life Cycle Geo, LLC, 403 River Bend Way, Colorado, United States, 81601, tom@lifecyclegeo.com

Machine learning algorithms are rapidly becoming an essential tool in the AMD practitioner's toolkit, with application across the entire mine project life cycle. During feasibility, machine learning-based sample selection, analysis of multivariate leachate and waste material characterization data streamline the practitioner's workflow, add considerable value, and can be followed by machine learning-supported materials classification, segregation and volume estimation. In permitting, unsupervised classification methods can be used towards development of a modern baseline in support of future compliance. During operations, both unsupervised and supervised algorithms provide considerable support in waste facility management, including seepage quality predictions, water treatment support and optimization of site-wide water management strategies. And in closure, machine learning algorithms add considerable value in understanding impact sources and informing closure plans.

Finally, large language models (LLMs) are increasingly being used to replace workflow inefficiencies and redundant tasks. LLMs can be used to streamline data ingestion, replace simple coding tasks and optimize various aspect of geochemical, transport and water balance modeling workflows.

The Tool for Acid Rock Drainage and Metal Leaching Prevention and Management: Transforming Global Leading Practices into Asset-Level Decision Support

R. Paisley[A], R. Verburg[A], N. Bezuidenhout[A], N. Korczak[A], J. Nicholls[B], G. Tremblay[C]
[A]WSP. rebecca.paisley@wsp.com
[B]ICMM
[C]International Network for Acid Prevention (INAP)

The Global Acid Rock Drainage (GARD) Guide developed by INAP describes leading practices and technologies that assist mine operations, regulators, and other stakeholders with acid and metalliferous drainage (AMD) prevention and management. It is primarily designed for specialists, scientists, and engineers with a reasonable background in chemistry and basic engineering. However, the responsibility to make AMD-related decisions, and implement leading practices, often falls on personnel at the mine operations (i.e., asset) level who are, typically, generalists. This can make it challenging for decisions to be made in a consistent, efficient, and practical manner.
In 2024, the 'Tool for Acid Rock Drainage and Metal Leaching Prevention and Management' was developed under the auspices of ICMM and INAP to support mining companies with the pro-active management of AMD. It aims to support personnel responsible for undertaking asset-level decisions regarding AMD management by presenting relevant information, in a concise framework.
The 'Tool' differentiates between external and internal controls, and between corporate- and asset-level decisions. External influences such as community needs, industry guidelines, and regulatory requirements are incorporated into the framework via corporate-level governance and strategy. At the asset level, the corporate strategy is translated into objectives and key performance indicators that consider the individual challenges, risks, and opportunities of the asset. The 'Tool' supports the development of an asset-level AMD management plan using findings from multiple studies, allowing for informed decision making on prevention and mitigation strategies. The 'Tool' further considers the importance of integrating AMD prevention and management actions into water management, mine waste management, closure planning, and adaptive management activities, ensuring actions remain relevant as conditions change.

This paper provides an overview of the 'Tool' and its functionality in operationalising the principles in the GARD Guide to empower users to make informed and consistent AMD prevention and management decisions.

CRC TiME Acid and Metalliferous Drainage test handbook

A.R. Gerson on behalf of the CRC TiME 3.10 Project Team
Blue Minerals Consultancy, Marlborough, New Zealand. andrea@blueminealsconsultancy.com.au

1.0 CRC TiME

The Cooperative Research Centre (CRC) Program was established by the Australian Government in 1990 to support Australian industries to solve critical issues, develop new technologies, products and services and compete on the world stage. The program is jointly funded by the Federal Government, industry participants and research organisations. CRC TiME (Transformations in Mining Economies), established in 2020, seeks to transform opportunities for community utilisation of post-mining impacted soil and water resources by providing an environment that enables subsequent sustainable utilisation, for example by agriculture, recreational facilities, forestry, aquaculture, or habitat conservation. CRC TiME has partnered with State Governments, mining companies, metallurgical companies, First Nations, and researchers to identify and develop these opportunities.

CRC TiME Project 3.10, Improved Prediction, Remediation and Closure of Acid and Neutral Metalliferous Drainage (AMD/NMD) Sites by Examination of Mine waste Behaviour at the Mesoscale, was approved in 2022 and will run for 5 years. The project is supported by CRC TiME, Flinders University; Newmont Mining Services; MMG Australia Limited; Rio Tinto Services Limited; Fortescue; BHP Group Operations Pty Ltd; Teck Resources Limited; Australian Genome Research Facility Limited; Okane; Minerals Research Institute of Western Australia; Department for Energy and Mining, South Australian Government; Australian Department of Agriculture, Water and the Environment; Mineral Resources Tasmania; The University of Queensland; University of Windsor, and Blue Minerals Consultancy.

2.0 BACKGROUND

It is now recognised that routine application of standard procedures for assessment of wastes as potentially acid-forming (PAF) or non-acid-forming (NAF) have been inadequate in many cases. Numerous case studies are outlined in Morin and Hutt (2001) where static and kinetic testing methods have failed to predict site outcomes. One striking example is the prediction, based on the alkalinity of leachate from kinetic leach columns, that a particular dump site would never give rise to acidic leachate. However, within 2 years dump leachate was <3.

Accurate forecasting and appropriate control of AMD/NMD remains a critical issue for mine sites with climate, geochemistry and microbiology all playing key roles. Incorrect forecasting can result in:

1) Inadequate environmental controls and strategies being put in place leading to downstream contamination of waterways, ecosystems and/or human health impacts and constraints on future site repurposing;
2) Inaccurate geochemical risk assessments, for example, non-acid forming waste rock and tailings being wrongly classified as potentially acid forming, resulting in inefficient utilisation of resources through expenditures that are not warranted;
3) Use of on-site remediation resources not being recognised; and
4) Lack of recognition of opportunities to understand and control beneficial microbial action.

In the last decade the narrative has evolved to better understanding the impact on water quality, with movement away from the binary NAF and PAF assessment to a more nuanced approach. The static methods remain focussed on relative amounts of PAF/NAF early in the AMD evolution profile with little integration of the relative rates of mineral leaching as aging and weathering takes place. For instance, NAF wastes may become PAF due to rapid dissolution of neutralising carbonate minerals that is not matched by the rate of dissolution of acid generating sulfide mineral. Additionally, liability associated with NAF materials needs also to be assessed as metalliferous drainage can result from reductive dissolution of tailings resulting in the release of metals.

3.0 CRC TiME ACID AND METALLIFEROUS DRAINAGE TEST HANDBOOK

The new Test Handbook builds on the ARD Test Handbook, AMIRA Project P387A Prediction & Kinetic Control of Acid Mine Drainage (AMIRA, 2002), which remains widely utilised by industry and has become an Australasian industry and government standard. Alternative predictive tools, also widely adopted globally, are outlined in the GARD Guide (GARD, 2010), such as the 2009 Canadian MEND Manual (MEND, 2002).

Many specific improvements and corrections in analytical methods and interpretation have been developed and used over the last 20 years but they are currently only found in reports, conference and journal papers or in shared information between AMD control consultants, government authorities and site environment managers. This Handbook is intended to collect these improved mineralogical and chemical methods and to add microbiological methods not included in previous Handbooks. **The objective is to produce a practical guide, consequently the length of the Handbook will be strictly monitored.**

The microbial component of AMD/NMD has been absent from previous handbooks due to difficulties in standardising sample collection, processing, data analysis, and data interpretation. The objective of including microbial characterisation into the updated test handbook is not to set standards, but to inform managers, authorities, and communities on the routes and options for microbial analysis and best practices. This will include:

1) Choice of analysis (culture-dependent *vs* culture independent (i.e., genomics, metagenomics)).
2) Best practices for designing microbial-based investigations on and off site.
3) Best practices for sample collection and preservation.
4) Inclusion of microbial characterisation into meso-scale kinetic testing.

Specific testing for metalliferous drainage has also not previously been a focus. Metalliferous drainage has on occasion been identified using the titration between pH 4.5 and 7.0 in the NAG test with >5 kg H_2SO_4 t^{-1} being defined as the concentration of risk. This will not, however, include metalliferous drainage due to Zn or Mn. A scheme is being trialled whereby the final NAG solution is assayed to identify remaining metalliferous components.

4.0 PUPROSE OF THE TEST HANDBOOK

This Handbook is intended as a resource for all people involved in aspects of mining geochemistry including:

- Environmental managers and staff in mining companies, to guide practical testing and monitoring of waste rock and tailings.

- Environmental protection assessment in government authorities to guide requirements for testing and monitoring with planning for containment and closure.
- Guidance to communities associated with mining operations to inform discussion and monitoring of release from operations.

It is not intended to set out site planning or remediation that may be needed after testing and monitoring information is collected. It is also not intended to provide a 'recipe' for testing requirements. It is intended to summarise and review testing methodologies with specific focus on their strengths, weaknesses and in what circumstances they can go wrong.

As the Test Handbook is to be an easily accessible document, the aim for the main body of the document is for it to be no more than 60 pages and to focus on readily accessible techniques. Techniques under development will be surveyed in an Appendix.

5.0 SURVEY

During 2024 an online Survey, focussing on identification of areas requiring new or improved practical test protocols for acid and metalliferous drainage prediction, was circulated to sponsoring company representatives. This survey was also made available, via the International Network for Acid Prevention (INAP) at the September 2024 International Conference on Acid Rock Drainage in Halifax, Canada. The questions asked in the survey are given below with a brief summary of the responses.

Q1 ***Briefly state your experience with AMD/NMD assessment?*** The replies to this spanned consultant geochemists, academics including microbiologists, government reviewers, laboratory managers and mine-site practitioners.

Q2 ***What sector do you belong to?*** Government, industry and academia.

Q3 ***What are the main concerns regarding current assessment methods for AMD/NMD?*** Ease of implementation, ability to predict lag time, prediction of metalliferous leaching, clarity, quantitative mineralogy, linkages/predictability, regulator expectation, using the results to inform dump/TSF/heap leach construction and final landform designs, lack of consistent approach, development of effective kinetic measurements.

Q4 **Are you aware of the GARD Guide and/or AMIRA P387A ARD Test Handbook? please specify.** Approximately half replies of yes, with the result not replying to the question and one reply of no.

Q5 **Rank your priorities (with 1 being the highest rank, average ranking is given) for inclusion in the CRC TiME AMD Assessment Handbook, considering the following**

– Mineralogical assessments and techniques	2.3
– Determination of acid generation	2.4
– Kinetic testing (methods, risk, tailings, rock, contaminants)	3.1
– Scale up studies (laboratory to site, both method and prediction of outcomes)	3.9
– Neutralisation strategies	4.5
– Microbiological assessment of AMD/NMD sites	4.8

Q6 **Please provide detailed suggestions for the CRC TiME AMD Assessment Handbook?** (Note: this section is highly abbreviated. We received many recommendations that are outside the scope of the Handbook with guidance requested for site/mineralogy specific conditions and regulatory frameworks.)

- Although this is an Australian guidance document, it should be transferrable to other regions. The net acid generation (NAG) test methods are not used in British Columbia, Canada, which is a missed opportunity.

- Include a set of quick reference calculation templates (acid base accounting (ABA), humidity cell test (HCT) depletion calculations, etc.) for people to copy into spreadsheets etc.
- Make it visually appealing and include pictures that demonstrate the concepts.
- Describe common interferences that may affect each test method.
- Clarity, simplicity and consistency in methods.
- AMIRA P387A Project ARD Test Handbook section 3 was low in detail, especially in relation to mineralogy.
- I advocate for early-stage testing that demonstrates results are statistically reliable for all waste types.
- GARD guide, AMIRA guide, Aus Gov leading practice on preventing ARD/NMD are all good resources, recommend CRC TiME work to complement these, not to create a new guide that says the same thing. Make it practical and useful to the mine site enviro that has limited resources, limited time, and limited budget.
- Adjust the methods for geochemistry/mineralogy/microbiology, and site climate.
- Ensure its circulated around global key stakeholders in various stages of the draft, starting with a table of contents and not completed in isolation. We do not need to re-invent the wheel, rather, we need to align current divergent assessment practice.
- We need to provide more standardised methods in the new handbook. For example, the heating temperature and time for ANC (acid neutralisation capacity) need to be accurately specified in the test handbook, as well as the cooling time prior to titration, etc. This is to minimise variations in the testing results from different laboratories.
- Recommendations for mineralogical/geochemical/microbiological assessments are required in the handbook.
- Emphasise the intent of the handbook is to be a reference and general guide (i.e., a toolbox), NOT a prescriptive protocol. AMD assessment should be specific to local environmental conditions, stage of project/mine development, geology and project needs.
- solid description of test methods and the modifications required (i.e., if siderite is present) in an easy-to-understand manner (i.e., table)

As far as is possible, within the bounds of a relatively brief and practical document, an attempt will be made to cover as many of the suggestions and concerns raised as possible.

6.0 LOGISTICS

The Test Handbook will be drafted by the CRC Project team with the first draft to be completed and internally reviewed by the end of the first quarter 2026. It will then be circulated to the project steering committee and CRC and sponsoring organisation representatives for editing and feedback. Thereafter it will be circulated to the broader community for input. We aim to have the Handbook completed by the end of 2026. Note: all contributors will be listed in alphabetical order in an Appendix. There will be no authors.

REFERENCES

AMIRA (2002) 'ARD test handbook: Project P387, A prediction and kinetic control of acid mine drainage' (Eds RSC Smart, WM Skinner, G Levay, AR Gerson, JE Thomas, H Sobieraj, R Schumann, CG Weisener, PA Weber, SD Miller, W Stewart) (AMIRA International Ltd.).

GARD (2010) Global Acid Rock Drainage Guide. International Network on Acid Rock Drainage, http://www.gardguide.com/index.php/Main_Page.

MEND (2002) 'Mine Environment Neutral Drainage'. https://mend-nedem.org/guidance-documents/, (Canada).

Morin, KA, Hutt, NM (2001) 'Environmental Geochemistry of Mine Site Drainage: Practical Theory and Cast Studies'. (MDAG Publishing, Vancouver, British Columbia, Canada).

Alternative kinetic leach test method for non-free draining samples of mine and process wastes

G. Campbell[A], A. Watson[B] and M. Stimpfl[C]

[A]Graeme Campbell and Associates, PO Box 247, Bridgetown, 6255, Western Australia.
gca@wn.com.au

[B]SRK Consulting (Australasia) Pty Ltd, Level 3, 18 - 32 Parliament Place, West Perth, 6005, Western Australia

[C]Superintendent Geo-Environmental, BHP Iron Ore Pty Ltd, Level 30, 125 St Georges Terrace, Perth, 6000, Western Australia

1.0 INTRODUCTION

Laboratory kinetic column leach tests were developed for sulfidic samples to assess the rate of sulfide oxidation, potential for acid generation and neutralisation, and longer-term leaching characteristics (e.g. pH, electrical conductivity and release of major ions and metals/metalloids).
Kinetic tests are experimental designs that allow the ongoing measurement of weathering and leaching rates and/or the potential drainage chemistry (Price, 2009). Testwork is often completed on samples with a particle size of <10 mm, where the samples are well flushed to ensure solute is eluted from the column and to reduce the potential for precipitation and accumulation of secondary weathering products.

Kinetic leach tests are suited to free draining samples; difficulties may arise when completing tests on samples that are not free draining – for example, fine grained tailings, samples with high clay content and/or dispersive properties. Current guidance documents provide limited instruction on how to manage samples that are not free draining, other than to stir the sample to promote solid-liquid contact and carefully decanting leachate off the top of the sample (Price, 2009).
This approach to testing poorly draining samples is unlikely to yield data representative of sulfide oxidation under optimum conditions. It will be difficult to ensure all particle surfaces are rinsed, particularly those towards the base of the column. Collection of water from the top of the column will result in incomplete flushing of the sample (excess pore water will remain within the solids matrix) and sub-optimal conditions for sulfide oxidation as the sample will remain saturated.

2.0 SAMPLE PROPERTIES AND LEACHABILITY

Coal processing wastes (i.e. tailings, mixed rejects and tailings, and coarse rejects) collected from coal mines in the Bowen Basin included a fine-grained fraction, clay minerals and coal (organic) macerals. The generally sodic samples may also be prone to slaking and dispersion with consequent breakdown of the aggregated solids following addition of deionised water, with liberated clays impeding gravity drainage during leaching.

Ten fine grained samples were submitted for AMIRA kinetic testwork. Sample preparation for the kinetic testing procedure included screening to remove large particles, with kinetic testwork taking place on the <4.75 mm size fraction of the dried solids. Kinetic testwork initially involved free draining columns, where 1.50 kg of sample was loaded into a Büchner funnel as per the AMIRA free draining column method (AMIRA, 2002) and rinsed with 1.00 kg high purity deionised water (HPDW). However, due to the abundance of clays and macerals, 80 % of samples were not free draining – the volume of

leachate recovered was either very low, or non-existent (i.e. no drainage) – and the leached solids remained in a fully saturated state. In addition, the water on the top of the column contained significant ultrafine particulate matter that remained suspended in solution.

3.0 ALTERNATIVE TEST METHOD DEVELOPMENT

To address the non-draining nature of the samples, an alternative test method was developed by Graeme Campbell and Associates (GCA) to generate data to reliably assess sulfide oxidation rates and leaching characteristics. The alternative method involved increased duration between flushing events (8 weeks) to allow time to establish weathering processes that will support the generation of weathering products. The method also included an extended contact between reacted solids and deionised water (one day) to maximise dissolution/elution of solutes for leachate analysis. Leachate recovery did not involve gravity drainage.

4.0 Test Outline

The novel kinetic testwork procedure (GCA method for non-free draining samples) is outlined below, together with a series of photographs showing selected steps in the procedure.

1. The sample is dried at low temperature (maximum 40^{o}C) and sieved to collect the <4.75 mm fraction for testing.
2. The first leachate, at t=0, is produced as follows: a representative 1.50 kg split of the sample is loaded into a polypropylene bowl and 1.00 kg HPDW water added (Figure 1). The sample is thoroughly mixed using a plastic spatula/scraper to produce a concentrated slurry (solids-density around 60 % w/w) thus ensuring good solid-liquid contact. After placing a lid over the slurried sample, the setup is left to sit for 1 day to maximise dissolution and elution of solutes for leachate analysis.
3. Leachate recovery is achieved using Rhizon® pore water samplers operated under a slight vacuum over a period up to 7-10 days, as governed by the solid hydraulic properties of the increasingly dewatered solids mass (Figure 2). The final dewatered reacted solids have a gravimetric water content of around 15-18 % (w/w) (Figure 3), and the yield of leachate for assaying is generally within the range 700-800 mL.
4. The final mass of dewatered solids is then chipped using a spatula to create aggregate like clods ranging up to 20 mm nominal in size for use in the subsequent unsaturated weathering cycle.
5. Weathering is undertaken using an incubator at 30^{o}C for a period of 8 weeks with weekly weighing of samples and addition of HPDW via misting to maintain the gravimetric water content within the above range. At this water content the matrix of the aggregates corresponds to a relative saturation around 50 %.
6. After 8 weeks, 1.00 kg HPDW is added to the sample and the leaching cycle is repeated.
7. The physicochemical conditions (viz. aeration and moisture status) during the weathering cycle are near-optimal for abiotic and biotic reactions, including oxidation of sulfides (predominantly pyrite) and decomposition of complex coal polymeric organic compounds during microbial and fungal respiration.

In addition to leachate analysis, gaseous measurement of oxygen concentration were undertaken for the estimation of oxygen consumption rates (OCRs) at 30^{o}C.

5.0 PRELIMINARY RESULTS

Table 1 summarises selected geochemical properties of two of the non-draining samples that underwent the GCA kinetic testwork protocol. The testwork program is currently ongoing, however

preliminary results showing the pH of the leachate collected and the sulfate release rate as a function of time are presented in Figure 4. The pH of the leachate is similar for the two samples – being relatively constant and mildly alkaline over the course of the test.

The sulfate release was highest in the first leach (around 600 mg kg^{-1} and 1,400 mg kg^{-1}) and decreased in subsequent leach events in a trend representative of salts being flushed from the samples. The latter measurements suggest sulfate release rates are trending towards near steady state conditions, with the sulfate elution rate (SER) representative of release of sulfate from sulfide oxidation. Sulfide oxidation rates calculated from SER for each sample are 4.9 x 10^{-12} kgO_2 kg^{-1} s^{-1} (GCA12135) and 2.3 x 10^{-11} kgO_2 kg^{-1} s^{-1} (GCA12138).

To validate the GCA kinetic protocol, OCR measurements were collected over the duration of the testwork at 8 weekly intervals. Figure 5 shows the results of OCR measurements completed on the samples immediately prior to rinsing with HPDW; results show that following an initial oscillation, OCRs are stabilising and that OCR is slightly higher for sample GCA12138 compared to sample GCA12135. Measured OCR values are 4 x 10^{-11} kgO_2 kg^{-1} s^{-1} (GCA12135) and 1 x 10^{-10} kgO_2 kg^{-1} s^{-1} (GCA12138).

Notably these preliminary results indicate that the measured OCR values (from O_2 consumption) are consistent with the values calculated from SERs. In particular, sample GCA12138 has higher sulfide oxidation rate compared to sample GCA12135, regardless of method; and sulfide oxidation rates estimated from OCR are SER are compatible with each other, although sulfide oxidation rates are 4-8 fold higher when derived from OCR compared to SER. The higher SERs for sample GCA12138 is associated with the higher CRS value for this sample (Table 1).

6.0 CONCLUSIONS

Conventional free draining kinetic column leach tests (such as the AMIRA column and humidity cell tests) are not suited for fine-grained materials that are not free draining under gravity.
The GCA method for non-draining samples ensures good contact between the solid and HPDW, to facilitate dissolution and elution of solutes from the sample, and to improve leachate recovery.
Utilisation of Rhizon® pore water samplers in the dewatering step (step 3) ensures that the physicochemical conditions in the dewatered sample are optimised to promote sulfide oxidation.
Analysis of leachates indicates that sulfate is generated and eluted from the samples, following the first flush, associated with ongoing sulfide oxidation. Calculated and measured OCR values obtained by two independent techniques (SO_4 elution vs O_2 consumption – measured on the same samples) are consistent, validating the GCA technique as a viable method for obtaining water quality and estimating sulfide oxidation rates in samples that do not drain under gravity.

The GCA method was developed for coal processing wastes. However, this test method has already been applied to other problematic fine grained and non-free draining samples across a range of commodities. This highlights the versatility of the GCA method for non-free draining samples as another kinetic testwork approach in the geochemistry tool box.

REFERENCES

AMIRA International Limited, 2002. ARD Test Handbook. *Project P387A Prediction and Kinetic Control of Acid Mine Drainage*, May 2002.

Price, W, 2009. *Prediction Manual for Drainage Chemistry from Sulphidic Geologic Materials*, MEND report 1.20.1 CANMET Mining and Mineral Sciences Laboratories.

Table 1. Selected sample properties

Parameter	Units	Sample ID	
		GCA12135	GCA12138
Total S	%	0.30	1.1
Sulfide S[A]	%	0.19	1.01
Sulfate S	%	0.11	0.09
ANC	$kgH_2SO_4\ t^{-1}$	19.5	15.5
Total C	%	19.5	16.8
Total Organic C	%	18.7	15.8
Total Inorganic C	%	0.8	1.0
Sample Classification	AMIRA	NAF-S	PAF

Notes: S – sulfur; ANC – acid neutralising capacity; C – carbon; NAF-S – non acid forming (sulfidic); PAF – potentially acid forming.
[A] Present as pyrite.

Fig. 1. Prepared slurry in polypropylene bowl allowed to soak for 1 day

Fig. 2. **Porewater extraction using Rhizon® pore water samplers**

Fig. 3. **Mass of reacted dewatered solids (left) and extracted water (right)**

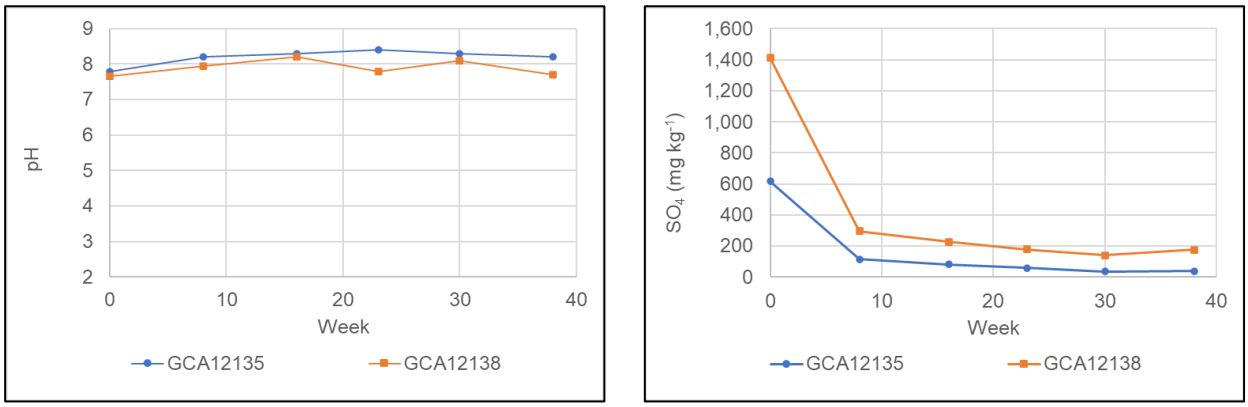

Fig. 4. **Leachate pH and mass of sulfate released as a function of leach event**

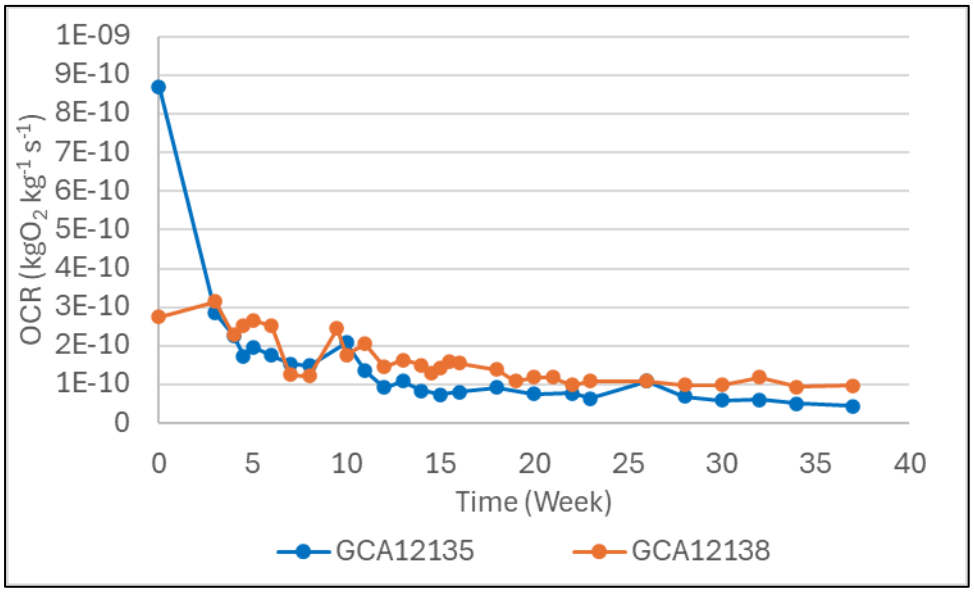

Fig. 5. Results of OCR measurements

Notes:

1. OCR – oxygen consumption rate.
2. Initial granular state corresponds to <4.5 mm fraction premoistened; following flushing, measurements completed on aggregated clods up to 20 mm nominal size.
3. Flushing of weathered solids via Rhizon® pore water samplers at weeks 0 ,8, 16, 23, 30 and 38.

A leading practice approach for field-scale cover system trials in Queensland

A. Volcich[A], and L. Nicolson[B]
[A]Principal Environmental Scientist, Environmental Geochemistry International, Brisbane.
antony.volcich@geochemistry.com.au
[B]Lead Technical Advisor, Office of the Queensland Mine Rehabilitation Commissioner, Brisbane

Keywords: mine waste, cover system design, trials, Queensland

1.0 ABSTRACT

Cover systems constitute one part of the total acid and metalliferous drainage management strategies required to arrest AMD on mines hosting potentially acid forming materials. Cover design is influenced by a range of factors such as the prevailing climate, materials available to construct the cover, the risk of mobilising contaminants and their potential impact on the environment. The cost of constructing a mine waste cover at scale in remote locations can be considerable.

Evaluating alternate cover system designs is an important step to develop the final, site-specific cover system design. Trials demonstrate the performance and constructability of a cover design and provide valuable field data to calibrate and validate the numerical model/s used to inform the cover design.

We developed a 5-step approach to conduct pragmatic, cost-effective field-scale trials that avoid prescribing excessive requirements. While focussed on environmental conditions in Queensland, the approach draws on international guidance and assumes a store-and-release design as the most appropriate type of cover system.

Using the leading practice approach, a field-scale trial will follow the steps below:

- Step 1 – Determine cover system objectives and design options (identify cover objectives, collect baseline information, model cover performance, identify a suitable cover design for a field-scale trial, prepare construction specifications).
- Step 2 – Plan the field-scale trial (identify trial objectives, determine the trial design, choose a suitable location, determine trial location and size of test cells, set study duration, and design the monitoring system).
- Step 3 – Undertake the field-scale trial (construct and monitor).
- Step 4 – Refine the design based on trial outcomes.
- Step 5 – Report on the trial.

The approach presents a strategy to develop a series of cover system design options, identify the most appropriate design, test its constructability and performance at field-scale and report on its effectiveness. We note that while cover systems provide one way to reduce AMD risks, priority must be given to source control for successful closure outcomes.

A case study assessment of the failure of net acid generation testing in the presence of Mn-containing phases

A.R. Gerson[A], G. Levay[B], P. Clay[C], A. Pandelis[D]
[A]Blue Minerals Consultancy, Marlborough, New Zealand. andrea@blueminealsconsultancy.com.au
[B]Levay & Co. Environmental Services, Edinburgh, South Australia
[C]MMG Rosebery, Rosebery, Tasmania
[D]MMG Rosebery, Rosebery, Tasmania

1.0 INTRODUCTION

The net acid generation (NAG) test is one of the two key components of the AMIRA classification system for assessment of the risk of acid mine drainage (AMD) from mine wastes (AMIRA, 2002). The objective of the NAG test is to dissolve all reactive sulfide minerals, resulting in the release of acid, and carbonate minerals, resulting in the release of neutralisation, to provide a measure of net acid generation.

Catalytic and/or rapid decomposition of peroxide (H_2O_2), used during NAG testing to promote sulfide mineral oxidation, has been reported in the literature (e.g. Stewart et al. (2003)) and is associated with rapid temperature increase. When H_2O_2 decomposition is sufficiently severe and rapid and is not the result of leaching of acid-forming minerals, their incomplete leaching can result, giving rise to erroneously elevated NAG pH values and the possibility of incorrect and reduced risk AMD classification.

H_2O_2 can act as both an oxidant and a reductant in acidic media, the half reactions for which are given in Eqn. [1] and Eqn. [2], respectively. For catalytic decomposition to occur 1) the non-peroxide reactant must have more than one oxidation state, 2) the energetics for both the oxidation and reduction reactions must be favourable and 3) the non-peroxide reactant used up in one of these reactions is reformed in the other. The catalytic decomposition of H_2O_2 by aqueous transition metal cations is a well-known phenomenon (e.g., Stadtman et al. (1990); Lin and Gurol (1998), Salem (2000)). However, as NAG test is carried out on solids, the examination of solid phases is focussed on herein.

Oxidant $\quad 0.5H_2O_2 + H^+ + e^- \rightarrow H_2O$ [1]
Reductant $\quad 0.5\,H_2O_2 \rightarrow 0.5O_2 + H^+ + e^-$ [2]

2.0 KNAG TESTING OF SYNTHETIC SAMPLES

It has been observed previously that samples containing elevated concentrations of sludge from the effluent treatment plant (ETP) at the MMG Rosebery (Tasmania, Australia) site gave rise to rapid H_2O_2 decomposition. These sludges are likely to contain Pb, Zn, Mn and Fe oxides/hydroxides. Hence, the presence of oxides/hydroxides of Mn and/or Fe, both of which have more than one oxidation state, in NAG test solids are likely culprits of rapid H_2O_2 decomposition.

The following methodology was used to prepare and test precipitated Mn (Fe) samples:

1. Prepare 500 mL of 10, 20, 100 and 750 mg L^{-1} Mn^{2+} solution with $MnCl_2{\cdot}4H_2O$ (Fe^{3+} solution with $FeCl_3$).
2. Mix 2.5 g quartz with 250 mL of each solution. Record the initial pH. Titrate to pH 10.5 with NaOH solution under constant stirring. Filter the mixture at the end of the titration. Dry the solid and filter paper at 40°C.

3. The final precipitated concentrations of Mn or Fe are the equivalent of 0.1, 0.2, 1.0 and 7.0 wt% corresponding to 10, 20, 100 and 750 mg L^{-1}.
4. Put the dried filter papers into 250 mL 15% H_2O_2 solution (pH adjusted to between 4.5 and 6.0, temp = 20±2 °C) in a conical flask. Carry out KNAG test overnight with continuous measurement of temperature and pH.
5. The next morning, carry out a heating stage (approx. 90°C for 2 h). Allow the solution to cool and measure the pH of the leach liquor to give NAG pH.

Figure 1a shows a graph of the maximum temperatures and times to maximum temperatures for a 10:90 wt/wt rhodochrosite and quartz mixture and all the precipitated systems. The rhodochrosite containing system did not show rapid decomposition of H_2O_2. In contrast the 20 ppm precipitated Mn system gave rise to rapid heating and pH increase (KNAG data shown in Figure 1b) likely due to the reaction given in Eqn. [3]. The acid generating oxidation reaction (Eqn. [4]) did not occur to a significant extent as demonstrated by the rapid and stable pH increase.

Precipitated Fe hydroxide had little effect on NAG testing until 750 ppm precipitated Fe at which time a marked temperature spike, albeit with long lag time (77 min), and increase in pH was observed most likely due to the reaction given in Eqn. [5] possibly followed by Eqn. [6].

$$0.5MnO_{2(s)} + H^+ + 0.5H_2O_2 \rightarrow 0.5Mn^{2+} + H_2O + 0.5O_{2(g)} \quad [3]$$

$$0.5Mn^{2+} + 0.5H_2O_2 \rightarrow 0.5MnO_{2(s)} + H^+ \quad [4]$$

$$FeOOH + 0.5H_2O_2 + 2H^+ \text{ ® } Fe^{2+} + 0.5O_2 + 2H_2O \quad [5]$$

$$Fe^{2+} + H^+ + 0.5H_2O_2 \text{ ® } Fe^{3+} + H_2O \quad [6]$$

It is concluded that rapid decomposition of H_2O_2 during NAG testing of MMG Rosebery site samples is most likely due to the presence of MnO_2, formed either on weathering of Mn-containing carbonates or precipitation resulting from the ETP. This appears to be semi-catalytic with slower regeneration of MnO_2 from surface formed Mn^{2+} (note: catalytic decomposition of H_2O_2 was not observed on testing of aqueous Mn).

3.0 KNAG TESTING OF SITE WASTE STREAMS

KNAG tests were carried out on site samples using the same methodology except the sample consisted of 2.5 g (<75 µm) of material. The following behaviours, based on sample type, were observed:

Mill feed – no evidence of rapid H_2O_2 decomposition but only one composite sample has had KNAG testing.

End of mill Zn circuit tails (pre-ETP) – two out of four composite samples showed signs of H_2O_2 decomposition during KNAG testing. These two composites contained elevated Mn-carbonate concentrations which could be indirectly responsible. A further composite showed signs of decomposition of H_2O_2 upon sequential NAG testing also suggesting formation of a H_2O_2 reaction decomposition product on NAG testing.

End of flume tailings (post-ETP)– composite samples showed H_2O_2 decomposition behaviour as a (rough) function of concentration of sludge from the ETP, with some very short lag times until the maximum NAG liquor temperature was achieved (<5 min).

Mine water solids (pre-ETP) – did not show rapid H_2O_2 decomposition behaviour.

Bobadil tailings storage facility (TSF) tailings (post-ETP) – surface samples containing ETP sludge have likely shown rapid H_2O_2 decomposition behaviour (based on previous in-house reports) and

NAG pH >4.5 despite elevated NAPP values. Older deep samples, from which this sludge may have dissolved, did not.

Bobadil stages 11 and 12 potential construction materials – did not show any rapid H_2O_2 decomposition behaviour.

Table 1 provides a summary of the site samples for which KNAG measurements have been carried out (excluding construction samples). The data in Table 1 has been ordered with respect to the time to the greatest temperature. The samples fall within three categories:

1. Samples that have not passed through the mill or ETP have long lag times until maximum temperature (171–150 min) and positive $\Delta[H^+]$ (i.e., pH decrease) during KNAG testing (shaded in green).
2. Samples that have passed through the mill but not the ETP, or have passed through the ETP but consist of composites that always contain tailings, or are from deep within a tailings storage facility, show decreasing time to maximum temperature (70–31 min) correlated to decreasing $\Delta[H^+]$ (positive to negative, i.e., pH decrease and increase respectively) and greater acid neutralisation capacity (ANC) (pink shading)
3. Samples that contain elevated levels of ETP sludge all have negative $\Delta[H^+]$ (i.e., increased pH), short lag times (12–4 min) and elevated ANC.

The presence of ETP sludge increases the rate of H_2O_2 decomposition so that even with highly positive NAPP values, NAG pH greater than 4.5 can result. Increasing ANC appears to decrease the lag time until rapid H_2O_2 decomposition. Although it was shown that this is not caused directly by Mn-carbonates it may be caused by their oxidation products.

4.0 CONCLUSION

The measurements described herein demonstrate that NAG testing is not always reliable for MMG Rosebery site samples due to the likely presence of Mn oxides/hydroxides. This is specifically the case for waste streams that have passed through the effluent treatment plant, that have been subjected to rapid increase in pH, e.g., polishing pond sludges, or that have been subjected to sequential NAG testing. In these cases, an uncertain classification may result (i.e., NAG pH $\geq$4.5 and NAPP >0), whereas classification as potentially acid forming would be correct. It is suggested that NAG testing should not be used as a standard test on these materials. Consequently, a neutralisation potential ratio classification scheme which is reliant only on ANC and maximum potential acidity (based on CRS S assay, NPR=ANC/MPA) is recommended for these waste types:

Non-acid forming	NAF	NPR >2
Uncertain	UC	NPR >1and $\leq$2
Potentially acid forming	PAF	NPR $\leq$1

There is currently no evidence to suggest that single stage NAG testing is unreliable for end of mill (Zn tails), mill feed or waste rock samples.

NPR classification of the site waste streams samples is shown in Table 1. This results in a general shift to more conservative classification as compared to AMIRA classification, with under the NPR (AMIRA) classification of 6 (10) NAF classification, 3 (2) uncertain classifications and 7 (4) PAF classifications. However, only the mill feed, TSF bore hole and Zn tails samples are NAPP negative. Of these only the bore hole samples have been identified as being at risk of resulting in unreliable single stage NAG test outcomes. Classification as uncertain due to NAG pH $\geq$4.5 for historic PAF Bobadil tailings is dependent on the concentration of remaining sludge from the effluent treatment plant so that the risk may reduce with depth/age. However, should contemporary post effluent treatment plant tailings become highly

NAPP positive, as was the case for historic tailings, due to changes in ore mineralogy, the likelihood of erroneous classification as uncertain is likely to increase. Incorrect classification of PAF tailings as uncertain has implications for both tailings management and closure.

Similar issues concerning NAG test reliability may arise for other sites and a critical analysis of the NAG test for each site is recommended before adoption of NAG testing as a site wide standard methodology for AMD classification.

REFERENCES

AMIRA (2002) 'ARD test handbook: Project P387, A prediction and kinetic control of acid mine drainage' (Eds RSC Smart, WM Skinner, G Levay, AR Gerson, JE Thomas, H Sobieraj, R Schumann, CG Weisener, PA Weber, SD Miller, W Stewart) (AMIRA International Ltd.)

Lin S-S, Gurol MD (1998) Catalytic decomposition of hydrogen peroxide on iron oxide: Kinetics, mechanism, and implications. *Environmental Science & Technology* **32**, 1417–1423.

Salem IA (2000) Catalytic decomposition of H_2O_2 over supported ZnO. *Monatshefte fur Chemie* **131** 1139–1150.

Stadtman ER, Berlett BS, Chock PB (1990) Manganese-dependent disproportionation of hydrogen peroxide in bicarbonate buffer. P*roceedings of the National Academy of Sciences of the United States of America* **87**, 384–388.

Stewart W, Miller SD, Smart R, Gerson A, Skinner W, Thomas J, Levay G, Schumann R (2003) Evaluation of the net acid generation (NAG) test for assessing the acid generating capacity of sulfide minerals. In 'Proceedings of Sixth International Conference on Acid Rock Drainage (ICARD) Application and Sustainability of Technologies' Brisbane Queensland 12–18 July 2003 (Eds T Farrell, G Taylor) pp. 617–625= (Carlton South, AUSIMM, Cairns).

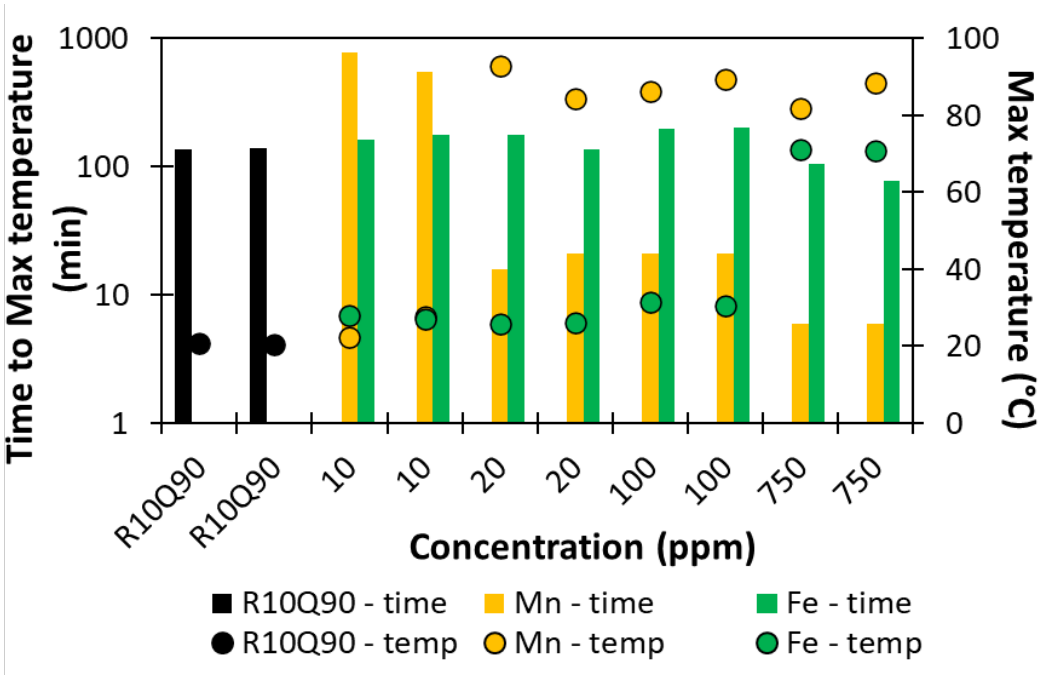

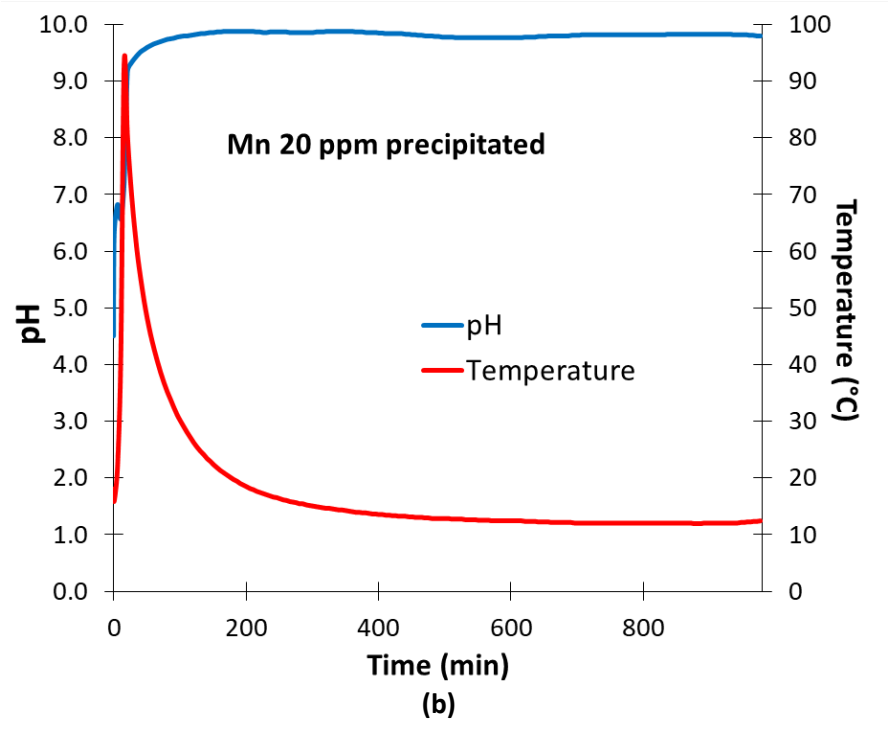

Fig. 1 **(a) maximum temperature and time (log scale) to maximum temperature for the rhodochrosite (R10Q90), and precipitated Mn and Fe KNAG tests. (b) Kinetic NAG test results for 20 ppm precipitated Mn.**

Table 1. **Summary of acid-base accounting for all Zn tailings, end of flume, and sludge samples on which KNAG testing has been undertaken. A positive $\Delta[H^+]$ value indicates a pH decrease and a negative value indicates a pH increase between the start of the NAG test and the maximum temperature. ANC and net acid production potential (NAPP = MPA–ANC) are in units of kg H_2SO_4 t^{-1}**

Description	ANC	NAPP	NAG pH	AMIRA class.	NPR	NPR class.	Time to peak temp. (min)	$\Delta[H^+]$ at max temp
Mill Feed	53	72	6.2	UC	0.4	PAF	171	9.35×10^{-6}
Mine water solids	40	−17	5.3	NAF	1.7	UC	150	6.08×10^{-5}
TSF bore hole	40	180	2.1	PAF	0.2	PAF	70	4.34×10^{-3}
TSF bore hole	42	125	2.4	PAF	0.3	PAF	60	4.24×10^{-3}
Zn tails	65	66	3.1	PAF	0.5	PAF	56	4.99×10^{-4}
Zn tails	109	33	4.1	PAF	0.8	PAF	41	4.11×10^{-4}
Post ETP, with tailings	111	−30	7.2	NAF	1.4	UC	40	-1.93×10^{-5}
Zn tails	99	24	8.3	UC	0.8	PAF	36	-1.98×10^{-5}
Zn tails	109	−40	8.4	NAF	1.6	UC	31	-1.58×10^{-5}
Polishing pond inlet	655	−649	9.3	NAF	112.9	NAF	8	-2.51×10^{-5}
Post ETP, no tailings	88	−12	9.0	NAF	0.9	PAF	12	-2.45×10^{-5}
Decant sludge	110	−79	9.1	NAF	3.5	NAF	9	-2.69×10^{-5}
Polishing pond	382	−376	9.0	NAF	65.9	NAF	9	-2.69×10^{-5}
Geotubes	652	−649	8.9	NAF	191.8	NAF	8	-2.69×10^{-5}
Post ETP, all combinations	128	−85	7.4	NAF	3.0	NAF	5	-1.58×10^{-5}
Post ETP, mine water	134	−84	8.6	NAF	2.7	NAF	4	-1.95×10^{-5}

Water quality modelling of backfilled pits in Australasia

L. Navarro[A] and P. Weber[B]
[A]Senior Environmental Research Scientist, Mine Waste Management, Christchurch, New Zealand.
leo.navarro@minewaste.com.au
[B]Principal Environmental Geochemist, Mine Waste Management, Christchurch, New Zealand.

Backfilling open-cut mine pits with waste rock is increasingly applied in Australasia as both a waste management solution and a closure strategy. It can provide environmental benefits such as reducing the footprint of surface waste rock dumps, stabilising final landforms, and, under saturated or sub-oxic conditions, promoting passive attenuation of contaminants (McCullough et al., 2024). However, it also presents risks, particularly the release of solutes directly into groundwater systems where interception and treatment are more difficult.

The performance of backfilled pits is highly site-specific. In some cases, saturated backfills have promoted denitrification and selenium reduction (Weilhartner et al., 2012), while in others, elevated sulfate and trace metal loads have been observed where readily soluble minerals are present (Watson et al., 2017). This variability highlights the need for robust testing and modelling approaches in closure planning.

We present two modelling backfill case studies from Australasia. The first case study mixes solute release from different geological units, using leachate data to define maximum and minimum ranges, with water volumes based on recharge through the backfill and mixing with aquifer inflows. The second case study represents a partially backfilled pit lake, where load release occurs during filling and is further constrained by solubility limits in PHREEQC.

These studies show how input datasets and conceptual models strongly influence predicted outcomes. Laboratory-based inputs yield higher and earlier concentration peaks, while scaled or solubility-limited cases produce more gradual release curves.

It is noted that laboratory leach tests such as SPLP, shake-flask, and kinetic column leaching experiments are commonly used to provide early indicators of solute release. These tests are valuable for identifying the “first flush” of salts and metals but often overestimate field conditions due to the use of finely crushed material with a high reactive surface area.To address these limitations, we propose intermediate-scale trials using IBCs (~1,000 L) and shipping containers (~30,000 L) filled with coarse waste rock. These trials better replicate field-scale particle packing, redox stratification, and heterogeneity, and are expected to generate leachates that more closely reflect actual backfill behaviour.

By linking laboratory testing, pilot-scale trials, in-situ validation, and modelling, we can build a stronger basis for closure planning and for balancing environmental benefits and risks of pit backfilling in Australasia.

References

McCullough, CD, Schultze, M, Vandenberg, J & Castendyk, D 2024, 'Mine waste disposal in pit lakes: a good practice guide', in AB Fourie, M Tibbett & G Boggs (eds), Mine Closure 2024: Proceedings of the 17th International Conference on Mine Closure, Australian Centre for Geomechanics, Perth, pp. 1063-1076, https://doi.org/10.36487/ACG_repo/2415_76

Weilhartner, A, Muellegger, C, Kainz, M, Mathieu, F, Hofmann, T & Battin, TJ 2012, 'Gravel pit lake ecosystems reduce nitrate and phosphate concentrations in the outflowing groundwater', Science of the Total Environment, vol. 420, pp. 222–228.

Watson, A, Linklater, C, Chapman, J & Marton, R 2017, 'Weathered sulfidic waste – laboratory-scale tests for assessing water quality in backfilled pits', 9th Australian Workshop on Acid Metalliferous Drainage, Sustainable Minerals Institute, The University

Use of x-ray fluorescence, thermogravimetric analysis and hyperspectral airborne survey to support and supplement geochemical mine waste characterisation

C.L. Burgers
Hancock Prospecting Pty Ltd, PO Locked Bag No. 2, West Perth, Western Australia, 6005, Australia.
colleen.burgers@hancrockrdg.com.au

1.0 Introduction

In Australia, in order to retain a tenement for exploration, an annual minimum expenditure must be met or the licence must be relinquished back to the State or Commonwealth. Specific legislation varies by state but the requirements are broadly the same. As a result, large amounts of survey, and cheaper non-intrusive data are collected, along with drilling. This paper presents how this information may be utilised for geochemical and mine waste characterisation at no additional analytical costs.

1.1 A terrestrial treasure trove of data

The application of automation in x-ray fluorescence (XRF) spectroscopy, lower-cost instrumentation, reduced counting times, and increased throughput in commercial laboratories has seen great advances in increased speed and lower costs for large volumes of sample assaying (Birch, et al., 1994). More consistent methods of sample preparation and instrument efficiency have expanded the element suite and achieved lower detection limits. The application of cloud-based laboratory information management systems has resulted in real-time grade control and more accurate geological block models. These factors have also greatly increased the volume of data available in exploration and conceptual project stages, such that even a resource at an inferred level (JORC, 2024)of definition, (particularly for base commodities of high volume, such as iron ore) may have tens of thousands of drillholes, with hundreds of thousands of data points. Thermogravimetric analysis (TGA) is required to measure the volatile mass liberated during preparation of the XRF fused bead, so that the sample will sum to 100% following the measurement of metal oxides.

1.2 An aerial abundance of surveys from the sky

Currently, several airborne survey technologies are used for exploration and geological and resource mapping. The primary use of these survey technologies is given briefly in **Table 4** from more detailed published reviews (Boyd & Isles, 2007; Mulè, et al., 2012; Minty, et al., 2009; Fairhead, et al., 2017; Bhargava, et al., 2024; Mehendale & Neoge, 2020). This type of geophysical data is incorporated into the geological models and seldom reviewed by as part of geochemical characterisation.

2.0 Supplemental Geochemical ASSESSMENT AND MATERIAL CHARACTERISATION

2.1 How to get more out of XRF

Sulfur and calcium (as CaO), silica, target metal oxides, as well as many minor and trace elements, are now included in standard analytical suites, as are at least three TGA temperatures: presented as integrated mass percent loss on ignition (LOI), for iron ore exploration in the Pilbara, WA. The

temperature ranges for TGA provide the integrated mass loss for the dehydration, dehydroxylation and combustion of the volatile component of a sample (Földvári, 2011).

In simple mineralogical assemblages, such as the Hammersley Group Brockman Iron Formation (BIF) and Marra Mamba Iron Formation (MMIF) of the Pilbara area of Western Australia the LOIs can be used to determine the presence of goethite, clay and carbonate minerals, as well as organic units. Sulfur by XRF is increasingly accurate with limits of reporting reaching 0.001%, which is lower than analysis by combustion (Sobek, et al., 1978). Hutt & Morin (2000) have demonstrated that even low-sulfur (<0.3% S) mine waste can generate acidity, so it is vital to be able to estimate neutralising potential from the assay database with a similar degree of confidence, prior to conducting geochemical characterisation.

2.1.1 Iron mineralogy

In XRF data iron content is reported as Fe%, as a molar conversion from the mass percentage of the oxide $FeO_{1.5}$. In weathered or hydrated iron formations, or secondary deposits such as Tertiary Channel Iron Deposits (CID), large portions of the Fe% is present as goethite (FeOOH). The mineralogy, whether Fe is present as goethite or hematite) has a significant effect on the grade and quality of the ore deposit and may be well estimated from dehydroxylation mass LOI to 371°C (more recent TGA report a higher temperature range to 425°C). The presence of hematite (Fe_2O_3) does not impact TGA mass changes and, a theoretically pure sample of Fe_2O_3 would show no LOI371%. Magnetite (Fe_3O_4) however, oxidises under combustion and gains mass, resulting in a negative LOI.

Figure 1 gives three arrangements of Fe % against LOI371%, LOI650 and Fe_3O_4%, as well as alumina% against LOI650%. The data populations have been labelled for the likely dominant iron mineral. Figure 1a) shows the 1:1 molar correlation for goethite (FeOOH) dehydroxylation (LOI371%) as a function of weight percentage, as well as a population of samples from the same site, containing magnetite, as indicated by Figure 1b). The hematite population demonstrates no mass loss or gain and no magnetism. The population labelled “Other Fe-mineral” is likely a combination of siderite ($FeCO_3$) (Kemp, et al., 2010)and stilpnomelane ($(K,Ca,Na)(Fe^{2+},Mg,Fe^{3+})_6\ Si_8\ Al(O,OH)_{27}\bullet 2\text{-}4H_2O$) (Hutton, 1938; Eggleton & S.W., 1964; Blake, 1965) both of which have significant Fe, combustion and dehydroxylation mass loss in the 650°C range. This is further supported by Figure 1d) that shows that the “Other Fe-mineral” population has low alumina, while the populations that contain goethite and hematite have been altered from the original magnetite and thus alumina is present along the kaolinite evolved water molar ratio.

For this deposit magnetite susceptibility was determined by Davis tube Recovery (DTR) while stilpnomelane and siderite were identified by x-ray diffraction (XRD). However, use of several XRF and TGA parameters in this method, can identify the presence of siderite or low alumina clays in waste material prior to XRD being conducted so that the much larger XRF database is validated and waste characterisation costs are reduced.

2.1.2 Clay Mineralogy

Phyllosilicate mineralogy can be complicated even when XRD is available. Using readily available XRF and TGA data can assist in upfront screening for more complicated mineralogy. Figure 2 shows the alumina (Al_2O_3) percent by XRF against the percent mass LOI at 650 °C (LOI650%) for a population of samples from the BIF. The mass ratio plots closely to a 1:2 molar ratio of Al_2O_3 to H_2O likely indicating kaolinite ($Al_2Si_2O_5(OH)_4$). Figure 3 shows the same plot for several different geological units where the

clay mineralogy is less simple. The Tertiary Detritals (TD) and MMIF are dehydrated with respect to kaolinite, likely indicating a mixture between a 1:2 and 1:1 alumina to water molar ratio mineral. Incorporation of cation data would assist in assessing the likelihood of smectite or serpentine groups. Also included in Figure 3 is the dolomitic Wittenoom Formation which shows that carbonate material can begin combusting at lower temperatures (Bartels, et al., 2024), and influence clay content determination. The presence of significant silicate minerals can thus be estimated in the screening phase and any potential contribution to acid neutralising capacity can be validated during laboratory testing (Weber, et al., 2005).

2.1.3 Carbonate mineralogy

In terms of mine waste management it is of great value to be able to quantify acid neutralising capacity (ANC) in the screening stages. The combination of magnesium (as MgO%) and calcium (as CaO%) assays by XRF and mass LOI at 1 000 °C (LOI1000%), which is the temperature of inorganic carbonate combustion, provides mineralogy (Kemp, et al., 2010; Földvári, 2011). Weber, et al., (2005) first demonstrated that the carbonate mineral content may be used to estimate ANC. Figure 4 shows the calcium and carbonate TGA range across several stratigraphies for a site in the Pilbara. It is clear that TD have distinct populations dominated by either dolomite or calcite, while the remaining units contain a fairly even mix between the two. Using the XRF-TGA data, it is simple to determine whether Ca, Mg or both, or LOI1000 is a better measure of carbonate-ANC and to identify populations that require further investigation. Figure 4 also shows that in the MMIF and Jeerinah Formation (JF) there is mass loss that is clearly not related to a calcium mineral and in these samples may either be organic matter or the presence of magnesite and that determinations of ANC cannot be predicated with CaO% or LOI1000%. The ANC assumptions based on this large assay database can then be validated with laboratory carbon-speciation and titratable ANC.

2.1.4 Impact of organic material

Combustion of organic material can occur across the entire standard temperature range with a slight correlation to degree of lithification. Figure 5 shows how the presence of an organic unit impacts the mass LOI in a population of samples from a CID by CO_2 evolution (Hutchinson & MacLennan, 1914). Total mass loss is high (>12%) and not proportional to the Fe, Al_2O_3 or CaO content.

2.2 A case study utilising airborne hyperspectral scanning

The aluminium-sulfate mineral, alunite ($KAl_3(SO_4)_2(OH)_6$), occurs either in primary deposits from hydrothermal or volcanic activity or as a secondary mineral from sulfide weathering. Equilibrium solubility products of low-pH mine waters, frequently indicate supersaturation with respect to jarosite or alunite, however, they are seldom detected by XRD in precipitates, suggesting either formation is slow at ambient conditions (Bigham & Nordstrom, 2000), or that, similarly to ferrihydrite minerals, the alunite group can be highly hydrated and poorly crystalline. Alunite is considered to be an acid generating sulfate but once formed, has low solubility in water (Chapman, et al., 1983).

While conducting waste characterisation at the Mulga Downs proposed development, in the Pilbara region, Western Australia, alunite was detected by semi-quantitative XRD in three samples in the basal Nammuldi Member of the MMIF and the upper JF shale. These units can contain significant sulfides and the presence of alunite is likely indicative of sulfide oxidation during a hydration event. However, unexpectedly, alunite between <1 to 4% was also detected in 10 samples of near-surface, TD with a low match probability (ICDD, 2023). Duplicate samples were sent to a second laboratory which

confirmed the initial detection. Alunite is considered to be an acid generating sulfate (Price, 2009) and the occurrence in this material was a concern for mineral waste management.

Airborne hyperspectral scanning, which delivers primary mineralisation of outcropping geology and maps showing variations in chemical composition and hydrothermal alteration (Bierwirth, et al., 1999), had been previously conducted for the Mulga area in 2013. The airborne hyperspectral scanner delivers 126 bands with approximately 18 nm width per band, of imagery over the 450 nm to 2 500 nm interval (Cudahy, et al., 2010). This information then undergoes several steps of processing to produce mineral maps of the regolith, which correlate well with mapped geological outcrops. In this way extensive soil mapping with significant detail of clay mineralogy, iron oxides, vegetation and carbonates may be determined (Haest, et al., 2013).

At Mulga Downs the hyperspectral survey detected large areas of dispersed alunite at the surface (Figure 6). When overlain with geological mapping, a strong correlation was found between the occurrence of alunite at surface and outcropping JF to the north, upgradient of the proposed mine. The addition of the hyperspectral survey indicates that the unexpected occurrence of alunite in weathered, surficial TD units in the Mulga Downs area, is likely from the weathering of sulfide-rich JF to the north and alluvial transport and deposition onto the site. The dissolution rates of alunite have been estimated to be low in several studies (Acero, et al., 2015; Miller, et al., 2014; Garvie, et al., 2014) and the apparent alluvial sediment transport of this material would also suggest that alunite is significantly resistent to weathering and does not pose an acid risk to water resources.

3.0 Conclusion

XRF and TGA assay data is routinely collected per metre, from surface to below mineralisation, with stratigraphy, rock type descriptions, 9 metal oxides, 2-3 minor anions (S, P, Cl), 3 TGA intervals and also frequently a suite of trace elements (As, Ba, Co, Cr, Cu, Ni, Pb, Se, Sn, Sr, V, Zn, Zr), often in enormous volumes. For example, at the Mulga Downs proposed mine more than 10,000 holes were drilled, with an average depth of 30 m below ground level, resulting in more than 6 million points of geochemical data, not including spatial, geological, weathering or groundwater data. Not all of this data is useful for mine waste management but as it is collected for resource definition, it presents “free” information that is statistically robust and should be relied on and referred back to.

The Pilbara iron ore mining assays data presented here leads to the following conclusions:

- The combination of Fe % against dehydroxylation mass loss at 371% can provide quantifiable estimations of goethite and hematite in conjunction with logging and stratigraphic data.
- The presence of other Fe-minerals such as siderite, magnetite and Fe-silicates may be detected with Fe% against LOI650% and other supplemental data such as DTR, if available.
- Investigating the alumina against evolved water at 650 °C provides quantifiable information on whether silicates are simple 1:1 layers or have variations that may be correlated with cation assays.
- The dominant carbonate mineral can be determined by plotting CaO% or MgO against LOI1000% so that ANC can estimated in initial screening and impact of clays, organic material, other calcium minerals or carbonates may be detected and accommodated with conservative waste characterisation parameters.
- The presence of unexpected material, such as organic lenses, can be identified and accurately logged with the TGA signature.
- Taking a broader view of the mining area to include geology offsite, and survey data not normally included in waste characterisation can provide crucial clues to the origin and evolution of waste units presumed to be weathered and inert.

References

Acero, P., Hudson-Edwards, K. A. & Gale, J. D., 2015. Influence of pH and temperature on alunite dissolution: Rates, products and insights on mechanisms from atomistic simulation. *Chemical Geology,* Volume 419, pp. 1-9.

Bartels, M. et al., 2024. Parts-Per-Million Carbonate Mineral Quantification with Thermogravimetric Analysis-Mass Spectrometry. *Analytical Chemistry,* pp. 96 (11), 4385-4393.

Bhargava, A. et al., 2024. Hyperspectral imaging and its applications: A review. *Heliyon,* 10 (e33208), p. 15.

Bierwirth, P., Blewett, R. & Huston, D., 1999. Finding new mineral prospects with HYMAP: early results from a hyperspectral remote-sensing case study in the west Pilbara. *Australian Geological Survey Organisation Research Newsletter,* Issue 31, pp. 1-3.

Bigham, J. M. & Nordstrom, D. K., 2000. Chapter 7: Iron and aluminium hydroxysulphates from acid sulphate waters. In: C. N. Alpers, J. L. Jambor & D. K. Nordstrom, eds. *Reviews in mineralogy and geochemistry: Sulphate Minerals – Crystallography, geochemistry and environmental significance.* Washington, D.C.: Mineralogical Society of America, 40 (1), pp. 351-403.

Birch, S. L., Norrish, K. & Metz, J. G. H., 1994. *Standard XRF Analytical Methods for the Mining, Mineral Processing and Metallurgy Industry.* Colorado, International Centre for Diffraction Data, pp. 353 - 359.

Blake, R., 1965. Iron Phyllosilicates of the Cuyuna District in Minnesotal. *The American Mineralogist,* 50(January-February), pp. 148-169.

Boyd, D. & Isles, D. J., 2007. *Geological Interpretation of Airborne Magnetic Surveys - 40 Years On.* In 'Proceedings of Exploration 07: Fifth Decennial International Conference on Mineral Exploration' Toronto, Canada., 9-12 September 2007. (Ed B. Milkereit) pp. 491-505.

Chapman, B. M., Jones, D. R. & Jung, R. F., 1983. Processes controlling metal ion attenuation in acid mine drainage streams. *Geochimica et Cosmochimica Acta,* Volume 47, p. 1957–1973.

Cudahy, T. et al., 2010. Mapping Soil Surface Mineralogy at Tick Hill, North-Western Queensland, Australia, Using Airborne Hyperspectral Imagery. In: R. V. Rossel, A. McBratney & B. Minasny, eds. *Proximal Soil Sensing - Progress in Soil Science 1.* Dordrecht: Springer, pp. 211-229.

Eggleton, R. & S.W., B., 1964. *The Crystal Structure of Stilpnomelane Part I. The Subcell..* Madison, Wisconsin, USA, Cambridge University Press, pp. 49-63.

Fairhead, J., Cooper, G. & Sander, S., 2017. *Advances in Airborne Gravity and Magnetics.* In 'Proceedings of Exploration 17: Sixth Decennial International Conference on Mineral Exploration'. Toronto, Canada, 22-25 October 2017, (Eds V. Tschirhart and M.D. Thomas), pp. 113-127.

Földvári, M., 2011. *Handbook of thermogravimetric system of minerals and its use in geological practice.* Volume 213, Geological Institute of Hungary,: Budapest, Pp 179.

Garvie, A. et al., 2014. *Oxidation and Solute Accumulation in Pit Wall Rock: Limiting Changes to Pit Lake Water Quality.* 29 April - 2 May 2014, Pp.339-350, Proceedings of the Eighth Australian Workshop on Acid and Metalliferous Drainage (Eds H Miller and L Preuss), Adelaide, South Australia.

Haest, M. et al., 2013. Unmixing the effects of vegetation in airborne hyperspectral mineral maps over the Rocklea Dome iron-rich palaeochannel system (Western Australia). *Remote Sensing of Environment,* Issue 129, pp. 17-31.

Hutchinson, H. B. & MacLennan, K., 1914. The determination of soil carbonates. *The Journal of Agricultural Science,* pp. 6 (3), 323-327.

Hutt, N. & Morin, K., 2000. *Observations and Lessons from the International Static Database (ISD) on Neutralizing Capacity.* Denver, USA, Society for Mining, Metallurgy, and Exploration, pp. Vol I, 603-611.

Hutton, C., 1938. The stilpnomelane group of minerals. *Mineralogical Magazine and Journal of the Mineralogical Society, 25 (163),* pp. 172-206.

ICDD, 2023. *International Centre for Diffraction Data.* [Online] Available at: https://www.icdd.com/

JORC, 2024. *Australasian Code for Reporting of Exploration Targets, Exploration Results, Mineral Resources, and Ore Reserves,* s.l.: The Joint Ore Reserves Committee (JORC) for Mineral Reserves International Reporting Standards .

Kemp, S., Wagner, D. & Mounteney, I., 2010. *Low level detection and quantification of carbonate species using thermogravimetric and differential thermal analysis,* Nottingham, UK: British Geological Survey.

Mehendale, N. & Neoge, S., 2020. *Review on Lidar Technology,* s.l.: SSRN.

Miller, J. L. et al., 2014. Alunite dissolution rates: Dissolution mechanisms and implications for Mars. *Geochimica et Cosmochimica Acta,* Volume 172, pp. 93-106.

Minty, B. et al., 2009. The Radiometric Map of Australia. *Exploration Geophysics,* 40(no. 4), pp. 325-333.

Mulè, S., Miller, R. & Carey, H. a. L. R., 2012. *Review of three airborne EM systems.* In 22nd International Geophysical Conference and Exhibition, Brisbane, Australia. 26-29 February 2012, ASEG Extended Abstracts, 2012:1, pp. 1-5. .

Price, W. A., 2009. *Prediction Manual for Drainage Chemistry from Sulphidic Geologic Materials,* Mine Environment Neutral Drainage Report 1.20.1; Natural Resources Canada;: Pp. 579.

Sobek, A. A., Schuller, W. A., Freeman, J. R. & Smith, R. M., 1978. *Field and Laboratory Methods Applicable to Overburdens and Minesoils,* Report Ref. EPA-600/2-78-054, United States Environmental Protection Agency (USEPA): Pp. 47-50.

Weber, P., Thomas, J., Skinner, W. & Smart, R., 2005. A Methodology to Determine the Acid Neutralization Capacity of Rock Samples. *The Canadian Mineralogist,* pp. Vol. 43, 1183-1192.

Table 4. A broad summary of airborne survey technologies, use and targets

Survey technology	Primary Use	Typical targets
Airborne Magnetic Surveys (AMR)	Structural mapping, magnetite bodies	Fe, Ni, intrusive targets
Airborne Electromagnetic Surveys (AES)	Conductivity anomalies	Sulfides, groundwater
Airborne Radiometric Surveys (ARS)	Surface lithology and alteration	K-rich rocks, U, Th, clays
Airborne Gravity Gradiometry (AGG)	Density contrast, deep structures	Iron ore, basins, kimberlites
Airborne Hyperspectral Imaging (HSI)	Surface mineral identification	Hydrothermal footprints
Airborne Light Detection And Ranging (LiDAR)	Terrain and structure mapping	Faults, veins, regolith

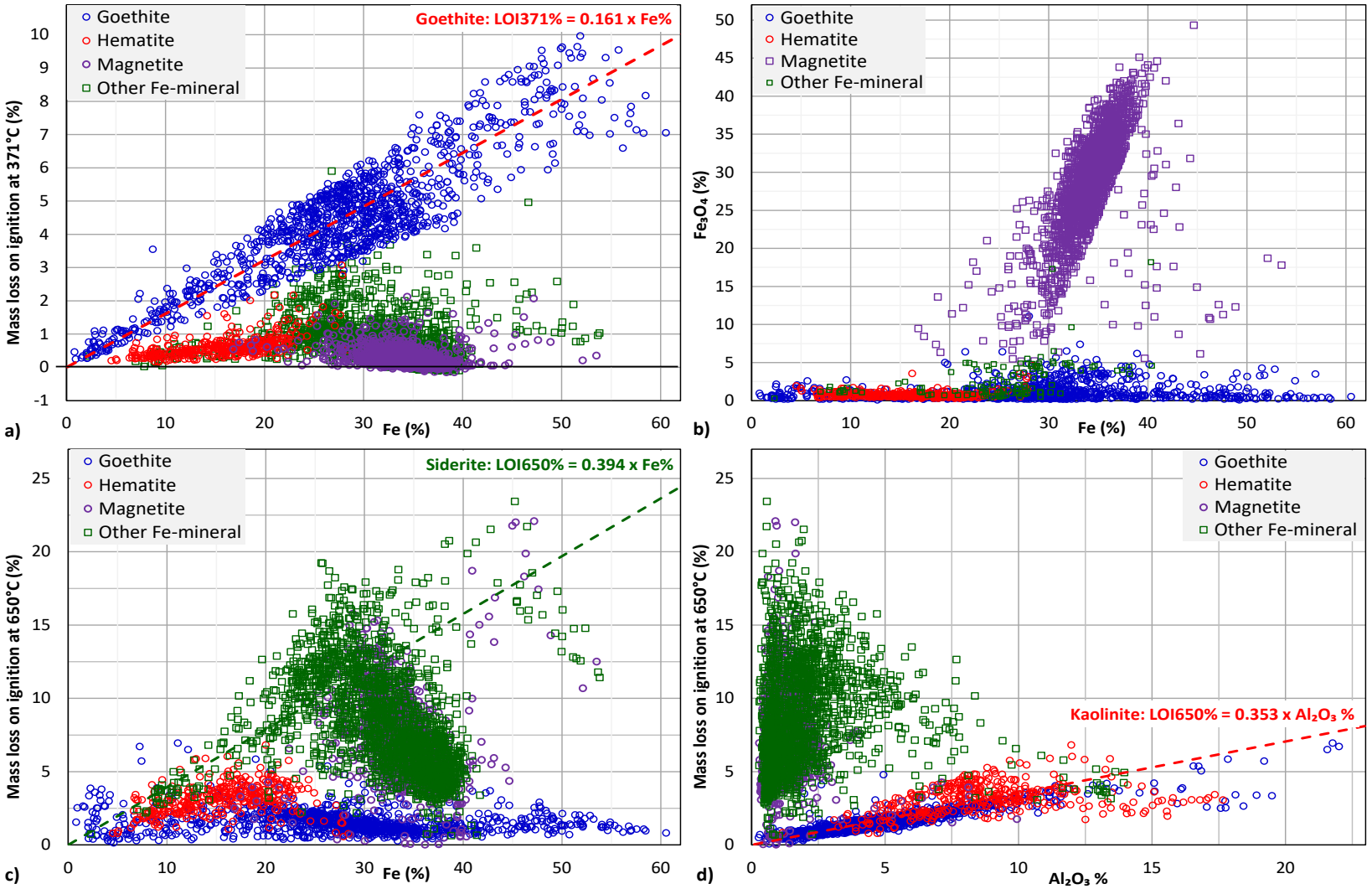

Fig 1. **Likely dominant iron minerals determined by XRF and TGA with supplemental magnetic data for selected populations from a magnetite deposit in the Pilbara: a) Fe% against LOI371% b) Fe% against Fe_3O_4% by Davis Tube Recovery (DTR), c) Fe% against LOI650% d) Al_2O_3% against LOI650%**

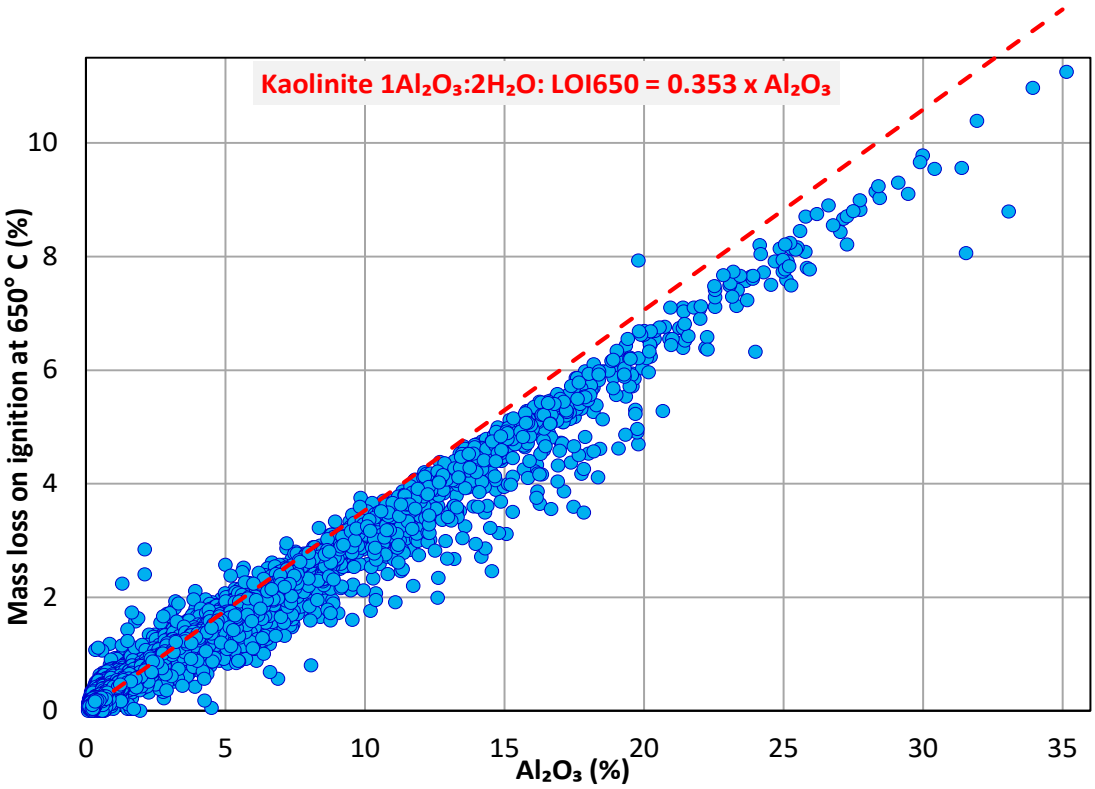

Fig 2. **Al_2O_3 mass percent by XRF against mass LOI at 650 °C % by TGA in Brockman Iron Formation indicating assays are close to the molar ratio of kaolinite**

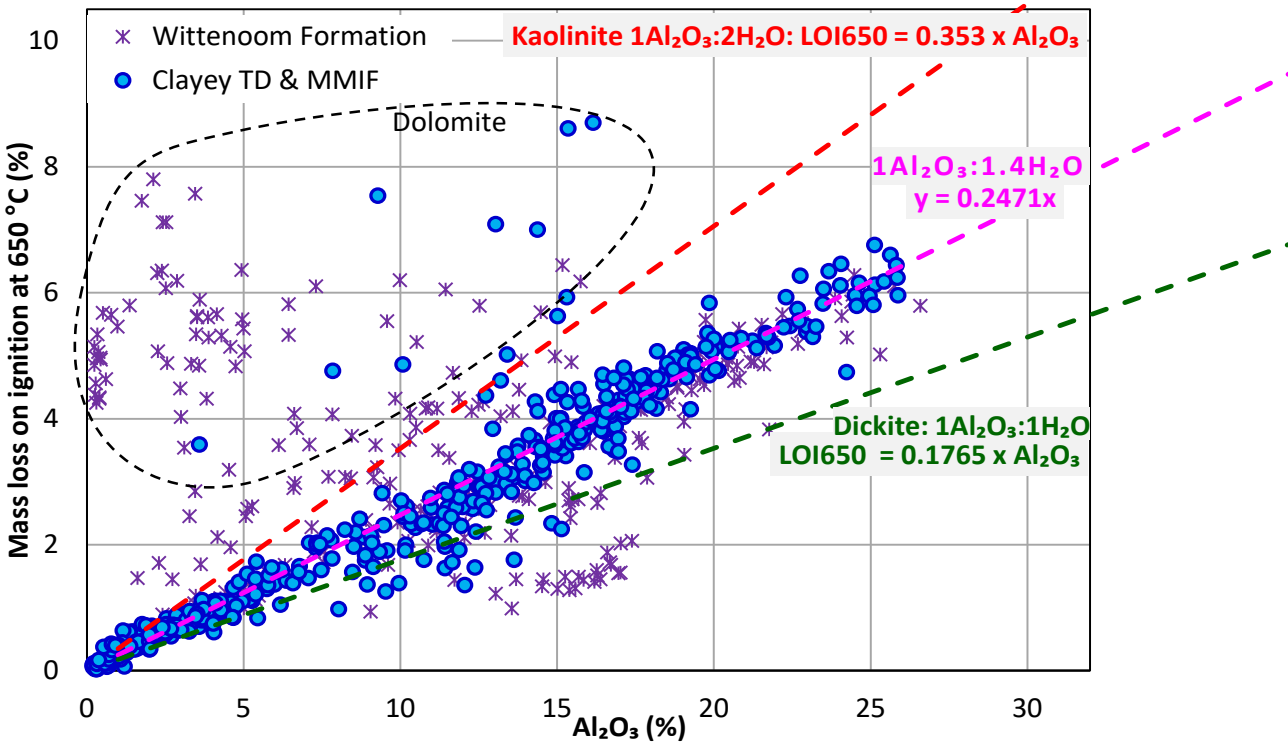

Fig 3. **Al_2O_3 mass percent by XRF against mass LOI at 650 °C % by TGA in clayey Tertiary Detritals and Marra Mamba Iron Formation indicating silicates are dehydrated with respect to the molar ratio of kaolinite and may comprise a mixture with dickite. Wittenoom Formation dolomite is also included to demonstrate that carbonate minerals can contribute mass loss below 650 °C**

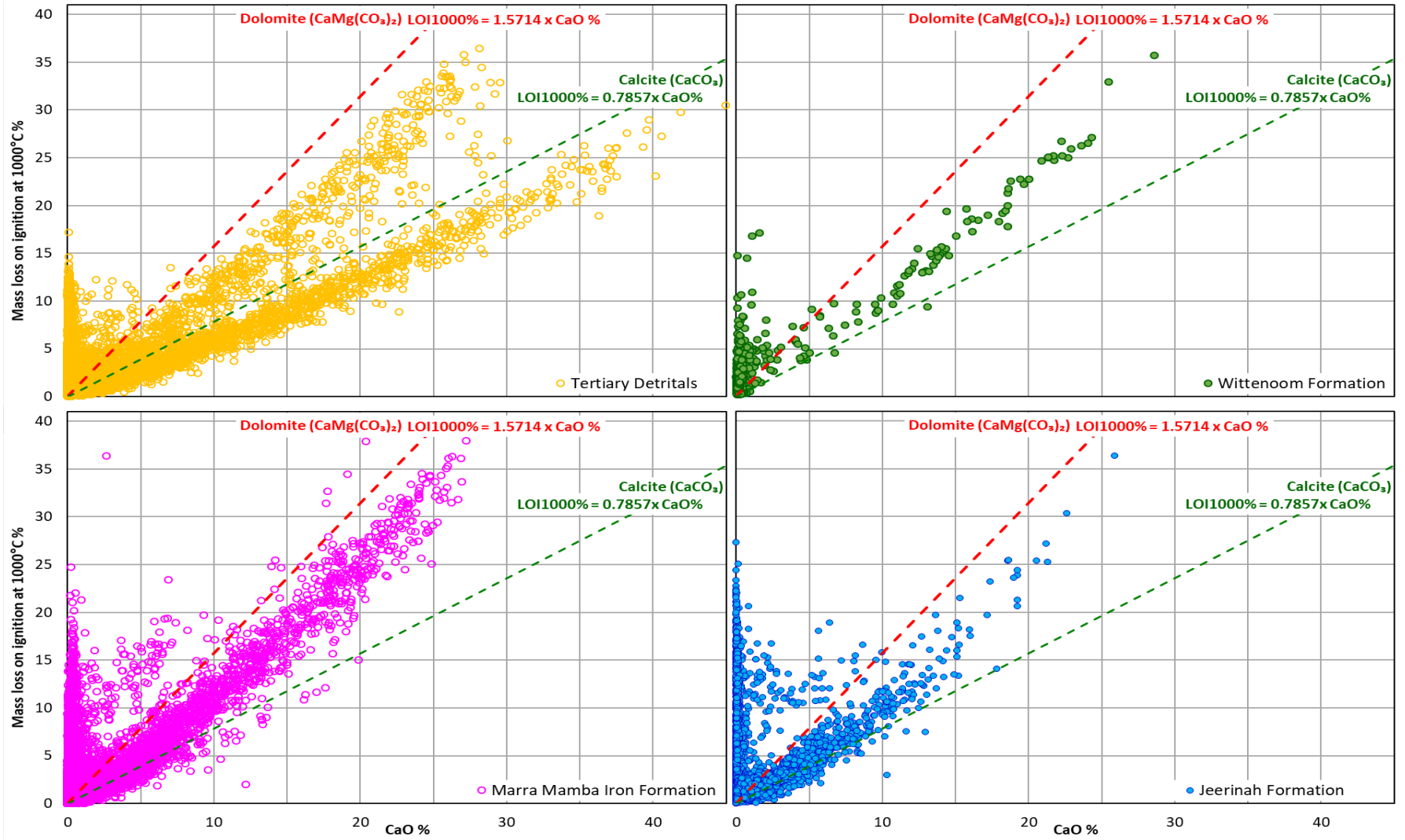

Fig 4. **Determining the mineralogy of calcium species and applicability as carbonate neutralising potential for drilling samples in Tertiary Detritals, Wittenoom Formation, and Marra Mamba Iron Formation, Jeerinah Formation organic shales**

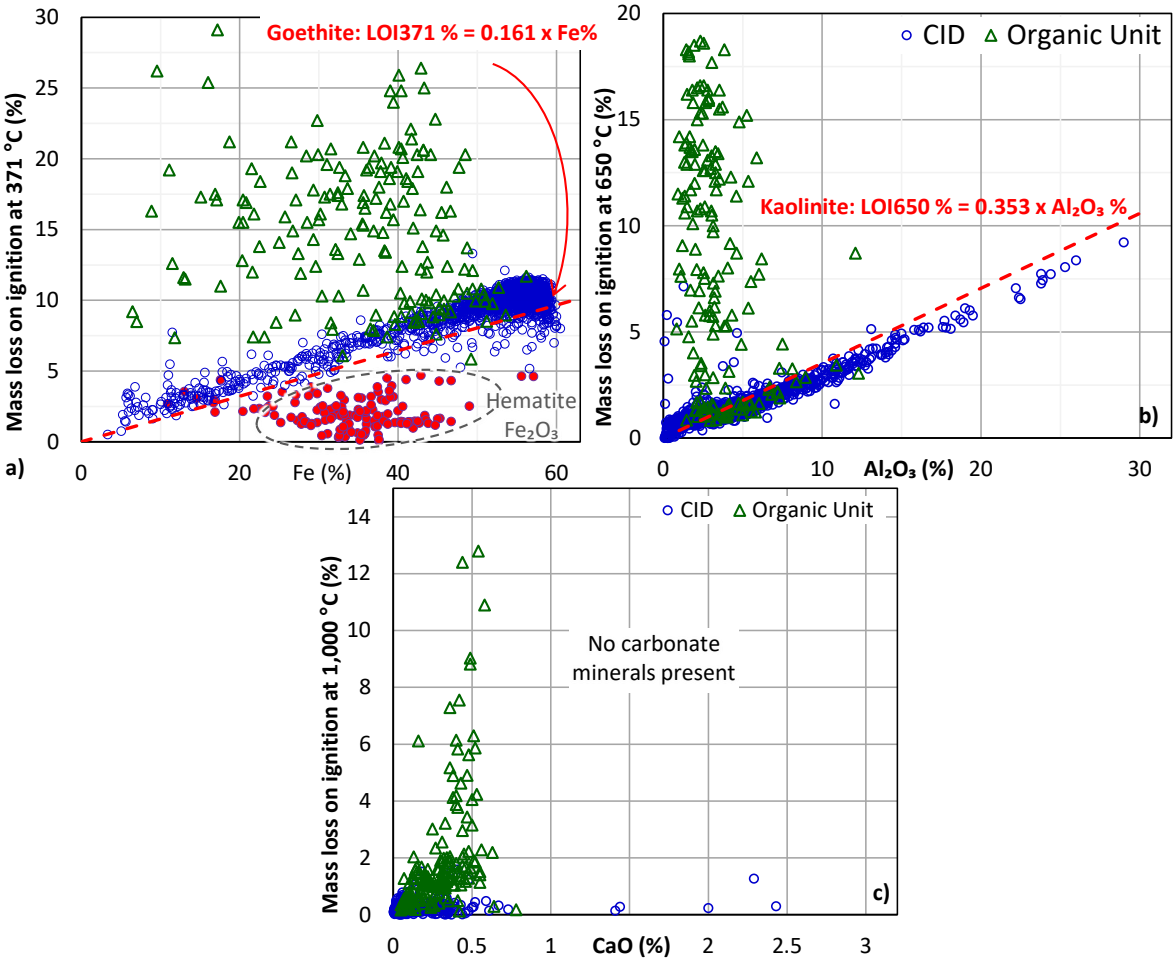

Fig 5. **An organic unit in Tertiary Channel Iron Deposits gives high LOI in all temperature ranges a) Fe % against LOI371% b) Al_2O_3 % against LOI650 % c) CaO% against LOI1000 % indicating material has no significant carbonate material**

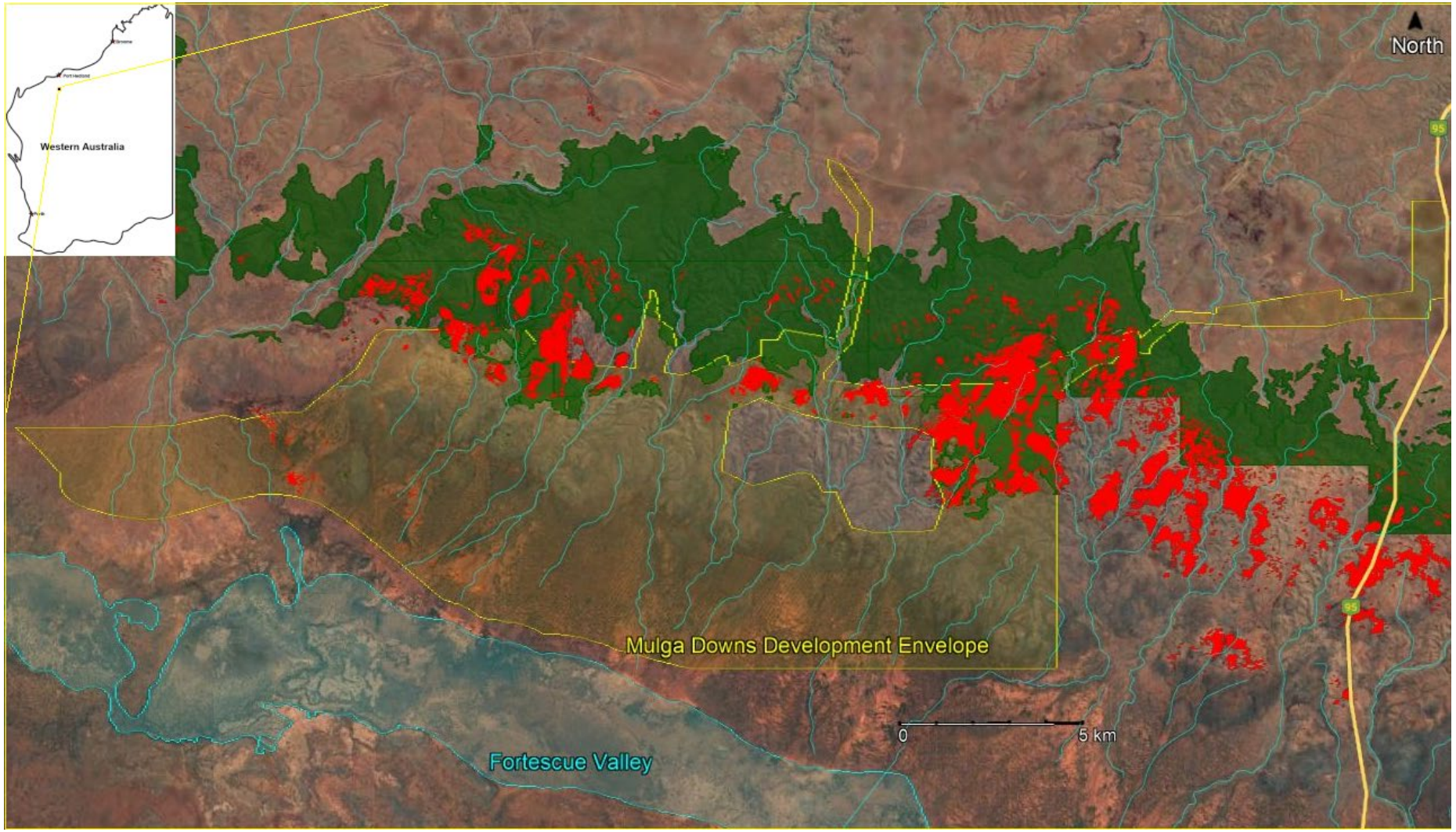

Fig 6. **Aerial image showing hyperspectral scanning results for alunite end-member spectra (red) and Jeerinah Formation outcrop (green) at the proposed Mulga Downs iron ore mine (development envelope shown in yellow) in the Pilbara region of Western Australia**

Understanding the sulfide oxidation behaviours in two AMD waste rocks from a gold mine

G. Qian[A], A. Gerson[B], N. Falk[A], T. Loney[A], M. de Groot[A], E. Dinsdale[A], H. Davies[C] and S. Harmer[A,D]

[A] College of Science and Engineering, Flinders University, Bedford Park, SA 5042, Australia.
gujie.qian@flinders.edu.au

[B] Blue Minerals Consultancy, Mahakipawa, Marlborough, 7281, New Zealand

[C] Newmont, Englewood, Colorado 80112, United States

[D] Flinders Microscopy and Microanalysis, Flinders University, Bedford Park, SA 5042, Australia

1.0 INTRODUCTION

In this study, two waste rock samples with contrasting acid and metalliferous drainage properties but similar pyrite contents, from a gold mine were examined with the objective of determining the cause of the different behaviours.

Acid and metalliferous drainage (AMD) is a global environmental issue, with the total cost of global environmental liabilities being in the order of US$100 billion (Wilson, 2008). AMD results primarily from the oxidation of pyrite (FeS_2) in the presence of both air (oxygen) and water (Johnson and Hallberg, 2005). In addition to oxygen and water, the presence of some oxidising bacteria (e.g., *Acidithiobacillus ferrooxidans*) can accelerate AMD formation (Baker and Banfield, 2003). Development of a long-term, sustainable AMD mitigation strategy require a complete understanding of AMD generation behaviours and any geochemical, mineralogical, and microbiological impacts.

This work was carried out as part of the CRC TiME 3.10 project to develop improved prediction and remediation strategies for AMD wastes from 12 national and international sites.

2.0 SAMPLES

The two waste rock samples were crushed to <4 mm for kinetic leach column (KLC) tests. Representative sub-samples (500 g) were pulverised into <75 µm for batch leaching, bulk assay, and acid-base accounting (Smart et al., 2002). A small portion of pulverised sample was further micronized for 10 min and spiked with 15 wt% corundum (internal standard; α-Al_2O_3) for quantitative X-ray diffraction (QXRD) analysis.

3.0 MINERALOGICAL AND GEOCHEMICAL CHARACTERISATION

QXRD showed that Samples A and B contained 3.9 and 3.5 wt% pyrite, respectively (Table 1). This is largely consistent with the chromium reducible S (S_{CRS}) assays of 2.44 and 2.30 wt%, corresponding to 4.6 and 4.3 wt% pyrite. Bulk assay revealed that 0.2 wt% fluorine and an extremely small amount of inorganic carbon (up to 0.02 wt%), likely as carbonate, were present in both samples.

Net acid generation (NAG) and acid neuralisation capacity (ANC) tests were performed as per Smart et al. (2002). NAG4.5 and NAG7 of both samples are in the range of 44 to 57 kg H_2SO_4/t, with NAGpH of 2.3 for both samples. The ANC of both samples are 2–3 kg H_2SO_4/t, indicating limited acid neutralisation potential. The maximum potential acidities (MPA = 30.6 × S_{CRS} wt%) are 75 and 70 kg H_2SO_4/t for Samples A and B, respectively. The net acid production potential (NAPP) values (MPA – ANC) were

calculated to be 73 and 68 kg H_2SO_4/t for A and B. These results suggest that both A and B are potentially acid-forming (PAF) waste materials.

4.0 BATCH DISSOLUTION AND ACTIVATION ENERGY CALCULATION

Batch leaching tests for A and B were carried out at 4, 20, 45 and 65 °C, with 10 g (±0.001) of sample (<75 µm) in 1 L Milli-Q water. An aliquot of 10 mL solution was collected at designated time intervals from each container and filtered through 0.22 µm syringe filters for solution ICP-OES analysis. After each solution collection, 10 mL fresh Milli-Q were added into each container. All containers were loosely capped throughout the batch leaching experiments to minimise evaporation and allow for oxygen saturation for sulfide oxidation. Solution levels were monitored 3–4 times per week, and fresh Milli-Q water was added to restore the original leachate volume when required.

Leachate S concentrations increased with temperature at a given reaction time, following *Arrhenius* behaviour (Putnis, 1992). Linear regressions were performed using the S concentrations from 14 to 63 days to obtain the 'long-term' rate constants (i.e., slopes from linear fittings) at different temperatures. Activation energy (E_a) values for sulfide oxidation for A and B were found to be 34.7 and 29.7 kJ/mol, respectively, using the *Arrhenius* method (He et al., 2025), suggesting that sulfide oxidation proceeds via an interface-reaction controlled mechanism (Brantley, 2008) and that the sulfide oxidation of A is slightly more temperature dependent (greater E_a). The E_a results here can be used to infer sulfide oxidation rates at any temperature, assuming the reaction mechanism does not change.

5.0 KINETIC LEACH COLUMNS

KLC (length 47 cm; diameter 12 cm) tests were carried out using 5 kg of crushed materials. Watering (166 mL Milli-Q water) and flushing (332 mL) were carried out weekly (except for the flushing weeks) and four-weekly, respectively, and completed within 1 min. After flushing, leachates were collected, filtered through 0.22 µm syringe filters, and measured to determine the leachate volume collected. Filtered leachate samples were then used for pH, EC, Eh, acidity titrations, and ICP-OES analysis to determine elemental concentrations.

Leachate pH dropped from pH 2.2–2.3 at week 8 to pH 1.7 for KLC A and to pH 1.9 for KLC B at week 12 and thereafter largely fluctuated within ±0.2 (Figure 1a). The acidity of KLC A increased from 17,000 at week 8 to around 27,000 mg $CaCO_3$/L at week 16 and thereafter constantly decreased until week 44 (6,500 mg $CaCO_3$/L). In comparison, the acidity of KLC B always decreased, from initially around 10,400 at week 8 to 4,400 mg $CaCO_3$/L at week 44 (Figure 1b). The acidities of KLCs A and B have almost doubled and tripled from weeks 44 to 92.

The significant decreases in pH and elevated acidities in the first 16 weeks appear to correlate with relatively high solution Eh and may be due to the dissolution of oxidised species, all of which coincide with initial high microbial activities (Falk et al. this proceeding). The Eh of KLC A decreased significantly from initially 675 mV (SHE) to around 610 mV after leaching for 40 weeks, whereas the Eh of the KLC B decreased from initially 625 mV to 607 mV at week 40. After week 40, Eh values of both KLCs have remained largely constant, with the average Eh being 611 and 612 mV (SHE) for KLCs A and B, respectively.

The concentrations of total Fe in the leachate samples and Fe/S molar ratios for KLC A are much greater than for KLC B (Figure 1c,d), despite that samples A and B have similar Fe (around 2.8 wt%) and pyrite contents (Table 1). Fe (oxy)hydroxides at 1 wt% were identified in sample A using TESCAN Integrated

Mineral Analyzer (TIMA). This phase, upon dissolution, is likely to lead to increased leachate Fe concentrations and consequent pyrite oxidation rates.

6.0 EXTENT OF REACTION AND ACID GENERATION/NEUTRALISATION RATES

The leachate S concentrations showed similar trends to the acidity profiles, with maximum S concentration observed at 16 weeks for KLC A (Figure 1e). Based on the leachate volumes and S concentrations, it was found that around 38% and 24% total S were dissolved after leaching for 92 weeks for KLCs A and B, respectively.

The calculated acid generation rate for KLC A, based on the leachate S data, was significantly greater than for KLC B (Figure 1f), with the greatest difference observed at week 20 (930 g H_2SO_4/week/t for KLC A *vs* 320 g H_2SO_4/week/t for KLC B). In comparison, acid neutralisation rates (ANR), calculated using Na, K, Mg and Ca leachate concentrations (data not shown), are largely similar for KLCs A and B, and remained almost constant after week 48. The relatively constant and small ANR (<10 g H_2SO_4/week/t) after week 48, as compared to much greater AGR (>150 H_2SO_4/week/t), suggests that neutralisation from silicate species does not contribute to the pH variations observed.

7.0 PRYITE OXIDATION RATE

Using leachate Eh, total Fe concentrations, and the Nernst equation (Li et al., 2016), ferric concentrations in leachates were calculated (Figure 1c). The ferric concentrations in the leachates for KLC A were found to be an order of magnitude greater than those for KLC B in the first 24 weeks, with the differences becoming smaller thereafter (average ferric 5.6 mg/L and 3.5 mg/L for KLC A and B, respectively).

Based on the ferric concentrations and the assumption of oxygen saturation in the KLCs, pyrite oxidation rates (per unit surface area per unit time) were calculated using the pyrite kinetic rate laws (ferric- and oxygen-controlled) developed previously (Williamson and Rimstidt, 1994). Pyrite oxidation in both KLCs is dominated by the ferric-controlled mechanism and is up to an order of magnitude faster than the oxygen-controlled pyrite oxidation (Figure 2a). Total calculated pyrite oxidation rate (sum of ferric- and oxygen-controlled rates) remained nearly constant after week 24 for both KLCs, with the average pyrite oxidation rate being 7.0×10^{-10} and 5.7×10^{-10} (mol/m^2/s), for KLCs A and B respectively.

The total pyrite oxidation rate and pyrite surface areas in KLCs A and B enables calculation of total pyrite dissolution per unit time (mol/s). The pyrite surface area changes with reaction time and can be calculated using the initial pyrite surface area (Figure 3) and the shrinking sphere model (Li et al., 2010). The calculated pyrite oxidation rates can then be compared to the experimental data. As shown in Figure 2b, the calculated pyrite dissolution rate per unit time (mol/s) remained almost constant after week 24 (3.5×10^{-9} in KLC A vs. 1.5×10^{-9} in KLC B).

Pyrite dissolution rate per unit time was also calculated using the leachate S concentrations ('measured' pyrite oxidation rate; Figure 2c), assuming that all the leachate S was from pyrite dissolution. Similar to the calculated pyrite dissolution, the 'measured' pyrite oxidation rate (mol/s) only showed small variations after week 24, with an average pyrite oxidation rate being 1.1×10^{-8} and 7.9×10^{-9} in KLCs A and B, respectively.

The calculated total pyrite surface area in KLC A is twice as much as that in KLC B, close to the ratio 2.3 of the calculated or 'measured' pyrite dissolution rate (per unit time) in KLC A to that in KLC B. This suggests that the larger total pyrite surface area in KLC A (Figure 3) is related to the faster pyrite

dissolution, in addition to the presence of 1 wt% Fe (oxy)hydroxide in sample A that possibly caused greater total Fe and ferric concentrations capable of accelerating pyrite oxidation.

In both KLC tests, the initial fast release of S in the first 24 weeks is possibly due to the dissolution of secondary sulfate species (0.27 wt% and 0.16 wt% sulfate S in A and B, respectively) and/or finer pyrite particles, likely resulting in an overestimation of initial pyrite dissolution rates. The differences between the calculated and 'measured' pyrite oxidation rates may result from application of the pyrite dissolution rate laws previously developed based on different pyrite batch dissolution methods (e.g., stirred and mixed flow reactors in the literature (Williamson and Rimstidt, 1994) vs. KLCs in this study) or potential microbial impacts on pyrite oxidation in KLCs A and B.

8.0 MICROBIOLOGICAL ANALYSIS

Both acidophilic Fe and S-oxidising bacteria capable of accelerating pyrite oxidation were detected in the leachate samples from KLCs A and B. KLC A showed greater RNA/DNA ratios, suggesting greater microbial activities, which may partly contribute to more rapid pyrite oxidation in KLC A. Different results (Fe, Eh, pH, cell counts) have also been observed between abiotic and biotic mini-batch leaching experiments, indicating that pyrite oxidation in samples A and B are partly microbially-controlled. For detailed results and discussion, readers are referred to the research work presented in Falk et al. (2025) in this proceeding.

9.0 CONCULSION

Two AMD wastes with similar pyrite contents (4.6 and 4.3 wt% pyrite in A and B, respectively) showed contrasting acid generation behaviours. Activation energies (E_a) resulting from batch leaching tests, suggest that pyrite oxidation in both samples proceeds via an interface reaction-controlled mechanism. These E_a may be used to predict pyrite oxidation at the site where the two samples were collected, assuming the reaction mechanism does not change. Pyrite oxidation rates, calculated using the leachate ferric and saturated oxygen concentrations, indicate that both control pyrite oxidation under the KLC conditions and that the ferric-controlled mechanism is predominant.

However, pyrite oxidation was found to be 50% faster in KLC A than in KLC B, possibly due to the larger total pyrite surface area and the greater leachate Fe (and ferric) concentrations contributed by the presence of 1 wt% Fe (oxy)hydroxides in A. The in-situ microbial communities in leachates were investigated by DNA sequencing. Acidophilic Fe and S-oxidising bacteria capable of accelerating pyrite oxidation were detected. Sample A exhibited higher microbial activity, which may also contribute to more rapid pyrite oxidation.

10.0 REFERENCES

Baker BJ and Banfield JF (2003) Microbial communities in acid mine drainage. *FEMS Microbiology Ecology* **44**, 139-152.

Brantley SL (2008) Kinetics of mineral dissolution, In ' Kinetics of Water-Rock Interaction' (Eds. SL Brantley, JD Kubicki, AF White) pp.151-210. (Springer New York).

He Z, et al. (2025) The mechanism and kinetics of the replacement of chalcopyrite by covellite under mild-hydrothermal conditions (120–200 °C). *Geochimica et Cosmochimica Acta* **401**, 122-135.

Johnson DB and Hallberg KB (2005) Acid mine drainage remediation options: a review. *Science of The Total Environment* **338**, 3-14.

Li J, et al. (2010) Chalcopyrite leaching: The rate controlling factors. *Geochimica et Cosmochimica Acta* **74**, 2881-2893.

Li Y, et al. (2016) Kinetics and mechanisms of chalcopyrite dissolution at controlled redox potential of 750 mV in sulfuric acid solution. *Minerals* **6**, 83.

Putnis A (1992) 'Introduction to mineral sciences'. (Ed A Putnis) (Cambridge University Press, U.K.).

Smart RSC, et al. (2002) ARD test handbook. *AMIRA International* http://www.amira.com.au/documents/downloads/P387AProtocolBooklet.pdf.

Williamson MA and Rimstidt JD (1994) The kinetics and electrochemical rate-determining step of aqueous pyrite oxidation. *Geochimica et Cosmochimica Acta* **58**, 5443-5454.

Wilson GW (2008) Why Are We Still Struggling Acid Rock Drainage? *Geotechnical News* **June**, 51-56.

Table 1. **QXRD results for Samples A and B.**

	Ab	Mc	Or	Ilt	Py	Ms	Ant	Qz	Kln	Amor.
A	47.7	28.6	11.2	5.6	3.9	2.4	0.3	0.3	--	--
B	37.8	22.6	11.0	16.0	3.5	1.6	--	1.5	2.0	4.1

Ab – albite; Mc – microcline; Or – orthoclase; Ilt – illite; Py – pyrite; Ms – muscovite; Ant – anatase; Qz – quartz; Kln – kaolinite; Amor – amorphous.

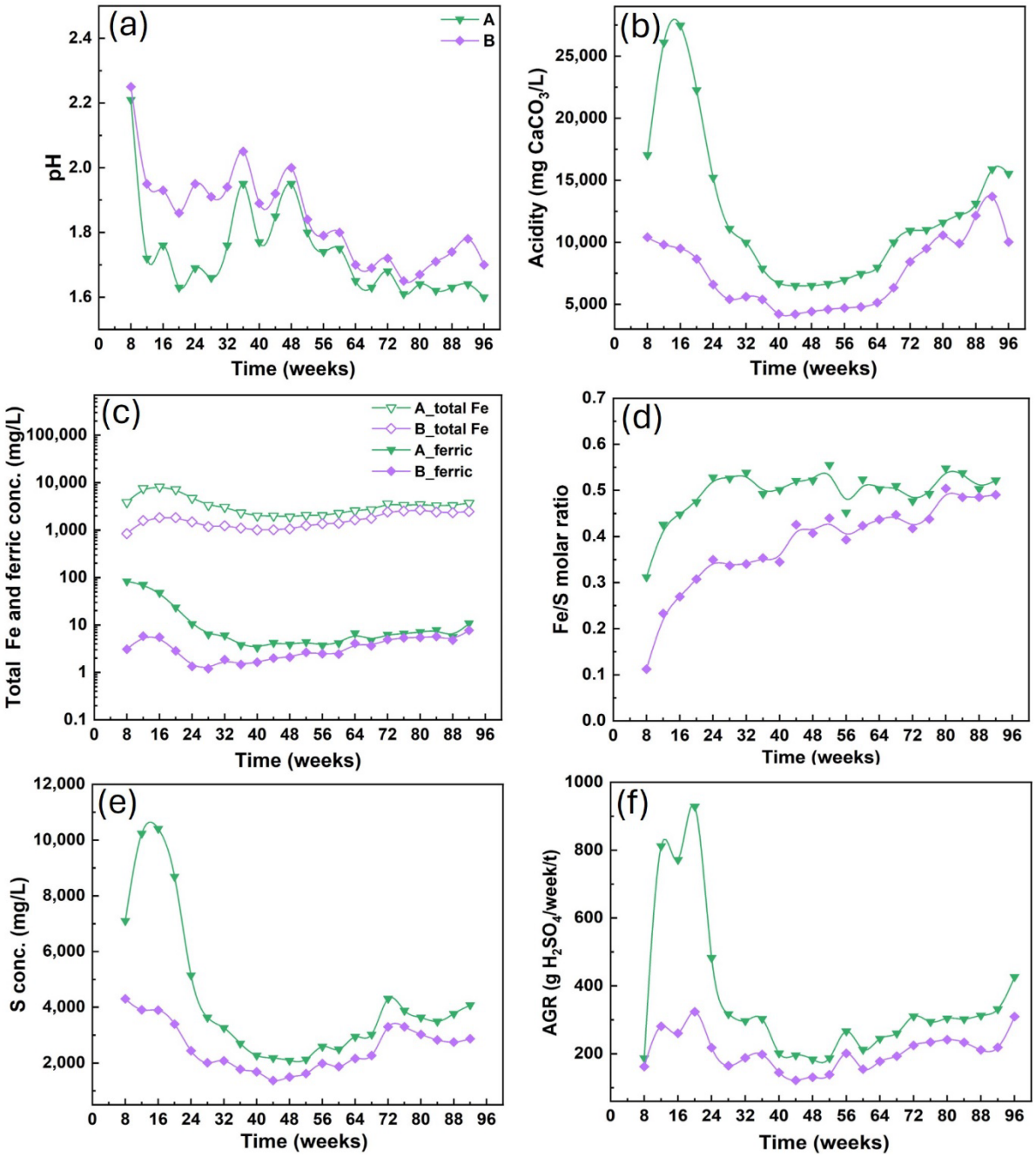

Fig. 1. **Leachate profiles for KLCs A and B. pH (a), leachate acidity (b), AGR (c), leachate S concentrations (d), total Fe and ferric concentrations (e), and Fe/S molar ratio (f)**

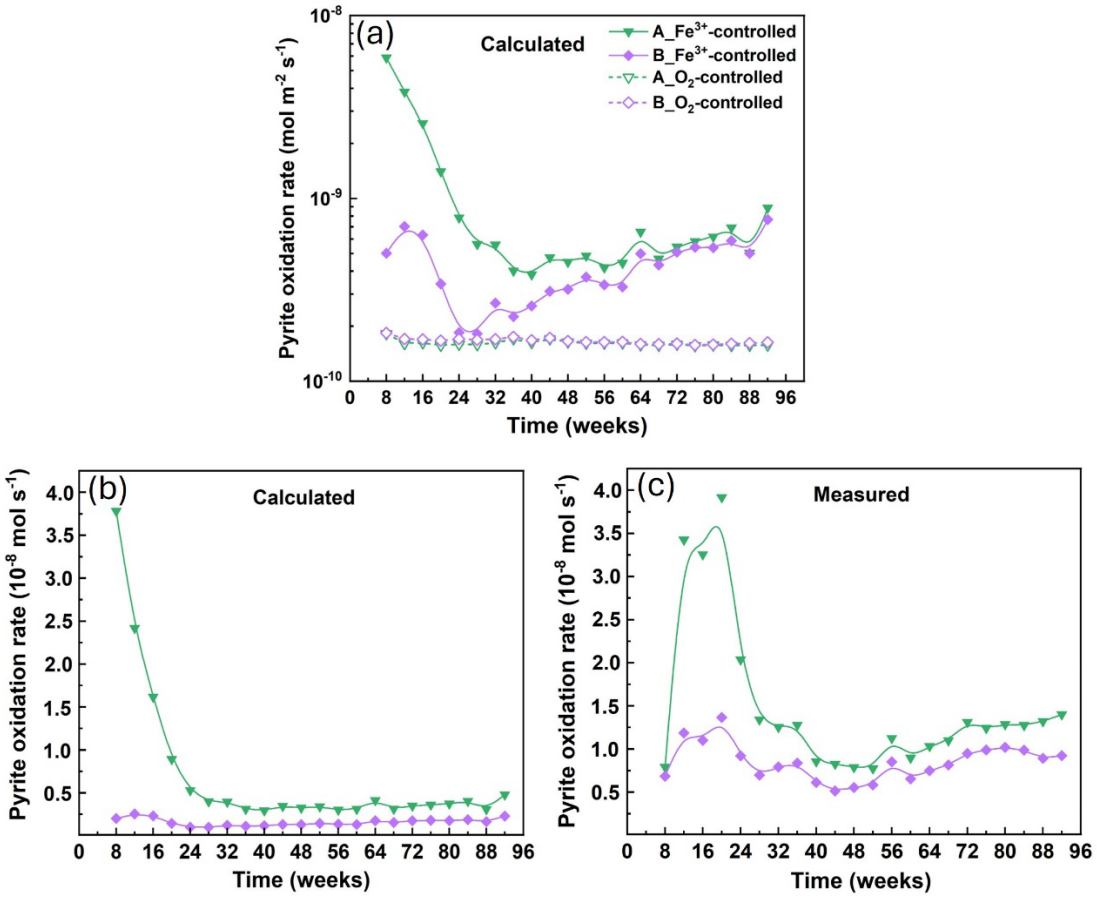

Fig. 2. **Pyrite oxidation rates for KLCs A and B. Calculated ferric- and oxygen-controlled pyrite oxidation rates (a), Pyrite oxidation rate per unit time (b), and pyrite oxidation rate per unit time based on measured leachate S data ('measured' pyrite oxidation rate) (c)**

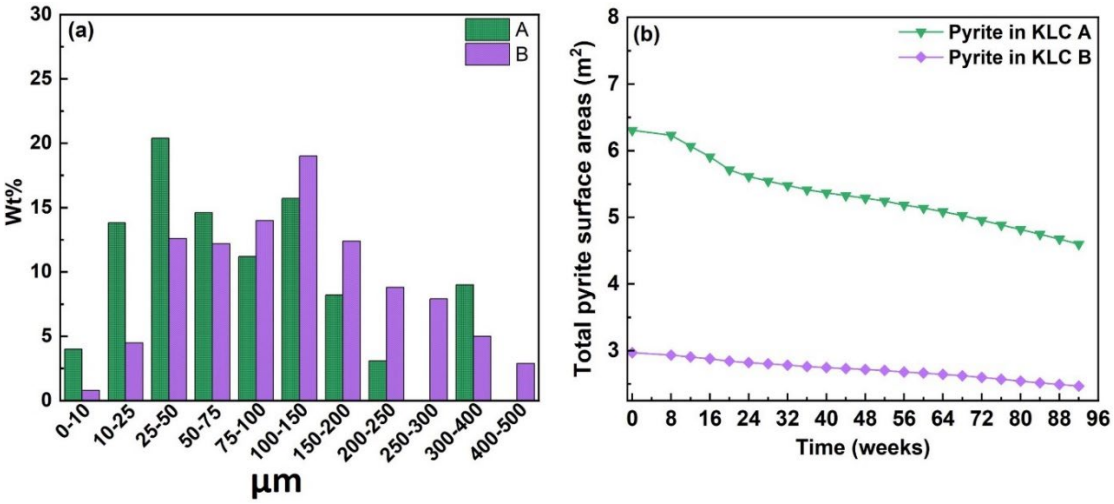

Fig. 3. **Pyrite grain size distribution in Samples A and B (a), and pyrite surface areas as a function of leach time in KLCs A and B (b). The initial total pyrite surface areas at time zero were calculated based on the pyrite grain size distribution, their relative mass fractions, and the pyrite contents in A and B from QXRD analysis**

Early Prediction of AMD through Integration of Hyperspectral and XRF Continuous Core Scanning-Based Geoenvironmental Indices in Queensland Mineral Systems

E.E. Sáez Salgado, A. Parbhakar-Fox, N. Fox and L.M. Jackson
W.H. Bryan Mining & Geology Research Centre, Sustainable Minerals Institute, The University of Queensland Experimental Mine Site, 40 Isles Road, Indooroopilly QLD 4068, Australia.
e.saezsalgado@uq.edu.au

1.0 INTRODUCTION

Acid and metalliferous drainage (AMD) remains one of the most pervasive geoenvironmental challenges in mining, capable of persisting for decades to centuries once triggered (Blowes et al., 2013; Lindsay et al., 2015). The environmental and socio-economic costs of AMD are profound, with global liabilities for remediation and treatment estimated at over US$100 billion (Vaziri, 2021). Conventional AMD forecasting methods, notably Acid-Base Accounting (ABA) and Net Acid Generation (NAG) tests, remain widely applied despite being costly and limited in their number and lack of mineralogical input (Parbhakar-Fox and Lottermoser, 2015; Dold, 2017). These limitations often result in heterogeneous materials being classified as uncertain or with their acid neutralisation capacity (ANC) being overlooked, constraining proactive risk management. Although modifications have been proposed (Dold, 2010; Mafra et al., 2020; Botero et al., 2024; El Aallaoui et al., 2024; Toubri et al., 2025), uncertainties persist, and these chemical laboratory tests continue as the industry standard.

Recent technological advances in drill core characterisation, such as continuous drill core hyperspectral imaging (HyLogger™, Schodlok et al., 2016; Fox et al., 2017b; Laukamp et al., 2023) and line-scan X-ray fluorescence (XRF; Croudace et al., 2019; Klawitter and Valenta, 2019), enable continuous, fast and non-destructive datasets integrating mineralogical and geochemical information. These datasets allow metre-scale evaluation of geoenvironmental indices and early domaining of mine waste materials. Building on previous work defining the Geoenvironmental Domaining Index (GDI; Jackson, 2020) and the HyLogger™ Geoenvironmental Index (Hy-GI; Parbhakar-Fox et al., 2018), this study tests their integration with line-scan calibrated sulphur measurements to predict AMD potential in four northern Queensland polymetallic deposits.

The main aim is to assess whether continuous drill core hyperspectral mineralogy combined with along-core XRF derived sulphur data can establish a scalable early workflow for AMD forecasting, bridging early exploration datasets with life-of-mine (LoM) waste management (Parbhakar-Fox and Baumgartner, 2023).

2.0 MATERIALS AND METHODS

2.1 Study Sites

The research focused on four representative mineral systems of northern Queensland: a) Baal Gammon (Sn-Cu) granite-related deposit, abandoned, with negligible ANC materials; b) Mount Isa (Cu-Pb-Zn-Ag) - SEDEX and epigenetic mineralisation, recently closed, known for carbonate occurrences; b) Ernest Henry (Cu-Au IOCG) large breccia pipe, currently operational, with ongoing AMD domaining efforts;

and d) Wolfram Camp (W-Mo) quartz-rich pipe deposit, abandoned, with locally calcite bearing horizons. Together, these sites provided >1,400 m of archived drill core from seven drill holes.

2.2 Hyperspectral Scanning

Approximately 1,466 m of drill core were scanned at the Geological Survey of Queensland (GSQ) Exploration Data Centre using the CSIRO HyLogger-3 system. This system measures spectral reflectance across the visible near- (VNIR; 350-1,000 nm), short wave- (SWIR; 1,000-2,500 nm), and thermal – infrared (TIR; 5,000-14,000 nm) ranges, enabling detection of hydrous silicates, iron oxides, sulphates, carbonates, and key silicates. Hyperspectral mineralogy was processed in The Spectral Geologist (TSG) software and composited at 1 m bins.

2.3 Geochemical Assays and XRF

Geochemical assays (ME-MS61™) for 79 core samples (26 m total) were used to calibrate sulphur contents. In parallel, Minalyzer CS line-scan XRF was applied to the 1,466 m of core, producing continuous profiles for 20 trace elements and 11 major oxides. Sulphur calibration was achieved by cross-matching 41 assay results, yielding a detection limit of 0.138% S.

2.4 AMD Validation Tests

Seventy pulp samples were subjected to static acid-base accounting (ABA) and net-acid generation (NAG) tests, while 48 samples underwent semi-quantitative X-ray diffraction (QXRD). These analyses enabled validation of sulphide and carbonate mineralogy, cross-checking hyperspectral indicators against established methods.

2.5 HyLogger™ Geoenvironmental Index (Hy-GI) Calculation

Hy-GI scores were calculated following Parbhakar-Fox et al. (2018), integrating mineral neutralisation potentials (NP) and reactivity ratios (RR) with relative hyperspectral intensities. When combined with sulphur values from assays or XRF, samples were classified into five AMD risk classes, ranging from classes with: a) high potential acid forming – high acid neutralisation capacity (Class 1 – High PAF and High ANC; Hy-GI >10,000; S >0.3%); b) high acid neutralisation capacity (Class 2 – High ANC; Hy-GI >40,000; S <0.3%); c) acid neutralisation capacity (Class 3 – ANC; Hy-GI: 10,000-40,000; S <0.3%); d) non-acid forming or Inert (Class 4 – NAF/Inert; Hy-GI: 0-10,000; S <0.3%); and e) potential acid forming (Class 5; Hy-GI <10,000; S >0.3%) future mine waste material.

3.0 RESULTS

The integration of hyperspectral mineralogy with calibrated sulphur values enabled a detailed classification of AMD risk across the four studied deposits (Figure 1). At Baal Gammon, three distinct domains were identified, including inert horizons, potentially acid-forming intervals, and mixed High PAF-High ANC zones where carbonate buffering was locally significant. In Mount Isa, the relative abundance of carbonates drove classifications, with large intervals falling into ANC or High ANC categories, while sulphide-rich zones were classified as High PAF-high ANC. Ernest Henry exhibited strong vertical zoning, transitioning from NAF/inert material near the surface to High PAF-High ANC horizons at intermediate depths, and sulphide-dominated PAF material at depth. Wolfram Camp was

largely inert, with only discrete horizons classified as PAF, although line-scan sulphur values tended to overestimate sulphide content.

4.0 CONCLUSIONS AND DISCUSSION

This study demonstrates the value of combining continuous drill core hyperspectral mineralogy with sulphur profiles for early AMD prediction. The approach provided conservative classifications, effectively capturing ANC domains overlooked by static AMD laboratory tests. It offers a scalable workflow for geoenvironmental domaining, producing high-resolution downhole profiles that inform waste segregation, blending, and facility design. By incorporating both sulphide and carbonate phases, the method enhances predictive accuracy and reduces uncertainty, supporting more sustainable mine planning.

REFERENCES

Blowes D, Ptacek C, Jambor J, Weisener C, Paktunc D, Gould W and Johnson D (2013) The Geochemistry of Acid Mine Drainage. Treatise on Geochemistry: Second Edition, 131-190, doi: https://doi.org/10.1016/B978-0-08-095975-7.00905-0

Botero YL, Demers I, Cisternas LA, Ávila A and Benzaazoua M (2024) A cleaner production strategy for acid mine drainage prevention of waste rock: A porphyry copper case. *International Journal of Mining Science and Technology* 34(8), 1163-1177, doi: https://doi.org/10.1016/j.ijmst.2024.07.012

Dold B (2010) Basic concepts in environmental geochemistry of sulfidic mine-waste management. *Waste management* 24, 173–198.

Dold B (2017) Acid rock drainage prediction: A critical review. *Journal of Geochemical Exploration* 172, 120-132, doi: https://doi.org/10.1016/j.gexplo.2016.09.014

El Aallaoui A, El Ghorfi M, Elghali A, Taha Y, Zine H, Benzaazoua M and Hakkou R (2024) Investigating the reprocessing potential of abandoned zinc-lead tailings ponds: A comprehensive study using physicochemical, mineralogical, and 3D geometallurgical assessments. *Minerals Engineering* 209, 108634, doi: https://doi.org/10.1016/j.mineng.2024.108634

Jackson L (2020). Mineralogical domaining of low grade and no grade zones using automated drill core logging. University of Tasmania. Thesis, 275, https://doi.org/10.25959/100.00034978

Klawitter M and Valenta R (2019) Automated Geological Drill Core Logging Based on XRF Data Using Unsupervised Machine Learning Methods. 6th International Conference on Geology and Mine Planning (GEOMIN - MINEPLANNING) 2019 Proceedings, Santiago, Chile.

Lindsay M, Moncur M, Bain J, Jambor J, Ptacek C and Blowes D (2015) Geochemical and mineralogical aspects of sulphide mine tailings. *Applied Geochemistry* 57, 157-177, doi: https://doi.org/10.1016/j.apgeochem.2015.01.009

Mafra C, Bouzahzah H, Stamenov L and Gaydardzhiev S (2020) Insights on the effect of pyrite liberation degree upon the acid mine drainage potential of sulfide flotation tailings. *Applied geochemistry* 123, 104774, doi: https://doi.org/10.1016/j.apgeochem.2020.104774

Parbhakar-Fox A and Baumgartner R (2023) Action versus reaction: how geometallurgy can improve mine waste management across the life-of-mine. *Elements* 19(6), 371-376. doi: https://doi.org/10.2138/gselements.19.6.371

Parbhakar-Fox A and Lottermoser, B (2015) A critical review of acid rock drainage prediction methods and practices. *Minerals Engineering* 82, 107-124, doi: https://doi.org/10.1016/j.mineng.2015.03.015

Parbhakar-Fox A, Fox N, Jackson L and Cornelius R (2018) Forecasting geoenvironmental risks: Integrated applications of mineralogical and chemical data. *Minerals* 8(12), 541, doi: https://doi.org/10.3390/min8120541

Toubri Y, Demers I, El Baroudi M and Benzaazoua M (2025) Combining static test outcomes with 3D numerical modeling as a new approach for upstream mine waste classification and acid mine drainage assessment. *Journal of Environmental Chemical Engineering* 13(2), 115967, doi: https://doi.org/10.1016/j.jece.2025.115967

Vaziri V, Sayadi AR, Mousavi A, Parbhakar-Fox A and Monjezi M (2021) Mathematical modeling for optimized mine waste rock disposal: Establishing more effective acid rock drainage management. *Journal of Cleaner Production* 288, 125124, doi: https://doi.org/10.1016/j.jclepro.2020.125124

a

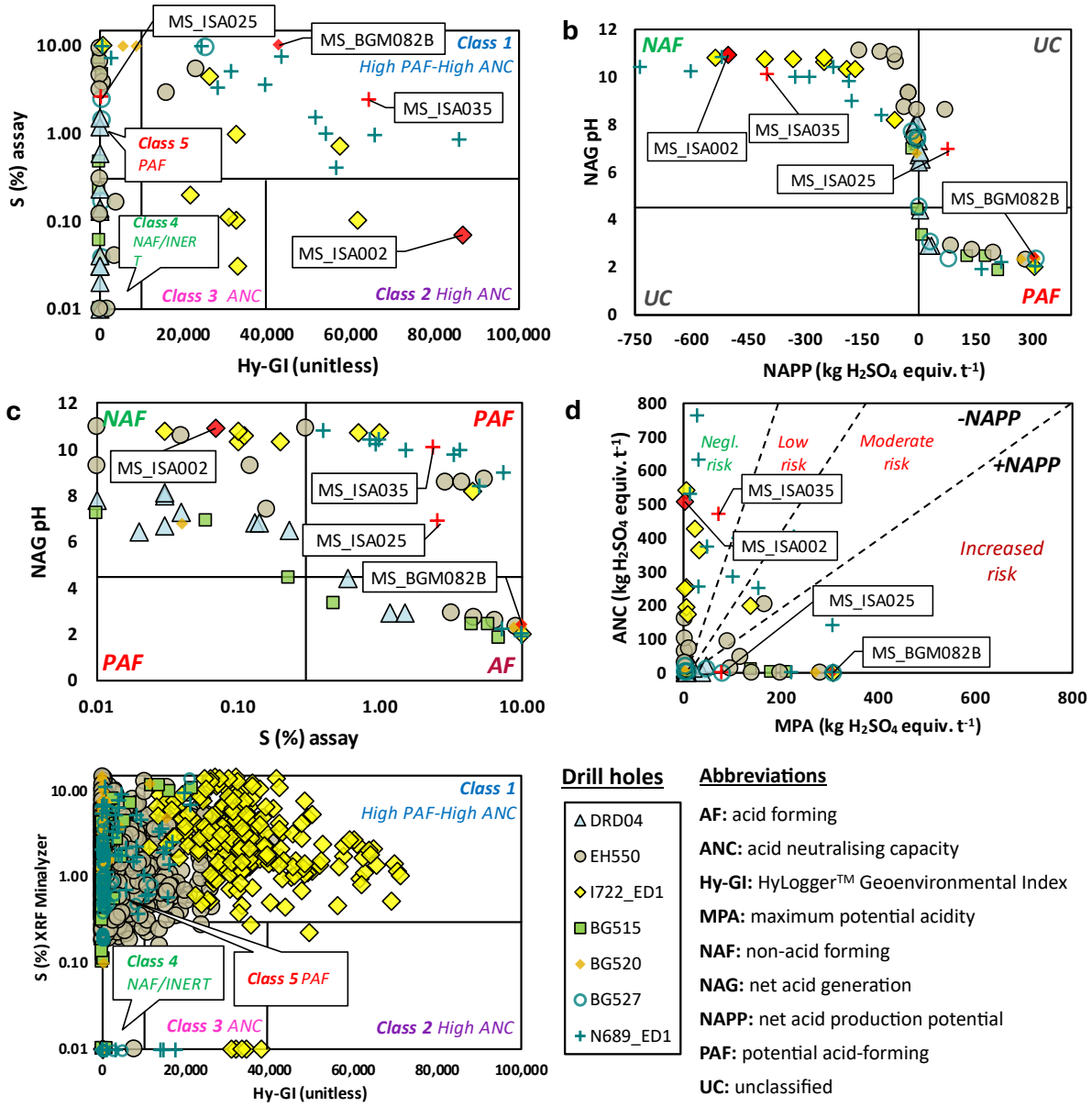

Fig. 1: **Classification of AMD conditions for samples (n= 79) from Baal Gammon (drill holes BG515, BG520 and BG527), Mount Isa (drill cores I722_ED1 and N689_ED1), Ernest Henry (drill hole EH550) and Wolfram Camp (drill core DRD04) deposits in northern Queensland. a) Hy-GI vs. sulphur values (S %) from assays - AMD risk zones; b) NAPP vs. NAG pH; c) Sulphur values (S%) from assays vs. NAG pH; d) MPA vs. ANC. Values from b, c and d are from static ABA-NAG classifications. Classification of samples MS_ISA002 (drill hole I722_ED1), MS_ISA025 and MS_ISA035 (N689_ED1), and MS_BGM082B (drill core BG520) is highlighted in red as example) Hy-GI vs. sulphur content (S %) from XRF Minalyzer CS analyses - AMD risk zones classification per metre for a total of 1,466 m of drill core.**

Estabilishing water quality crtiteria for protection of AMD-Impacted rivers using biological and chemical monitoring datasets: Hercules Mine Case Study

T. Robson[A], J. Crosbie[B] and C. Steyn[C]
[A]SRK Consulting (Australasia) Pty Ltd, Level 3/18-32 Parliament Pl, West Perth WA 6005.
trobson@srk.com.au
[B]Crosbie ESG Pty Ltd, Doonan QLD 4562
[c]MMG Australia Limited, 28 Freshwater Place, Southbank, VIC, 3006

1.0 INTRODUCTION

Acid and metalliferous drainage (AMD) source control and water treatment are primary tools in limiting deleterious effects on river systems. If these tools are to protect the biological health of receiving waters, and for financial resources spent on management to yield meaningful impact, it is essential that water quality objectives reflect the sensitivity of local aquatic ecosystems to acidity, sulfate salinity and metals/metalloids. In this case study, we present approaches and findings from an assessment of the Hercules Mine (Hercules), an inactive historical polymetallic operation in Tasmania. Historical mining practices between 1894 and 1999, left ongoing AMD discharge via adits and natural drainages, which are associated with influences on downstream aquatic ecosystems. The current tenement holders, MMG Australia, have commissioned multiple studies to understand the AMD source hazards, their relative contribution to discharged loads, and the key transport pathways in the system. These studies are informing rehabilitation and closure options and closure completion criteria for the site (Haywood et al. 2022). The primary aim of the assessment reported in this case study, was to derive site-specific surface water quality criteria (SWQC) for downstream freshwater creeks and rivers. We focus on the value of using a multiple-lines of evidence approach, particularly harnessing field-based data to extrapolate threshold toxicant concentrations that are protective of aquatic ecosystem function.

2.0 Environmental context

2.1 Mine location and surface water interactions

Hercules is located within the Pieman River catchment on the west coast of Tasmania, which has a wet climate (3,714 mm annually), 8 km south of Rosebery on the western flanks of Mt Hamilton. The steeply-inclined location and abundant rainfall encourage the transport of AMD-related contaminants into downstream freshwater creeks and rivers. Baker Creek and several natural flowlines, which drain the slopes of Mt Hamilton, transport AMD into the Ring River. The Ring River then flows northwest, where it enters the Pieman River near the location of the Bluestone Renison Tin Operation (Figure 1).

2.2 Protected environmental values, priority contaminants and default guideline values

The Tasmanian Government has established protected environmental values (PEVs) for Baker Creek (aesthetic water quality), Ring River below Baker Creek (aesthetic water quality, protection of modified aquatic ecosystems) and Lake Pieman (aesthetic water quality, protection of modified aquatic ecosystems, recreational water activities). The PEVs inform management goals for these three watercourses, and were informed by stakeholder engagement (DPIWE 2000). A holistic review of monitoring data (Section 5.2) and current site activities found that the current Hercules Mine discharge

is unlikely to materially compromise aesthetic and recreational use PEVs; therefore, protection of aquatic ecosystems was the focus when deriving SWQC. A systematic review of water quality datasets identified priority contaminants for management: pH, electrical conductivity (EC), Al, As, Cd, Cu, Fe, Pb, Mn, Ni, sulfate and Zn. Although the Tasmanian Environmental Protection Agency (EPA) has established stressor default guideline values (DGVs) for the Pieman catchment (pH, nutrients, salinity), which were informed by regional datasets (EPA 2021), catchment-specific DGVs have not been established for metals and metalloids.

3.0 Local water characteristics and implications for aquatic toxicity

Watercourses of the Pieman catchment are atypical of many regions in Australia, tending to be naturally acidic (typically <pH 6 and in some cases <pH 5) due to enrichment in humic/fulvic acids from soil runoff (dissolved organic carbon (DOC) in the order of 6–11 mg L^{-1}). Local waters are also soft (~7 mg L^{-1} as $CaCO_3$) and have low alkalinity (order of 2 mg L^{-1} $CaCO_3$). Some of these characteristics limit the capacity of the system to attenuate acidity from AMD inflows (low alkalinity, acidic water) and can increase toxicity of metals/metalloids (low hardness). However, the presence of elevated DOC can potentially partially mitigate metals/metalloid toxicity and local aquatic species are also necessarily adapted to acidic, organic waters (discussed further in Section 5.2). For instance, standard synthetic freshwater media compositions used for laboratory testing could not support the locally abundant water flea (*Ceriodaphnia* cf *spinata*), and a modified test method using catchment water was required. For these reasons, applying toxicant DGVs established for Australia as a whole is sub-optimal, both in terms of representativeness of local conditions and toxicological studies upon which they are based.

4.0 ASSESSMENT APPROACHES

4.1 Laboratory toxicological data

For the reasons discussed in Section 3, locally relevant laboratory toxicology data was limited to direct toxicity assessment (DTA) studies on locally prevalent water flea (*Ceriodaphnia* cf *spinata*), algae (*Auxenochlorella protothecoides*) and rainbow trout (*Oncorhynchus mykiss*), yielding median effective and lethal concentrations (EC_{50}, LC_{50}) and no-observable and lowest observable effective concentrations (NOEC and LOEC) for Zn (all species), as well as Cu and sulfate for *Ceriodaphnia* cf *spinata*.

4.2 Water quality and biological health monitoring

MMG and previous operators have maintained an extensive water quality sampling program (108 monitoring locations, sampled between 2000 and 2025) and biological survey (benthic macroinvertebrate diversity and abundance, algae coverage and fish counts) program at locations along Baker Creek and the Ring, Stitt and Pieman rivers (Figure 1). These monitoring programs, which have been running for 25 years in some locations, were driven by compliance requirements of environmental permits.

To supplement laboratory toxicological data, time-series data from water quality and biological monitoring location pairs, were used to correlate priority contaminant concentrations and biological metrics on a seasonal and interannual basis. Monitoring locations were selected to reflect the spectrum of mine water impacts along stretches of local rivers, also considering spatial relatedness and dataset quality for water quality locations. Reference sites, considered unimpacted by mining, were selected from Sterling River (location STR1), another tributary within the Pieman catchment, and locations on Baker Creek and Ring River upstream of known mining impacts (Figure 1). Surveys at STR1 informed biological reference conditions against which impacted sites were assessed, to extrapolate threshold

contaminant concentrations for biological health. An example of plots used to estimate threshold concentrations is given in Figure 2. Water quality data from reference sites were also used to estimate upper range (95% percentile), naturally occurring concentrations of priority contaminants and key parameters within the catchment.

5.0 RESULTS & DISCUSSION

5.1 Current biological health of the Ring River

Biomonitoring data showed that, relative to Stitt River locations and the reference site (STR1), Baker Creek and the Ring River have diminished benthic macroinvertebrate abundance and diversity (Figure 3). Further, no fish have been recorded during electrofishing surveys in the Ring River, whilst trout are observed in the Stitt and Pieman catchments. This supported the inference that Baker Creek and the Ring River (below Baker Creek) are highly disturbed systems (i.e., measurably degraded ecosystems of lower ecological value) as per relevant national and state level guidelines (EPA 2020; ANZG 2018), and that 80% species protection level (SPL) toxicant DGVs are the most appropriate generic guidelines for comparison with site-specific criteria.

5.2 Findings from laboratory DTA studies

Laboratory studies indicated that catchment-specific water quality characteristics affect toxicity of several priority contaminants. The NOECs derived for *Ceriodaphnia* cf *spinata* (Table 1) exceed relevant toxicant DGVs (80% SPL toxicant DGVs) by factors of 16 (Zn) and 21 (Cu). Acute Cu toxicity appeared to be affected most strongly by DOC, whereby the EC_{50} increased by a factor of 45 when individuals were exposed in water containing 8 mg L^{-1} DOC versus <1 mg L^{-1} DOC. The protective nature of DOC on zinc toxicity was also observed to a lesser extent, yielding a 65% increase in the EC_{50} for *Ceriodaphnia dubia* (unpublished data). Acclimation to elevated DOC (~10 mg L^{-1}) and zinc (0.02–0.08 mg L^{-1}), to mimic catchment conditions, reduced the LC_{50} for zinc in *Oncorhynchus mykiss* by a factor of 3 (Koehnken 1992). Acidic pH also influenced toxicity, whereby zinc toxicity was reduced for *Ceriodaphnia dubia* (by a factor of 2 at pH 6.5 vs 7.5) and *Auxenochlorella protothecoides* (by a factor of 5 at pH 6 vs 7).

5.3 Findings from field-based datasets and SWQC derivation

It is important to recognise that correlations between water quality and biological datasets are not in themselves proof of causal toxicological relationships. Therefore, as part of a multiple lines-of-evidence approach, estimated threshold concentrations were compared with laboratory toxicity endpoints, Australian and international toxicant DGVs (ANZG 2018) and upper background reference concentrations. Concentrations of priority contaminants in this case study were correlated in the 'toxicant mixture' given they share a common source (polysulfide mineral oxidation). Where concentrations of a toxicant/stressor of interest are correlated with other more toxic contaminants, threshold concentrations for the metal of interest may instead reflect sensitivity of receptors to the more toxic counterparts. For example, estimated threshold concentrations for sulfate were in the order of 10 mg L^{-1}, despite laboratory DTA results suggesting a NOEC of ~200 mg L^{-1} and literature-derived values being in the order of 130 mg L^{-1} (Elphick et al. 2011). This disparity exists because sulfate is naturally present at low concentrations (≤6 mg L^{-1}) and higher concentrations in this catchment reflect sulfide oxidation and hence elevated levels of metallic toxicants.

Threshold values estimated for Cd, Cu, Pb and Zn were found to be useable and were broadly consistent with other lines of evidence. Threshold concentrations estimated for Zn (0.1 – 4 mg L^{-1}) based on various biometric endpoints are given in Table 2. The estimated zinc threshold concentrations are

compatible with relevant laboratory toxicological endpoint concentrations (Table 1). The NOEC for *Ceriodaphnia* cf *spinata* (0.5 mg L^{-1}) sits between estimated threshold concentrations for benthic macroinvertebrate diversity and abundance. The estimated NOEC for *Oncorhynchus mykiss*, which was 0.07 mg L^{-1} when acclimated to zinc and exposed in organic acid-rich water, is slightly lower than the estimated threshold concentration for adult/juvenile fish. Estimated threshold concentrations for fish and macroinvertebrate diversity are similar to NOECs (pH 6 and 7) for *Auxenochlorella protothecoides*, which are in the range 0.04–0.19 mg L^{-1}.

The range of threshold concentrations indicate that fish abundance and benthic macroinvertebrate diversity are most sensitive to Zn exposure. The threshold concentration for macroinvertebrate abundance, which was an order of magnitude greater than that for macroinvertebrate diversity, most likely reflects variable sensitivity of benthic species to metal exposure and a similar pattern was also noted for Cd and Cu. Based on this finding, two sets of SWQC were developed for Hercules, acknowledging the practical challenges of achieving the substantial reduction in priority contaminant concentrations required to improve the biological health of the Ring River. Intermediate improvement criteria, presented in Table 3, are considered protective of aquatic biota recorded along Pieman tributaries (Ring, Stitt and Sterling rivers) with some apparent tolerance to priority contaminants. The intermediate criteria objective is to improve water quality so that the Ring River could support an improved modified ecosystem comprising benthic photosynthetic algae (primary producer) and more metal-tolerant benthic macroinvertebrates at an abundance consistent with the reference location. Maximum practicable improvement criteria, considered protective of more sensitive benthic species as well as fish, were also derived with the objective to provide conditions reflecting minimally impacted reference locations. The intermediate improvement protection criteria value derived for Cd (0.0005 mg L^{-1}), based on benthic macroinvertebrate abundance/diversity, was similar to the DGV (80% SPL) and background reference levels (0.0002 mg L^{-1}). Copper threshold concentrations based on adult fish and benthic macroinvertebrate abundance (0.004–0.05 mg L^{-1}), overlap with the DGV (0.012 mg L^{-1}) and the estimated NOEC for *Ceriodaphnia* cf *spinata* (0.05 mg L^{-1}), providing multiple corroborating lines of evidence.

Contaminant correlation effects confounded the estimation of threshold concentrations for arsenic, manganese, nickel and sulfate. Given the current lack of locally relevant DTA data for these elements, literature values and DGVs were adopted as the most reliable line of evidence to inform the SWQC. Estimated threshold concentrations were lower than, or consistent with, upper background reference values for aluminium, iron and EC. Given that concentrations cannot practicably be reduced below background levels, the upper background reference values were adopted as the SWQC for these parameters. Background reference data for pH show that values as low as pH 4.1 occur naturally within the catchment, despite the Pieman catchment DGV being set at pH >6.2. Observations of acidic pH, low EC and low concentrations of metals/metalloids (i.e. Lewis acids) at reference locations suggest that acidic pH can be attributed to presence of organic acids. The SWQC value for pH was established as pH ≥4.5, to be conservative and to minimise potential influence of outliers.

6.0 CONCLUDING REMARKS

This case study draws attention to the substantial, but perhaps often unrealised value of compliance-driven, long-term environmental monitoring datasets. It would not have been possible to derive site-specific criteria for multiple priority contaminants without a high quality dataset collected across contamination gradients, over multiple seasons and years. For companies operating mines with viable source-pathway linkages to surface waters, there is substantial opportunity to maximise value from compliance-driven water quality monitoring, by investing in concurrent biomonitoring programs. These rich datasets offer defendable, directly relevant insights to provide regulators with confidence when implementing site-specific water quality criteria for protection of aquatic biota.

REFERENCES

ANZG (Australia and New Zealand Governments) (2018) Australian and New Zealand Guidelines for Fresh and Marine Water Quality [online]. Available at www.waterquality.gov.au/anz-guidelines.

DPIWE (Department of Primary Industries, Water and Environment, Tasmania) (2000) Environmental management goals for Tasmanian surface waters. Catchments within the Circular Head & Waratah/Wynyard municipal areas. January 2000.

Elphick JR, Davies M, Gilron G, Canaria EC, Lo B and Bailey HC (2011) An aquatic toxicological evaluation of sulfate: the case for considering hardness as a modifying factor in setting water quality guidelines. *Environmental toxicology and chemistry*, 30(1), 247–253.

EPA (Environmental Protection Authority, Tasmania) (2020) Technical guidance for water quality objectives (WQOs) setting for Tasmania. August 2020.

EPA (Environmental Protection Authority, Tasmania) (2021) Default Guideline Values (DGVs) for Aquatic Ecosystems of the Pieman Catchment. August 2021.

Haywood MG, O'Farrell C, Jones DR, Crosbie J and Osgerby B (2022) Integration of surface and groundwater studies to support closure planning at the legacy Hercules Mine, Tasmania, In 'Proceedings of the 15th International Conference on Mine Closure'. Perth, Western Australia. (Eds AB Fourie, M Tibbett & G Boggs) pp 725-738. (Australian Centre for Geomechanics, Perth).

Koehnken L (1992) Pieman River Environmental Monitoring Programme. August 1992.

USEPA (2018) Final aquatic life ambient water quality criteria for aluminum. December 2018.

Table 1. Summary of laboratory toxicological data

Taxa/Toxicant	48-h EC_{50}	72-h LC_{50}	NOEC	LOEC
Ceriodaphnia cf *spinata*[1]				
Zn (mg L^{-1})	0.68	-	0.5	1
Cu (mg L^{-1})	0.074	-	0.052	0.104
SO_4 (mg L^{-1})	-	-	-	-
Hardness 7 mg L^{-1} $CaCO_3$	361	-	193	385
Hardness 30 mg L^{-1} $CaCO_3$	1,700	-	1,000	3,000
Oncorhynchus mykiss[2]				
Zn (mg L^{-1})	-	-	-	-
DOC ~8 mg L^{-1}, 80–100 µg L^{-1} Zn acclimation	-	0.7	0.07[3]	-
DOC <1 mg L^{-1}, 80–100 µg L^{-1} Zn acclimation	-	0.2	0.02[3]	-
Auxenochlorella protothecoides[4]				
Zn (mg L^{-1})	-	-	-	-
pH 6/DOC ~8 mg L^{-1}	-	-	0.19	>0.19
pH 7/DOC ~8 mg L^{-1}	-	-	0.041	0.081

Table 2. Estimated biological threshold concentrations for total zinc

Biological endpoint	Estimated threshold concentration (mg L^{-1})
Benthic macroinvertebrate diversity	0.1
Benthic macroinvertebrate abundance	1
Adult fish (*Salmo trutta*) abundance	0.1
Juvenile fish (*Salmo trutta*) abundance	0.1
Algal coverage	4

Table 3. Summary of site-specific surface water criteria

Toxicant/Stressor	Intermediate improvement criteria	DGV (80% SPL) / Pieman Catchment DGV[A]	Reference value / rationale
Al (mg L^{-1})[C]	≤0.44	0.021[B]	Upper background concentration
As (mg L^{-1})	<0.013	0.14	Reference value – DGV (95% SPL)
Cd (mg L^{-1})	<0.003	0.00022	Benthic macroinvertebrate abundance
Cu (mg L^{-1})	<0.04	0.012	Benthic macroinvertebrate abundance
Fe (mg L^{-1})	≤0.47	-	Upper background concentration
Mn (mg L^{-1})	<1.9	3.6	DGV (95% SPL)
Ni (mg L^{-1})	<0.005	0.0049	DGV (adjusted 80% SPL), acknowledging that the draft revised DGV (very high reliability) is greater than the current (low reliability) DGV by a factor of >5.
Pb (mg L^{-1})	<0.03	0.0015	Benthic macroinvertebrate abundance/diversity
Sulfate (mg L^{-1})	<129	-	Literature study findings (Elphick et al 2011)
Zn (mg L^{-1})	<1	0.009	Benthic macroinvertebrate abundance
pH	≥4.5	6.2	Background reference data
EC (µS cm^{-1})	≤90	123	Upper background level

[A] DGVs adjusted for pH, hardness, alkalinity and DOC as appropriate for catchment conditions.

[B] No reliable guideline value is currently established for Al under ANZG (2018). The 2018 USEPA (2018) ALAWQC, adjusted for pH (5.5), DOC (2.5 mg L^{-1}) and hardness (7 mg L^{-1} as $CaCO_3$), is presented.

[C] Concentrations are for unfiltered ('total') samples.

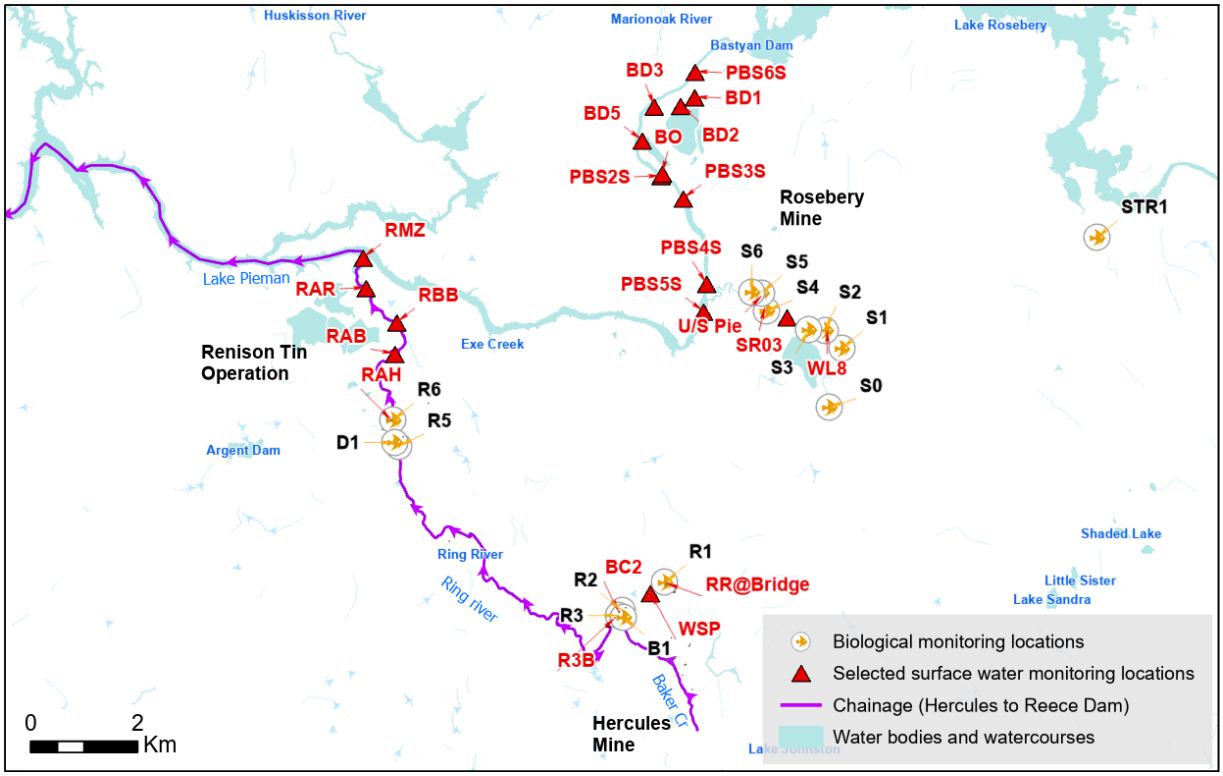

Fig. 1. **Site locality including selected water quality and biological monitoring locations**

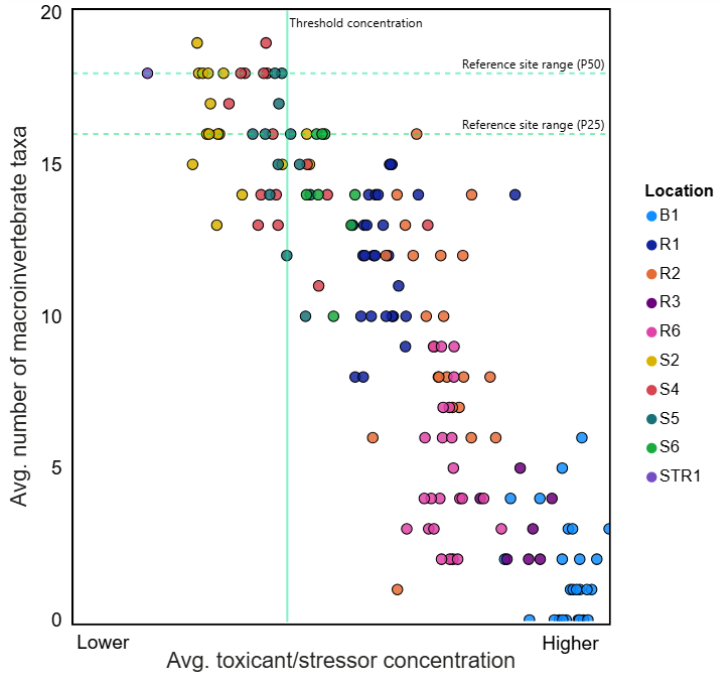

Fig. 2. **Benthic macroinvertebrate diversity and abundance versus toxicant concentration**

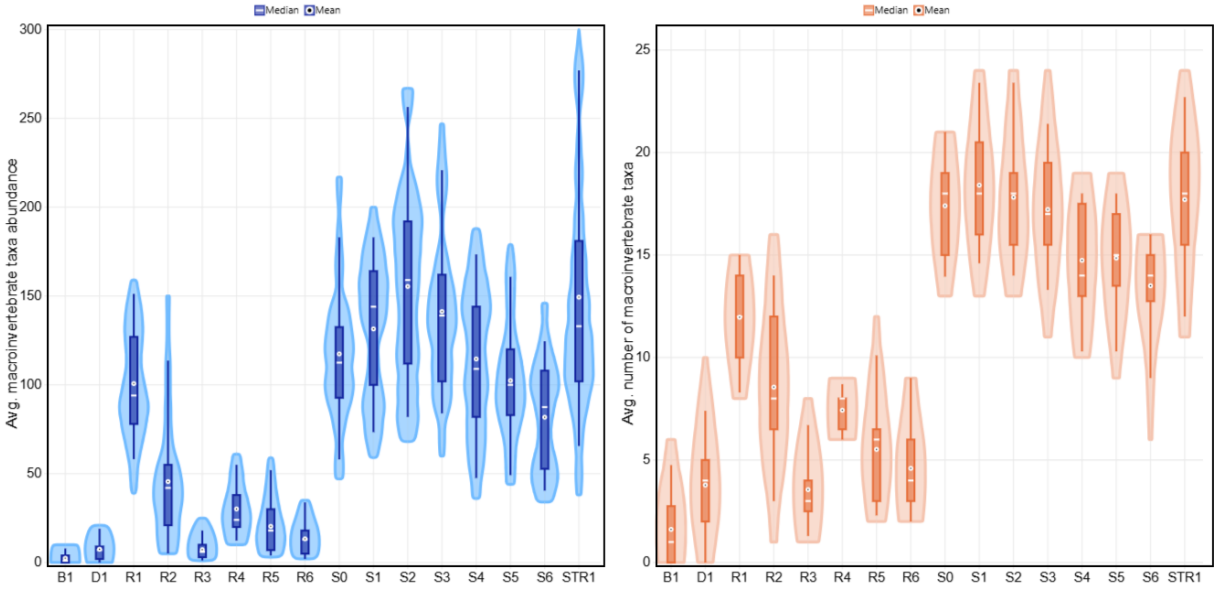

Fig. 3. **Benthic macroinvertebrate diversity and abundance: frequency distribution and central tendency**

Field and Laboratory Scale Investigations of AMD Potential in Mine Waste at Three Coal Mines in the Bowen Basin, Australia

A.M. Garvie[A], A. Watson[B], M. Stimpfl[C] and N. Thompson[D]

[A]Principal Consultant, SRK Consulting (Australasia) Pty Ltd, Level 20, 44 Market Street, Sydney, 2000, NSW, Australia. agarvie@srk.com.au

[B]Principal Consultant, SRK Consulting (Australasia) Pty Ltd, Level 3, 18 - 32 Parliament Place, West Perth, 6005, Western Australia, Australia

[C]Principal Geo-Environmental Advisor, BHP Iron Ore Pty Ltd, Level 30, 125 St Georges Terrace, Perth, 6000, WA, Australia

[D] Specialist Geochemist, BHP, Level 11, 480 Queen Street, Brisbane, 4000, QLD, Australia

1.0 Introduction

A program of field work was initiated in 2022 to investigate geochemical processes and gas transport mechanisms in mine waste landforms at three coal mines located in the Bowen Basin, Australia. The landforms contain various coal processing wastes. In some cases, more than one waste type is present, for example rejects placed over tailings or layers of dewatered tailings mixed with spoil. The objective of the work is to assess the potential for acid and metalliferous drainage (AMD) from the landforms, which typically have low sulfide sulfur contents and some neutralising capacity. Outcomes of initial modelling and measurements were reported by Garvie et al. (2024).

Data collection and interpretation are currently ongoing as part of multiyear studies at the sites. This paper describes the scope of these studies, the project status and interim results.

2.0 Background

Sulfide mineral oxidation is a critical step in the generation of AMD. Acid generated may be neutralised by carbonate minerals, with the consequent production of carbon dioxide (CO_2). CO_2 is also a product of reactions involving carbonaceous material, e.g. low temperature (T) oxidation (Kim, 1995; Wang et al., 2003; Lee et al., 2015; Li et al., 2019), microbial induced biodegradation (Fuertez et al, 2017), and desorption from coal (Kim, 1973).

Processes that occur in coal mine waste landforms are presented in Figure 1. Where O_2 is available, sulfide minerals and carbonaceous materials may oxidise. Generally, O_2 is supplied to the interior of waste landforms by gas advection and O_2 diffusion. The material property that controls gas advection is the intrinsic permeability and the property that controls diffusion is the O_2 diffusion coefficient.

Oxidation reactions are exothermic and therefore lead to increases in landform temperatures above the long-term average ambient T. Heat is conducted from regions of higher T to regions of lower T; therefore, the T distribution within the landform may change with time, depending on the balance of the rate of heat generation and heat loss by conduction in the landform. Heat is also transported by gas and liquid movement.

Data describing the spatial and temporal distribution of gaseous components and T within the interior of landforms can provide valuable insight to processes taking place and form an important basis for forecasting the potential for AMD.

3.0 Study scope

Waste landform characterisation investigations have taken place at three mines:

- Mine A – one landform containing end- and paddock- dumped spoil, tailings and mixed plant rejects (MPR)
- Mine B – one landform containing end-dumped coal rejects
- Mine C – three landforms: tailings, end-dumped rejects placed on tailings, and remnants of a ROM coal stockpile.

Investigations have included drilling, sampling and instrument installation. Instruments were installed within the drilled holes to measure O_2 and CO_2 concentrations, and T versus depth.

Sample characterisation included a suite of static testing (e.g. acid-base accounting, net acid generation testing, multi-element composition) and, for a subset of samples, kinetic testing to quantify rates of oxidation at laboratory-scale (see companion paper, Campbell et al., 2025) and examine leachate composition. A summary of selected characteristics of the landform materials is in Table 1.

Intrinsic permeabilities of the mine wastes were estimated using two methods. The first involved measuring the saturated hydraulic conductivity at 4 depths in the top 1.2 m of waste and subsequently calculating the intrinsic permeability. The second method involved flowing nitrogen gas into the mine waste at selected positions below the 6 m depth using a nylon tube and measuring the gas pressure rise in the waste as a function of nitrogen flow rate.

4.0 Selected interim field results

4.1 Mine A

Monitoring locations are shown in Figure 2 and examples of depth profiles of O_2 and CO_2 concentrations and T at two locations (H1 and H4) in the landform are presented in Figure 3. The landform was instrumented in 2022.

At both locations, the O_2 concentration decreases with depth. The decrease is steep initially, within the near surface portions of the depth profile, becoming shallower with depth. The shape of the O_2 depth profiles in June 2022 is consistent with diffusive transport of O_2 from the landform surface. The more recent measurements (June 2025) show that O_2 levels are increasing with time over. The trend is possibly due to a reduction in oxidation rates in the landform.

CO_2 concentrations at some depths exceed atmospheric CO_2 concentration (20 v% compared to atmospheric 0.042 v%). More recent measurements (June 2025) indicate that CO_2 concentrations have increased over time and suggest CO_2 generation or desorption within the landform.

The T is slightly elevated (28-30°C) when compared to long-term ambient T at the site (25°C) at most depths. Temperatures in the top 8 m are influenced by seasonal variations in climate. Below 8 m temperatures are constant within the uncertainty of the measurements (±0.5°C). These temperatures suggest that the rate of heat generation in the waste has decreased and combined with the trends in O_2 concentration indicate that the spoil oxidation rates have decreased.

4.2 Mine B

At Mine B, the investigation focused on a coal rejects landform up to 60 m high, 1,400 m wide and 2,200 m long. The coal rejects were end-dumped and dozed into position. A pair of vertical drill holes, approximately 40 m deep and separated by approximately 20 m, were drilled at each of two locations in May 2023 (MB001 to MB004, Figure 4). MB001 and MB003 were drilled close to nearby crests.

Examples of depth profiles of O_2 and CO_2 concentration, and T at one of the paired locations are presented in Figure 5 (MB003 and MB004). Figure 6 illustrates schematically the landform construction staging and shows that the near-surface material at the MB003/004 locations had been in place for only a few months prior to the installation of the measurement equipment.

The O_2 concentration profiles are more complex than those at Mine A. The near-surface portions of the profiles suggest diffusion plays a significant role in O_2 supply from the landform surface to newly placed oxidising material. There are intervals at depth with higher O_2 concentrations than both overlying and underlying materials. The distribution of O_2 at depth may be influenced by the three-dimensional O_2 distribution that existed immediately prior to placement of newer material; these profiles would be expected to evolve over time due to O_2 consumption and diffusion. CO_2 concentrations at most depths exceed atmospheric CO_2 with maxima at 19 v%, but typically between 1 and 10 v%.

T profiles are nearly constant with depth at MB003 in May 2023 but show evidence of heating (up to 42°C) within the upper portion of the depth profile by April 2025 (the recently placed material, Figure 6). At MB004, moderate heating (to around 37°C) was observed between the 10 and 15 m depths in May 2023 and temperatures have cooled (to around 34°C) by April 2025. The cooling may be a result of landform construction – with the advance of the landform crest away from MB004 over time leading to reduced oxygen supply and oxidation rates associated with the low O_2 concentrations.

4.3 Mine C

At Mine C, three landforms were investigated – see Figure 7. Installation of monitoring equipment occurred in late September and earlier October 2023. Selected examples of depth profiles of O_2 and CO_2 concentration, and T are presented in Figure 8. The shapes of the O_2 profiles are broadly consistent with oxygen supply by diffusion from the landform surfaces.

The CO_2 profiles observed within the three landforms at Mine C are quite distinct. In all cases, the CO_2 concentrations markedly exceed the atmospheric concentration (as was the case with Mine A and B). In Mine C, maxima in excess of 60 v% (are observed in the reject landform (MB148) at depths between 5 and 15 m, and at depths greater than 35m in the ROM landform (MB140).

Oxygen and therefore oxidation and heating are confined to the near surface tailings (MB110). Heat near the surface is readily conducted to the atmosphere resulting in temperatures being similar to the long-term average ambient T. The monitoring locations in the rejects and ROM coal are, within a horizontal distance of 10 m of the crest of the batter where oxygen is more likely to be supplied by convection compared to locations further from the side of the landform (Cathles and Schlitt, 1980). This combined with the marginally elevated temperatures in the rejects (MB140) indicates that convection may not be a significant oxygen supply mechanism away from the batters.

Temperatures in the ROM coal (MB148) have been elevated (40-45°C) and peaked at approximately the 25 m depth. This indicates that the oxidation rate was relatively high near this depth. The decreasing T in the ROM coal over the last 2 years indicates that oxidation rates have decreased since their peak values due to the low oxygen concentrations.

4.4 Estimates of intrinsic permeability and saturated hydraulic conductivity

Estimated intrinsic permeability values determined from measurements are shown in Figure 9. At all three mines, estimates of intrinsic permeability at depth varied widely, from 10^{-13} m^2 to maxima of 10^{-10} m^2 (Mine C), 10^{-8} m^2 (Mine A) and 10^{-7} m^2 (Mine B). The measurement uncertainty on these values has not yet been estimated. Near the surfaces of the landform, as inferred from the saturated hydraulic conductivity measurements, permeability ranged from 10^{-16} to 5×10^{-12} m^2. The generally lower range

of values in near surface locations may reflect the influence of compaction due to movement of heavy vehicles on the surface of the landforms.

5.0 Discussion

Several waste landforms have elevated pore gas CO_2 concentrations, but the source of the CO_2 is yet to be determined.

The work of others provides a means of interpreting the intrinsic permeabilities. Pantelis and Ritchie (1991) showed that during the first 4 years after dump construction, convection would not be significant for intrinsic permeabilities below 1×10^{-10} m^2 (grey shaded area in Figure 9). Similarly, numerical modelling of gas transport and sulfide mineral oxidation demonstrated that high intrinsic permeability values ($> 1 \times 10^{-9}$) would be required to develop convective gas transport at the Questa and Sullivan (Lefebvre et al., 2002; Lahmira and Lefebvre, 2008) mines. These studies suggest that intrinsic permeabilities of less than 10^{-10} m^2 may not support convection. Together with the measured low intrinsic permeability values and the O_2 and T distributions, the studies suggest that diffusion is currently the dominant oxygen supply mechanism in the landform regions studied. Another contributing factor potentially limiting convection is the low sulfide sulfur densities of some waste types, which are expected to be associated with low heating rates and T gradients, consequently the driver of gas convection is relatively small.

One key observation is that, despite the landforms having been constructed by end-tipping, diffusion appears to be the dominant form of oxygen supply. It is noted that in some volumes of recently placed waste, the T is increasing – thus, future advection cannot be discounted.

Data collection continues and will be used to build a robust dataset describing changes in the distribution of key gaseous components and T with time. As more data are collected, the implications for and the required function of any closure covers will be better understood.

6.0 Acknowledgements

This paper is the outcome of inputs from many people with various skills to whom the authors are grateful. The following are acknowledged for major inputs: Calum Thompson, Bronwen Forsyth, Anat Paz, Karan Jain, Camila Espinoza, Arena Palacio, Claire Linklater.

7.0 References

Campbell, G., Watson, A. and Stimpfl, M, (2025) Development of alternative kinetic leach test method for non-free draining coal mine wastes. Proceedings of the AMD Workshop, Brisbane, 19 – 21 October

Cathles, L.M. and Schlitt, W.J., 1980 A Model of the Dump oxidation leaching process that incorporates oxygen balance, heat balance, and two-dimensional air convection. Proceedings of the Las Vegas Symposium, 26 February 1980, Sponsored by the Solution Mining Committee, Society of Mining Engineers of AIME

Fuertez, J., Boakye, R., McLennan, J., Adams, D.J., Sparks, T.D. and Gottschalk, A., (2017) Developing methanogenic microbial consortia from diverse coal sources and environments. Journal of Natural Gas Science and Engineering, Vol. 46 pp. 637-650. https://doi.org/10.1016/j.jngse.2017.07.028

Garvie, A., Stimpfl, M., Watson, A., Thompson, N., Thompson, C, and Forsyth, B., 2024, Initiation of Field- and Laboratory-scale Investigations of Acid and Metalliferous Drainage Potential in Mine Waste at Three Coal Mines: The Roles of Sulfide Mineral and Organic Carbon, Proceeds of ICARD 2024, Halifax, Canada.

Kim, A.G. (1973) The Composition of Coalbed Gas. Report of Investigations. United States Bureau of Mines.

Kim, A.G., (1995) Relative Self-Heating Tendencies of Coal, Carbonaceous Shales, and Coal Refuse. Report of Investigation/1995. Bureau of Mines, United States Department of the Interior.

Lahmira, B and Lefebvre, R, 2008. Numerical Modeling of Gas Flow in the No. 1 Shaft Waste Rock Dump, Sullivan Mine, B.C., Canada, Institut national de la recherche scientifique, Centre Eau Terre Environnement, Research Report R-970.

Lee, D.G., Isworo Y.Y., Park, K.H., Kim, G.M., Kim, S.M., Jeon, C.H., (2020) Low-Temperature Oxidation Reactivity of Low-Rank Coals and Their Petrographic Properties. ACS Omega 2020, (30):18594-18601. https://doi.org/10.1021/acsomega.0c00840.

Lefebvre, R, Lamontagne, A, Wels, C and Robertson, A, 2002. ARD Production and Water Vapour Transport at the Questa Mine, in Proceedings Ninth International Conference on Tailings and Mine Waste, Tailings and Mine Waste ’02, pp. 479-488 (AA Balkema Publishers: Lisse).

Li, J., Li, Z., Yang, Y., Niu, J. and Meng, Q., (2019) Room temperature oxidation of active sites in coal under multi-factor conditions and corresponding reaction mechanism. Fuel (2019). https://doi.org/10.1016/j.fuel.2019.115901.

Luo, J., Wu, Y., Mi, D., Ye, Q., Huang, H., Chang, Z., Chen, Q., Zhang, T., Sun G., Wang, X., Wang, Y. and Liu, X., (2020) Analysis of the Distribution and Microscopic Characteristics and Disintegration Characteristics of Carbonaceous Rocks: A Case Study of the Middle Devonian Luofu Formation in Western Guangxi of China. Advances in Civil Engineering, Hindawi, Vol. 2020, 15 pages. https://doi.org/10.1155/2020/8810648.

Pantelis, G and Ritchie, A I M, 1991. Macroscopic transport mechanisms as a rate-limiting factor in dump leaching of pyrite ores, Appl. Math. Modelling, 15: 136-143.

Wang, H., Dlugogorski, B.Z., Kennedy, E.M., (2003) Coal oxidation at low temperatures: Oxygen consumption, oxidation products, reaction mechanism and kinetic modelling. Progress in Energy and Combustion Science. Vol. 29 (6): 487-513. https://doi.org/10.1016/S0360-1285(03)00042-X.

Table 1. **Summary of selected characteristics of landform materials**

Mine	Waste type	Total sulfur		Cr-reducible sulfur (sulfide sulfur)		Acid neutralising capacity		Total organic carbon	
		%		%		kgH_2SO_4/t		%	
		Range	Average	Range	Average	Range	Average	Range	Average
A	Spoil	0.01 - 0.57	0.071	<0.005 - 0.44	0.046	13 - 218	59	0.1 - 21	2.8
	MPR	0.02 - 1.6	0.35	0.019 - 1.4	0.22	4.2 - 168	29	0.57 - 30	13
	DT	0.04 - 0.44	0.24	0.034 - 0.35	0.16	17 - 96	36	0.46 - 23	14
B	Rejects	0.31 - 1.7	0.61	0.078 - 1.1	0.34	1.3 - 175	27	20 - 38	28
C	Tailings	0.12 - 11	1.5	0.008 - 11	1.2	<0.5 - 31	14	4.3 - 55	34
	Rejects	0.01 - 1.3	0.53	0.013 - 0.73	0.14	<0.5 - 21	3.5	0.09 - 62	27
	ROM Coal	0.04 - 2.3	0.82	0.011 - 1.4	0.51	<0.5 - 31	13	3.2 - 23	14

MPR – mixed plant reject; DT – dewatered tailings; ROM – run-of-mine

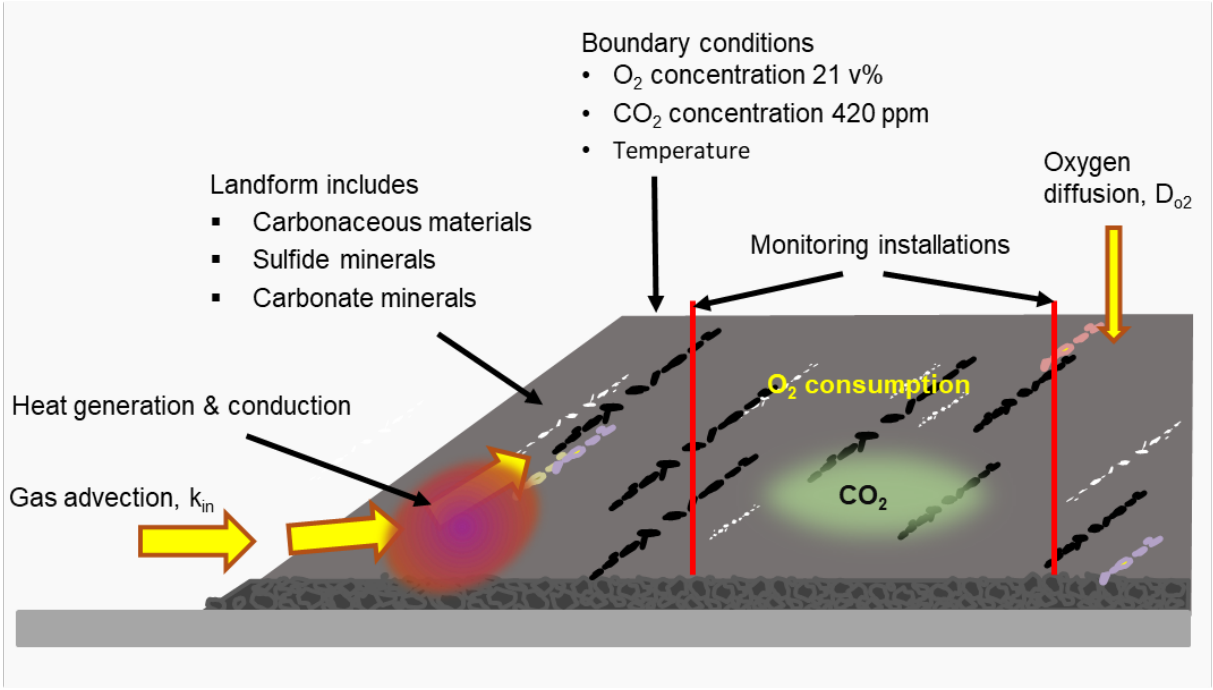

Fig. 1. **Coal mine waste landform processes**

Fig. 2. **Mine A monitoring locations**

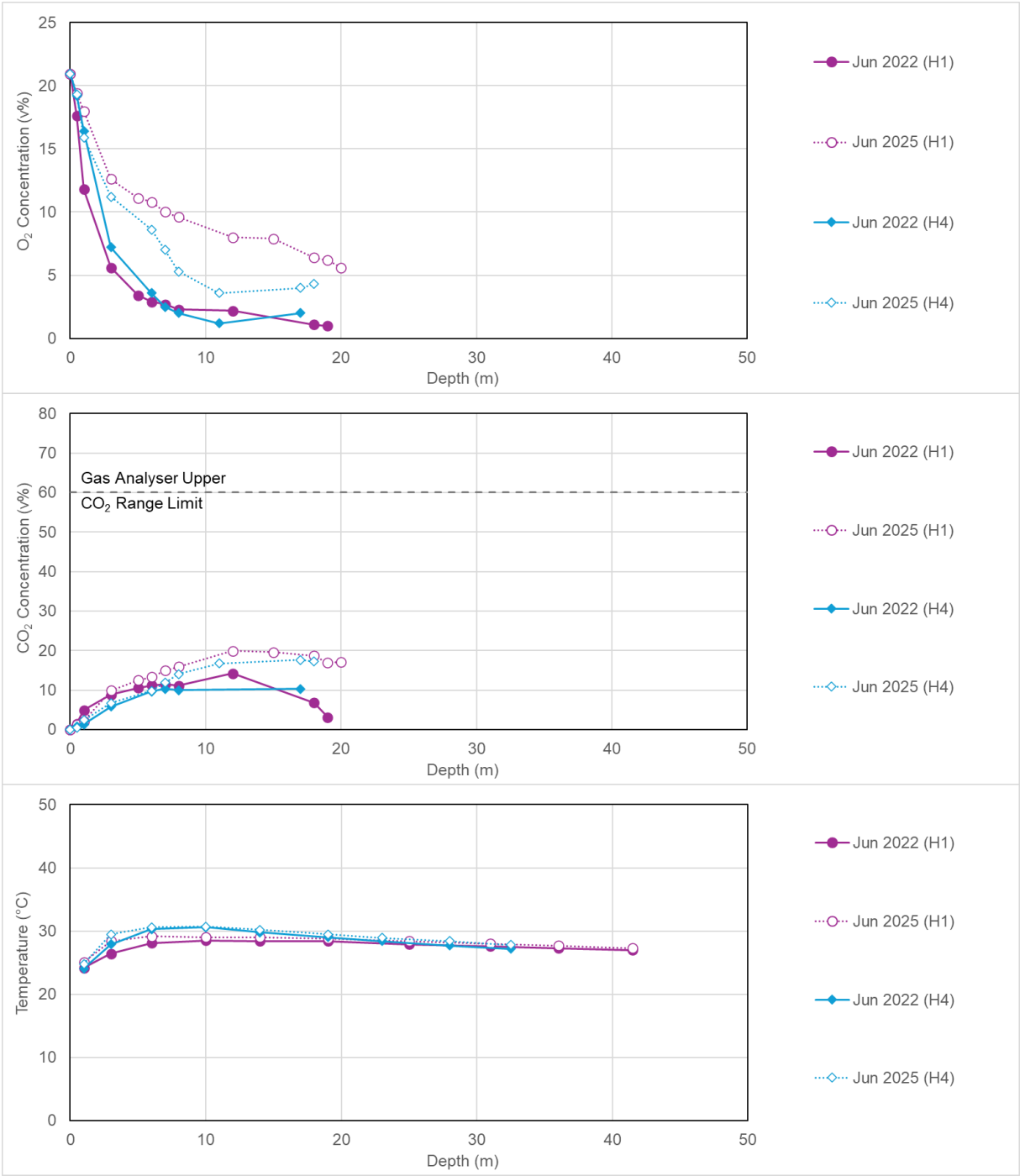

Fig. 3. **Depth profiles of (a) O_2 and (b) CO_2 concentrations, and (c) temperature, measured at Mine A**

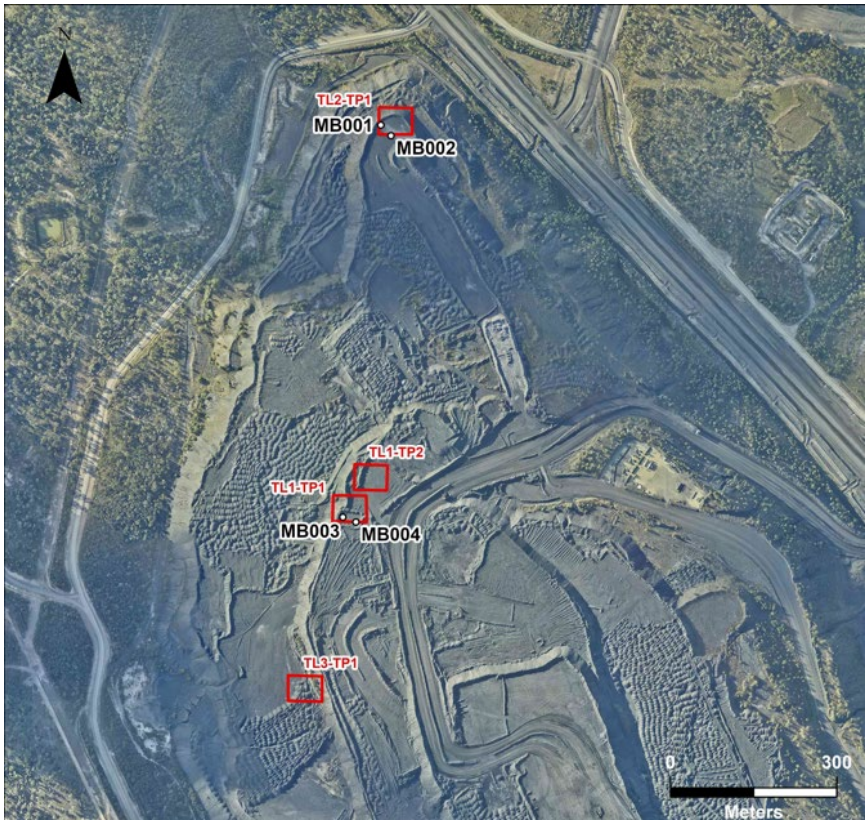

Fig. 4. **Mine B monitoring locations**

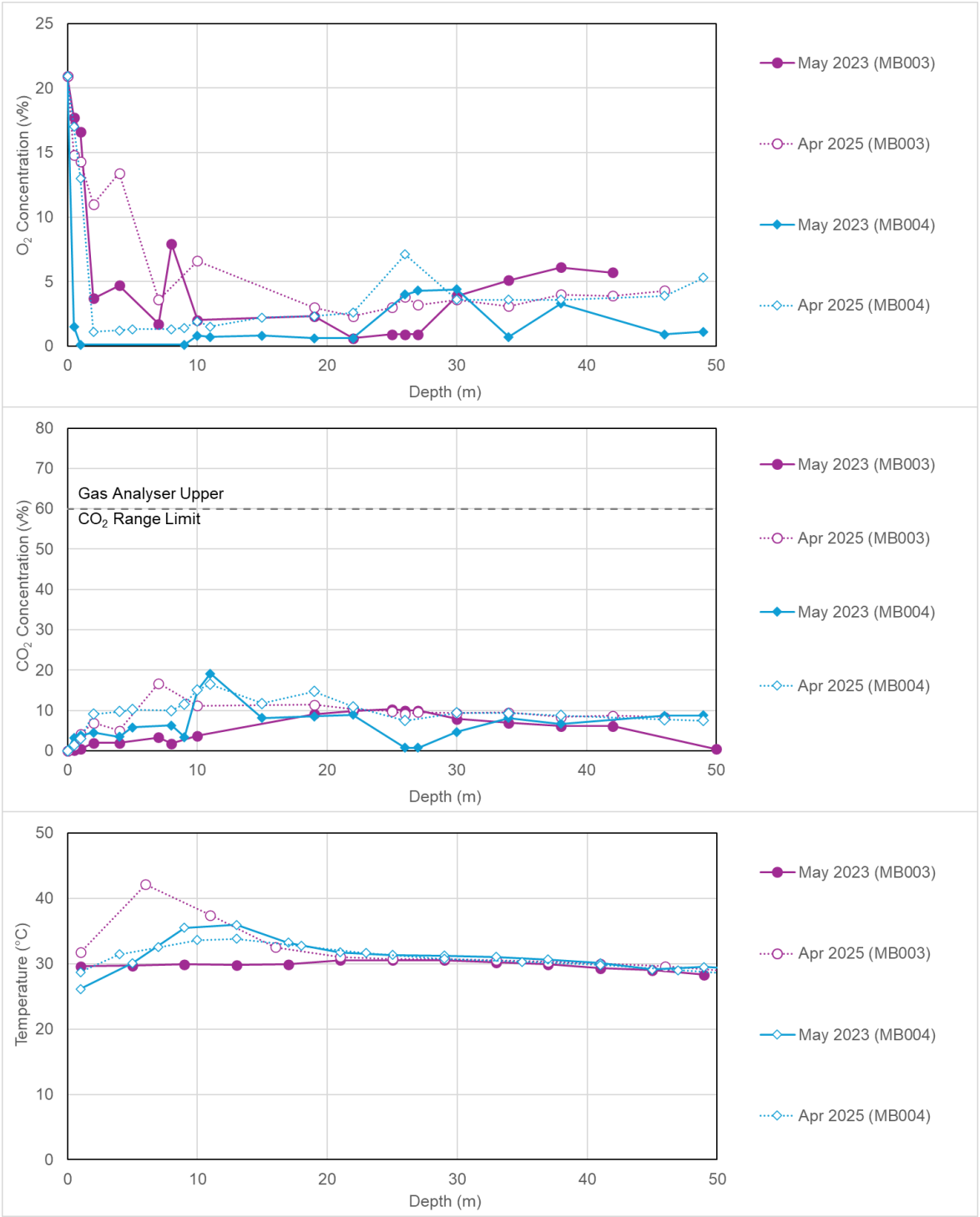

Fig. 5. **Depth profiles of (a) O_2 and (b) CO_2 concentrations, and (c) temperature, measured at Mine B**

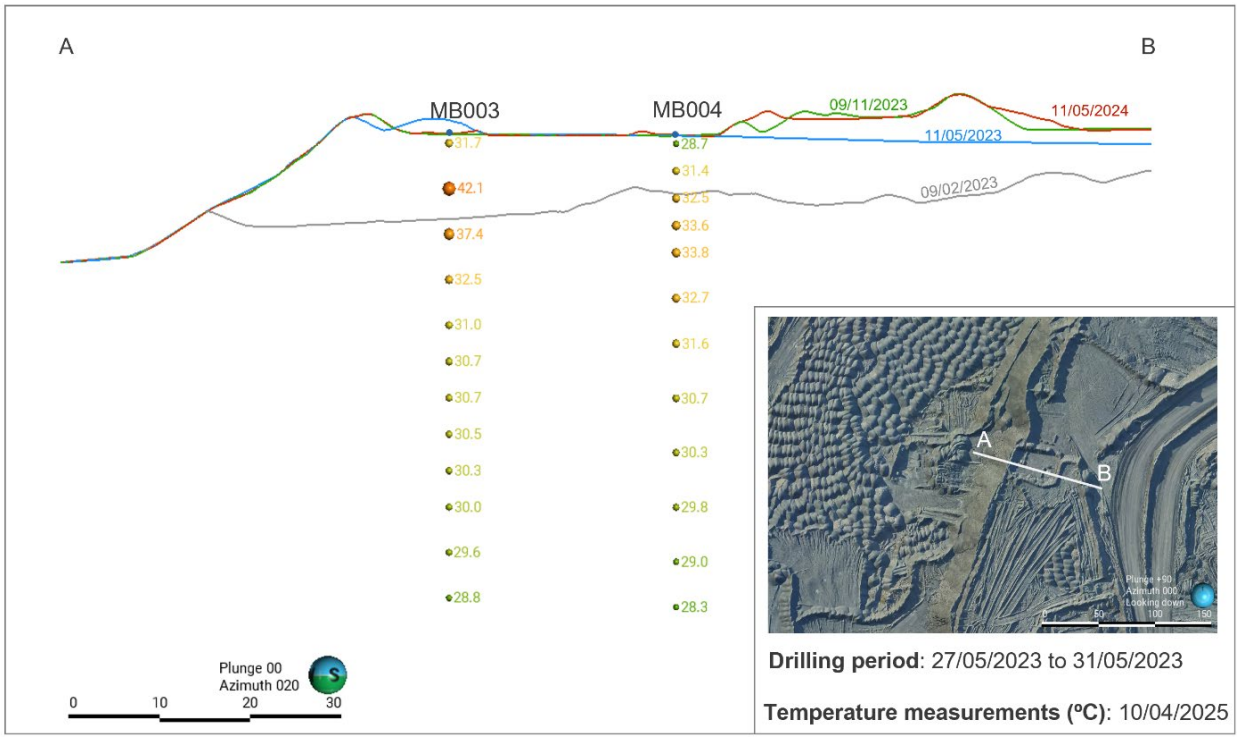

Fig. 6. **Schematic illustration showing the landform construction staging and temperature profiles measured in April 2025 (Mine B)**

(a)

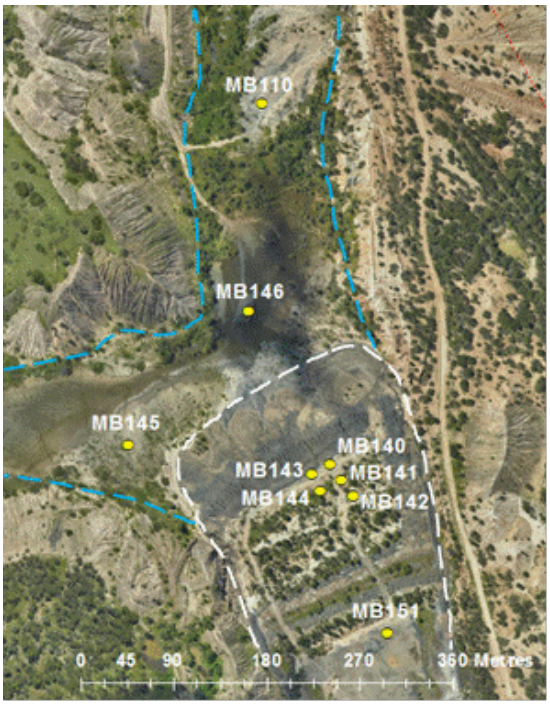

(b)

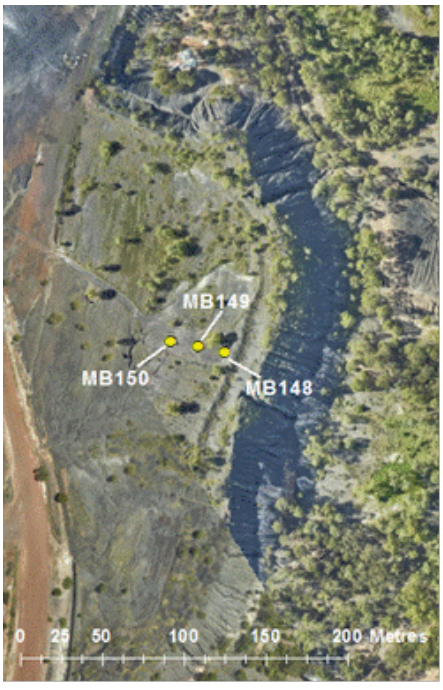

Fig. 7. **Mine C monitoring locations a) in-pit tailings to the north within blue dashed lines and rejects on tailings to the south within white dashed lines, b) remnant ROM coal**

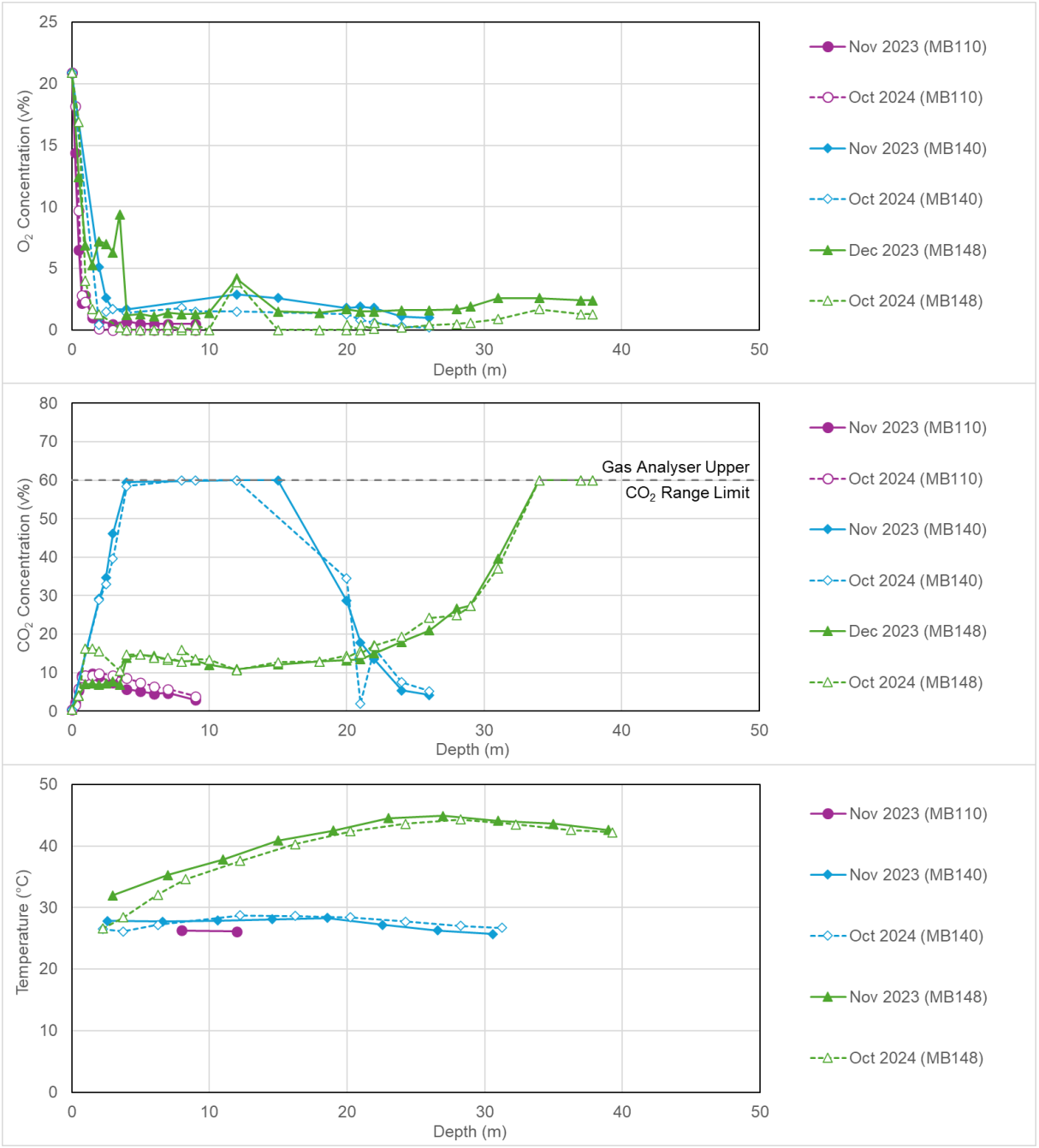

Fig. 8. **Depth profiles of (a) O_2 and (b) CO_2 concentrations, and (c) temperature, measured at Mine C**

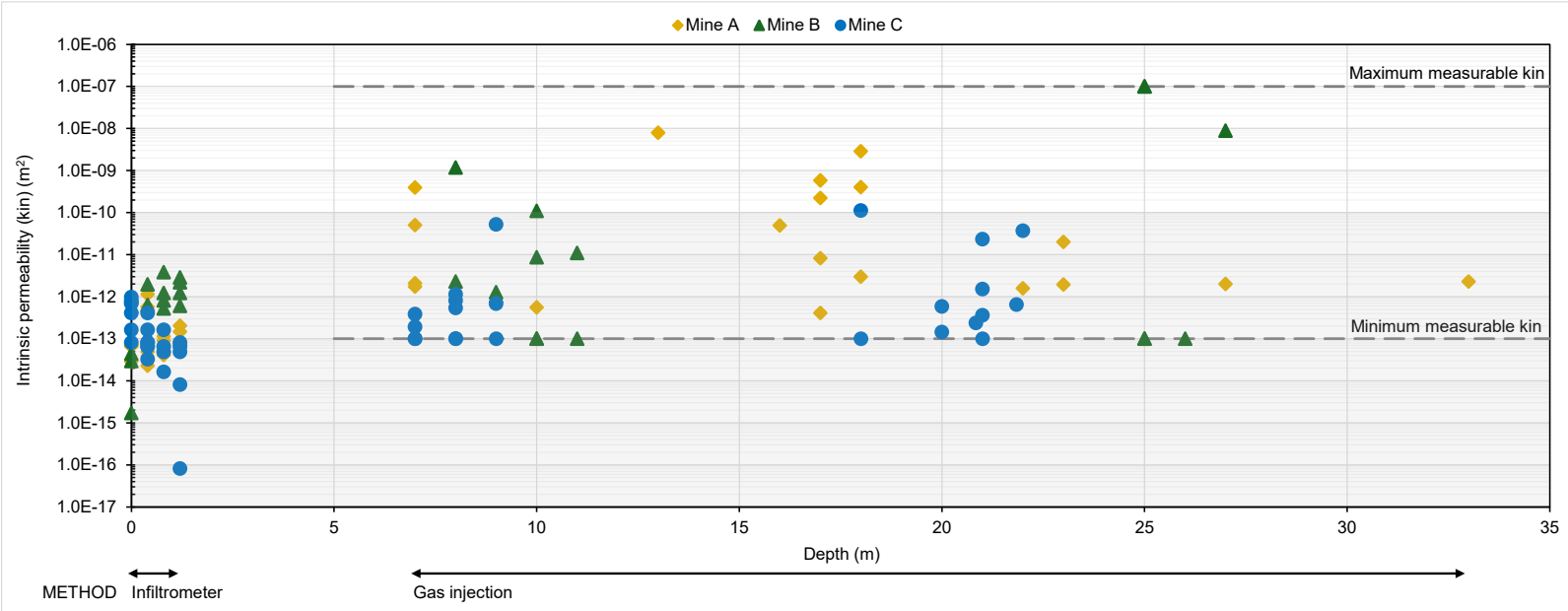

Fig. 9. Measured intrinsic permeability values across the three mines

The darker grey region corresponds to low permeability values that modelling suggests do not support convective oxygen supply.

Improved mining sulfur management through biological strategies

L.A. Warren[A], L.E. Twible[A], F.Y.L. Liu[B], K. Whaley Martin[C], T.E.C. Nelson[C], L.X. Chen[D], H. Sonnenberg[E], S. Neault[F], S.D. Marshall[G], L. Yestrau[F], S. McCarry[H], J.F. Banfield[I], and S.C. Apte[J]

[A]Department of Civil and Mineral Engineering, University of Toronto, Toronto, ON, M5S 1A4 Canada.
lesley.warren@utoronto.ca

[B]WSP 6925 Century Ave, Suite 600 Mississauga, ON L4N 7K2 Canada

[C]ERM 120 Adelaide St W., Toronto, ON M5H 1T1 Canada

[D]University of Science and Technology, 6, JinZhai Road, Baohe District, Hefei, Anhui, 230026 China

[E]Ecoreg Solutions, 279 Woolwich Rd. Guelph, ON N1H 3V8 Canada

[F]Hudbay Minerals, 25 York St., #800, Toronto, ON M5J 2V5 Canada

[G]Glencore Copper, 2 Longyear Drive, Falconbridge, ON P0M 1S0 Canada

[H]Glencore Sudbury INO, Strathcona Mine Rd. Levack ON P0M 1J0 Canada

[I]Earth and Planetary Science, University of California Berkeley, 307 McCone Hall, Berkeley CA 94720-4767 USA

[J]College of Asia and the Pacific, The Australian National University, Acton ACT 0200 Australia

1.0 INTRODUCTION

Sulfur compounds are a common by-product of operations processing sulfide minerals resulting in their occurrence in tailings and tailings impoundments (TI). These sulfur compounds, e.g. thiosalts ($S_nO_x^{2-}$), are reactive, with their oxidation linked to linked to impacts such as acid mine drainage (AMD) and toxicity failures. They remain a global mining environmental challenge, indicating the need for improved understanding not only of the possible S compounds that can occur in mining impacted waters, but also the possible microbial cycling of these S compounds that can affect S associated risks to receiving environments (RE).

The dominant S compounds observed in tailings streams, e.g., thiosulfate, sulfite, tetrathionate, are the presumed to be the dominant forms of S compounds also occurring in TI and thus monitoring methods, whether in house or more typically through analytical laboratories, have focused on their quantification (Figure 1a). However, the range of possible S oxidation states, from -2 (i.e., ΣH_2S, S^{2-}) to +6 (i.e., SO_4^{2-}) facilitates both a wider array of intermediate oxidation state S compounds (SOI), as well as microbial redox cycling that can lead to different water quality outcomes than those predicted by assumption of only thiosalts as the dominant S compounds in abiotic models. As treatment technologies do not fully remove all S compounds (Miranda-Trevino et al. 2013), there is a growing awareness of the need to address escalating risks associated with the incomplete understanding of reactive sulfur compounds in mining impacted waters, as well as the factors affecting their possible alteration/generation or removal through microbial biogeochemical redox cycling (Figure 1b, Whaley Martin et al. 2023), to improve environmental performance and reduce risks.

An overview of the results of a five-year case study that integrated characterization of physicochemistry, S geochemistry and sulfur oxidizing bacteria (SOB) microbiology of TI and RE waters from 4 Canadian base metal mines are summarized, highlighting how these results inform S management and treatment.

2.0 METHODS

All site descriptions, sampling methodology and analyses are described in detail in recent publications (Liu et al. 2024, Twible et al. 2024, Whaley Martin et al. 2020, 2023). Briefly, water samples were collected from four Canadian base metal TI and associated RE, when possible, over four consecutive years (2016-2019) as well as 2021. Each water sample was analyzed for sulfur speciation and microbial community composition (16S rRNA gene sequencing) and for some samples, metagenomic determination of functional S metabolism (genomic DNA) and RNA analysis of gene activity. Aqueous chemical characterization included analyses of total sulfur (Total S), sulfate (SO_4^{2-}), thiosulfate ($S_2O_3^{2-}$), and sulfite (SO_3^{2-}) concentrations and mass balance determination of reactive sulfur (S_{React}); all S atoms capable of oxidation; determined by [Total S] – [SO_4^{2-}] (Whaley Martin et al. 2020). Field measured TI / RE depth dependent water cap physicochemical parameters included temperature, pH, dissolved oxygen (DO; concentration and % saturation) and conductivity or salinity data (YSI 600 XLM, ProDSS water quality meter or ThermoScientific Orion Star A329 Multiprobe).

3.0 RESULTS AND DISCUSSION

3.1 Reactive Sulfur Compounds in TI and RE Waters

Tailings associated with sulfide mineral hosted ores contain residual sulfide minerals, as well intermediate sulfur oxyanion compounds of the form $S_nO_x^{2-}$, such as thiosulfate $S_2O_3^{2-}$, sulfite, SO_3^{2-}, and tetrathionate, $S_4O_6^{2-}$, that are generated during the metal extraction process. However, these are not the only sulfur oxidation intermediate compounds (SOI) that can occur, and current monitoring techniques do not consider or fully constrain, nor do current treatment approaches fully remove all possible reactive sulfur compounds (reactive sulfur =Total S – SO_4^{2-}; representing all possible S atoms capable of oxidation and thus creating environmental impacts (Figure 1, Miranda Trevino et al. 2013). Results from this case study indicate that reactive S does make it through treatment to RE contexts for all four mines investigated, and that often thiosalts are less than 4% of the total SOI or reactive S risk that occurs in both TI and RE (Figure 2; Whaley Martin et al. 2020) underscoring that current monitoring methods are underreporting potential S risks and highlighting the need for more conservative S monitoring and treatment strategies to mitigate possible S risks.

3.2 TI and RE Water SOB Communities and S Oxidation Repertoires

The occurrence of a diverse SOI pool in these TI and RE contexts underscores active microbial S cycling occurs once tailings are deposited in TI and in RE. A common set of SOB (7 major sulfur cycling Families; Figure 3) were identified to occur across these 4 base metal mines in both TI and RE waters, often dominating the total microbial community abundance (> 50-80%; Twible et al. 2024) and highlighting their significant role in S outcomes. The most abundant genera were *Halothiobacillus* spp., *Sediminibacterium* spp., *Thiobacillus* spp., *Sulfuricurvum* spp., *Thiovirga* spp., *Sulfuritalea* spp., *Sulfurimonas* spp., *Sulfuriferula* spp. and *Thiomonas* spp. (Figure 2; Twible et al. 2024). The four most abundant genera in these four TI collectively possess the capacity for sulfur oxidation via all three universal pathways (Friedrich et al. 2008), complete Sox (cSox) (*Halothiobacillus*, S*ulfuricurvum*), incomplete Sox (iSox) + rDsr (*Thiobacillus*), and S4I (*Halothiobacillus,* Sediminibacterium and *Thiobacillus*) underscoring well adapted SOB communities that can differentially mediate sulfur cycling in response to ambient water chemistry characteristics (Twible et al. 2024; Liu et al. 2024, Whaley Martin et al. 2023, Houghton et al. 2016). Reactions catalyzed by the cSox pathway favour the complete oxidation of SOI to SO_4^{2-}, resulting in increased acidity and SO_4^{2-} production, while more energy efficient pathways used by non-cSox SOB (iSox/rDsr/S4I pathways) commonly generate free SOI, and in some cases, may consume H^+ (Liu et al. 2024, Whaley Martin et al. 2023).

3.3. Physicochemical and S Geochemical Influences on SOB Genera and S Pathways

SOB genera abundance was consistently correlated with pH, [O_2] and [$S_2O_3^{2-}$] across these water samples indicating ecological habitat preferences amongst genera and thus which pathway operates differentially impacting reactive S and acidity outcomes. Peak abundances of non-cSox dominant SOB occurred within circumneutral pH values (~6 - ~8.5) while the highest abundances of cSox dominant SOB occurred at pH values below 6.5. Specifically, two key pH dependent niches occurred: cSox dominant SOB (*Thiomonas* spp. or *Halothiobacillus* spp.) associated with lower pH and [$S_2O_3^{2-}$]; and non-cSox dominant SOB (iSox and/or rDsr pathways, e.g. *Thiobacillus* spp., *Sulfuriferula* spp.), associated with more circumneutral pH conditions and higher [$S_2O_3^{2-}$]. The cSox pathway, responsible for the direct oxidation of $S_2O_3^{2-}$ to SO_4^{2-}, generates more acidity, decreased [$S_2O_3^{2-}$] and increased [H^+]/[SO_4^{2-}] values than the S4I, iSox, or rDsr pathways. Samples above pH ~ 8.5 had low abundances of SOB, suggesting this may be the upper ecological pH limit for SOB viability in TI water caps. (Liu et al. 2024, Twible et al. 2024, Whaley Martin et al. 2023)

Whaley Martin et al. 2023 identified two dominant SOB genera carrying out distinctive sulfur oxidative strategies (*Halothiobacillus* (cSox) and T*hiobacillus* (iSox+rDsr)) connected with acidity generation and thiosulfate concentrations dependent on TI water [O_2] and thus depth dependent niches where these different SOB were active. Field results identified higher oxygen conditions observed in upper waters, drove higher abundances of *Halothiobacillus* and increased net acid production. While lower to no oxygen concentrations occurring at deeper TI water column depths were associated with higher activity of *Thiobacillus* (iSox + rDsr; capability to use NO_3^- in addition to O_2 for S oxidation reactions), and lower acidity and sulfate concentrations. Mines commonly focus TI water management on suppression of AMD, by discharging tailings under water to minimize oxygen exposure and thus oxidation reactions (based on abiotic understanding). Results here highlight how the specific management conditions aimed at preventing AMD, namely, lower [O_2] and circumneutral pH values, favour SOB containing the iSox + rDsr pathways, associated with the generation of higher reactive sulfur. Thus, while these conditions result in less acidity generation on site, they increase the risk of sulfur impacts to downstream RE, as recalcitrant SOI are not destroyed with currently available static, chemical and energy intensive treatment technologies (Figure 4).

4.0 CONCLUSIONS

Results of a five-year case study on 4 Canadian base metal tailings impoundment and receiving environment waters sulfur chemistry and microbiology identified a suite of largely novel SOB common to both TI and RE waters. These TI-RE SOB communities possess diverse sulfur oxidation/disproportionation capabilities in their genetic repertoires that lead to different sulfur and water quality outcomes. SOB communities, and thus which sulfur reactions occur, dynamically responded to changes in water physicochemistry and sulfur chemistry affecting S and acidity outcomes. Applying classic modeling to prevent ARD formation, i.e. disposal of tailings under water to limit O_2 exposure, favours iSox SOB, and the persistence of reactive S compounds, thus exacerbating possible S risks to RE. Further, typical polishing pond pH conditions (i.e. > 9) limit SOB and thus remove the potential for SOB to degrade any remaining reactive S before treatment and discharge to RE. Results demonstrate how such microbially integrated investigation addresses long-standing critical sulfur knowledge gaps, and pave the way for development of smart, nature-based solutions to improve sulfur management.

REFERENCES

Friedrich CG, Bardischewsky F., Rother D. Quentmeier A and Fisher J (2005) Prokaryotic sulfur oxidation *Current Opinion in Microbiology* **8** 253-259

Houghton JL, Fousoukos DI, Flynn TM, Vetriani C, Bradley AS, and Fike DA (2016) Thiosulfate oxidation by Thiomicrospira tehermophila: metabolic flexibility in response to ambient geochemistry Environmental Microbiology **18** 3057-3072

Liu FYL, Twible LE, Nelson TCN, Whaley Martin K, Yan Y, Arrey JLS and Warren LA (2024) Determinants of microbial sulfur cycling and implications for environmental impacts. *Chemosphere* **372** 144084

Miranda-Trevino JC, Pappoe M, Hawboldt K and Bottaro C (2013) The importance of thiosalts speciation: review of analytical methods, kinetics and treatment. *Critical Reviews in Environmental Science and Technology* **43** 2013-2070

Twible LE, Whaley Martin K, Chen LX, Nelson TEC, Arrey JLS, Jarolimek CV, King JJ, Ramilo L, Sonnenberg H, Banfield JF, Apte SC and Warren LA (2024) pH and thiosulfate dependent microbial sulfur oxidation strategies across diverse environments. *Frontiers in Microbiology* **15** 1426584

Whaley-Martin K, Marshall S, Nelson TEC, Twible LE, Jarolimek CV, King JJ, Apte SC and Warren LA (2020) A mass-balance tool for monitoring potential dissolved sulfur oxidation risks in mining impacted waters. *Mine Water and Environment* **39** 291-307

Whaley-Martin, KJ, Chen LX, Nelson TEC, Gordon J, Kantor R, Twible LE, Marshall S, Rossi L, Bessette B, Baron C, Apte SC, Banfield JF and Warren LA (2023) O_2 partitioning of sulfur oxidizing bacteria drives acidity and thiosulfate distributions in mining waters. *Nature Communications* **14** 2006

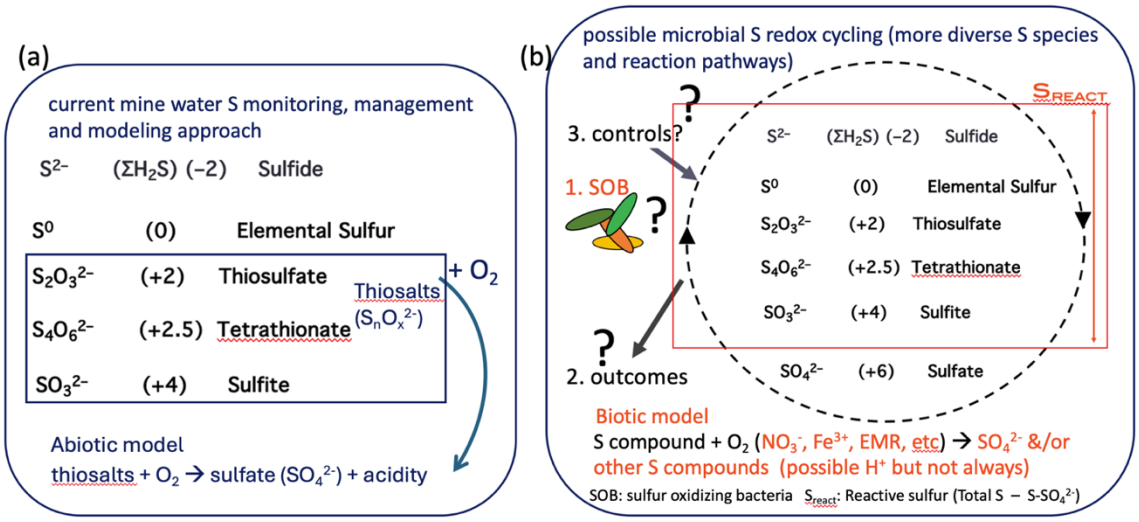

Fig. 1. **(a) Current mine wastewater management and modeling approach; (b) Possible microbial redox cycling of sulfur compounds that includes a wider array of possible S compounds, controls and outcomes than those currently considered in abiotic models.**

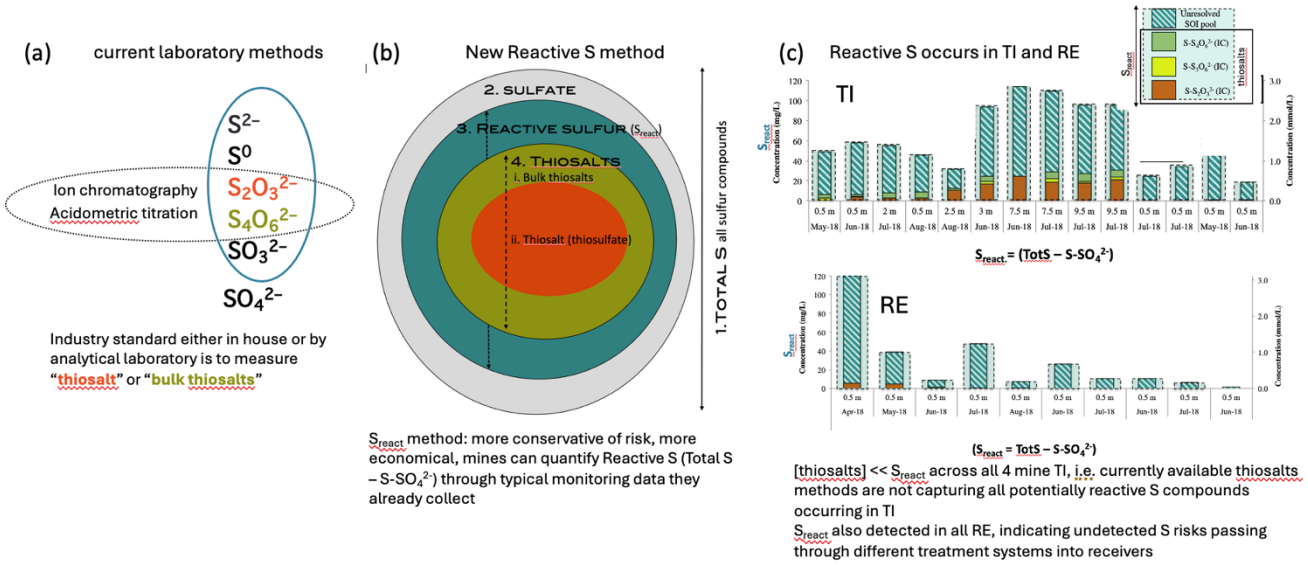

Fig. 2. (a) Current analytical methods commonly used to monitor thiosalts (thiosulfate and tetrathionate assumed to be dominant S species) versus the range of possible S compounds that can occur of oxidation state less than 6+ (i.e. sulfate) and thus capable of oxidation and impact generation; (b) New Reactive Sulfur method, calculated by [Total S] – [sulfate], capturing all S atoms of oxidation state less than 6+, irrespective of speciation and thus capable of oxidation and impact generation; (c) results across all 4 mines indicating the presence of other S compounds in both TI and RE (indicating that S compounds are making it through current treatment to RE, beyond typically monitored thiosalts; Whaley Martin et al. 2020).

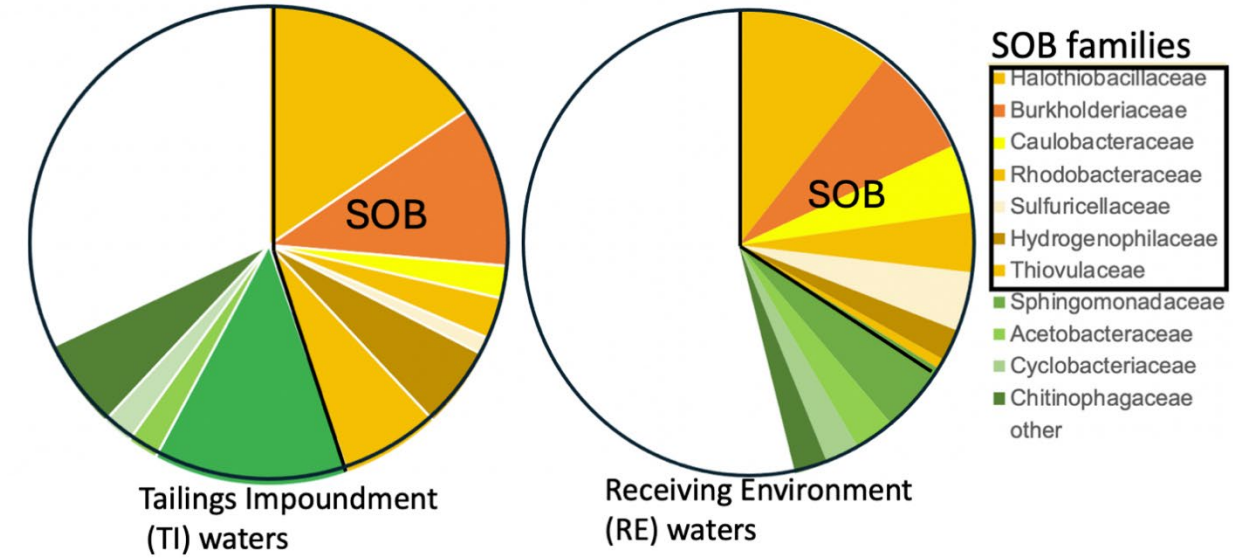

Fig. 3. Composite relative abundance of the seven major sulfur oxidizing bacteria (SOB) families that were found to occur in TI and RE waters across four base metal mines investigated over five years (see Twible et al. 2024 for greater detail).

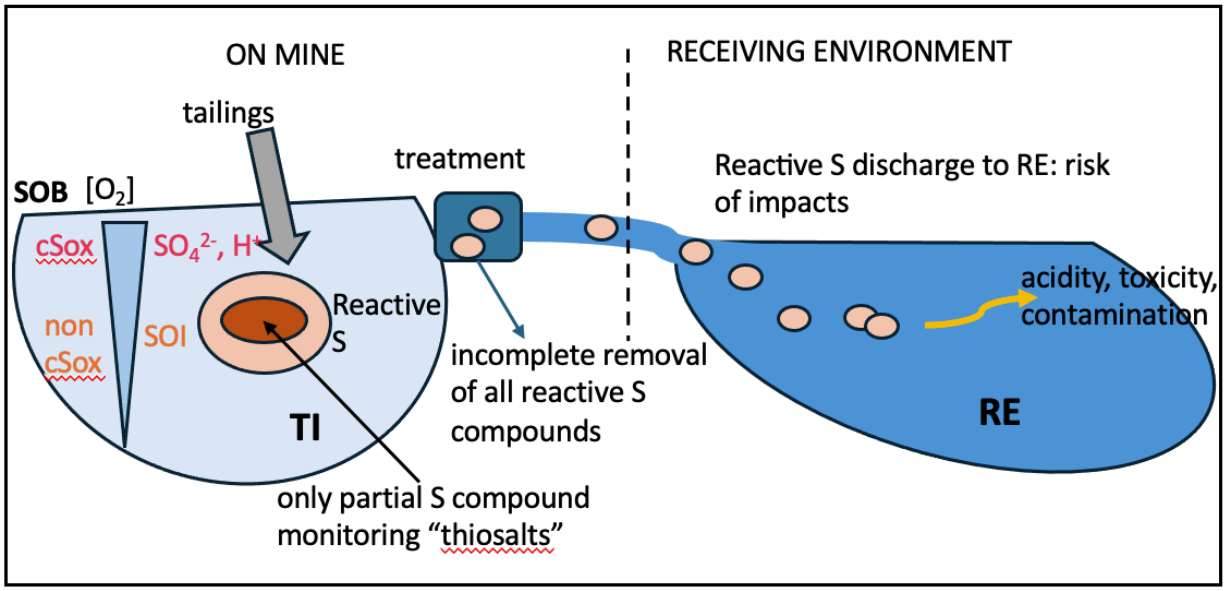

Fig. 4. **Identified challenges associated with current TI modeling, monitoring, management and treatment strategies that lead to RE impacts from partial reactive S monitoring focusing only on thiosalts, inefficient treatment that does not remove all possible SOI and the occurrence of O_2 dependent SOB that catalyze different S oxidation pathways resulting in more sulfate and acidity at higher O_2 and more SOI or reactive S at lower O_2.**

Geochemical study of pyrrhotite and pyrite reactivity in tailings Eloise copper mine, Queensland, Australia

C. Nikagolla [A], A.M. Robertson [A], A.R. Gerson [B], S. Cole [C], N. Jones [C] and Q. Bruwer [C]
[A]RGS Environmental Consultants Pty Ltd, PO Box 3091, Sunnybank South, Qld 4109, Australia.
chandima@rgsenv.com
[B]Blue Minerals Consultancy, Marlborough, New Zealand
[C]AIC copper Pty Ltd, Eloise Copper Mine; PO Box14, Cloncurry, Qld 4824, Australia

1.0 Predicting Acid and Metalliferous Drainage risk

Understanding the Acid and Metalliferous Drainage (AMD) risk from tailing materials is crucial to limit the potential for environmental impact and promote a sustainable closure model that complies with relevant industry standards and guidelines (e.g. COA 2016 and INAP 2025). This understanding also enables the development of a financially viable and environmentally robust management strategy based on risk.

The AMD potential of mine materials is typically predicted using standard Acid-Base Accounting (ABA) and test methods on representative samples (AMIRA 2002). Recent laboratory and field investigations confirm that these standard methods can overestimate the AMD risk, due to the lack of consideration for variability in oxidative reactivity among different sulfide minerals (Robertson et al. 2015; Schumann et al. 2015; Gerson et al. 2019; Smart et al. 2024).

Gerson et al. (2019) developed an improved method for estimating the maximum potential acidity (MPA) from mine materials containing both pyrite and pyrrhotite, considering their respective sulfide contents and oxidative behaviour. The methodology considers different pyrrhotite oxidation pathways that may occur over time within tailing materials in a TSF. The non-acid-forming (NAF) pathway Eqn. [1] produces elemental sulphur, while the acid-forming pathway Eqn. [2] occurs rapidly under highly oxidising conditions, or slowly during longer term weathering processes.

$$Fe_{(1-x)}S + 3(1-x)/4O_2 + (1-x)/2H_2O \rightarrow (1-x)FeOOH + S^0 \quad [1]$$

$$Fe_{(1-x)}S + 3(3-x)/4O_2 + (3-x)/2H_2O \rightarrow (1-x)FeOOH + H_2SO_4 \quad [2]$$

2.0 Case Study

Historical geochemical and mineralogical investigations found that Eloise Copper Mine (ECM, 60 km SE of Cloncurry, Queensland) tailing materials have an elevated total S concentration, most of which presents as pyrrhotite. The tailings also have appreciable inherent Acid Neutralising Capacity (ANC), mainly in the form of reactive calcite. In the past, the significant difference between the geochemical nature of pyrite and pyrrhotite was not fully recognised. Tailing materials were previously assessed using standard static geochemistry test methods (AMIRA 2002) and were classified as, and assumed to be Potentially Acid Forming (PAF). The TSF at ECM was therefore ranked in the “high risk” Consequence Category as defined in the Queensland Estimated Rehabilitation Cost Guideline and Calculator, and currently requires a complex, multi-layered engineered cover system for rehabilitation.

3.0 SAMPLES

Twenty tailing samples were collected between December 2022 and July 2024 under the ECM monthly tailing sampling and characterisation program. The individual samples were subjected to ABA testing at Australian Laboratory Services (ALS) at Stafford, Queensland. While most samples were classified as "NAF", three samples were classified as "Uncertain" and three samples were classified as "PAF". A total of four composite tailing samples were prepared by combining equal proportions of the monthly tailing samples, with composites selected using the geochemical characteristics of the individual samples.

4.0 MINERALOGY

The XRD results of the four composite tailing samples are shown in Error! Reference source not found.. The major minerals in the samples are quartz (32 to 35 wt%), biotite (9 to 14 wt%), sodium plagioclase (9 to 13 wt%), and amphibole (9 to 10 wt%). Minor minerals include potassium feldspar (2 to 5 wt%), pyrrhotite (3 to 7 wt%), calcite (3 to 4 wt%), chlorite (3 to 7 wt%), pyrite (1 to 2 wt%), rutile (1 to 2wt%), and ankerite (0.5 to 1 wt%). The MLA-SEM results for the tailings samples align well with the XRD results and confirm that the main sulfide mineral present is pyrrhotite with smaller amounts of pyrite, which are highly liberated, and a considerable amount of calcite.

5.0 AMD CLASSIFICATION

The acid-forming nature of four composite tailing samples was further investigated using the standard ABA test method that reflects Australian (AMIRA 2002; COA 2016) and international (INAP 2025) guideline criteria for classifying mine materials. The MPA was calculated using the conventional method Eqn. [3]. The samples were also re-classified using the modified methodology Eqn. [4] by Gerson et al. (2019).

$$\text{NAPP} = \text{Total sulfur wt \%} \times 30.6 - \text{ANC} \quad [3]$$

$$\text{NAPP} = [(\text{pyritic sulfur wt \%}) + (0.2 \times \text{pyrrhotite sulfur wt \%})] \times 30.6 - \text{ANC} \quad [4]$$

The ABA results for the four composite tailings samples obtained using conventional methodology (AMIRA 2002) are provided in **Table 1**. The total sulfur content ranges from 1.63 to 2.72 wt% and, based on Scr test results, is mainly present as sulfide. The ANC varies from 76.1 to 101.7 kg H_2SO_4/t, with an elevated median value of 85.5 kg H_2SO_4/t. Based on the Net Acid Producing Potential (NAPP = MPA – ANC) and ANC:MPA ratio results, the tailings samples are classified as "NAF" or "Uncertain". When the tailings samples were re-classified using the modified methodology Eqn. [4] developed by Gerson et al. (2019), all four samples were classified as "NAF" with strongly negative NAPP values ranging from -84.9 to -46.8 kg H_2SO_4/t and an ANC:MPA ratio which varied from 2.4 to 6.0 (**Table 2**).

6.0 KINETIC LEACH COLUMN TESTING

The four composite ECM tailing samples were combined into a single composite sample and subjected to a Kinetic Leach Column (KLC) test program under fully oxidising and free draining conditions (AMIRA 2002) at the RGS in-house laboratory. The KLC test program was completed over a period of six months to determine the likely contact water quality generated from the materials over time under conditions similar to the surface tailings at the TSF.

The pore water leached from the composite tailing sample remained pH neutral to slightly alkaline and contained negligible acidity and excess alkalinity. The tailing sample retained over 96 % and 94 % of its inherent sulfur content and ANC value, respectively, and the average oxygen consumption rate, calculated from the measured sulfate generation rate, was 2.63 x 10^{-8} kg (O_2) m^{-3} s^{-1}.

7.0 Discussion

The geochemistry results demonstrate that the ECM tailings contain over 1 wt % sulfur, most of which is present as sulfide, dominated by pyrrhotite rather than pyrite. Pyrrhotite has significantly less potential to generate acidity than finely disseminated pyrite. Hence, the application of standard geochemical ABA test methods has the potential to misclassify the tailing materials as "PAF" and overestimate the capacity of the materials to generate acidity.

The oxidative behaviour of pyrrhotite can significantly reduce the AMD hazard classification of the ECM tailing. According to the conventional classification method, two of the four ECM composite tailing samples were classified as "NAF" and two were classified "Uncertain" for AMD production. When the improved methodology by Gerson et al. (2019) was applied, the MPA (and thereby NAPP) was significantly reduced. The calculated NAPP values and ANC:MPA ratios indicate that all tested tailing samples are "NAF" despite containing more than 1 wt% sulfur (**Table 2**).

The low AMD potential of the ECM tailing samples was further evidenced by the KLC program, which indicated that most sulfide was retained and was accompanied by a low sulfide oxidation rate over the duration of the six-month KLC test program.

Given that the tailings have an appreciable and available excess ANC value, the oxygen consumption rate, calculated from the measured sulfate generation rate, is lower than the rate (5×10^{-8} kg (O_2) m^{-3} s^{-1}) identified by AMIRA (1995) and Bennett et al. (2000) above which there may be some risk of AMD, thus providing a satisfactory factor of safety with respect to potential for AMD. Hence, the tailing materials are predicted to generate circumneutral to slightly alkaline leachate under free draining conditions and with a greater factor of safety for bulk tailings under saturated anoxic conditions at the TSF.

The amount of acid potentially generated by the oxidation of the ECM tailing materials containing a sulfide component, comprised mainly of pyrrhotite, is likely to be neutralised by inherent excess ANC. The findings of this study help to explain the absence of field monitoring evidence of AMD from the TSF, despite ECM having been in operation for over 30 years.

8.0 CONCLUSIONS

The results of this geochemistry and mineralogical work program completed on the ECM tailing samples indicate that the application of standard static geochemical characterisation techniques can overestimate the amount of acidity generated from mine materials containing appreciable pyrrhotite. The ECM tailing samples, where mineralogical data is available to verify the proportions of pyrrhotite and pyrite, are all classified as "NAF".

The revised AMD classification of the ECM tailings will provide significant advantages for ECM mine operations, rehabilitation, and closure. There is an increased level of confidence that the current TSF "high risk" Consequence Category is not valid and should be re-assessed. Hence, the requirement for a complex multi-layered engineered cover system for the TSF is essentially unwarranted. This paper emphasises the importance of integrating geochemical and mineralogical studies and field monitoring data to predict the likelihood of AMD production from mine materials and will help to optimise the rehabilitation strategy for the final TSF landform.

References

AMIRA (1995) ARD Test Handbook. AMIRA Project P387: Mine Waste Management: Prediction & Kinetic Control of Acid Mine Drainage. (Environmental Geochemistry International).

AMIRA (2002) ARD Test Handbook. AMIRA Project P387A: Prediction & Kinetic Control of Acid Mine Drainage. (Ian Wark Research Institute and Environmental Geochemistry International).

Bennett JW, Comarmond MJ and Jeffery JJ (2000) Comparison of oxidation rates of sulfidic mine wastes measured in the laboratory and field. (Australian Centre for Mining Environmental Research: Brisbane).

COA (2016) Leading Practice Sustainable Development Program for the Mining Industry. Prevention of Acid and Metalliferous Drainage. (Commonwealth of Australia, Canberra).

Gerson AR, Rolley PJ, Davis C, Feig ST, Doyle S and Smart RSC (2019) Unexpected Non-Acid Drainage from Sulfidic Rock Waste. *Scientific Reports*. **9 (1)** 4357.

INAP (2025) Global Acid Rock Drainage Guide (GARD Guide). (Golder Associates on behalf of the International Network on Acid Prevention: http://www.inap.com.au/).

Robertson AM, Kawashima N, Smart RC and Schumann R (2015) Management of pyrrhotite tailings at Savannah Nickel Mine – a decade of experience and learning. In proceedings of the 10th International Conference on Acid Rock Drainage (ICARD). Santiago, Chile. 21-24 April 2015. Chapter 2, pp11.

Schumann R, Robertson AM, Gerson AR, Fan R, Kawashima N, Li J and Smart RC (2015) Iron sulfides ain't iron sulfides. A comparison of acidity generated during oxidation of pyrite and pyrrhotite in waste rock and tailings materials. In proceedings of the 10th International Conference on Acid Rock Drainage (ICARD). 21-24 April 2015. Santiago, Chile. Chapter 2, pp11.

Smart R, Gerson A, Robertson A and Schumann R (2024) Long Term Storage and Closure of Pyrrhotite-Containing Mine Wastes. Manuscript MMM-2024-1 submitted to the Journal of Minerals and Mineral Materials.

Table 1. **Acid Base Account results and AMD classification using the conventional methodology**

Sample No.	Total S (%)	ANC ($kg\ H_2SO_4/t$)	MPA ($kg\ H_2SO_4/t$)	NAPP ($kg\ H_2SO_4/t$)	ANC:MPA Ratio	Sample Classification
E_C301	1.65	101.7	50.4	-51.3	2.2	NAF
E_C302	1.63	76.1	50.0	-26.0	1.5	NAF
E_C303	2.93	90.9	89.7	-1.2	1.0	Uncertain
E_C304	2.72	80.1	83.2	-4.4	1.1	Uncertain

Table 2. **Acid Base Account results and AMD classification using the improved methodology**

Sample No	Pyrite:Pyrrhotite ratio	MPA ($kg\ H_2SO_4/t$)	NAPP ($kg\ H_2SO_4/t$)	ANC:MPA Ratio	Sample Classification
E_C301	1:5	16.8	-84.9	6.0	NAF
E_C302	1:3	20.0	-56.1	3.8	NAF
E_C303	1:7	26.9	-64.0	3.4	NAF
E_C304	1:3	33.3	-46.8	2.4	NAF

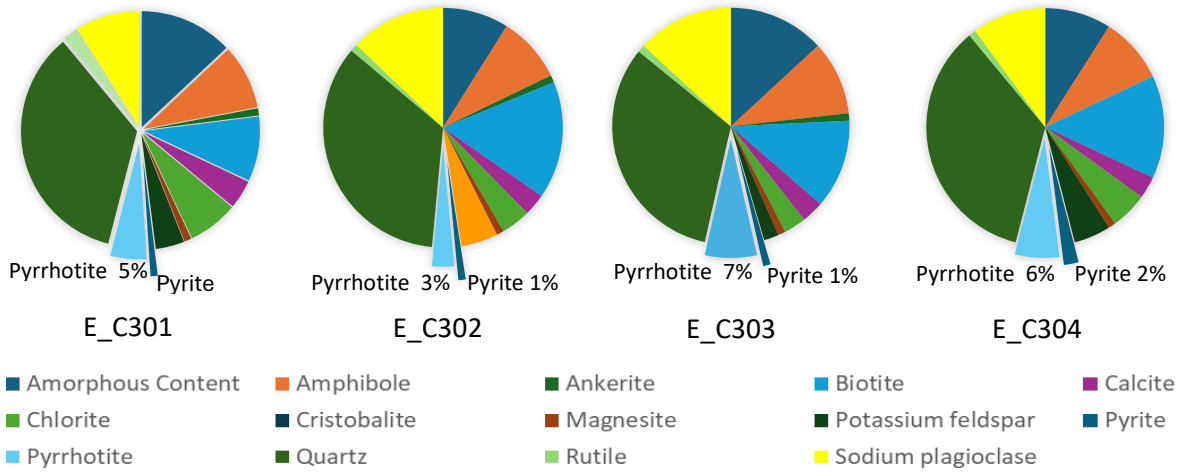

Fig. 1. **Mineralogy composition of ECM composite tailings samples**

Combining Genomics and Kinetic Leaching Tests to Quantify Microbial Influence on Sulfide Oxidation

N.W. Falk[AB], G. Qian[B], B. Papudeshi[AB], A.R. Gerson[C], H. Davies[D], S.L. Harmer[BE], E.A. Dinsdale[AB]

[A]Flinders Accelerator for Microbiome Exploration (FAME), Flinders University, Bedford Park, SA 5042, Australia. nick.falk@flinders.edu.au

[B]College of Science and Engineering, Flinders University, Bedford Park, SA 5042, Australia

[C]Blue Minerals Consultancy, Mahakipawa, Marlborough, 781 New Zealand

[D]Newmont, Englewood, Colorado 80112, United States

[E]Flinders Microscopy and Microanalysis, Flinders University, Bedford Park, SA 5042, Australia

1.0 INTRODUCTION

The study presents a novel kinetic leach column (KLC) framework for predicting microbial influence on mine waste weathering, with the abiotic/biotic test offering a practical screening tool for industry use.

Exposure to oxygen and water initiates pyrite (FeS_2) oxidation, producing acidity and releasing toxic metals/metalloids that can degrade ecosystems and water quality if unmanaged. Acidophilic Fe- and S-oxidising microorganisms thrive in these conditions, accelerating pyrite oxidation. They act directly by forming biofilms on mineral surfaces and indirectly by oxidising Fe^{2+} to Fe^{3+} in solution, which further drives abiotic oxidation (Gleisner et al., 2006). While numerous field (Chen et al., 2016; Goltsman et al., 2015) and laboratory (Meruane & Vargas, 2003; Mielke et al., 2003) studies have deepened understanding of mine drainage microbial communities and biotic sulfide oxidation, microbial assessments are rarely used in routine mine waste evaluations. Key barriers include the variability of site conditions (e.g., resource type, processing, climate), which complicates standardisation, and the largely reactive nature of current microbial tools, whether culture-dependent or culture-independent (i.e., omic-based), which offer limited predictive power. As a result, microbial data are underutilised in acid and metalliferous drainage (AMD) prediction frameworks, despite the potential for improved forecasting when paired with trusted geochemical tests (Qian et al., 2021).

2.0 KINETIC LEACH COLUMNS

Two bulk waste rock samples (A and B) were crushed to < 4 mm. Each 5 kg sample was packed into acrylic columns (42 cm × 12 cm) with a 4–8 µm glass filter disk and rubber plug at the base. Columns were watered weekly using a four-week cycle: three applications of 166 mL DI water, followed by one of 332 mL. This continued over 72 weeks. Microbial and geochemical samples were collected at weeks 8, 12, 16, 20, 24, 32, 48, and 72. Leachate was weighed, split into triplicates, and filtered through 0.2 µm Sterivex™ filters. Filters were flash-frozen in liquid nitrogen and stored at −80 °C. Filtered leachate was analysed for pH, Eh, and total Fe and S via ICP-OES. Acidity (mg $CaCO_3$ L^{-1}) was determined by titration to pH endpoint of 8.3 with 0.5 M NaOH solutions.

2.1 Microbial Activity and Geochemical Trends in Leachate

DNA and RNA were co-extracted from Sterivex™ filters using the Qiagen RNeasy PowerSoil Total RNA Kit and DNA Elution Kit. The internal filter membrane was removed in fragments using sterile tweezers and placed into the PowerBead tube provided. For improved RNA recovery, 2 mL of Tri-Reagent and 0.4 mL of chloroform were added in place of the standard phenol/chloroform/isoamyl alcohol.

Subsequent steps followed the manufacturer's instructions. DNA and RNA were eluted separately and quantified for concentration using a Qubit4 Fluorometer. The ratio of RNA:DNA concentration was calculated, with higher values indicative of greater microbial community activity (Loeppmann et al., 2018).

In total, 46 DNA samples (23 each from samples A and B) were sequenced on an Illumina MiSeq. Reads were filtered using Trimnami (Roach, 2023) with Fastp and Prinseq++. Taxonomy was assigned using MMseqs2 (Steinegger & Söding, 2017) and GTDB. Sulfur oxidation genes were annotated with SUPER-FOCUS (Silva et al., 2016) using the SEED classification. Fe-oxidation genes were identified using FeGenie (Garber et al., 2020) on contigs assembled with SPAdes (Bankevich et al., 2012). Relative gene abundances (%) were calculated per sample. Metagenome Assembled Genomes (MAGs) were binned with VAMB (Nissen et al., 2021), assessed via CheckM2 (Chklovski et al., 2023), and taxonomically assigned with GTDB-Tk.

Leachate from waste rock A exhibited greater concentrations of DNA, RNA, Fe, and S, and lower pH values compared to leachate from waste rock B (Figure 1). In waste rock A, nucleic acid concentrations peaked at 8 weeks, with DNA and RNA levels reaching 6.8 ng μL^{-1} and 20.7 ng μL^{-1}, respectively. These concentrations declined over time; however, RNA:DNA ratios remained >1 up to week 24, suggesting sustained in-situ microbial activity for several months. By contrast, waste rock B showed lower peak DNA and RNA concentrations (1.1 ng μL^{-1} and 2.9 ng μL^{-1}, respectively), with a pronounced decline by week 16, indicating reduced microbial activity throughout the leaching period. Total acidity was greater in waste rock A leachate, with pronounced acid generation occurring from weeks 8–24, which corresponded with maximums in microbial activity (Table 1).

2.2 Taxonomic and Functional Diversity of Leachate Microbial Communities

Microbial diversity, measured using the Shannon (*H*) diversity index, was significantly less in waste rock A leachate (mean $H = 1.3$) compared to waste rock B (mean $H = 1.7$) (Mann-Whitney $p = 0.0137$; statistic = 153). The 25 most abundant microbial genera identified in leachate samples are displayed in Figure 2. The two waste rock communities were dominated by well-known acidophilic, Fe/S-metabolizing bacteria, including *Acidiferrobacter*, *Acidiphilium*, and *Sulfobacillus*. In addition to these characterized taxa, several unclassified genera belonging to the families and orders *Acidiferrobacteraceae*, *Acidimicrobiales*, *Sulfobacillaceae*, and *Alicyclobacillales* were also highly abundant.

Waste rock A exhibited pronounced dominance by the Fe-oxidizing genus *Acidiferrobacter* at 8 weeks, with relative abundance over 90%. By weeks 20 and 24, *Sulfobacillus* became more prominent. In contrast, waste rock B maintained a more diverse community over time, with *Acidiferrobacter* present at 46% relative abundance at 8 weeks, and *Acidiphilium*, a known Fe-reducing genus, remaining abundant throughout the experiment.

2.3 Metagenomic Evidence for Microbial Iron and Sulfur Cycling

High quality genomes for *Acidiferrobacter* were assembled from DNA sequences in week 8 samples from both waste rock A and B and were confirmed to possess genes for Fe-oxidation. The community-wide potential for microbial-influenced sulfide oxidation in the two waste rocks was further explored through the abundance of Fe- and S-oxidation genes detected in contigs built from all DNA sequences for each timepoint. Fe-oxidation gene abundances ranged from 0% - 0.06% in waste rock A and from 0.01% - 0.05% in waste rock B. For S-oxidation genes, the ranges were 0.001% - 0.009% for waste rock A and 0.003% - 0.008% for waste rock B.

Waste rock A exhibited significant positive correlations between Fe and S concentrations, Fe and RNA:DNA, and S and RNA:DNA, and significant negative correlations between Fe and microbial Fe-oxidation %, and S and microbial Fe-oxidation % (Figure 3A), suggesting microbial regulation in Fe and S loads in leachate. Waste rock B exhibited fewer significant correlations, with only microbial Fe-oxidation % and microbial S-oxidation % showing a significant positive correlation (Figure 3B).

3.0 Assessing Microbial Influence via Abiotic/Biotic Leach Testing

A small-scale leaching experiment using waste rock A was conducted to assess microbial contributions to acid generation via iron speciation. Subsamples of 50 g of crushed (< 4 mm) waste rock A were placed into 50 mL luer-lock syringes (plungers removed), positioned vertically with a 5 µm syringe filter at the base to simulate miniature leaching columns. Two treatments were set up in duplicate: a biotic treatment (sterile deionised water) and an abiotic treatment (ampicillin-supplemented water, 500 µg mL^{-1}) to suppress microbial activity. Over 25 weeks, columns received 3 mL of treatment solution weekly. At weeks 8, 14, 18, 20, and 25, leachate was collected by flushing each column with 50 mL of sterile deionised water.

Leachates were analysed for pH, Eh, and iron speciation using the ferrozine method (Viollier et al., 2000), which measures Fe^{2+} and total Fe; Fe^{3+} was calculated by subtraction. Microbial cell counts were determined by flow cytometry. Pyrite oxidation rates were estimated from Fe^{2+}/Fe^{3+} data, considering dissolved oxygen as the primary oxidant (Williamson & Rimstidt, 1994).

The abiotic treatment (wetted with 500 ug mL^{-1} ampicillin) consistently exhibited lower leachate concentrations of Fe, lower Eh, and higher pH than the biotic treatment (Figure 4). This was most evident after 25 weeks, where there was a sharp divergence in leachate pH and Fe between treatments. Rate calculations showed that the biotic treatment had pyrite oxidation rates 1.5× and 1.7× greater than abiotic treatment rates at collection weeks 18 and 25, respectively. Cumulative cell counts were significantly greater in the biotic treatment leachate (2.0×10^6 cells mL^{-1}) compared to the Abiotic (9.5×10^4 cells mL^{-1}), with cell counts below detection limits at week 25 for the abiotic treatment.

4.0 DISCUSSION

This study demonstrates how integrating microbial analysis into standard KLC testing can offer valuable insights into the biological drivers of AMD. Results show that microorganisms can significantly accelerate sulfide oxidation and acid generation in certain waste rock types, information that is often unexplored in conventional static geochemical assessments.

Waste rock A, which showed elevated acid generation during a 72-week KLC test, also exhibited greater microbial activity, as evidenced by elevated RNA:DNA ratios, and the presence of known Fe- and S-oxidising bacteria (e.g., *Acidiferrobacter* and *Sulfobacillus*). These taxa carried Fe- and S-oxidation genes (identified via DNA sequencing) and were strongly correlated with Fe and S leaching, reinforcing the role of biological processes impacting AMD. In contrast, waste rock B exhibited lower microbial activity and acid release and exhibited no statistical correlations between geochemical and microbial variables.

To directly quantify the influence of microbial processes on waste rock A, miniature batch leaching experiments were conducted with and without microbial inhibition. The biotic treatment exhibited Fe^{3+}-driven pyrite oxidation rates nearly 2× greater than the abiotic control, evidence that microbial activity significantly enhances pyrite oxidation rates under realistic conditions.

4.1 Implications for Industry

Current AMD prediction tools rely heavily on geochemical tests that do not account for microbial contributions, despite well-established evidence that microbes can accelerate sulfide oxidation by several orders of magnitude (Colmer et al., 1950; Gleisner et al., 2006; Makaula et al., 2017; Nordstrom, 1985; Singer & Stumm, 1970). This study provides a practical, field- and/or lab-relevant framework to close that gap.

Key industry-relevant findings are:

- Microbial monitoring can identify biogeochemical "hotspots": Waste rocks like sample A that are microbially active may pose greater long-term AMD risk, even if static geochemical tests appear marginal.
- The abiotic/biotic leach test is easy to implement: The low-cost batch test can be incorporated into early-stage waste rock screening programs to flag samples for further investigation using the same material, particle size, and setup as existing protocols. The use of less manipulated waste rock provides a more realistic simulation of the current microbial-colonization state of the material.
- Microbial risk profiling can guide more targeted management strategies**:** By identifying waste rock types prone to biologically accelerated sulfide oxidation, operators can prioritise those materials for additional cover, blending, or encapsulation. This approach also provides insight into the relative susceptibility of different rock types to microbially driven leaching over time. In cases where microbial contributions are minimal, conventional geochemical management strategies may be sufficient. Conversely, if microbial activity plays a significant role, the use of targeted microbial mitigation (e.g., biocide application) will need to be evaluated from a cost-benefit perspective, allowing for more informed and adaptive planning.
- Supports adaptive risk-based frameworks: This microbial-inclusive KLC method complements current static and kinetic tests and can be used to inform decision-making under frameworks like the GARD Guide and AMIRA Handbook (Moyo et al., 2025).

4.2 Toward Practical Implementation

The approach presented here bridges the gap between academic understanding and operational needs. Rather than relying on artificial cultures or controlled systems, it assesses in-situ microbial activity directly from leachate, using unmanipulated waste rock. While this method does not resolve the exact mechanisms of microbial oxidation, it does provide a strong early indicator of microbial influence, enabling a tiered approach: routine screening via biotic/abiotic tests, followed by deeper genomic or mineralogical analysis as needed.

In summary, integrating microbial screening into AMD assessments enhances predictive power and provides an early-warning tool for biologically driven sulfide oxidation. Adoption of this approach can significantly improve long-term risk assessments and support more sustainable mine waste management practices.

REFERENCES

Bankevich, A., Nurk, S., Antipov, D., Gurevich, A. A., Dvorkin, M., Kulikov, A. S., Lesin, V. M., Nikolenko, S. I., Pham, S., Prjibelski, A. D., Pyshkin, A. V., Sirotkin, A. V., Vyahhi, N., Tesler, G., Alekseyev, M. A., & Pevzner, P. A. (2012). SPAdes: A new genome assembly algorithm and its applications to single-cell sequencing. *Journal of Computational Biology*, *19*(5), 455–477. https://doi.org/10.1089/cmb.2012.0021

Chen, L. xing, Huang, L. nan, Méndez-García, C., Kuang, J. liang, Hua, Z. shuang, Liu, J., & Shu, W. sheng. (2016). Microbial communities, processes and functions in acid mine drainage ecosystems. In *Current Opinion in Biotechnology* (Vol. 38, pp. 150–158). Elsevier Ltd. https://doi.org/10.1016/j.copbio.2016.01.013

Chklovski, A., Parks, D. H., Woodcroft, B. J., & Tyson, G. W. (2023). CheckM2: a rapid, scalable and accurate tool for assessing microbial genome quality using machine learning. *Nature Methods*, *20*(8), 1203–1212. https://doi.org/10.1038/s41592-023-01940-w

Colmer, A. R., Temple, K. L., & Hinkle, M. E. (1950). An Iron-Oxidizing Bacterium From The Acid Drainage Of Some Bituminous Coal Mines. *Journal of Bacteriology*.

Garber, A. I., Nealson, K. H., Okamoto, A., McAllister, S. M., Chan, C. S., Barco, R. A., & Merino, N. (2020). FeGenie: A Comprehensive Tool for the Identification of Iron Genes and Iron Gene Neighborhoods in Genome and Metagenome Assemblies. *Frontiers in Microbiology*, *11*. https://doi.org/10.3389/fmicb.2020.00037

Gleisner, M., Herbert, R. B., & Frogner Kockum, P. C. (2006). Pyrite oxidation by Acidithiobacillus ferrooxidans at various concentrations of dissolved oxygen. *Chemical Geology*, *225*(1–2), 16–29. https://doi.org/10.1016/j.chemgeo.2005.07.020

Goltsman, D. S. A., Comolli, L. R., Thomas, B. C., & Banfield, J. F. (2015). Community transcriptomics reveals unexpected high microbial diversity in acidophilic biofilm communities. *ISME Journal*, *9*, 1014–1023. https://doi.org/10.1038/ismej.2014.200

Loeppmann, S., Semenov, M., Kuzyakov, Y., & Blagodatskaya, E. (2018). Shift from dormancy to microbial growth revealed by RNA:DNA ratio. *Ecological Indicators*, *85*, 603–612. https://doi.org/10.1016/j.ecolind.2017.11.020

Makaula, D. X., Huddy, R. J., Fagan-Endres, M. A., & Harrison, S. T. L. (2017). Using isothermal microcalorimetry to measure the metabolic activity of the mineral-associated microbial community in bioleaching. *Minerals Engineering*, *106*, 33–38. https://doi.org/10.1016/j.mineng.2016.12.012

Meruane, G., & Vargas, T. (2003). Bacterial oxidation of ferrous iron by Acidithiobacillus ferrooxidans in the pH range 2.5-7.0. *Hydrometallurgy*, *71*(1–2), 149–158. https://doi.org/10.1016/S0304-386X(03)00151-8

Mielke, R. E., Pace, D. L., Porter, T., Southam, G., & Gordon, S. (2003). A critical stage in the formation of acid mine drainage: Colonization of pyrite by Acidithiobacillus ferrooxidans under pH-neutral conditions. In *Geobiology* (Vol. 1).

Moyo, A., Parbhakar-Fox, A., Meffre, S., & Cooke, D. R. (2025). An accelerated kinetic leach test for geochemical and environmental characterisation of acid and metalliferous drainage. *Environmental Technology and Innovation*, *38*. https://doi.org/10.1016/j.eti.2025.104092

Nissen, J. N., Johansen, J., Allesøe, R. L., Sønderby, C. K., Armenteros, J. J. A., Grønbech, C. H., Jensen, L. J., Nielsen, H. B., Petersen, T. N., Winther, O., & Rasmussen, S. (2021). Improved metagenome binning and assembly using deep variational autoencoders. *Nature Biotechnology*, *39*(5), 555–560. https://doi.org/10.1038/s41587-020-00777-4

Nordstrom, K. D. (1985). Receiving Acid Mine Effluent. In *Selected Papers in the Hydrologic Sciences* (Vol. 2270, p. 113).

Qian, G., Fan, R., Huang, J., Pring, A., Harmer, S. L., Zhang, H., Rea, M. A. D., Brugger, J., Teasdale, P. R., Gibson, C. T., Schumann, R. C., Smart, R. S. C., & Gerson, A. R. (2021). Oxidative dissolution of

sulfide minerals in single and mixed sulfide systems under simulated acid and metalliferous drainage conditions. *Environmental Science and Technology*, *55*(4), 2369–2380. https://doi.org/10.1021/acs.est.0c07136

Roach, M. J. (2023). *Trimnami: Trim Lots of Metagenomics Samples All at Once*.

Silva, G. G. Z., Green, K. T., Dutilh, B. E., & Edwards, R. A. (2016). SUPER-FOCUS: A tool for agile functional analysis of shotgun metagenomic data. *Bioinformatics*, *32*(3), 354–361. https://doi.org/10.1093/bioinformatics/btv584

Singer, P. C., & Stumm, W. (1970). Acidic mine drainage: The rate-determining step. *Science*, *167*(3921), 1121–1123. https://doi.org/10.1126/science.167.3921.1121

Steinegger, M., & Söding, J. (2017). MMseqs2 enables sensitive protein sequence searching for the analysis of massive data sets. In *Nature Biotechnology* (Vol. 35, Issue 11, pp. 1026–1028). Nature Publishing Group. https://doi.org/10.1038/nbt.3988

Viollier, E., Inglett, P. W., Hunter, K., Roychoudhury, A. N., & Van Cappellen, P. (2000). *The ferrozine method revisited: Fe(II)/Fe(III) determination in natural waters*.

Williamson, M. A., & Rimstidt, J. D. (1994). The kinetics and electrochemical rate-determining step of aqueous pyrite oxidation. In *Geochimlca et Cosmochimica Acta* (Vol. 58, Issue 24).

Table 1. Leachate Total Acidity (mg CaCO3 L-1) in Waste Rock A and Waste Rock B leachate

Timepoint	Waste Rock A	Waste Rock B
Week 8	17033	11710
Week 12	26110	13100
Week 16	27480	14300
Week 20	22270	14100
Week 24	15215	11850
Week 32	9981	5610
Week 48	6512	4423
Week 72	10929	8427

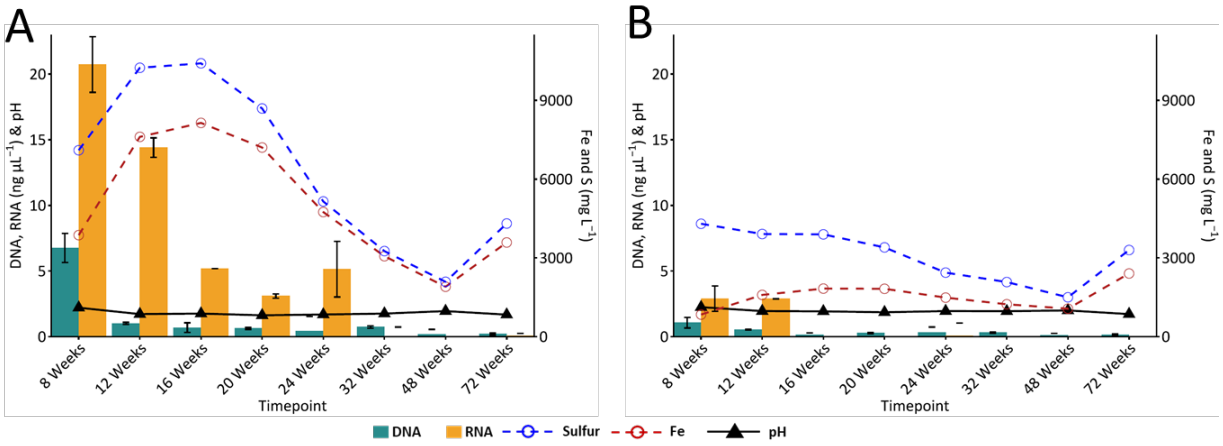

Fig. 1. **Kinetic leach column (KLC) leachate characteristics for waste rock A (A) and waste rock B (B) over 72 weeks**

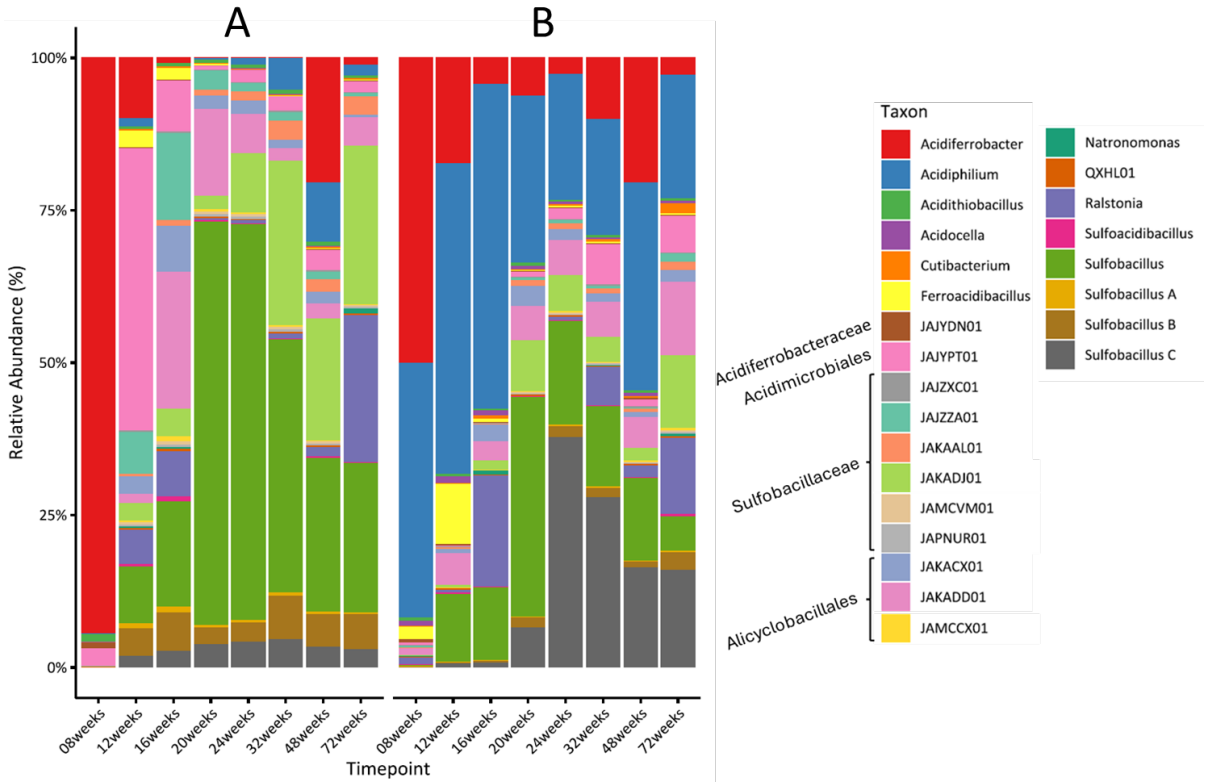

Fig. 2. **Microbial community analysis of Waste Rock A and Waste Rock B leachate. The top 25 most abundant genera are displayed by relative abundance (%)**

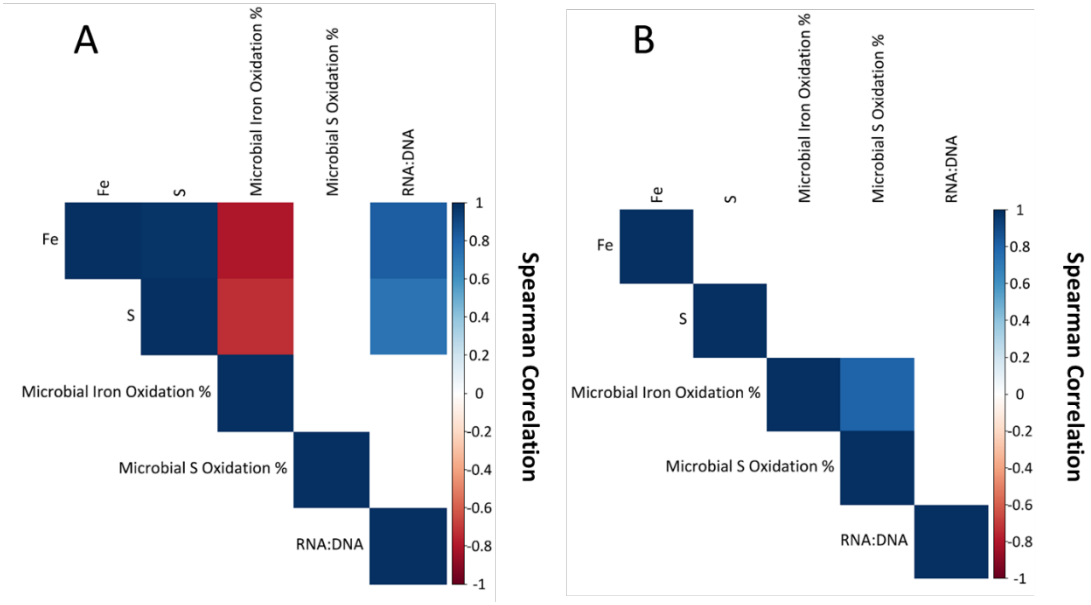

Fig. 3. **Significant Spearman correlations ($p < 0.05$) for select geochemical and microbiological variables from Waste Rock A and Waste Rock B. Variables include total Fe, Total S, Microbial Iron Oxidation %, Microbial Sulfur Oxidation %, and RNA:DNA ratio**

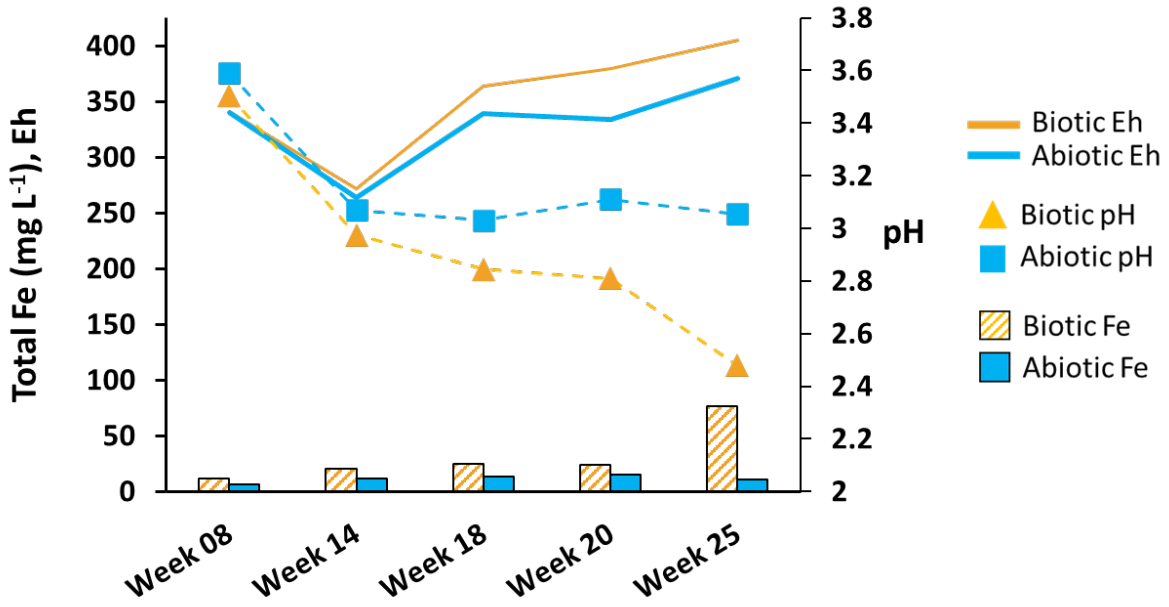

Fig. 4. **Leachate characteristics (Total Fe, Eh, and pH) from waste rock A biotic/abiotic batch leaching experiment. Biotic treatments were leached with deionised water, and abiotic treatments leached with ampicillin-spiked deionized water (500 µg mL-1) for 25 weeks**

Iron ore mine AMD management Hey people, it's not just about Acid Rock Drainage!

A. Botfield[A] and R. Cooke[B]

[A]Environmental Geochemistry International (EGi), 7/2a Gladstone Street Newtown, New South Wales, Australia, 2042. andrew.botfield@geochemistry.com.au

[B]Fortescue, Ground Floor, 256 St Georges Terrace, Perth, Western Australia, Australia 6000,

For a large iron ore operation, the challenges of effectively managing Acid and Metalliferous Drainage (AMD) are not immediately obvious. Afterall, most mined rock types that are disturbed are geochemically benign in terms of sulfide mineral content and those that are not, usually represent a minor proportion of the mining envelope. However, the implementation of AMD management planning from project conception to closure for a large iron ore operation not only requires rollout across large and complex mining operations but also needs to be nimble and adaptable to the ongoing changes to best practice and the regulatory requirements for project approval and licensed operation.

Recent guidance on the implementation of AMD management planning is provided by the Tool for Acid Rock Drainage and Metal Leaching Prevention and Management (INAP & ICMM 2025). At its core, as illustrated by Figure 1, is a staged risk-based approach centred around continual refinement of a site-specific AMD source to receptor conceptual site model. The model requires fit for purpose data collection to inform potential environmental impacts and validation of mitigation strategies. Based on the incorporation of the site model into a Microsoft Excel based macro, the management tool can also link specific AMD management scenarios to typical data collection activities and international best practice guidelines for AMD characterisation and environmental impact assessment.

Scale is a key factor for an iron ore operation. Mine waste volumes are often very large as are the volumes of water that must be handled to enable ore extraction and processing. Consequently, to realise an effective set of AMD management strategies, the modes of data collection need to be carefully thought through to ensure both site specific relevance, and that they can be applied practically at scale and are not cost or time prohibitive. However, there is often a significant disconnect with the data collection requirements stipulated by a regulator and what can be achieved based on the scale of the operation and the site-specific nature of mined materials.

One of the most valuable modes of AMD data collection for an iron ore operation is the geological model of the mined rock types. Target iron ore bearing rock types associated with all iron ore mines across the Pilbara region of Western Australia are part of the Hamersley Group (Thorne et al., 2008). Most of these rock types are continuous for hundreds of kilometres with consistent and well described geological controls on the distribution and forms of sulfur and carbonate minerals (Rio Tinto 2010; and Green et al, 2019). This alone enables the identification of rock types that are most likely to represent a potential AMD risk to the environment, such as the pyritic Mount McRae Shale unit. When that information is used in conjunction with a typically very large geo-assay database from resource definition and grade control drilling programs, the distribution of these problematic rock type materials can be well defined. This information is highly valuable in informing the assessment of AMD and associated risk to the environment, as it can be incorporated into the same block model that is used for many aspects of mine waste scheduling and waste landform design (Green et al., 2019).

However, AMD assessment requirements for mine approval and licensing in Australia often does not acknowledge the significant understanding of deposit geology and can place far more importance on a

proponent undertaking often quite arbitrary geochemical sampling and test work programs with no thought to the scale or the nature of the ore and waste rock that may be produced by the mine. For an iron ore mine, scale is important, and modes of data collection must be relevant, targeted and where possible collected incidentally with other tasks or functions to maximise value and save cost, e.g., regular sampling and testing of process facility tailings and supernatant concurrent with other operational practices; and use of compliance surface / groundwater quality monitoring programs to inform the identification of emerging AMD water quality issues across a site.

Additionally, over the last few years regulators have specified a requirement for several tests adapted from other industries and environmental regulatory environments that don't provide geochemical data that can be readily interpreted in the context of water-rock interactions in the natural environment. Examples include the *Synthetic Precipitation Leaching Procedure* (USEPA 1994) and sequential extraction techniques such as *Sequential Extraction Procedure for the Speciation of Particulate Trace Metals* (Tessier 1979) and *Method 1313 of the USEPA LEAF series - Liquid-Solid Partitioning as a Function of pH Using a Batch Equilibrium Procedure* (USEPA 2017). What these tests have in common is the use of strong acids, bases and/or organic extractants intended to mimic the range of potential conditions of waste storage, water infiltration and resultant drainage water quality. However, such tests are often too far removed from field conditions to reliably inform the probable geochemical behaviour of a material and are often unnecessary since a wide range of field conditions can be described by conventional water quality modelling approaches. For example, unscaled water extract or environmental compliance water quality data can be used to define source term chemistry and coupled with surface and groundwater balance information, for chemical equilibrium modelling using programs such as PHREEQC (Parkhurst and Appelo 2013).

Another example is the requirement to undertake the free draining kinetic column test (AMIRA (EGi & IWRI) 2002) and in the case of an iron ore operation, often on iron formation rock units that are geochemically benign in terms of acid forming and/or neutralisation potential. This test method is regularly used to provide reliable quantification of several geochemical aspects including sulfide reactivity, oxidation kinetics, metal solubility and overall short to longer term leaching behaviour under optimised oxidising conditions. This is achieved via exposing a fixed mass of material within a large buchner funnel, as depicted in Figure 2, to a weekly wet-dry cycle and a monthly leaching cycle. This test method is known to provide valuable insights into how pyritic mine materials may behave on exposure to air, but what insights are gained for non-pyritic materials that could be obtained using quicker, simpler and cheaper static leachate test methods such single or multi-stage water extraction tests?

For illustration we are using a comparison of leachate quality data from a free draining kinetic column operated for six-months with 3-stage (1 part solid :2 parts de-ionised water) and single stage (1 part solid: 5 parts de-ionised water (EGi 2002) extraction data sets. The test work was undertaken by EGi from 2024 to 2025 using samples of Brockman Iron Formation rock with very low total sulphur and carbonate mineral content referred to as 'Pilbara BIF X', collected from two different iron ore mine sites within the Pilbara. These two mines are separated by over 200 km and referred to as 'Mine A' and 'Mine B' in summary Tables 1 to 2 and time-based plots Figures 3 to 8.

Overall, the free draining kinetic column data sets suggests the short to longer term leaching characteristics of Pilbara BIF X from the two different mine sites are very similar and, although initially releasing moderate concentrations of salinity and bicarbonate alkalinity, concentrations of these parameters would attenuate to relatively low concentrations in the medium to longer term and concentrations of all metals, metalloids and trace non-metals such as boron and fluoride are expected to be either negligible or low both in the short or longer term. To enable comparison between the

kinetic column and 3-stage (1:2) and single stage (1:5) water extraction data sets, the cumulative mass release of constituents as a function of the changing ratio of kinetic column flush volume to sample mass that occurs over time, was compared to the solute mass release as a function of the batch water extract volume to mass ratio. Figure 9 compares cumulative mass release for total dissolved solids (TDS).

Results suggest the 3-stage (1:2) water extraction provides a reasonable estimation of kinetic column cumulative mass release for TDS at week 15 and the extrapolated probable order of magnitude for TDS for column flush to mass ratios of 4 and 6 if the kinetic column work was to continue up to the timeframe equivalent of those ratios. Results also suggest although the single stage (1:5) water extraction data set has a wide range in equivalent cumulative mass release the median TDS value provides a reasonable estimation of probable order of magnitude of cumulative mass release if the kinetic column work was to continue until a column flush to mass ratio of 5 was reached. Note also, the 1:5 batch extracts were performed using similar but not the same sample used in the leach column and sequential 1:2 batch extracts.

Overall, although both these static test methods represent leaching conditions that are quite different to the kinetic column method, i.e., chemical equilibrium driven dissolution of constituents rather than strongly oxidising conditions with cycles of evaporation and water infiltration, these batch extraction methods do appear to provide a reasonable indication of short to longer term leachate quality for this non-acid forming (NAF) Brockman Iron Formation rock type. Further support of this inference can be seen for constituents that did not record concentrations above the limit of detection across the two different mine sites for the same NAF Brockman Iron Formation rock type, i.e., the two independent data sets demonstrate a very similar leaching profile. Provided samples capture the geochemical variability of a NAF material, these results suggest that batch extraction tests can be used to identify key constituents that may be released due to short to longer term contact with an unbuffered water source such as rainfall run-off or relatively fresh groundwater.

The Tool for Acid Rock Drainage and Metal Leaching Prevention and Management defines characterisation as “actions to complete the characterisation of all potential ARD/ML sources at a level that is sufficient for the prediction of drainage chemistry, identification of potential environmental impacts, and evaluation of prevention/mitigation/treatment alternatives” (INAP & ICMM 2025). However, what a large iron ore company and industry guidance or regulators define as sufficient is often not the same. With unrealistic expectations for mining companies to undertake very detailed and long-term geochemical test work, consideration needs to be given to alternatives for demonstration of how mined materials are likely to behave, particularly where that material is geologically consistent over 100s of kilometres and where conclusions are supported by decades of historical data collection.

Figure 10 outlines the AMD management process that a large iron ore company implements for new iron ore projects. This is typically underpinned by a highly integrated corporate document framework such as shown in Table 3. The framework ranges from a high-level corporate management plan outlining the company’s philosophy regarding AMD management, to site-specific operations manuals, which ensures all internal stakeholders are aware of their requirements to be compliant across different stages of a project from planning to operations. Table 3 also outlines how these documents can link to the Tool for Acid Rock Drainage and Metal Leaching Prevention and Management leading practice activities.

Typically, the process begins with systematic sampling for new deposits where hundreds of samples across geological units undergo static geochemical test work. The priority at this stage is the integration of baseline geochemical data into the geological model as early as possible to produce mine-material

inventories and inform management strategies for operations. Once the landforms have been designed, long-term test work such as detailed geochemical modelling and seepage assessments can be completed. Long-term test work is often required for early environmental approvals and if not completed, the assessment may leverage data derived from other sites. Usually, the mining company acknowledges that there will be information gaps, but these are within the company's internal risk tolerance. This process must be flexible, as inputs may change at various times based on advice from internal subject matter experts and requests for information from the regulatory bodies.

Once a project moves into operations, the focus shifts to the implementation of a robust sampling program to validate the baseline geochemical predictions. Results can be reported externally through compliance reports and demonstrate the company's commitment to understanding the ongoing risk from the operation. Systematic sampling during operations continually builds on the company's understanding of geological materials which will inform future projects.

As detailed in the Tool for Acid Rock Drainage and Metal Leaching Prevention and Management, it is imperative we create success criteria that are SMART (specific, measurable, achievable, relevant and time bound). Such criteria should be defined based on regulatory requirements, stakeholder inputs, and the company's internal risk tolerance (INAP & ICMM 2025), keeping in mind that these may not always align. From an operational and corporate risk management perspective, clearly a staged risk-based approach can be applied to AMD management planning at an iron ore operation. However, there remains a need to further educate mining companies, consultants and regulators on how best to undertake fit for purpose data collection that informs probable AMD behaviour of mined materials and validation of mitigation strategies.

REFERENCES

AMIRA (EGi & IWRI) (2002). ARD Test Handbook. Project P387A Prediction & Kinetic Control of Acid mine Drainage. AMIRA International Limited. May 2002. Authored by Environmental Geochemistry International (EGi) and Ian Wark Research Institute (IWRI).

EGi (2002). Single and Sequential Batch Extraction Test. Internal test method. July 2002.

Green and Borden (2011). Geochemical Risk Assessment Process for Rio Tinto's Pilbara Iron Ore Mines. Chapter 19. Integrated Waste Management. Rosalind Green and Richard K Borden. Published: August 23rd, 2011.

Green et al., (2019). Rio Tinto's framework for evaluating risks from low sulfur waste rock. R. Green. C. Linklater. S. Lee. L. Terrusi. K Glasson. Mine Closure 2019.

INAP & ICMM (2025). Tool for Acid Rock Drainage and Metal Leaching Prevention and Management. International Network for Acid Prevention (INAP) and International Council on Mining and Metals (ICMM).

INAP (2014). Global Acid Rock Drainage Guide (GARD Guide), International Network for Acid Prevention (http://www.gardguide.com/).

MEND (2009). Prediction Manual for Drainage Chemistry from Sulphidic Geologic Materials. Report 1.20.1. Mining Environment Neutral Drainage (MEND) Program, Natural Resources Canada. December 2009.

Parkhurst and Appelo (2013). Description: PHREEQC (Version 3)—A Computer Program for Speciation, Batch-Reaction, One-Dimensional Transport, and Inverse Geochemical Calculations. USGS Techniques and Methods, Book 6, Chapter A43. U.S. Geological Survey, Reston, Virginia.

Rio Tinto (2010). Geology and mineralogy of the Hamersley Province ore. Year 2010 update.

Tessier et al, (1979). Sequential Extraction Procedure for the Speciation of Particulate Trace Metals. A. Tessier, P.G.C. Campbell, and M. Bisson.

Thorne et al., (2008). Chapter 8. Banded Iron Formation-Related Iron Ore Deposits of the Hamersley Province, Western Australia. Warren Thorne. Steffen Hagemann. Adam Webb. John Clout. 2008 Society of Economic Geologists. SEG Reviews vol. 15, p. 197–221.

USEPA (1994). Method 1312. Synthetic Precipitation Leaching Procedure. Revision 0. September 1994.United States Environmental Protection Agency.

USEPA (2017). Method 1313: Liquid–Solid Partitioning as a Function of Extract pH Using a Parallel Batch Extraction Procedure (EPA SW-846 Test Method 1313, Rev. 0). U.S. Environmental Protection Agency. 2017.

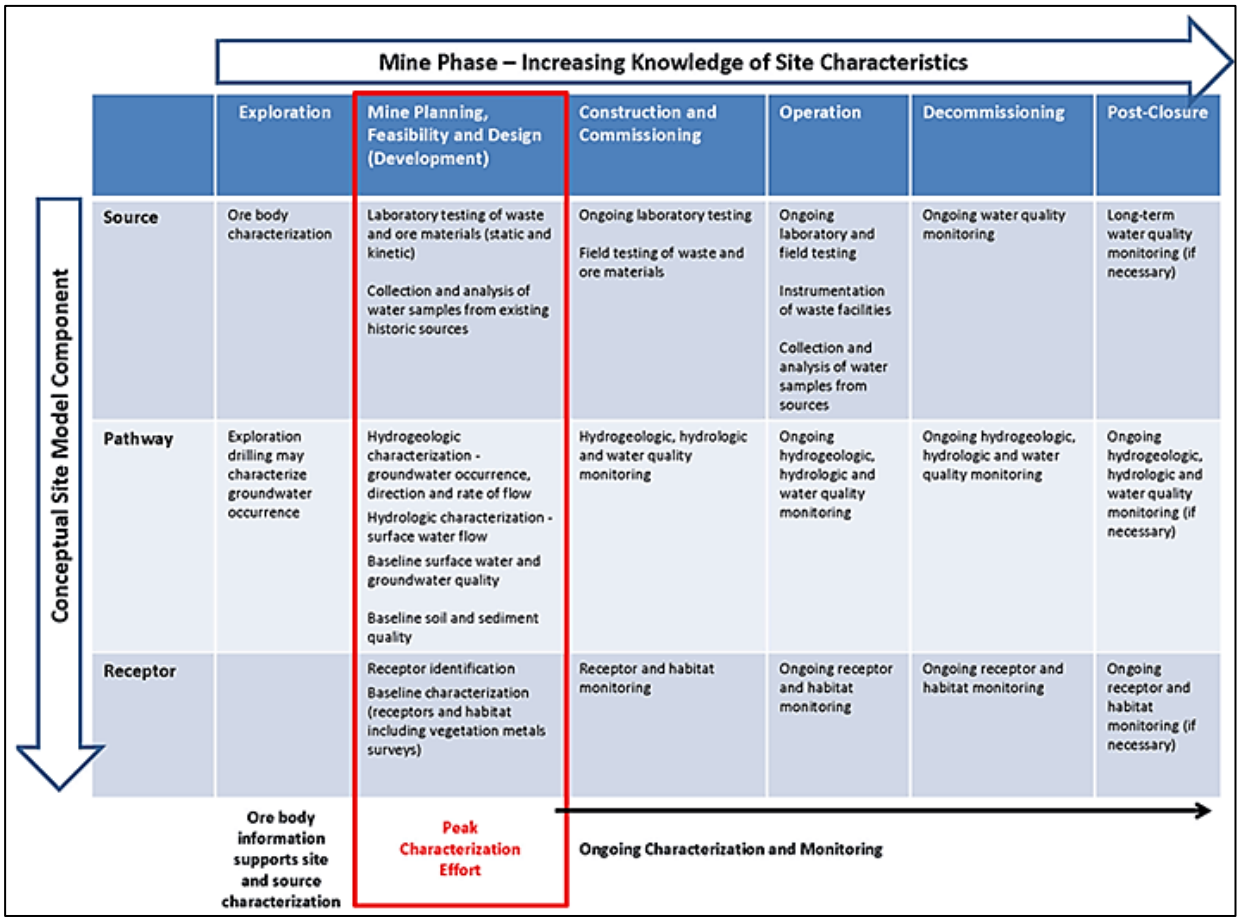

Fig. 1. **Example output from the Tool for Acid Rock Drainage and Metal Leaching Prevention and Management (INAP & ICMM 2025)**

Fig. 2. **Typical set up of free draining columns that are subject to a weekly wet-dry cycle and a monthly leaching cycle.**

Table 1. **Comparison of free draining column data with 3 Stage Batch Extracts (1:2) and Single Stage (1:5) extracts for Pilbara BIF X at Mine A**

Parameter		Free Draining Column (six months)		3 Stage Batch Extracts			1:5 Extracts (13 samples)		
		First Flush	Median	1st 1:2	2nd 1:2	3rd 1:2	Max	Median	Min
pH	-	7.66	7.74	7.5	7.8	7.5	8.3	7.8	6.7
EC	µS/cm	1580	125	291	138	88	246	94	65
TDS (calc)	mg/L	1120	115	223	115	78	271	71	29
Alkalinity (CaCO3)	mg/l	200	59	77	52	42	51	30	15
HCO3 equiv	mg/L	244	72	94	63	51	62	37	18
Ag	mg/l	0.00005	0.00005	0.00005	0.00005	0.00005	0.00005	0.00005	0.00005
Al	mg/l	0.003	0.115	0.0025	0.0025	0.023	0.045	0.003	0.003
As	mg/l	0.0001	0.0003	0.0004	0.0001	0.0001	0.0002	0.0001	0.0001
B	mg/l	0.387	0.209	0.173	0.116	0.090	0.223	0.092	0.053
Ba	mg/l	0.042	0.015	0.579	0.895	0.808	1.230	0.645	0.188
Be	mg/l	0.00005	0.00005	0.00005	0.00005	0.00005	0.00005	0.00005	0.00005
Ca	mg/l	37	5	7	4	3	8.000	5.000	1.000
Cd	mg/l	0.000025	0.000025	0.000025	0.000025	0.000025	0.000025	0.000025	0.000025
Cl	mg/l	370	9	48	16	6	124	13	4
Co	mg/l	0.0005	0.0002	0.0001	0.00005	0.00005	0.0007	0.0001	0.0001
Cr	mg/l	0.0001	0.0004	0.0004	0.0006	0.0005	0.0011	0.0005	0.0001
Cu	mg/l	0.0038	0.0032	0.0073	0.0033	0.0020	0.0045	0.0017	0.0007
F	mg/l	0.60	2.50	0.6	0.7	0.6	0.8	0.3	0.2
Fe	mg/l	0.001	0.108	0.003	0.006	0.050	0.349	0.004	0.001
Hg	mg/l	0.00002	0.00002	0.00002	0.00002	0.00002	0.00002	0.00002	0.00002
K	mg/l	11	2	4	1	0.5	3.0	1.0	0.5
Mg	mg/l	70	8	12	7	5	8.0	5.0	2.0
Mn	mg/l	0.033	0.014	0.010	0.005	0.005	0.040	0.003	0.001
Mo	mg/l	0.001	0.016	0.0008	0.0015	0.0018	0.0028	0.0002	0.0001
Na	mg/l	239	19	41	18	9	71	12	4
Ni	mg/l	0.002	0.002	0.0007	0.00025	0.0008	0.0013	0.0003	0.0003
Pb	mg/l	0.00005	0.00005	0.00005	0.00005	0.00005	0.00005	0.00005	0.00005
Sb	mg/l	0.0010	0.0004	0.0002	0.0001	0.0001	0.0006	0.0001	0.0001
Se	mg/l	0.0020	0.0004	0.0002	0.0001	0.0001	0.0003	0.0001	0.0001
Si	mg/l	7.2	8.5	5.1	4.7	4.3	6.29	1.90	0.72
Sn	mg/l	0.0004	0.0001	0.0001	0.0001	0.0001	0.0	0.0	0.0
SO4	mg/l	149	8	17	6	3	36	4	1
Sr	mg/l	0.37	0.04	0.062	0.038	0.028	0.045	0.030	0.018
Th	mg/l	0.0001	0.00005	0.00005	0.00005	0.00005	0.00005	0.00005	0.00005
Tl	mg/l	0.00008	0.00001	0.00001	0.00001	0.00001	0.00001	0.00001	0.00001
U	mg/l	0.000025	0.000025	0.000025	0.000025	0.000025	0.000025	0.000025	0.000025
Zn	mg/l	0.011	0.0010	0.078	0.073	0.047	0.057	0.017	0.007

Note: underlined values are below detection and recorded above at half the reporting limit.

Table 2. **Comparison of free draining column data with Single Stage (1:5) extracts for Pilbara BIF X at Mine B**

Parameter		Free Draining Column (six months)		1:5 Extracts (5 samples)		
		First Flush	Median	Max	Median	Min
pH	-	7.03	7.03	8.60	7.90	7.20
EC	µS/cm	496	68	463	106	94
TDS (calc)	mg/L	286	26	283	55	55
Alkalinity (CaCO3)	mg/l	16	16	28	27	18
HCO3 equiv	mg/L	20	20	34	33	22
Ag	mg/l	0.0005	0.0005	0.0005	0.0005	0.0005
Al	mg/l	0.005	0.005	0.06	0.01	0.005
As	mg/l	0.0005	0.0005	0.0005	0.0005	0.0005
B	mg/l	0.08	0.025	0.18	0.11	0.025
Ba	mg/l	0.004	0.001	0.786	0.351	0.076
Be	mg/l	0.0005	0.0005	0.0005	0.0005	0.0005
Ca	mg/l	2	0.5	5	2	0.5
Cd	mg/l	0.00005	0.00005	0.00005	0.00005	0.00005
Cl	mg/l	119	0.5	115	16	7
Co	mg/l	0.0005	0.0005	0.0005	0.0005	0.0005
Cr	mg/l	0.0005	0.0005	0.001	0.0005	0.0005
Cu	mg/l	0.004	0.0005	0.004	0.002	0.0005
F	mg/l	1	0.7	0.7	0.3	0.2
Fe	mg/l	0.1	0.025	0.54	0.09	0.025
Hg	mg/l	0.00005	0.00005	0.00005	0.00005	0.00005
K	mg/l	10	0.5	7	0.5	0.5
Mg	mg/l	5	1	11	1	0.5
Mn	mg/l	0.003	0.002	0.238	0.053	0.005
Mo	mg/l	0.012	0.006	0.0005	0.0005	0.0005
Na	mg/l	81	3	73	11	10
Ni	mg/l	0.0005	0.0005	0.0005	0.0005	0.0005
Pb	mg/l	0.0005	0.0005	0.0005	0.0005	0.0005
Sb	mg/l	0.0005	0.0005	0.0005	0.0005	0.0005
Se	mg/l	0.005	0.005	0.005	0.005	0.005
Si	mg/l	2.6	2.6	3.87	1.94	0.77
Sn	mg/l	0.0005	0.0005	0.0005	0.0005	0.0005
SO4	mg/l	49	0.5	50	4	1
Sr	mg/l	0.011	0.003	0.013	0.009	0.003
Th	mg/l	0.0005	0.0005	0.0005	0.0005	0.0005
Tl	mg/l	0.0005	0.0005	0.0005	0.0005	0.0005
U	mg/l	0.0005	0.0005	0.0005	0.0005	0.0005
Zn	mg/l	0.009	0.0025	0.09	0.011	0.005

Note: underlined values are below detection and recorded above at half the reporting limit.

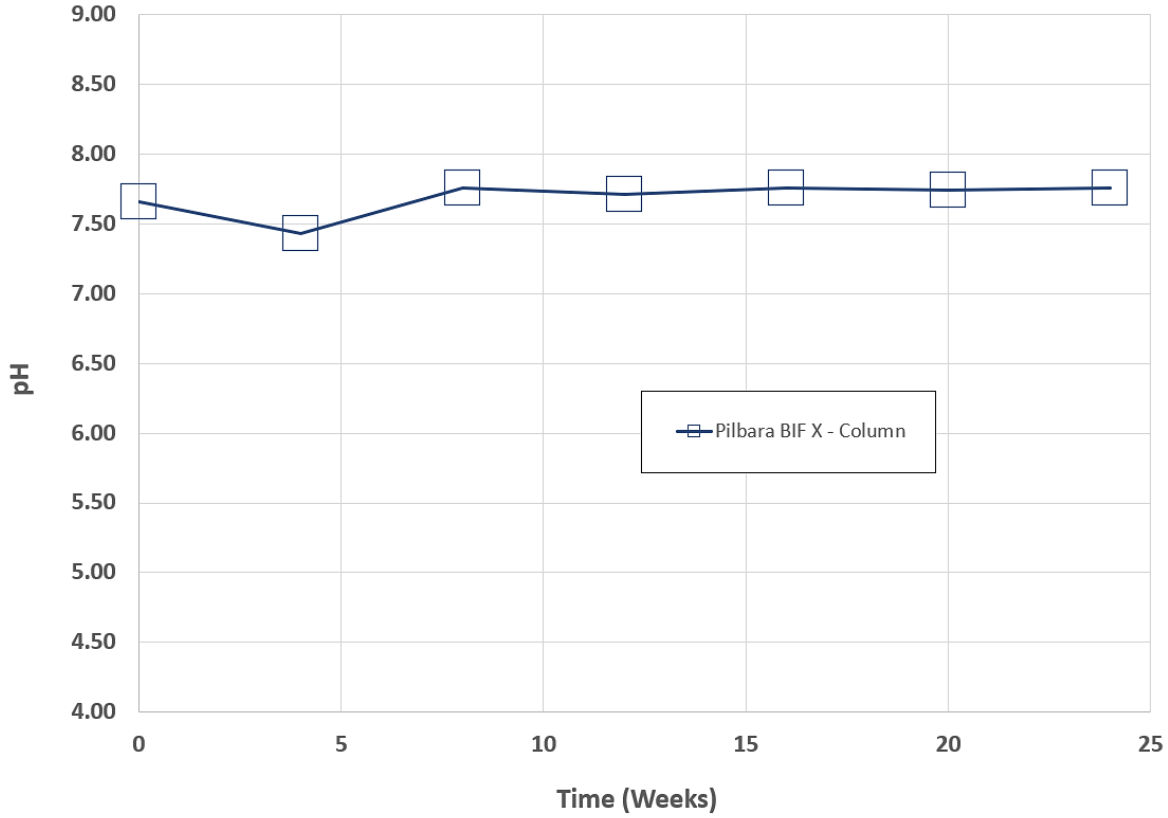

Fig. 3. **pH values for free draining column test work on Pilbara BIF X from Mine A**

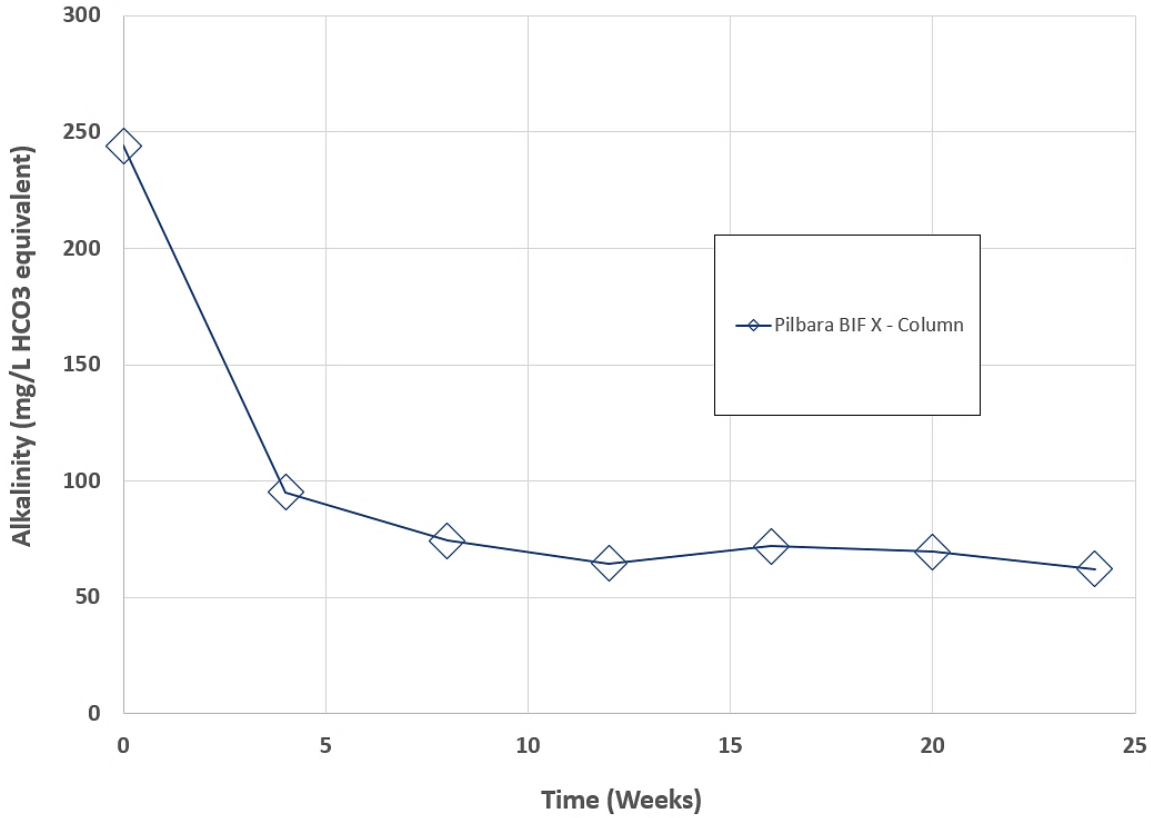

Fig. 4. **Alkalinity values (bicarbonate equivalent) free draining column test work on Pilbara BIF X from Mine A**

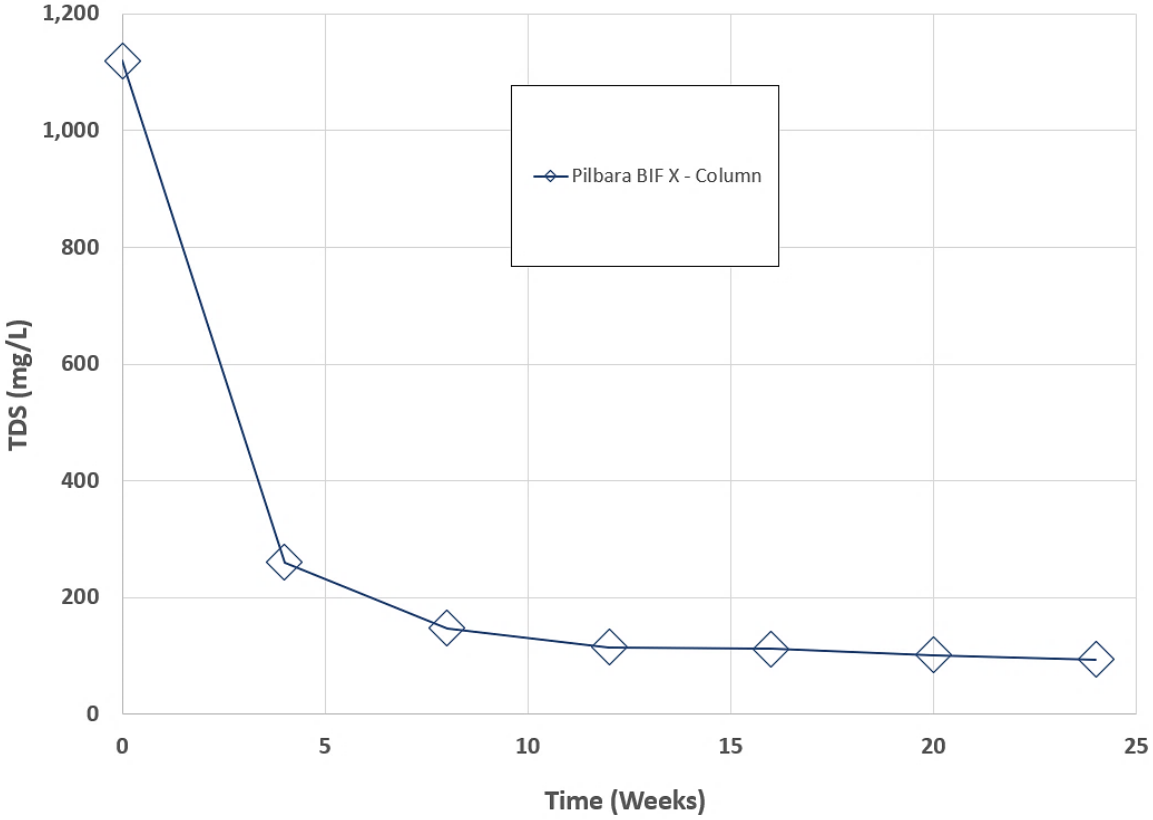

Fig. 5. **TDS values for free draining column test work on Pilbara BIF X from Mine A**

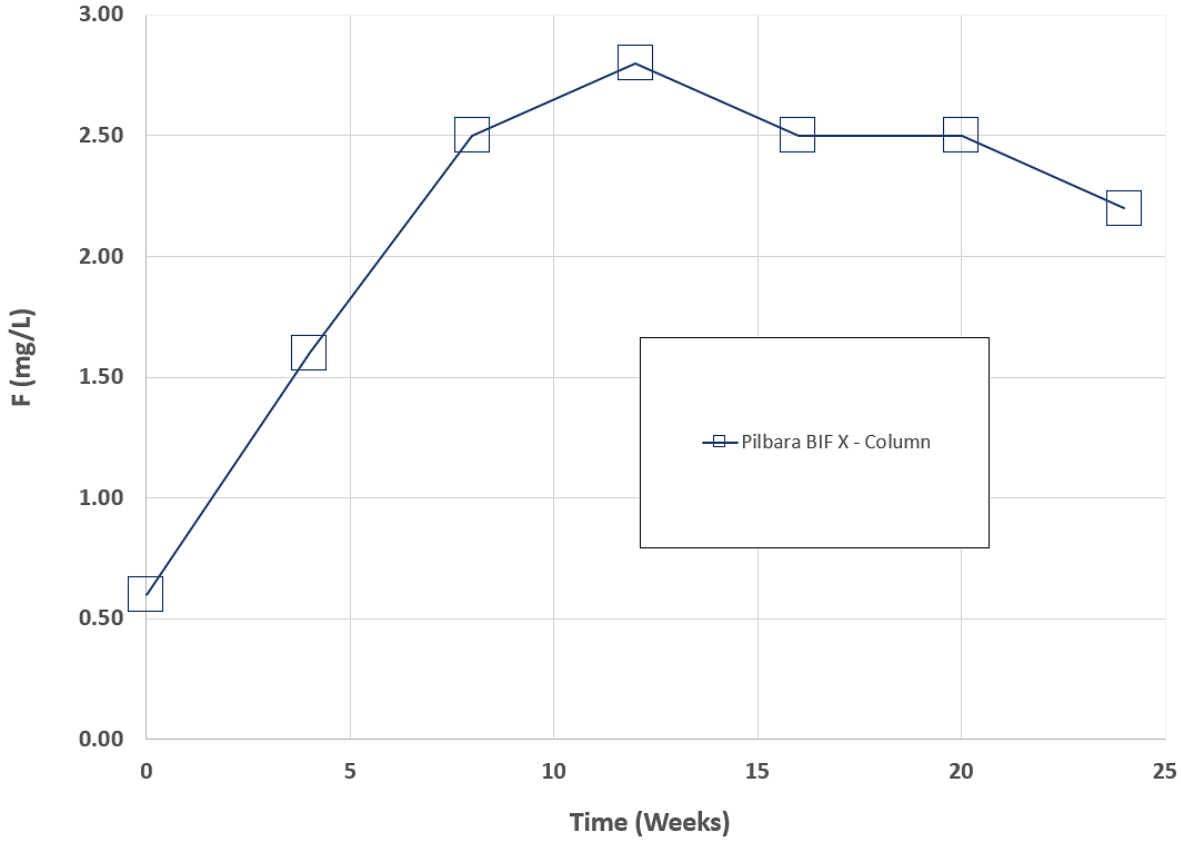

Fig. 6. **Fluoride values for free draining column test work on Pilbara BIF X from Mine A**

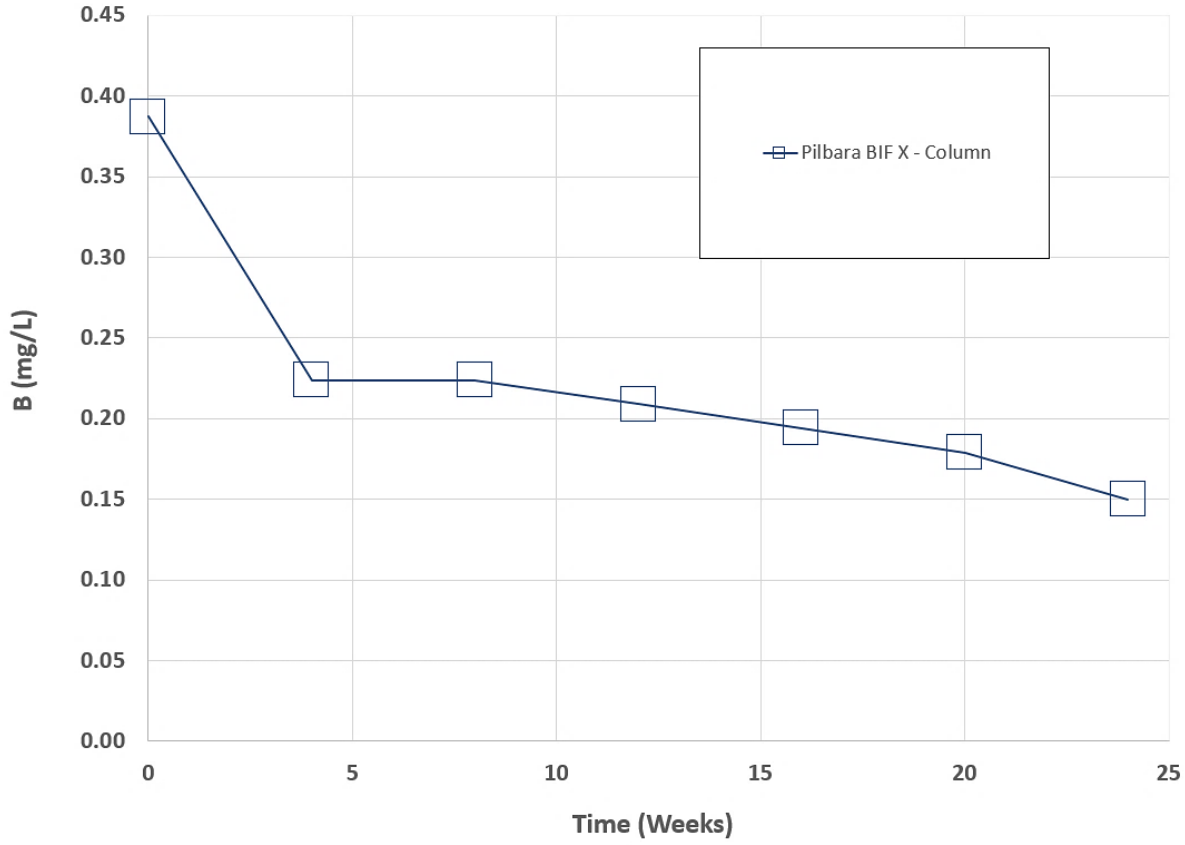

Fig. 7. **Boron values for free draining column test work on Pilbara BIF X from Mine A**

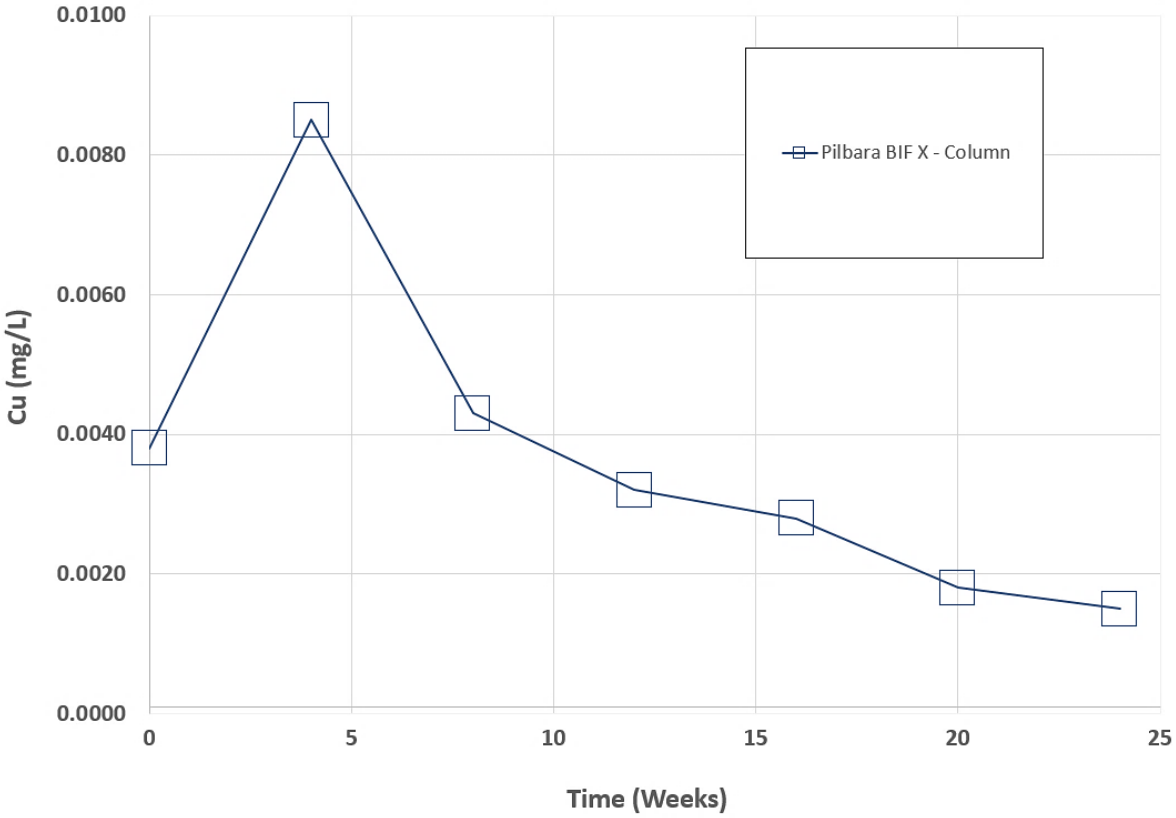

Fig. 8. **Copper values for free draining column test work on Pilbara BIF X from Mine A**

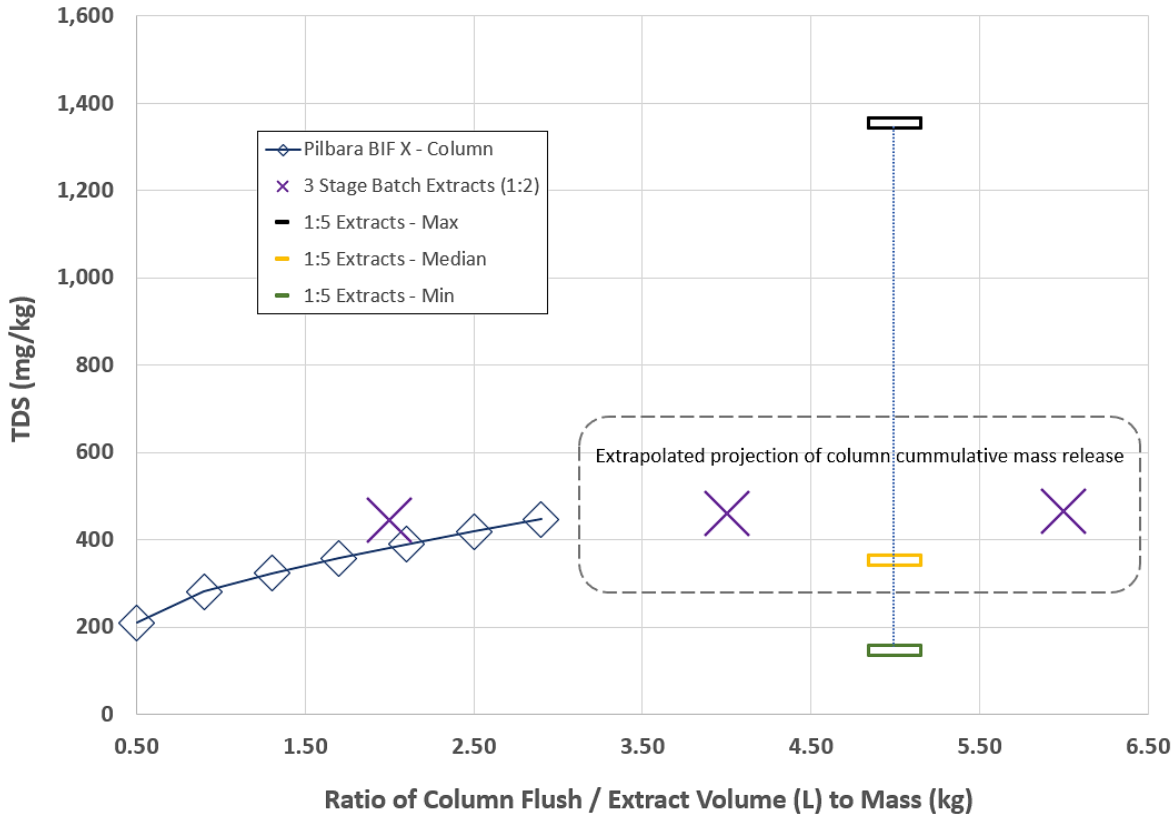

Fig. 9. **Comparison of cumulative mass release of TDS from Pilbara BIF X from Mine A, actual extrapolated compared to 3 Stage Batch Extracts (1:2) for same sample as column and Single Stage (1:5) extracts for 13 samples of same material**

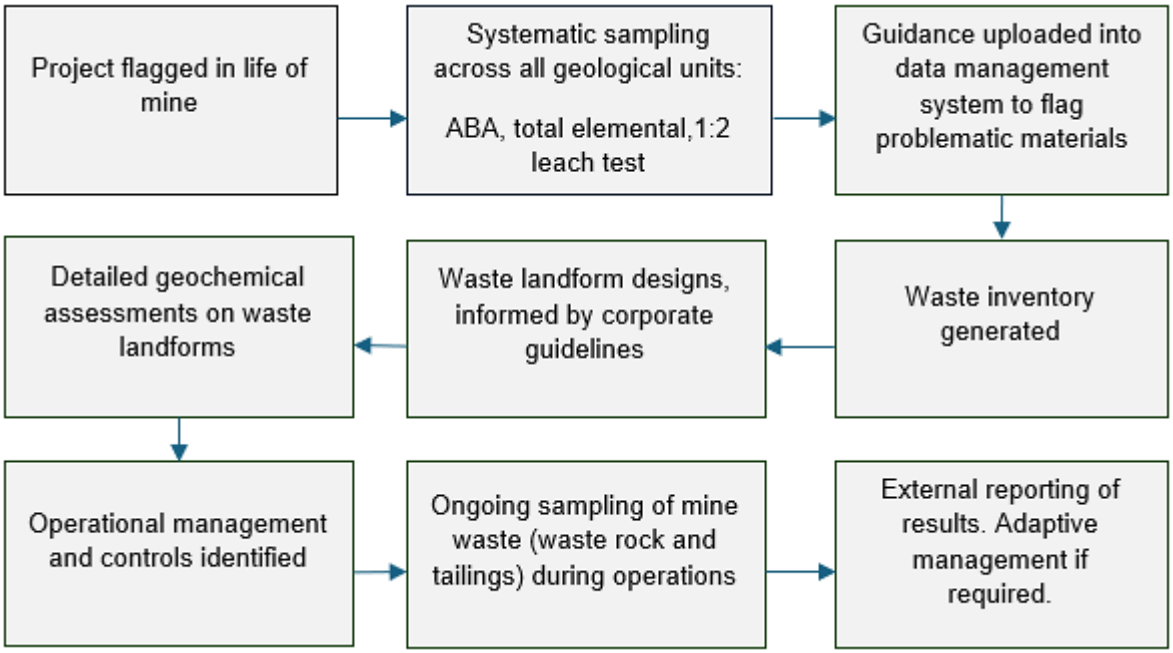

Fig. 10. **Example of AMD identification and management process implemented by a large iron ore mining company.**

Table 3. Typical corporate documents and the link to the relevant leading practice activities (INAP & ICMM 2025).

Document	Purpose	Relevant Leading Practice Activities (INAP & ICMM 2025).
Corporate AMD Management Plan	Outlines the mandatory minimum requirements to ensure that the identification, disturbance, and disposal of mine material does not adversely impact health, safety, and environmental values. Provides a framework to maintain these values in a way that minimises potential negative impacts to mine plans and schedules.	**ARD/ML Governance and strategy**
AMD Management Key Performance Indicators and Objectives	Outlines the suitable asset-level targets and review requirements in accordance with the *Tool for Acid Rock Drainage and Metal Leaching Prevention and Management* (INAP & ICMM, 2025).	**ARD/ML objectives, standards and KPIs**
AMD Characterisation Guideline	Provides a standardised approach to AMD sampling and investigation activities across all sites.	**Characterisation**
Landform Guideline	Provide a standardised approach for the management of mine materials through the design of landforms including waste rock dumps and backfill.	**Prevention, mitigation and treatment**
AMD Procedure (Planning)	Outlines the process by which hazards and risks pertaining to mined material are identified and communicated during the planning phase: - Inputs that each department requires to perform their tasks with respect to identifying and communicating mined material hazards. - Outputs that each department is responsible for with respect to identifying and communicating mined-material hazards. - Internal approvals required for any outputs generated.	**Characterisation** **Prediction** **Prevention, mitigation and treatment**
Operations Manuals (Operations)	Describes the process for how operations will undertake the management of potential risks from mined material at a site during operations including: - Outlining each operational departments responsibilities to manage the risk during operations. - Outlining the site-specific regulatory commitments - Specifying site-specific sampling requirements to validate the predictions.	**Prevention, mitigation and treatment** **Monitoring program plan**

Modelling hydrological and geochemical processes in large in-situ waste rock leaching columns under natural weather conditions

C. Zhang[A], Z. Zhao [B], C. Ptolemy[C], T. Ferguson[D], S. Quintero[E], L. Tan[F] and D. Williams[G]

[A] University of Queensland, St Lucia, 4072. chenming.zhang@uq.edu.au

[B] ATC Williams, Newmarket, QLD 4051.

[C] Grange Resources, Tasmania, Burnie, 7320.

[D] Grange Resources, Tasmania, Burnie, 7320.

[E] University of Queensland, St Lucia, 4072.

[F] University of Queensland, St Lucia, 4072.

[G] University of Queensland, St Lucia, 4072.

1.0 Background

Managing acid mine drainage (AMD) is an ongoing challenge within the mining industry, particularly due to its potential long-term environmental impacts on soil, water resources, and ecosystems. The generation of acid mine drainage occurs primarily when sulphide-bearing minerals, such as pyrite, are exposed to oxygen and water, resulting in oxidation processes that produce sulphuric acid. If unmanaged, AMD can significantly degrade water quality, affect biodiversity, and lead to costly remediation efforts. Consequently, understanding and controlling the geochemical and hydrological processes in waste rock storage facilities is essential for sustainable mining practices.

To evaluate the long-term behaviour and effectiveness of alternative waste management and co-disposal strategies, Grange Resources, in collaboration with the University of Queensland, initiated a comprehensive monitoring and modelling study using large-scale column leaching tests. These tests aimed to replicate realistic field conditions, offering insights into the complex interactions between hydrological flow, oxygen ingress, and geochemical reactions over an extended period.

2.0 EXPERIMENTAL SETUP

Six large concrete columns, each with a diameter and height of 1 meter per segment and stacked to reach a total height of 4 meters, were constructed between December 2017 and February 2018, shown in Figure 1 and Figure 2. These columns were designed to represent different waste rock scenarios typically encountered at the Savage River Mine. The upper column is open to atmospheric allowing for evaporation, rainfall, water infiltration and oxygen ingress. A water outlet was installed at the base of the column to drain excess pore water and maintain the water table at approximately 10 cm above the internal base. A U-bend system was incorporated to limit atmospheric venting, restricting oxygen ingress from the bottom of the column. Leachate was collected from the base and sampled quarterly for water quality analysis.

3.0 HYDROGEOCHEMICAL MODELLING

Numerical modelling was conducted using TOUGHREACT, a reactive transport simulator designed to capture coupled hydrological and geochemical processes in porous media (Xu et al., 2006). The model domain replicated the physical dimensions and boundary conditions of the experimental columns, using 40 discretised vertical layers to capture detailed variations, as shown in Figure 3.

Hydraulic conditions were represented using atmospheric boundary conditions at the column surface and constant head boundary conditions at the base, replicating the real-world scenario of gravity-driven percolation and restricted oxygen ingress provided by the U-bend.

Key geochemical reactions modelled included (Table 1):

- Pyrite oxidation, generating acidity and sulphate;
- Carbonate mineral dissolution (calcite and dolomite), providing acid-neutralising capacity;
- Muscovite and albite dissolution, contributing to alkalinity and silica release;
- Gypsum precipitation, capturing calcium and sulphate ions.

Mineral volume fractions were derived from pre-leaching XRD analyses, and reaction kinetics parameters were sourced from established literature, with subsequent calibration against observational data. The calibration involved adjusting kinetic parameters such as dissolution and precipitation rates and surface area calculations to align simulated and observed leachate chemistry trends, particularly sulphate, calcium, magnesium concentrations, and pH.

Through iterative model calibration and validation against five years of observational data, the hydrogeochemical model effectively simulated the coupled hydrological and chemical processes within the column tests. This robust modelling approach validated the conceptual understanding of mineral reaction dynamics and solute transport, thereby enhancing confidence in predicting long-term AMD behaviour in mine waste management.

4.0 MODEL CALIBRATION

The numerical model developed using TOUGHREACT (Xu et al., 2006) was calibrated rigorously using five years of observed leachate chemistry and hydrological data. Calibration focused primarily on sulphate concentrations, pH, calcium, and magnesium levels, as these were critical indicators of pyrite oxidation and buffering reactions.

Due to uncertainties in mineral liberation, the representativeness of mineral fractions from XRD analyses, changes in waste porosity and hydraulic conductivity, and the omission of other reactions that may influence pyrite oxidation and acid generation, some model discrepancies were expected. The initial mineral volume fractions derived from XRD were only minimally adjusted during calibration, indicating that the initial mineralogical characterisation was robust. However, minor adjustments to reaction kinetics — including dissolution and precipitation rates and reactive surface areas — were required to achieve close agreement between model predictions and observed data.

Model calibration effectively replicated observed sulphate dynamics across columns (Figure 4), predicting the initial spike and subsequent decline associated with pyrite oxidation. Similarly, simulated pH levels closely matched measured values, confirming the accuracy of buffering reactions involving carbonate and aluminosilicate minerals (Figure 5). The model also reliably captured the trends in calcium and magnesium concentrations (Figure 6 and Figure 7), validating the representation of mineral precipitation processes, notably gypsum formation. Note that the model overestimated Ca^{2+}, SO_4^{2-} and Mg^{2+} concentrations in Column 1 during the first two years, likely due to the gradual liberation of pyrite and carbonate minerals as the surrounding aluminosilicate matrix weathers and disintegrates. This process cannot be simulated by the model, which assumes that all minerals are fully liberated and immediately available for reaction.

Note the TOUGHREACT model was constructed using initial mineral volume fractions derived directly from pre-leaching XRD characterisation. Although amorphous phases were not detected in XRD results, sensitivity adjustments were implemented during calibration. These included modifying reactive surface areas and kinetic parameters of silicate minerals to account for potential reactivity associated with undetected, fast-dissolving components. This approach was employed to bracket uncertainty

arising from uncharacterised phases and helped ensure robust alignment with observed leachate chemistry.

5.0 MODEL RESULTS

The results of the hydrogeochemical modelling using TOUGHREACT provided detailed insights into the key geochemical processes driving acid generation and neutralisation in the columns. The calibrated model successfully simulated the temporal evolution of sulphate concentrations, pH, calcium, and magnesium levels, effectively capturing the complex interplay of hydrological and geochemical dynamics observed during the five-year monitoring period.

Simulated sulphate concentrations closely matched observed values, accurately capturing the initial sharp increase due to pyrite oxidation and the subsequent decline as reactive sulphides were progressively depleted. The model indicated that sulphate release was largely governed by oxidation kinetics, influenced significantly by oxygen availability and moisture content. The simulations showed reduced sulphate production in columns with compacted cover materials, highlighting their effectiveness in limiting oxygen ingress and pyrite oxidation.

The pH simulations confirmed effective acid buffering provided primarily by carbonate dissolution, especially calcite and dolomite, which were generally well represented in the model. Columns with limited carbonate content, such as the B-Type waste column, showed consistent maintenance of pH through aluminosilicate weathering, particularly muscovite dissolution. The modelling further confirmed that this aluminosilicate weathering released essential cations (K^+, Na^+) into the leachate, sustaining alkalinity and buffering pH effectively over time.

The simulation of calcium dynamics reflected a close coupling with sulphate concentrations, indicative of gypsum precipitation processes within the columns. Model outputs suggested gypsum precipitation was particularly active in columns containing higher sulphate and calcium concentrations, effectively immobilising both ions and reducing their mobility in leachate. Magnesium dynamics were similarly well-represented, with the model accurately simulating gradual declines in magnesium concentration due to precipitation processes and interactions with carbonate minerals.

Overall, the modelling results provided robust validation of the conceptual model developed from field observations, confirming the critical role of mineralogical composition and waste management strategies in controlling AMD processes. The calibrated TOUGHREACT model thus served as a reliable tool for predicting long-term geochemical stability and evaluating potential management interventions.

6.0 CONCLUSIONS

This study presented comprehensive results from the long-term monitoring and hydrogeochemical modelling of waste rock columns at the Savage River Mine, highlighting critical insights into hydrological and geochemical processes controlling AMD. Detailed monitoring confirmed that moisture dynamics reached equilibrium rapidly, with compacted and mixed-waste configurations demonstrating significantly improved water retention and reduced oxygen ingress compared to loosely placed materials. Oxygen measurements further established that compacted layers and mixed waste configurations effectively limited oxygen diffusion, thus minimising oxidative processes and acid generation.

Geochemical analyses of leachate samples revealed distinct temporal trends in sulphate, calcium, magnesium, and pH across different waste types. Columns containing potentially acid-forming (D-Type) waste initially exhibited elevated sulphate concentrations due to rapid pyrite oxidation, with subsequent decreases as reactive pyrite was depleted. Non-acid-forming waste types, particularly B-

Type waste, maintained consistently high alkalinity, driven predominantly by aluminosilicate weathering processes.

The calibrated hydrogeochemical model developed using TOUGHREACT effectively replicated observed geochemical trends, validating the conceptual understanding of mineral reactions and buffering mechanisms. Modelling results emphasised the critical role of mineralogical composition, waste layering, compaction, and mixing strategies in controlling AMD processes. The simulation outcomes clearly demonstrated effective sulphate immobilisation through gypsum precipitation, robust carbonate buffering, and sustained alkalinity from aluminosilicate weathering. While XRD analysis did not detect amorphous phases, their potential presence below detection thresholds was acknowledged and indirectly addressed during model calibration via sensitivity adjustments to aluminosilicate reaction kinetics.

Ultimately, this study provides valuable practical insights and robust predictive tools that support the implementation of innovative waste management strategies at mining operations. The validated hydrogeochemical modelling approach offers reliable forecasting capabilities to inform decision-making processes, enhancing environmental stewardship and operational sustainability in the mining industry.

REFERENCES

Blowes, D. W., Ptacek, C. J., Jambor, J. L., and Weisener, C. G. (2003) The geochemistry of acid mine drainage. In J. L. Jambor, D. W. Blowes, & A. I. M. Ritchie (Eds.), Environmental Aspects of Mine Wastes (Vol. 31, pp. 149–204). Mineralogical Association of Canada.

Nordstrom, D. K. (2011) Mine waters: Acidic to circumneutral. Elements, 7(6), 393–398. https://doi.org/10.2113/gselements.7.6.393

White, A. F., and Brantley, S. L. (2003) The effect of time on the weathering of silicate minerals: Why do weathering rates differ in the laboratory and field? Chemical Geology, 202(3–4), 479–506. https://doi.org/10.1016/j.chemgeo.2003.03.001

Xu, T., Sonnenthal, E., Spycher, N., and Pruess, K. (2006) TOUGHREACT – A simulation program for non-isothermal multiphase reactive geochemical transport in variably saturated geologic media: User's Guide. Lawrence Berkeley National Laboratory Report LBNL-55460.

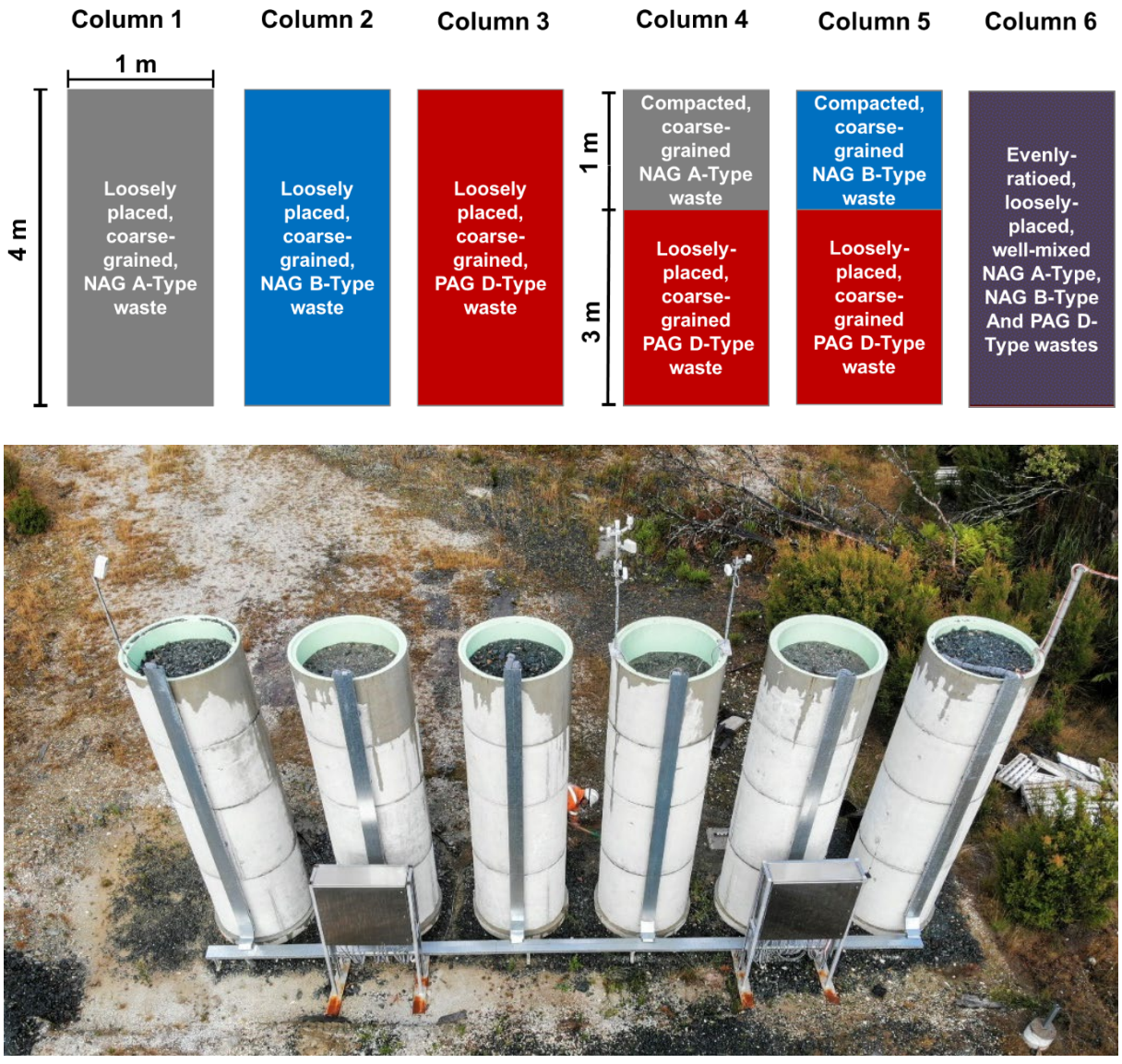

Fig. 7. **Column design and photograph**

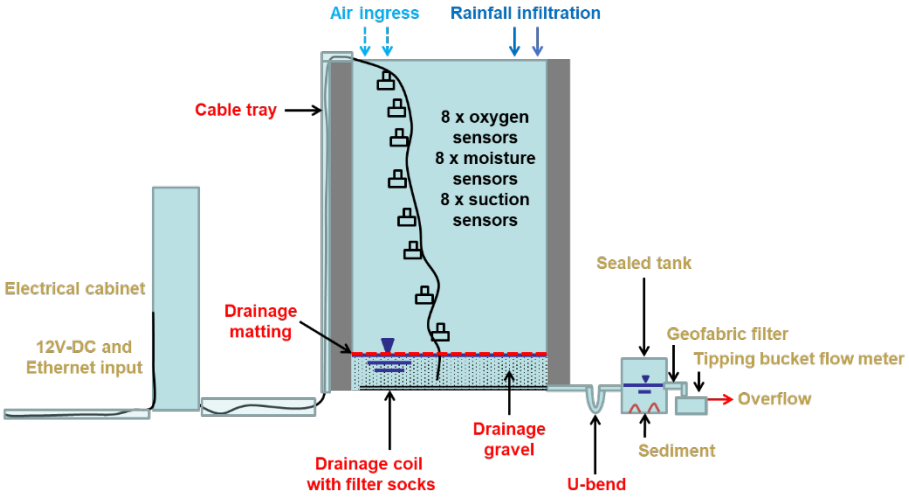

Fig. 8. **Schematic design and instrumentation layout of each column**

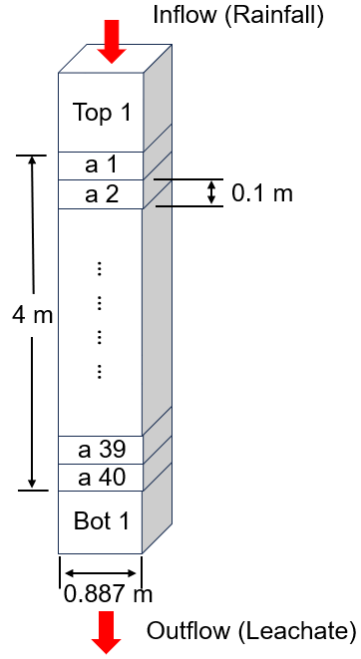

Fig. 9. **Model Domain Setup**

Table 5. **List of minerals considered in the geochemical model and associated equations**

Mineral Name	Reaction Equation
Pyrite	$FeS_2 + 3.5O_2 + H_2O \rightarrow Fe^{2+} + 2SO_4^{2-} + 2H^+$
Calcite	$CaCO_3 + 2H^+ \rightarrow Ca^{2+} + HCO_3^-$
Dolomite	$CaMg(CO_3)_2 + 2H^+ \rightarrow Ca^{2+} + Mg^{2+} + 2HCO_3^-$
Muscovite	$KAl_2(AlSi_3O_{10})(OH)_2 \rightarrow K^+ + 3SiO_2 + 3AlO_2^- + 2H^+$
Albite	$NaAlSi_3O_8 \rightarrow Na^+ + 3SiO_2 + AlO_2^-$
Gypsum	$CaSO_4 \rightarrow Ca^{2+} + SO_4^{2-}$
Quartz	Assumed non-reactive

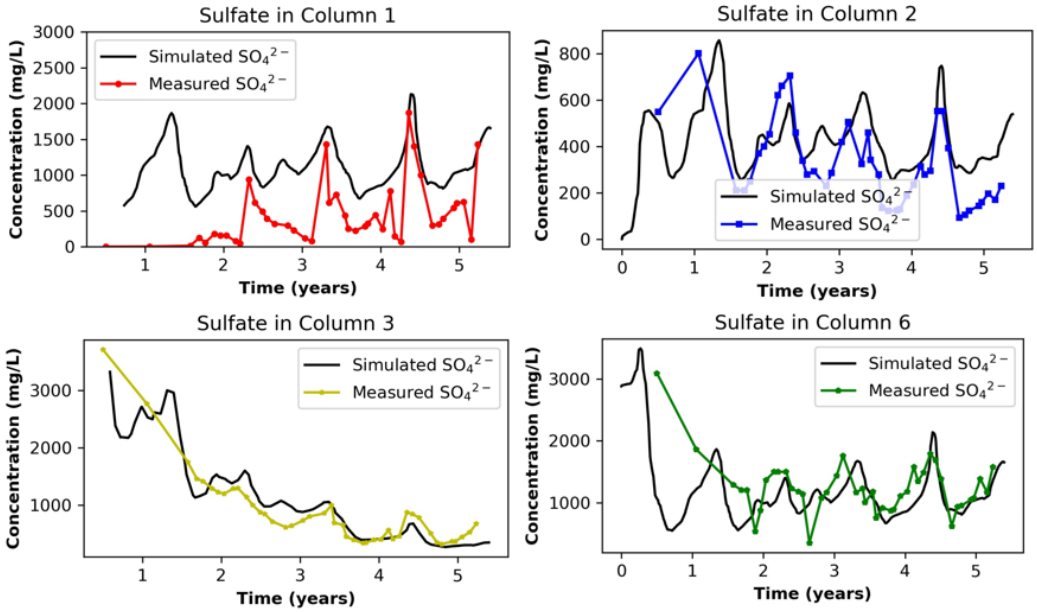

Fig. 10 . **Model Calibration Results – Sulphate**

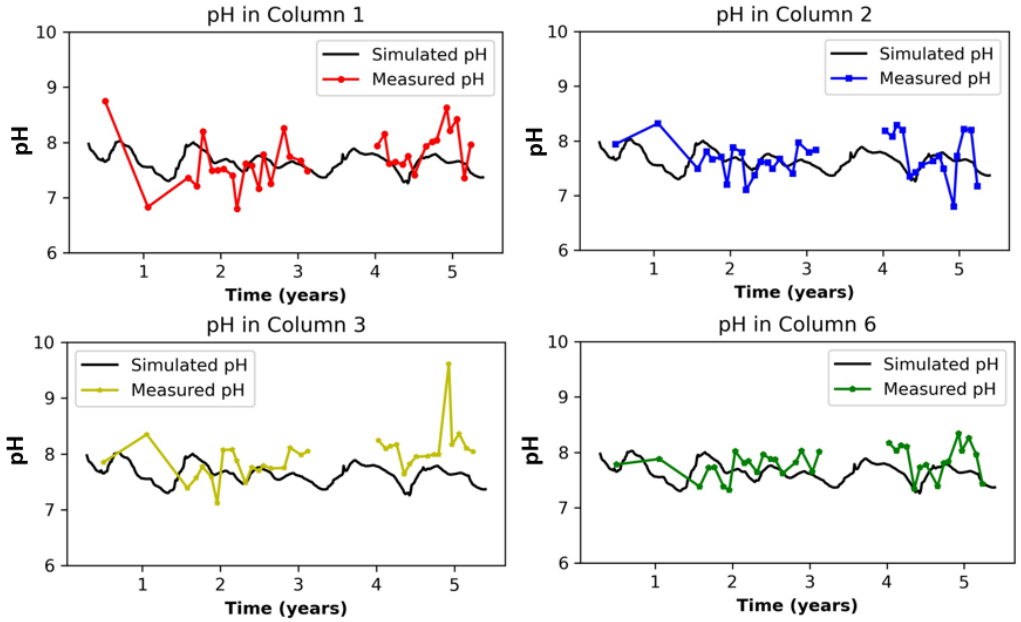

Fig. 11. **Model Calibration Results – pH**

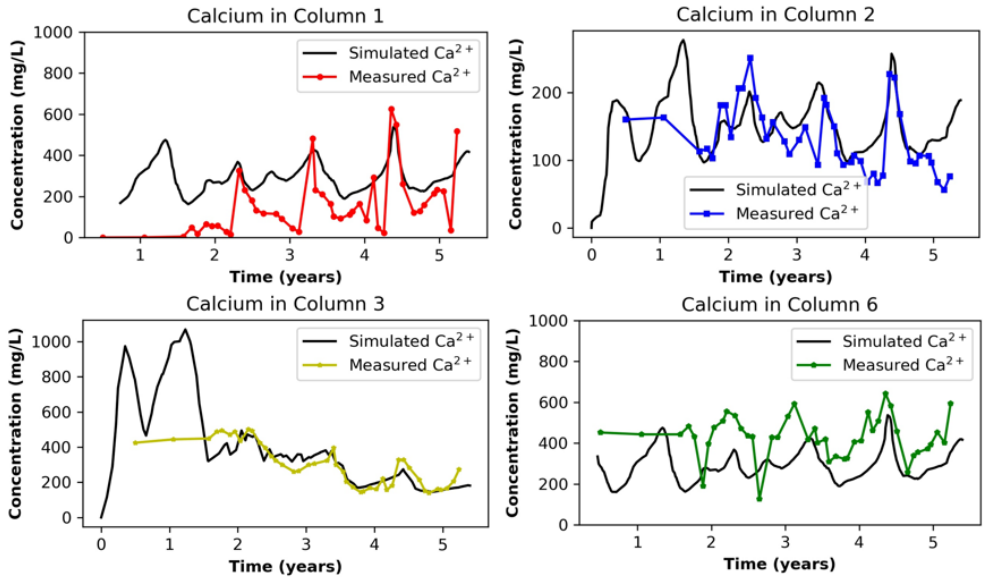

Fig. 12. **Model Calibration Results – Calcium**

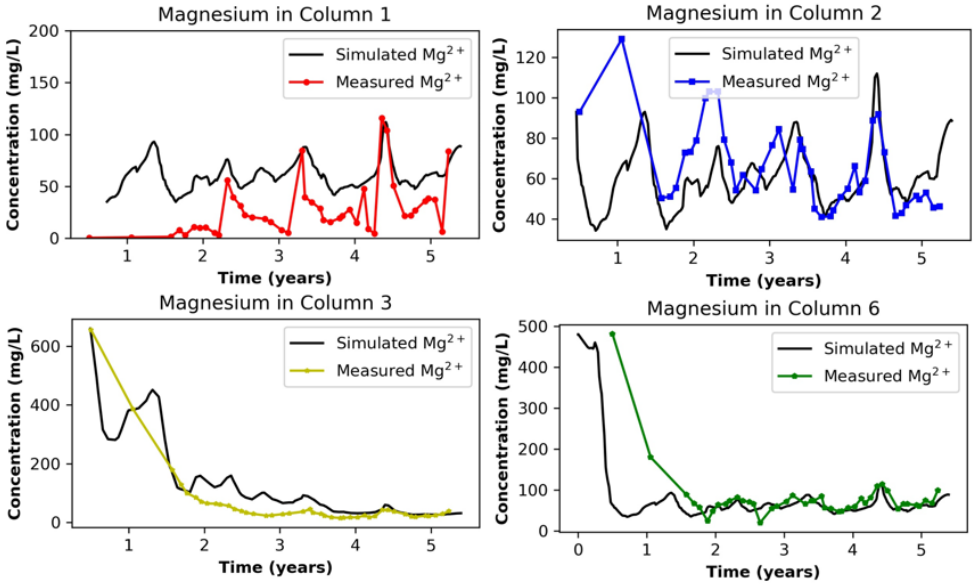

Fig. 13. **Model Calibration Results – Magnesium**

Impacts of AMD on TSF Seepage Pathways and Physical Stability

B. H Usher[A], J Durocher[B] and D Sprague[C]
[A]Klohn Crippen Berger, Level 3, 150 Mary Street, Brisbane, QLD 4000, Australia. busher@klohn.com
[B]Klohn Crippen Berger, Unit 101 - 1361 Paris Street, Sudbury Ontario P3E 3B6, Canada

1.0 INTRODUCTION

While the processes of sulfide oxidation leading to acid mine drainage (AMD) are understood and now form part of mine site characterisation at most sites, under most jurisdictions, the potential impacts of these processes on seepage pathways and physical stability have not received as much attention. In sulfide-rich mine waste, AMD processes can result in high loads of iron-rich drainage. This drainage, through oxidation and acid neutralisation, can result in significant accumulation of secondary mineral precipitates that can alter or completely clog drainage pathways. Some examples are shown below (Figure 1) for a tailings facility drainpipe clogged by precipitates and a seepage zone at the toe of a different facility where widespread precipitates along the seepage zone have clogged the pathway. In both cases, drainage pathways were reduced, with concerns about increase phreatic levels behind these points.

2.0 PRECIPITATE DEVELOPMENT

Secondary mineral precipitation in tailings occur because of chemical weathering reactions in the tailings that are often driven by changing conditions of the surrounding environment. These processes include oxidation-reduction (redox reactions); acid/base reactions (neutralization reactions); and dissolution-precipitation (solubility reactions).

The processes occur because the tailings and construction materials contain sulfide minerals which are exposed to water, atmospheric gases (most importantly in this case, oxygen), and changing pore water concentrations (including acidic or neutral conditions). Pyrite and pyrrhotite are common sulfide minerals in tailings and their oxidation releases iron, metals, sulfate, and acidity from the solid to liquid phase. Their oxidation products react to form secondary minerals (precipitates) that are more stable under the changed geochemical conditions. In several tailings systems, the elevated aqueous concentrations can result in the precipitation of secondary (i.e., precipitates) metal(oid)-oxyhydroxides and -sulfates. In parallel to the sulfide reactions, neutralisation of the acidity through carbonates, silicate, and oxides can also result in the precipitation of secondary metal(oid)-oxyhydroxides.

These processes occur widely and depend on key factors including composition of the tailings (i.e., sulfide content and neutralizing capacity); grain size of the tailings (i.e., reaction surfaces and influence on permeability); physiochemical conditions (i.e., pore water pH, oxidant availability); moisture content; geochemical characteristics of the infiltration, seepage, and pore water ; depositional history and age of the tailings; depositional strategies (e.g., prolonged beach exposure permits oxidation and alteration); dam design (e.g., finger drains, foundation conditions, starter dam material); water management practices (e.g. pond extent, seepage recirculation or lime dosing); and remediation efforts. Sulfide oxidation reactions release aqueous Fe^{2+}, sulfate, acidity and metal(loid)s from the sulfide minerals to surrounding pore waters that migrate in the tailings towards the phreatic surface. Mobilized (aqueous) Fe^{2+}can be oxidized to Fe^{3+} to form semi-stable precipitates and/or can be further transported deeper in the profile with infiltration, or with the pore water. The types of precipitates formed in this zone depend on pH and can include iron oxy-hydroxides such as ferrihydrite[$Fe_{10}O_{14}(OH)_2$] at neutral pH or iron oxy-sulfates such as schwertmannite

[$Fe_{16}O_{16}(OH)_{12}(SO_4)_2$] and jarosite [$KFe_3(SO_4)_2(OH)_6$] at acidic pH. Precipitates are moderately soluble and re-mobilized Fe^{3+} from these precipitates can reach the phreatic surface and can remain in solution if the pH is low or be reduced to soluble Fe^{2+} in sub-oxic and sub-neutral porewaters by reaction with sulfide minerals. Precipitate forms when mobile (aqueous) Fe^{3+} reaches zones where acid neutralizing conditions occur and when mobile (aqueous) Fe^{2+} reaches oxidizing conditions. Based on observations from drilling, geochemical laboratory testing, and field observations, a general weathering and alteration profile from an older high sulfide area provides a good illustration of the processes (Figure 2). Alteration of tailings, including weathering and oxidation reactions, is ubiquitous, but the extent of the reactions is observed to occur across a spectrum, with a general weathering profile that can be described by processes in the "oxidized", "partially oxidised", and "unoxidized" zones.

2.1 General observations from the oxidised zone

The oxidized zone is usually near surface and typically penetrates to a depth of 1.5 m to 4.5 m (depending on the area and age of tailings; Figure 2). Tailings are typically acidic with pH between 2.5 and 4, depleted of neutralizing potential and trace elements (that may include depleted iron, sulfur, nickel, cobalt, copper, selenium, and aluminium). Tailings are often coated with Fe-rich precipitates (typically Fe-oxyhydroxides and -oxysulfates). In this zone, sulfur speciation is dominated by sulfate-sulfur. Secondary minerals in this zone can form weak to strong cementation that result in structures that range from blocky to cementitious hardpans.

2.2 General observations from the partially oxidized zone

The partially oxidized zone is located below the oxidized zone and has been observed to penetrate to the phreatic level (Figure 2). This can occur at depths of more than 20 m below surface (depending on the area and age of tailings). In this zone, tailings are typically less acidic (pH ranges from 4 to 5), visible signs of oxidation are variable and, where they exist, can occur gradationally or as intermittent oxidized layers. In this zone, ANC is seen to increase with depth and trace element concentrations typically stabilize, and the relative sulfate content decreases. Secondary minerals in this zone are typically observed as thin coatings of Fe-oxyhydroxides and -oxysulfates.

2.3 General observations from the unoxidized zone

The unoxidized zone is typically located below the phreatic level (Figure 2). Tailings are often neutral to sub-neutral and can range from pH 5 to above pH 8, depending on tailings type; the tailings in this zone often have similar properties to the freshly-produced tailings. Visible oxidation is rare; trace element concentrations remain stable and secondary minerals are less abundant and typically only observed as sub-millimetre coatings. In these unaltered tailings there is limited reduction of ANC (compared to the fresh tailings) and most of the sulfur content is sulfidic.

3.0 IMPACTS OF PRECIPITATE FORMATION

In broad terms, mineral precipitation can significantly alter the properties of the materials, especially in terms of drainage pathways, leading to impacts to performance of filters and drains in tailings dams (as shown in Fig 1). Precipitated minerals accumulate in pore spaces, leading to reduced permeability, which may increase phreatic surfaces/pore pressures. From a geotechnical perspective, this can lower the stability of the facility, since, broadly, elevated pore pressures reduce effective stress within the dam structure, potentially leading to reduced shear strength, slope instability, and even catastrophic

failure if not properly controlled. Porosity reduction can occur by means of chemical clogging as precipitates are deposited in the pore space.

Several porosity-permeability relationships are used to estimate the change in permeability as effective porosity changes. The Kozeny-Carman relationship is the most widely used empirical equation for estimating these aspects, but general observations suggest that reduction in pore space has a log linear impact on hydraulic conductivity (i.e. as the clogging proceeds the impacts on permeability become exponentially pronounced in the flow zone). As an example, to illustrate the impacts, a recent field trial was by KCB conducted at a site with acidic drainage to assist with quantification of timing of clogging and to inform design measures to mitigate against clogging of drains. Field barrels and columns were filled with various TSF construction materials, and the rates of hydraulic conductivity change from interaction with water from drains (pH ~ 4 and dissolved iron concentrations between 300 to 500 mg/L). Preliminary results suggest that chemical precipitate formation within pore spaces reduced porosity by approximately 30 to 50%, with a log-linear reduction in field measured hydraulic conductivity within a three-month period (Fig 3 provides a visual illustration of the observed precipitate formation and clogging in a coarse filter sand).

4.0 GEOCHEMICAL CONSIDERATIONS IN DESIGN AND OPERATION

The Global Industry Standard on Tailings Management (GISTM) was developed to prevent catastrophic tailings dam failures by establishing a global, comprehensive standard for safer, more accountable, and transparent tailings management. The framework was developed for safe management of tailings facilities throughout their life cycle and geotechnical stability is the key consideration. Importantly, GISTM recognises the importance of integrated understanding and management of risks, acknowledging the importance of tailings chemistry, water quality, and geochemistry in long-term containment performance.

Controlling iron solubility is critical for mitigating precipitate formation and maintaining effective drainage performance. Eh and pH are the primary geochemical control considerations governing solubility-based mitigation strategies that can be implemented in stabilization upgrades. By implementing Eh and pH controls to maintain Eh and pH within specific ranges, iron can remain in its soluble form, minimizing the risk of precipitate formation. Key mitigation measures include limiting the availability of oxidants (atmospheric oxygen, rainfall carrying dissolved oxygen, and Fe3+ from soluble sources), reduce or eliminate oxygen ingress into the structure (i.e. tailings slope and buttress) and measures to limit changes in tailings water quality from when it exits as pore water to when it exits the facility. The latter may include reduced retention/reaction time in the drainage pathways and/or isolating incompatible water types (e.g., isolation of oxic sources from anoxic sources to preserve reducing conditions).

Consideration of material properties can play an important role in mitigation strategies. From a geochemical perspective, it is important to avoid the use of reactive/high ANC fill materials in buttress drainage zones, as these can alter water chemistry and promote precipitate formation by pH adjustment. Equally important is selecting materials that will provide high permeability for the life of the facility. This supports effective drainage and minimizes the risk of hydraulic performance decreases. Incorporating these considerations into design process helps identify and mitigate against long-term geochemical and hydraulic performance risks.

Experience at sites with elevated dissolved iron in tailings water has shown that appropriate design of drains can significantly reduce clogging from precipitate formation. Free-draining oxic drains may be suitable when the tailings water contains relatively low concentrations of dissolved iron and/or when the tailings water is already highly oxidised. At the other extreme, when tailings pore water contains

significant dissolved iron and is susceptible to oxidization or neutralisation before the water can exit the facility, a fully submerged and encapsulated drain may be necessary. This design minimizes exposure to oxygen and pH changes, thereby reducing the likelihood of iron precipitate formation and prevents build-up of pore pressures in the facility.

5.0 CONCLUSIONS

From the perspective of safe tailings facility operation, incorporating geochemical processes into design and management allows for more accurate quantification of the factors and rates of precipitation that may alter geotechnical or hydraulic properties. By accounting for these processes, improved design and construction practices can be implemented to mitigate potential impacts on physical stability. With advancements in understanding these processes, geochemists, in addition to understanding potential environmental risks, now also play an important role in the responsible storage of mine waste by integrating geochemical insights into designs and construction practices that can reduce risks to physical stability, consistent with the requirements of modern leading practices and aligned to global standards such as the Global Industry Standard for Tailings Management.

Fig 1. Examples of clogged pathways from TSFs: Drain pipe (L) and seepage zone (R)

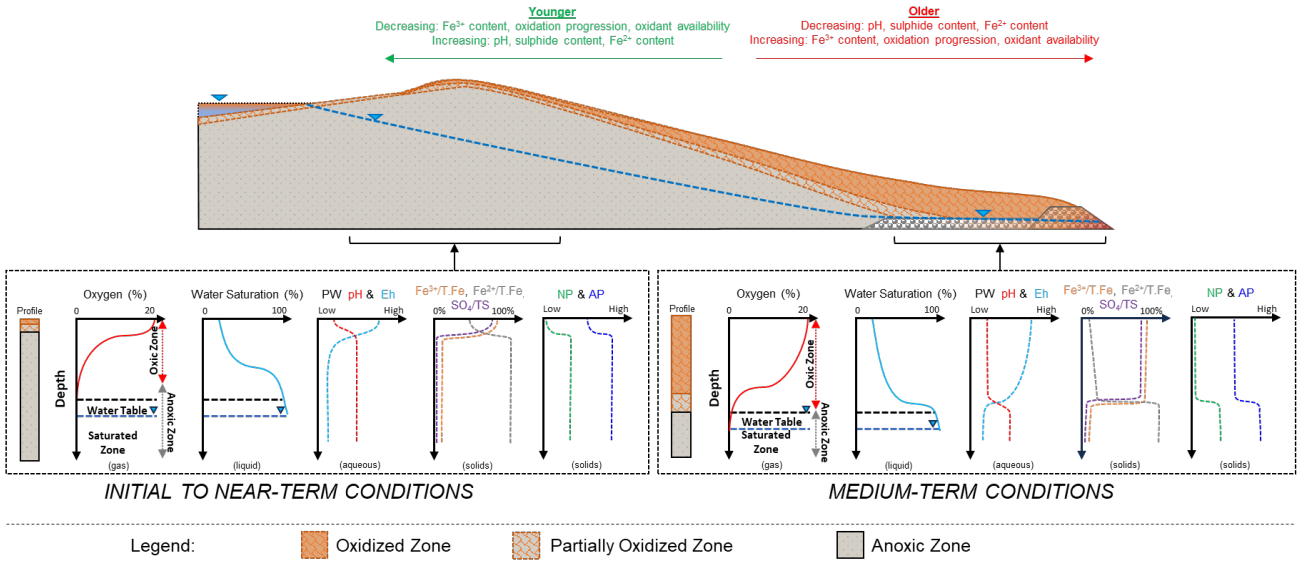

Fig 2. Typical conditions observed in different parts of the TSF over time

Fig 3: Filter sand (a) initial conditions and (b) conditions after 97 days

Advanced real-time continuous monitoring of Acid Mine Drainage

A. Nolan, T. Carlson and R. Campbell
HydroTerra Pty Ltd, 42/328 Reserve Road, Cheltenham, VIC 3192.
anolan@hydroterra.com.au

1.0 INTRODUCTION

Acid mine drainage (AMD) is characterised by high acidity and high iron and sulfate concentrations. As a result of increased solubility at low pH, many other toxic metals may also be present at elevated concentrations. For example, aluminium, copper, zinc and to lesser extents, lead, arsenic, cadmium, nickel and manganese. The combination of low pH and high metal concentrations can cause a range of environmental issues, including:

- Vegetation dieback and ecosystem deaths (e.g. fish kills)
- Contamination of drinking and agricultural water
- Corrosion of infrastructure and equipment

2.0 MONITORING OF AMD FOR SITE ASSESSMENT AND MANAGEMENT

Monitoring of pH, electrical conductivity (EC), oxidation-reduction potential (ORP) and flow rates in AMD waters are common approaches for AMD site management, with real-time continuous monitoring providing the most effective insights. Real-time continuous monitoring of these key parameters at AMD sites can provide immediate insights for improved compliance monitoring and site management, and captures critical insights into temporal variability related to climatic conditions, including first flush events (the first rainfall after a prolonged dry period, generally characterised by high acidity and high metal loading) as well as peak flows etc.

However, pH is a measure of H^+ ions only, whereas total acidity is a measure of both H^+ and dissolved metals (e.g. iron, aluminium, manganese), which produce acid when they precipitate. Total acidity can be measured by titrating against a strong base (reported as mg $CaCO_3$/L) or calculated using H^+ and metal concentrations. Therefore, pH monitoring data trends may not always provide the best early indicator of AMD onset conditions, as demonstrated in the Figure 1 (INAP 2009).

Figure 1 shows seepage water quality data from two waste rock dumps over a six-year period. The onset of AMD conditions is characterised by decreasing pH and increasing metal and sulfate concentrations. However, notably the seepage pH remained near neutral for several years before acidic conditions were evident. The water quality data in Figure 1 show that alkalinity, as opposed to pH, may be a better early indicator of the onset of AMD conditions as the decreasing trend in alkalinity was evident before the decreasing pH trend.

Real-time continuous concentrations of other key AMD parameters (such as metals, sulfur, total acidity or alkalinity) are more difficult to monitor, therefore an estimate of these parameters using an alternative real-time parameter, such as EC, can provide critical insights into the onset of AMD conditions and provide a rapid screening method for site management and compliance assessment.

In a study by Smith et al. (2022), EC was shown to provide statistical correlations with key AMD parameters. It was demonstrated that EC could be used for prediction of total acidity, dissolved iron and sulfur concentrations in acidic AMD waters. From these findings, empirical correlations were used to derive regression equations, which were used to derive the EC values corresponding to the respective water quality limits for total dissolved solids (TDS), dissolved iron and sulfur to provide a rapid screening method, as demonstrated in Figure 2.

This presentation will include a case study where EC was shown to correlate well with concentrations of some metals and sulfate. Real-time flow rates were also monitored to allow an estimate of metal loads over time and in response to rainfall.

3.0 INNOVATIONS IN REAL-TIME CONTINUOUS MONITORING AND REMOTE SAMPLING TECHNOLOGIES

Innovations in sensors and telemetry, as well as remote sampling technologies such as drones and autosamplers, support the capture of long-term monitoring data and essential trends at AMD sites, particularly in response to rainfall and seasonal variation.

This presentation will highlight recent advances in sensor technologies, such as solid-state multi-parameter sensors, capillary zone electrophoresis and ion selective electrodes, to provide advanced real-time monitoring systems and data visualisation.

REFERENCES

Guide (GARD Guide). http://www.gardguide.com'.

Smith, J., Sheridan, C., van Dyk, L. and Harding, K. (2022). Critical evaluation of the chemical composition of acid mine drainage for the development of statistical correlations linking electrical conductivity with acid mine drainage concentrations. Environmental Advances. **8**. 100241. 10.1016/j.envadv.2022.100241.

The International Network for Acid Prevention (INAP) (2009). Global Acid Rock Drainage

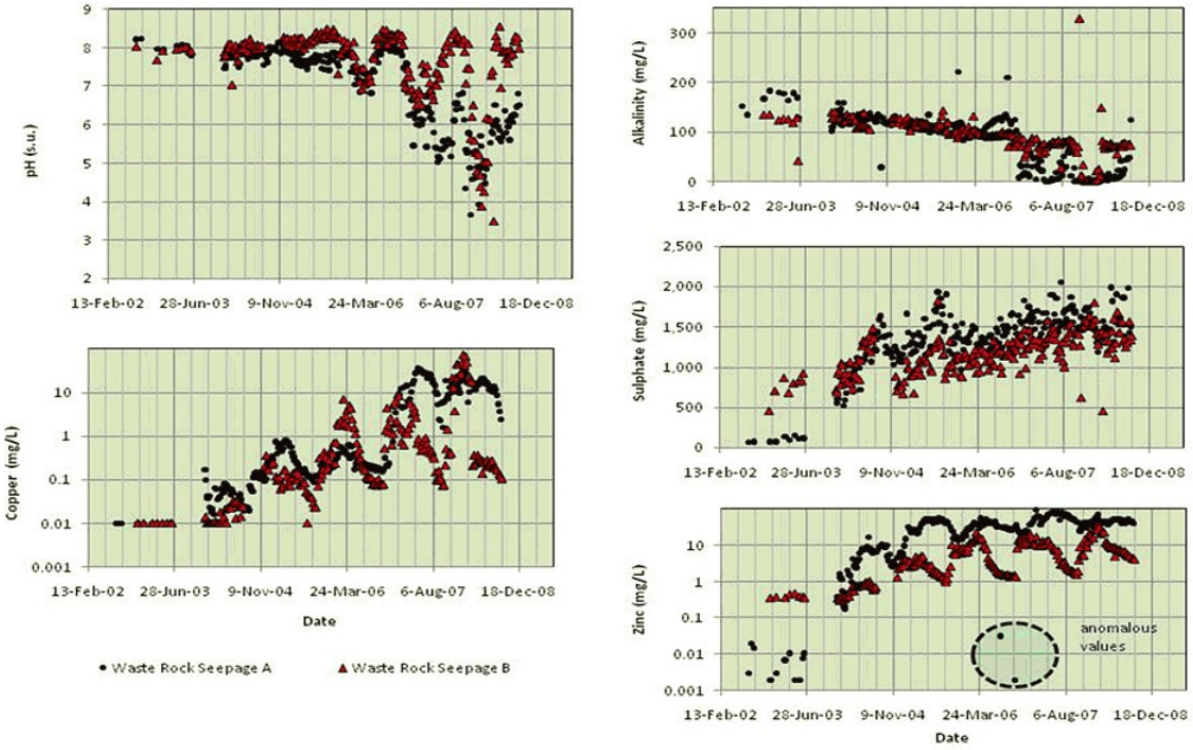

Fig. 1. Waste Rock Seepage Water Quality Trends. Source: INAP 2009 (GARDGuide, Chapter 8).

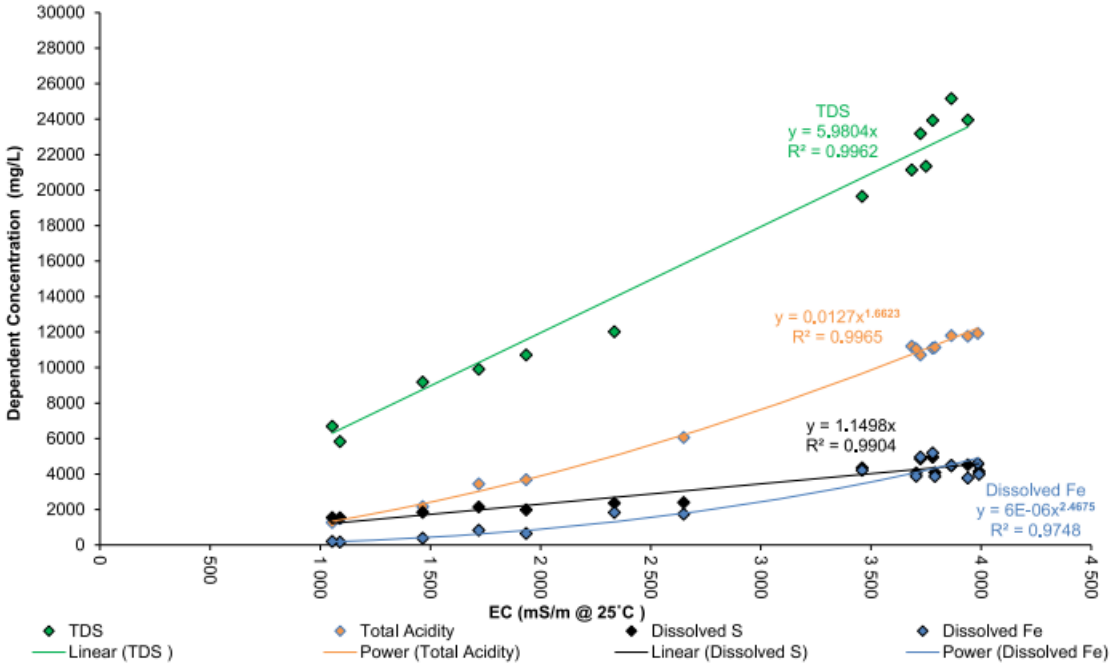

Fig. 2. Total dissolved solids (TDS), total acidity, dissolved iron and dissolved sulfur as a function of electrical conductivity (EC): Linear regression (intercept set to zero) or power regression equations, after rejection of outliers. Source: Smith et al. 2022.

Early steps towards understanding risks of increased temperature in mineralised waste rocks

D. Sharma[A,B], B. Usher[B], J. Fourie[B] and M. Edraki[A]
[A]Sustainable Minerals Institute, The University of Queensland, St Lucia, QLD 4072, Australia.
d.sharma@uq.edu.au
[B]KCB Australia Pty Ltd, Level 3, 150 Mary Street, Brisbane, QLD 4000

1.0 INTRODUCTION

Sulfide minerals are crucial in ore formation but also play a significant role in pollution through processes like Acid and Metalliferous Drainage (AMD) and spontaneous combustion (self-heating). AMD can arise from the high sulfide content in metalliferous mine waste materials such as waste rocks and slurry tailings (Australian Government Department of Industry, Innovation and Science., 2016; Betrie, 2014; Vaughan & Corkhill, 2017). The problem of sulfides self-heating is less well-documented (Moon et al., 2020; Payant et al., 2012). Sulfide self-heating is also known as sulfide spontaneous combustion and is commonly linked with pyrite, pyrrhotite, chalcopyrite, sphalerite and galena; in pure and mixed forms of sulfur (Kim et al.,2023).

Sulfide self-heating is an exothermic oxidation reaction that has the potential to result in increased reactivity and lost working time from the gases generated. Sulfide self-heating is consistent with the standard AMD generation process:

Sulfide minerals + Oxygen + H_2O (can be gaseous or liquid) → Heat + Acidity + Metals + Sulfate

The oxidation of sulfide minerals in waste rock represents a branching geochemical pathway where water availability acts as the determinant between AMD formation and spontaneous combustion initiation (Bergholm, 1995). Under water saturated conditions, the exothermic oxidation reactions produce mobile acid products. While under moisture-limited conditions, the identical oxidation processes generate accumulated elemental sulfur that subsequently ignites at temperatures below 100°C (Bergholm, 1995). Spontaneous combustion events may then alter the geochemical reactivity of waste rock, potentially amplifying subsequent AMD generation when these heat-affected materials are later exposed to water and oxygen.

The most referenced theory in the literature that explains sulfide self-heating is the three sequential staged theory, termed Stage A, Stage B and Stage C (Payant et al., 2012; Rosenblum & Nesset, 2020). The three stages are divided into ambient temperature ranges, with Stage A classified for ambient temperature to 100°C, Stage B classified for ambient temperature between 100°C to 350°C, and Stage C classified for ambient temperature beyond 350°C (Rosenblum & Nesset, 2020). In each stage, the heat generated is a result of exothermic oxidation reactions. In Stage A, sulfides oxidise to form elemental sulfur with moisture content an important consideration. Stage B involves oxidation of the elemental sulfur while Stage C involves the direct oxidation of the sulfide. In literature, Stage C is commonly referred to as ignition, roasting or runaway temperature (Beamish & Theiler, 2019). Factors that influence the rate of reaction include the type and quantity of sulfide mineral/s present in the waste rocks, the particle sizes and surface area, the oxygen content, moisture conditions, the galvanic interactions, and bacterial interactions.

Electrochemical reactions at the mineral-solution interface control the rate of oxidation of sulfides (Chopard et al., 2017). A sulfide mineral in a typical mine waste environment can act as an electrode with the order of rest potentially generally as follows (Payant et al., 2012):

Pyrite > Chalcopyrite > Sphalerite > Pentlandite > Pyrrhotite > Galena

Direct contact of sulfide minerals with different rest potentials initiates the galvanic effect. Despite the research progress made in the field of sulfide self-heating in the last century, the mechanisms are still not yet fully understood. Preliminary results are presented in this paper from a multimodal analytical approach applied to waste rocks from an operational sulfide-rich zinc-lead mine site where sulfide self-heating has been observed.

2.0 MATERIALS AND METHODS

This paper focuses on 6 drill core samples that are representative of waste rock types from a stratiform, sediment-hosted Zn-Pb-Ag deposit, hosted in dolomitic shales. Pyrite (FeS_2), sphalerite (Zn(Fe)S), and galena (PbS) are the dominant minerals. Samples entailed are representative Pyritic Shale (n=2) and Black Bituminous Shale (n=4) samples.

A range of sulfide spontaneous combustion tests and analytical methods have been completed. Standard testing included Acid-Base Accounting (ABA), Acid Buffering Characterisation Curve (ABCC), Net Acid Generation (NAG), whole rock analysis (X-Ray Fluorescence (XRF),4 acid digestion, and total elemental sulfur). Extended mineralogical assessment included X-Ray Diffraction (XRD), thin section petrology, Scanning Electron Microscopy/Energy Dispersive Spectroscopy (SEM-EDS) and Mineral Liberation Analysis (MLA). The characterisation was supplemented by self-heating testing comprising combustion propensity testing (standard in the coal industry), adiabatic oven incubation testing, isothermal oven self-heating testing and oxygen consumption rate (OCR) assessment.

3.0 RESULTS AND DISCUSSION

The total sulfur content ranges from 3.1 wt% to 20.4 wt%. Although the paste pH values of the samples are relatively neutral (ranging between 7.6-8.4), the NAG pH values range between 2.2 to 8.5 which can reflect the high sulfide content because of all the samples having more than 200 kg H_2SO_4 t^{-1} equivalent acid neutralising capacity (ANC), which the ABCC testing indicates is largely available above pH 5.5 (Table 7).

The OCR for the samples ranged from 4.1×10^{-10} to 3.1×10^{-9} kg (O_2) kg^{-1} s^{-1}, with higher rates correlating to increased pyrite content. Samples 3 and 4, containing 30-34 wt% pyrite, exhibited the highest OCR values, while samples 1, 2, 5, and 6 (8-15 wt% pyrite) showed lower consumption rates. The presence of variable sphalerite and dolomite in these samples potentially creates different galvanic interactions that may influence the overall oxidation behaviour. Although carbonate neutralisation reactions are exothermic, their thermal contribution is minimal compared to sulfide oxidation. Moreover, the temperature-dependent reduction in carbonate solubility means that the neutralisation capacity of the waste rocks decreases as self-heating progresses, potentially accelerating thermal runaway conditions (Sherlock et al., 1995).

Petrographic results showed pyrite grains in three distinct textures: (1) coarse angular grains (50-100 µm) disseminated randomly within the matrix with sharp grain boundaries against silicate and carbonate minerals; (2) coarse rounded to sub-rounded grains (50-100 µm) with shared boundaries with sphalerite, where areas of elevated Fe and Zn occur at fused grain boundaries; and (3) fine-grained rounded to sub-rounded pyrite (<1 to <50 µm) as individual disseminated grains. Galena, where present, forms larger sub-angular grains (>1 mm) and shares grain boundaries with sphalerite. Pyrite was not observed in assemblage with galena.

Self-heating testing typically performed in the coal industry was conducted for all samples. Additional self-heating testing was conducted using an adiabatic method on selected samples (Beamish & Theiler, 2019). All samples showed moderate volatile matter content indicating the samples have a portion of organic combustible content that can potentially contribute additional heat once the oxidation process

begins. Generally, samples with higher total sulfur content, also showed higher calorific values which are a measure of the energy content of a sample when it is completely combusted. All samples reported RIT >199°C, with only one sample transitioning from Stage A to B (~100°C) under adiabatic conditions. Calorific values followed the expected trend with sulfide content, but the results also indicated a decrease in elemental sulfur post-heating. This latter finding is currently being investigated as it is inconsistent with expectations, with ongoing focus on the role of mineral textures in limiting reactions.

4.0 CONCLUSIONS AND FUTURE WORK

This paper has presented preliminary results from six drill core samples that are representative of waste rock types from a stratiform, sediment-hosted Zn-Pb-Ag deposit. This study underscores the dual environmental risks of AMD and spontaneous combustion posed by sulfide-rich waste rocks. Key findings from the work to date include:

- High total sulfur content correlates with higher AMD potential and faster oxygen consumption.
- Fine-grained pyrite and intergrowths with sphalerite increase combustion risk.
- Existing self-heating models may not fully explain observed behaviour.

The following work is in progress to improve the understanding of the likelihood of spontaneous combustion to occur in samples from this deposit:

- Quantifying the galvanic interaction between the sulfide minerals experimentally. Specifically, the interactions between pyrite, sphalerite and galena needs to be understood which are the most abundant sulfide minerals noted in the six samples.
- The accurate quantification of the distribution of the sulfide minerals relative to the carbonate minerals in more samples can prove to be beneficial. Especially, understanding the likelihood of spontaneous combustion for sulfide minerals in contact with carbonate minerals compared to sulfide minerals not in contact with carbonate minerals.
- Impacts of moisture content and oxygen consumption rates.
- Depth/mass relationships for storage of the material.

5.0 REFERENCES

Australian Government Department of Industry, Innovation and Science. (2016). Preventing acid and metalliferous drainage. chrome-extension://efaidnbmnnnibpcajpcglclefindmkaj/https://www.industry.gov.au/sites/default/files/2019-04/lpsdp-preventing-acid-and-metalliferous-drainage-handbook-english.pdf.

Beamish, B. B., & Theiler, J. (2019). Coal spontaneous combustion: Examples of the self-heating incubation process. International Journal of Coal Geology, 215, 103297. https://doi.org/10.1016/j.coal.2019.103297

Bergholm, BA. (1995). Oxidation of Pyrite (Open-File Report Nos. 95-389). US. Geological Survey.

Betrie, G. D. (2014). Risk management of acid rock drainage under uncertainty. https://doi.org/10.14288/1.0074404

Chopard, A., Plante, B., Benzaazoua, M., Bouzahzah, H., & Marion, P. (2017). Geochemical investigation of the galvanic effects during oxidation of pyrite and base-metals sulfides. Chemosphere, 166, 281–291. https://doi.org/10.1016/j.chemosphere.2016.09.129

Kim, H. (2023). Self Heating of Sulphide Ores, A Study of Chemical Interaction between Elemental Sulphur and Pyrrhotite [Master of Science]. McGill University.

Kim, H., Rosenblum, F., Kökkılıç, O., & Waters, K. (2023). Role of Elemental Sulphur in Stage B Self-Heating of Sulphide Minerals, and the Potential Role of Polysulphides. Minerals, 13(7), 923. https://doi.org/10.3390/min13070923

Moon, S., Rosenblum, F., Tan, Y., Waters, K. E., & Finch, J. A. (2020). Transition of Sulphide Self-Heating from Stage A to Stage B. Minerals, 10(12), 1133. https://doi.org/10.3390/min10121133

Payant, R., Rosenblum, F., Nesset, J. E., & Finch, J. A. (2012). The self-heating of sulfides: Galvanic effects. Minerals Engineering, 26, 57–63. https://doi.org/10.1016/j.mineng.2011.10.019

Rosenblum, F., & Nesset, J. (2020). The Basics of Self-heating of Sulphide Mineral Mixtures. MLARD Conference.

Sherlock, E. J., Lawrence, R. W., & Poulin, R. (1995). On the neutralization of acid rock drainage by carbonate and silicate minerals. Environmental Geology, 25(1), 43–54. https://doi.org/10.1007/BF01061829

Vaughan, D., & Corkhill, C. (2017). Mineralogy of Sulfides. Elements, 13, 81–87. https://doi.org/10.2113/gselements.12.3.xx

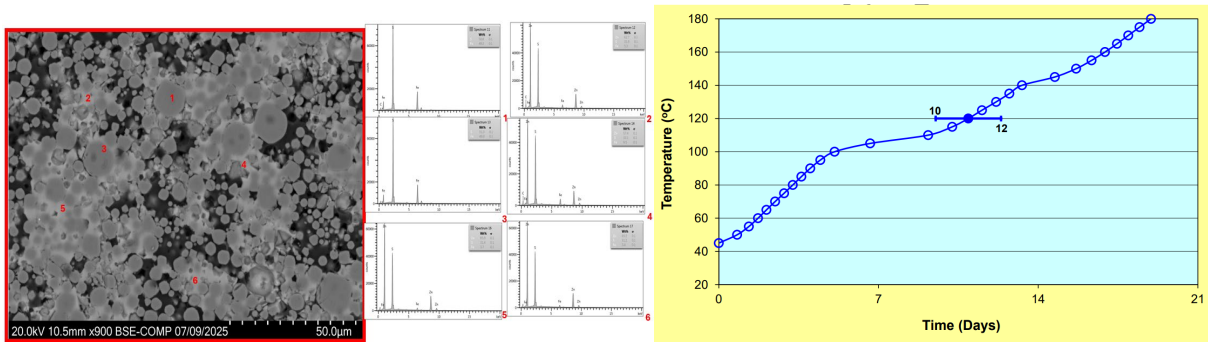

Fig. 1 Sample 4 Results: Rounded pyrite grains (1, 3) with sphalerite (containing <10 wt% Fe) between the pyrite grains (2, 4, and 6); the grain boundaries between the minerals are fused. Incubation self-heating testing results.

Table 6 **Summary of ABA, and OCR results**

Sample	Lithology	Paste pH	NAG pH	Total Sulfur**	Total Org. Carbon**	MPA*	ANC*	NPR	OCR***
1	Pyritic Shale	8.3	8.1	8.7	0.44	266.8	740	1.8	1.70E-09
2	Black Bituminous Shale	8.4	8.5	6.6	1.63	202.6	349	1.7	5.50E-10
3		8.0	2.2	19.4	1.36	593.6	272	0.5	1.80E-09
4	Pyritic Shale	7.6	2.3	20.4	0.34	624.4	284	0.5	2.80E-10
5	Black Bituminous Shale	7.6	3.0	9.7	3.13	296.8	222	0.8	2.60E-09
6		8.4	3.3	3.1	1.31	95.5	316	3.3	2.20E-09

* (kg H_2SO_4 t^{-1} rock), ** (weight %), *** (kg (0_2) kg^{-1} s^{-1})

Table 7 **Summary of ABCC results**

Sample	Lithology	pH 6.5		pH 5.5		pH 4.5	
		Reacted ANC*	% of Total ANC	Reacted ANC*	% of Total ANC	Reacted ANC*	% of Total ANC
1	Pyritic Shale	42.9	9.12	368	78.2	459	97.7
2	Black Bituminous Shale	98.0	28.1	319	91.3	361	104
3		42.9	15.8	245	90.1	245	90.1
4	Pyritic Shale	12.3	4.31	165	58.2	276	97.1
5	Black Bituminous Shale	12.3	5.52	190	85.5	233	105
6		12.3	3.88	221	69.8	306	96.9

* (kg H_2SO_4 t^{-1} rock)

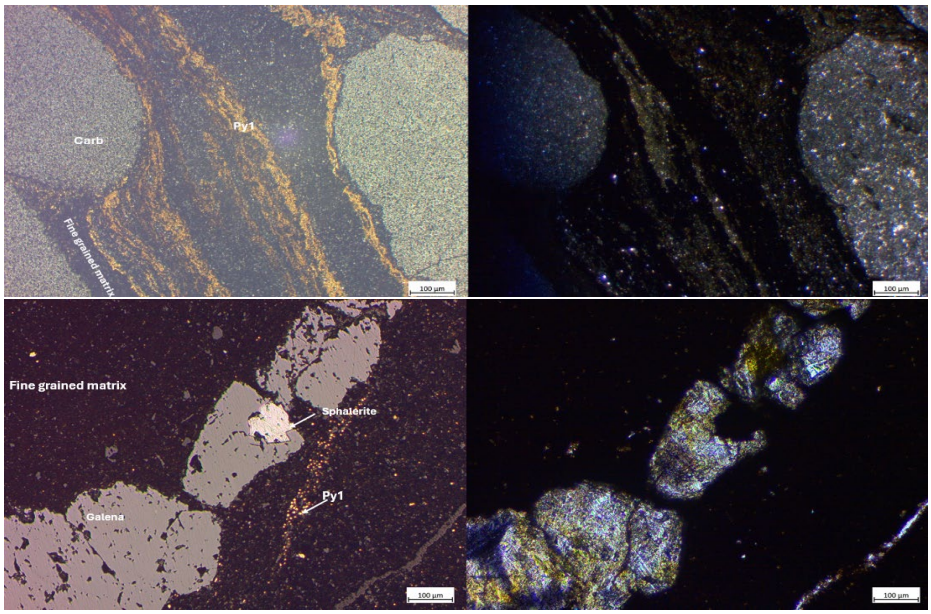

Fig. 2 **Fine grained pyrite and dolomite in Sample 1 (top). Sphalerite and galena grains in a discontinuous vein in Sample 5 (bottom).**

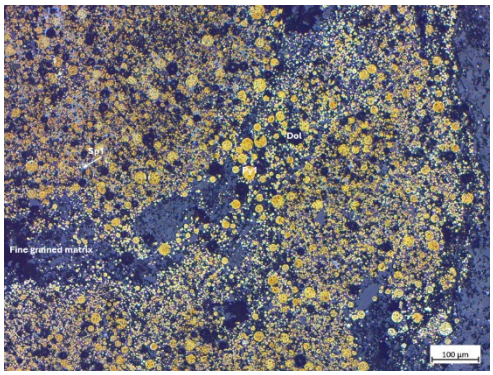

Fig. 3 **Rounded pyrite grains throughout Sample 3 with some pyrite grains showing replacement with silicate and dolomite minerals.**

Reprocessing of Mine Wastes – The circular economy providing opportunities to improve the management of sulfidic materials.

PL Defferrard
Sibanye Stillwater, Australia. pascal.defferrard@sibanyestillwater.com

1.0 Abstract

Sibanye-Stillwater's Century operation, located in Queensland, Australia, represents the largest tailings retreatment project in the country and stands among the top 15 global zinc producers. The operation involves the hydraulic mining and retreatment of legacy tailings from the original Century Mine, leveraging a progressive and economically sustainable rehabilitation strategy. The core of this strategy is the removal of tailings material from the original tailings storage facility (TSF) using high-pressure hydraulic cannons, with supplementary mechanical intervention where necessary. The mobilised slurry is then transported via pipeline to the original Century open pit, where it is deposited subaqueously, effectively isolating the material from oxygen and significantly reducing the potential for acid metalliferous drainage and other geochemical risks.

This innovative approach aligns with regulatory closure objectives while maximising resource recovery from historical tailings, ensuring the long-term stability and environmental integrity of the site. The model enables concurrent rehabilitation by progressively reducing the tailings dam footprint as material is removed and re-deposited in a controlled, engineered repository. Additionally, it supports post-mining land use objectives and demonstrates a sustainable model for mine closure that balances environmental responsibility with economic viability. This method also provides a replicable framework for other large-scale mining operations managing extensive tailings legacies. The Century operation illustrates the potential of integrated mining, retreatment, and rehabilitation processes to deliver both economic and environmental outcomes, positioning Sibanye-Stillwater as a leader in sustainable mine closure practices.

Assessing waste critical metals potential and acid and metalliferous drainage risks at an abandoned gold lode mine in Normanby, South-East Queensland

F.Colombi[A], K.Johnson[B], A.Iqbal[A], S.Baldwin[A], E. Jennings[A] and A.Parbhakar-Fox[A]

[A] WH Bryan Mining Geology Research Centre, Sustainable Minerals Institute (SMI), University of Queensland, UQ Experimental Mine Cnr Finney Road and Isles Road Indooroopilly QLD 4068 Australia. f.colombi@uq.edu.au

[B] Department of Natural Resources and Mines, Manufacturing and Regional and Rural Development, (GSQ), PO Box 5318, Townsville QLD 4810, Australia

1.0 Abstract

The drive toward sustainable resource recovery and environmental rehabilitation has amplified the interest in the valorisation of mine waste. Abandoned mine sites are increasingly recognised not only as a source of environmental pollution, but also as potential and unconventional secondary resources of critical metals. This study investigates the waste rock dumps and surrounding drainage systems of the historic Normanby Au-lode, located near Mount Perry in southeast Queensland. An integrated multi-analytical approach was applied to waste rock samples (n=53) and slag (n=2), including Inductively Coupled Plasma Mass Spectrometry (ICP-MS), X-ray Diffraction (XRD), Mineral Liberation Analysis (MLA) and Laser Ablation Inductively Coupled Plasma Mass Spectrometry (LA-ICP-MS), complemented by drone-based surveys and drainage water analysis. The study identified Cu sulfides and their alteration products (e.g., iron oxides) as primary hosts of critical metalloids such as bismuth (Bi), antimony (Sb), silver (Ag), and copper (Cu). Additionally, Cu concentrations exceeding 10 mg/L were recorded in surface waters downstream off the waste dumps. The findings highlight the hidden potential of abandoned mine sites for metal recovery, and also the significant environmental risks they may pose to surrounding ecosystems. A broader evaluation of similar legacy sites across Queensland is essential to guide sustainable remediation and resource development.

2.0 Introduction

The shift toward low-carbon technologies is driving global demand for critical and strategic metals, which are essential for batteries, renewable energy infrastructure, electronic components, and other key applications. At the same time, the supply of these elements is constrained by geopolitical instability, trade limitations, and declining ore grades. As a result, secondary sources, particularly mine wastes, are emerging as viable alternatives as critical metal resources (Tayebi-Khorami *et al.,* 2019). Abandoned mines, historically considered environmental liabilities, may now offer economic and strategic values. Mine waste often contains residual concentrations of metals that were either uneconomic to recover at the time or left unprocessed due to historical technology inefficiencies. Tailings from abandoned mines often contain higher concentrations of critical metals than the original ore (Sarker *et al.,* 2022). Moreover, mine drainage waters can mobilize significant quantities of critical metals over time. In some cases, precipitates from mine drainage can contain up to 0.02% cobalt, a concentration comparable to that found in some ore-grade deposits (Ziwa *et al.,* 2020).

This study investigates the critical metals and metalloids in historical mine waste from the Normanby deposit, an abandoned historical Cu-Au mine near Mount Perry in Queensland (Figure 1), and the environmental risk associated with its natural weathering. The aim is to evaluate the reprocessing

potential of the historical mine waste, assess the geochemical and mineralogical hosts of critical metalloids and understand the contamination footprint from the surrounding drainage systems. These insights are intended to support regional rehabilitation and circular economy approaches for legacy mine sites in Australia and globally.

3.0 Methods

The Normanby site contains several small waste rock dumps distributed around an abandoned underground gold mine. The country rock is dominated by felsic intrusives, in particular the Tenningering granodiorite. Waste rock samples (n=53) were collected from four major waste rock dumps, capturing variability in lithology and degree of weathering. Two slag samples were also retrieved from the nearby smelter site. A total of 14 water samples were collected along the primary drainage pathways originating from the waste rock piles and extending downstream to areas including the Mount Perry township (Figure 2). Waste rock and slag samples were prepared and analysed by ALS Geochemistry (Brisbane) using ICP-MS. The samples were processed with the ALS methods ME-MS61 and ME-MS81 to assay a suite of 86 major and trace elements. Nine waste rock and one slag sample with high metalloid content were selected for further characterisation via XRD at Sietronics Laboratory Services (Australian Capital Territory), MLA at the Sustainable Minerals Institute (University of Queensland), and LA-ICP-MS at Adelaide Microscopy (University of Adelaide). Water quality parameters such as pH and electrical conductivity were collected during field sampling, while alkalinity, sulfur, major cations/anions and dissolved metalloids were analysed by ALS Geochemistry (Brisbane). To 3D map the mine waste, a DJI Air 3 drone with pre-designed flight plans was used with a Waypoint Map. The data was processed using WebODM for the generation of georeferenced orthomosaic and 3D models.

4.0 Results

Bulk-rock geochemical data revealed that waste rock samples are enriched in critical metalloids such as Ag, As, Bi, Cu, Sb, Se and Te, often exceeding 1,000 times their average crustal abundances (Levinson, 1974; Rumble, 2021). These elements are also important pathfinder indicators for Au ± Cu mineralisation. Similarly, the slag is enriched in critical metalloids including As, Cu, Bi and Sb (Figure 3). Statistical parameters for bulk-rock composition of the waste rock and slag are summarised in Table 1. X-ray diffraction and MLA revealed mineralogical dominance of quartz, plagioclase, pyrite, chalcopyrite, chalcocite and Fe oxides (Figure 4). In contrast, the composition of the slag is mainly composed of Si-Fe, Al-Si-Ca-Fe and Fe-Si bearing-phases (Figure 5).

The distribution of critical metalloids was investigated by LA-ICP-MS in Fe and Cu sulfides (e.g., pyrite, chalcopyrite, chalcocite, bornite, covellite) and Fe oxides (including goethite). Compositional characterization of pyrite reveals an enrichment in Co (up to 7,853 ppm) and Te (up to 124 ppm), while chalcopyrite is enriched in Zn (up to 11,882 ppm). Bornite contains high concentrations of Ag (3,982 ppm) and Bi (3,142 ppm), whereas chalcocite and covellite also host these critical metalloids, although at lower concentrations. Finally, iron oxides including goethite, are highly enriched in Ag (up to 4,335 ppm), As (up to 7,079 ppm), Cu (up to 24,579 ppm), Pb (up to 6,754 ppm), Sb (up to 26,419 ppm) and Bi (up to 35,749 ppm; Table 2).

All drainage samples collected near the waste rock dumps show elevated concentrations of dissolved Cu (up to 30 mg/L), and strongly acidic pH values (down to 1.91) (Figure 6A-B). This is especially evident for drainage from waste rock dumps NBs4 and NBs5 (see Figures 1 for location). Water draining from

these two dumps often contain sulfate concentration exceeding 1,000 mg/L and Cu concentration above 17 mg/L, both surpassing the Australian and New Zealand Guidelines for Fresh and Marine Water Quality (ANZG) values (Figure 6, Table 3) (ANZG, 2023). Additionally, a sample collected from the top of NBs5 contains As at a concentration above 0.0025 mg/L, also exceeding the relevant ANZG threshold. Dissolved Cu concentrations tend to decrease with increasing pH (Table 3), and a similar pH-dependent trend is observed for other dissolved metalloids, including Ni, Zn and As (Table 3). However, these elements are not present in high dissolved concentrations in the water. Downstream attenuation is observed (Figure 6A), although some downstream areas within the town of Mount Perry still exhibit low pH and elevated dissolved Cu concentrations (Table 3).

The volumes of the mine waste features, including the waste rock dumps and the slag pavement near Mount Perry were calculated by testing a consumer-grade drone using the WebODM method. Orthomosaics and 3D models were generated from drone imagery in WedODM and subsequently imported into ArcGIS Pro for the analysis and visualization of boundary polygons delineating the waste rock piles, as shown in Figure 7a. Based on the estimated volume of approximately 10,000 m^3 for NBs5 (Figure 7a), an average material density of 4.2 g/cm^3, and the median assay values (in ppm) of As, Bi, Sb, Ag, and Cu from the 30 samples collected within NBs5, the approximate tonnages of these metals of interest were calculated (Figure 7b).

5.0 Discussion

The integration of geochemical, mineralogical, and remote sensing data in this study reveals a potential re-processing opportunity, coupled with an environmental impact associated with the Normanby mine waste. The elevated concentrations of critical metalloids such as Cu, Bi, Sb, Ag, and As in both waste rock and slag suggest options for underexplored secondary and possibly primary resources. Although funding constraints did not allow for Au fire assay, the presence of key pathfinder elements and Ag enrichment, when considered in light of the historical gold fineness of the region, strongly suggest that considerable quantities of Au may remain in the waste materials, warranting further investigation (Stuart, 2016).

LA-ICP-MS analyses indicate that Cu and Fe sulfides, including pyrite, chalcopyrite, and bornite, are key mineral hosts for elements such as Co, Zn, Ag and Bi. Particularly noteworthy is the highly enriched levels of Sb, As and Bi in iron oxides, likely formed during oxidative weathering of primary sulfides. The presence of elevated concentrations of critical metalloids in goethite and other Fe oxides suggests secondary phases may act as both short-term sinks and long-term sources of environmental contamination. These findings are consistent with previous studies that document the role of Fe oxides in adsorbing or incorporating metalloids during sulfide weathering (Parbhakar-Fox and Lottermoser, 2017).

The water chemistry results further highlight the potential environmental risks associated with the site. The presence of acidic pH values and elevated dissolved Cu concentrations indicates active acid and metalliferous drainage (AMD) processes, in line with previous findings on AMD generation from the weathering of sulfidic mine waste (Parbhakar-Fox *et al.,* 2014; Amar *et al.,* 2021). In addition, several water samples exceeded the Livestock Drinking Water Guidelines values for sulfate and Cu, and one sample for As (ANZG, 2023). Although there is no documented evidence of livestock using the downstream water, these guidelines were considered the most appropriate, as livestock use is the most likely scenario downstream. Under the ANZG guidelines, sulfate concentrations > 1,000 mg/L indicate a risk of chronic effects for livestock consuming the water. Although only one sample exceeded the As trigger value of 0.0025 mg/L, this may still pose a hazard. Dissolved Cu concentrations are well above

the ANZG livestock guideline of 0.5 mg/L. While Cu is an essential micronutrient, at these levels it can be toxic. Further work on Cu speciation is warranted to better constrain mobility, bioavailability and risk. While downstream attenuation is observed, some areas within Mount Perry still exhibit low pH and elevated metal loads, posing a potential risk to local water quality and ecosystems. The limited mobility of other metalloids (e.g., As, Zn, Ni) may reflect the pH-dependent solubility or retention by secondary minerals, plants (e.g., ferns) and organic matter in the drainage pathway. It is important to note that, although the Normanby site likely represents a localized source of environmental contamination, Mount Perry and the surrounding region has been affected by over a century of sporadic historical mining activity, contributing to widespread contamination across the region not isolated to this specific occurrence.

Drone-based volumetric analysis adds a spatial dimension to this evaluation, allowing for the quantification of waste volumes and a better understanding of potential resource availability and contamination extent. The accurate delineation of waste rock piles provides an essential input for planning future remediation or valorisation strategies, including selective reprocessing, passive treatment systems, or phytoremediation. Altogether, these findings indicate that legacy mine waste, such as that at Normanby, represents both a challenge and an opportunity. While environmental risks associated with weathering and leaching are evident, the significant concentrations of critical metalloids suggest that targeted recovery may be viable, especially if coupled with remediation efforts.

6.0 Conclusions

This study demonstrates that historical mine waste at the Normanby Au-lode contains considerable concentrations of critical and strategic metalloids, particularly Cu, Bi, Sb, and Ag. These are primarily hosted within Cu-Fe sulfides and secondary Fe oxides. The presence of high dissolved Cu concentrations and low pH in nearby drainages highlights the environmental risks associated with ongoing weathering processes.

However, the multi-analytical approach adopted here also reveals the potential for selective metal recovery, particularly from mineral phases enriched in valuable elements. Drone-based volumetric assessments offer key insights into the scale of the waste features, facilitating resource estimation and spatial planning.

Overall, the Normanby site exemplifies the dual nature of abandoned mine waste as both a source of contamination and a potential resource. The findings support broader efforts to re-evaluate legacy sites across Queensland for their contribution to circular economy models and sustainable critical metal supply chains. Future work should expand this approach to other legacy sites, incorporating leaching trials, passive remediation design, and economic feasibility studies to guide practical implementation.

References

Amar, H., Benzaazoua, M., Edahbi, M., Villeneuve, M., Joly, M. A., & Elghali, A. (2021). Reprocessing feasibility of polymetallic waste rock for cleaner and sustainable mining. Journal of Geochemical Exploration, 220, 106683.

ANZG (2023). Livestock drinking water guidelines. Australian and New Zealand Guidelines for Fresh and Marine Water Quality. Australian and New Zealand Governments and Australian state and territory governments, Canberra.

Levinson, A. A. (1974). Introduction to exploration geochemistry.

Parbhakar-Fox, A. K., Edraki, M., Hardie, K., Kadletz, O., & Hall, T. (2014). Identification of acid rock drainage sources through mesotextural classification at abandoned mines of Croydon, Australia: Implications for the rehabilitation of waste rock repositories. Journal of Geochemical Exploration, 137, 11-28.

Parbhakar-Fox, A., & Lottermoser, B. (2017). Principles of sulfide oxidation and acid rock drainage. In Environmental Indicators in Metal Mining (pp. 15-34). Cham: Springer International Publishing.

Rumble, J. R. (Ed.). (2021). CRC Handbook of Chemistry and Physics (102nd ed.). CRC Press.

Sarker, S. K., Haque, N., Bhuiyan, M., Bruckard, W., & Pramanik, B. K. (2022). Recovery of strategically important critical minerals from mine tailings. Journal of Environmental Chemical Engineering, 10(3), 107622.

Stuart N. F. "MDL 265 - Combined Report for Periods from 2000 to 2016." Unpub. Rpt. For Belanda Pty. Ltd. to Dept. Natural Resources and Mines, Qld.

Tayebi-Khorami, M., Edraki, M., Corder, G., & Golev, A. (2019). Re-thinking mining waste through an integrative approach led by circular economy aspirations. Minerals, 9(5), 286.

Ziwa, G., Crane, R., & Hudson-Edwards, K. A. (2020). Geochemistry, mineralogy and microbiology of cobalt in mining-affected environments. Minerals, 11(1), 22.

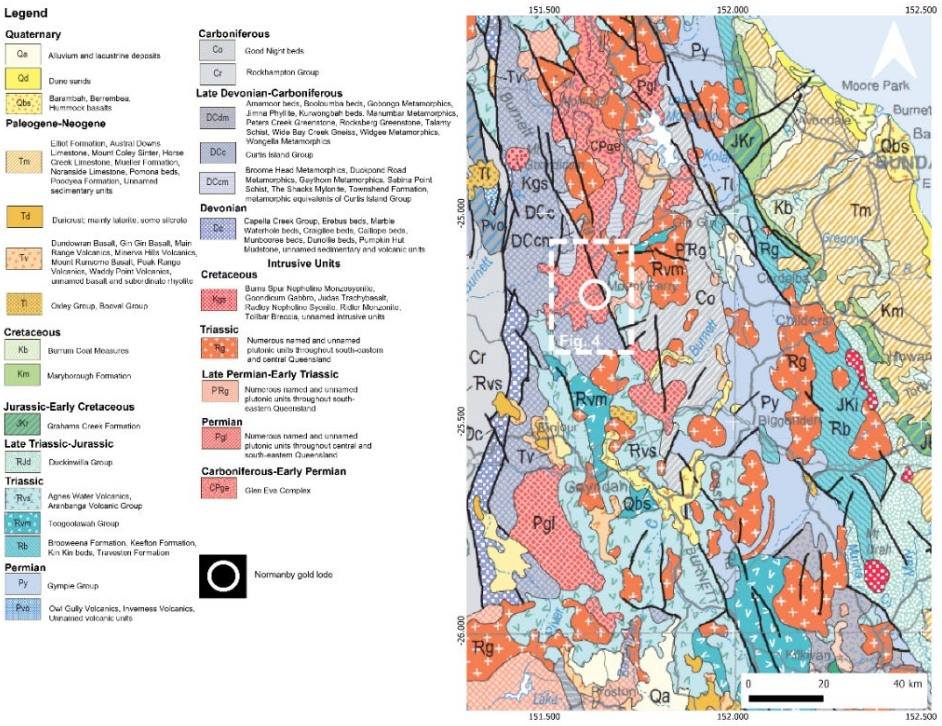

Fig. 1. **Regional geological map with location of the Normanby lode within the Gympie Province**

Table 1. **Summary statistics for selected elements (ppm) measured in the Normanby mine waste (C.a.v. = crustal abundance values; Rumble *et al.*, 2021)**

	Ag	*As*	*Bi*	*Co*	*Cu*	*Mo*	*Pb*	*Sb*	*Se*	*Te*	*Zn*
C.a.v.	0.08	1.8	0.0085	25	68	1.1	14	0.2	0.5	0.001	70
					Waste rock (n=53)						
Min	0.1	1	0.3	1	33	0.3	2	1	1	0.1	2
Max	352	1,590	4,180	300	302,000	176	841	4,240	45	37	910
Mean	46	116	325	53	26,932	20	73	350	13	5	80
Median	10	54	38	19	4,040	10	18	70	6	3	36
					Slag (n=2)						
Min	3	56	7	81	3,930	12	77	696	1	0.4	775
Max	6	321	70	96	5,460	21	392	2,400	2	0.4	2,140
Mean	4	189	39	88	4,695	17	235	1,548	2	0,4	1,458
Median	3	56	7	81	3,930	12	77	696	1	0.4	775

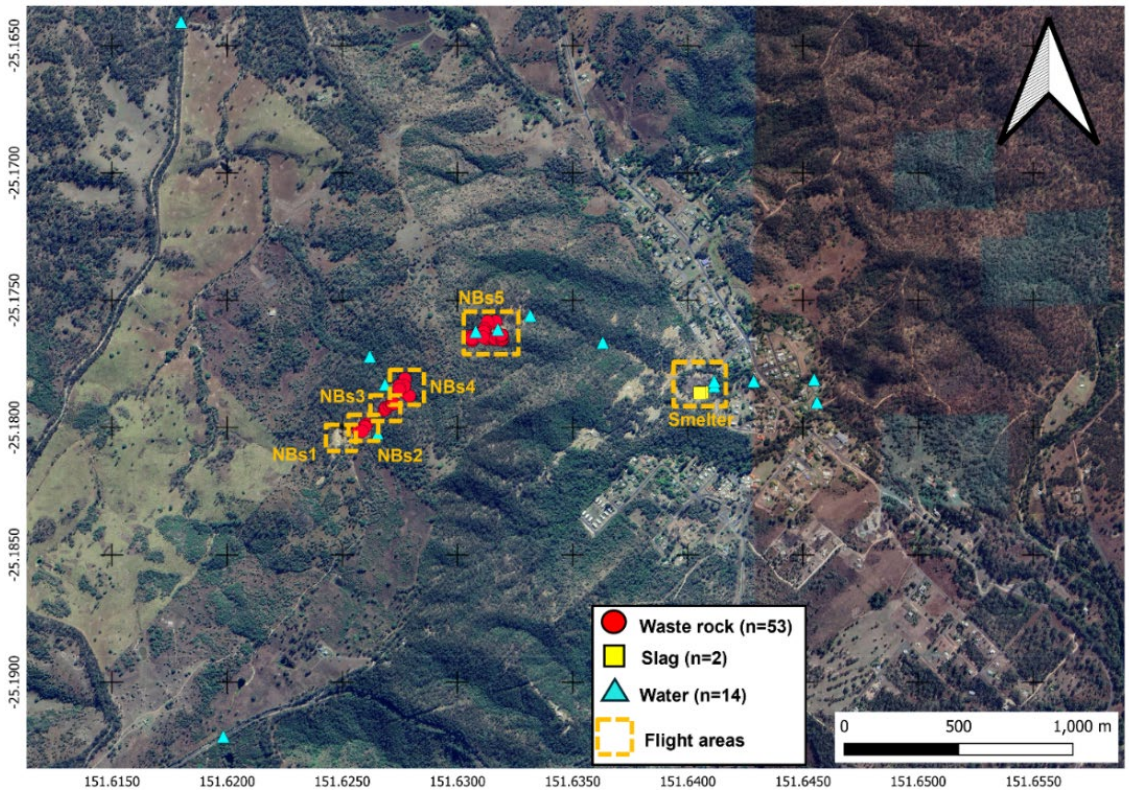

Fig. 2. **Normanby mine waste sampling and drone survey locations**

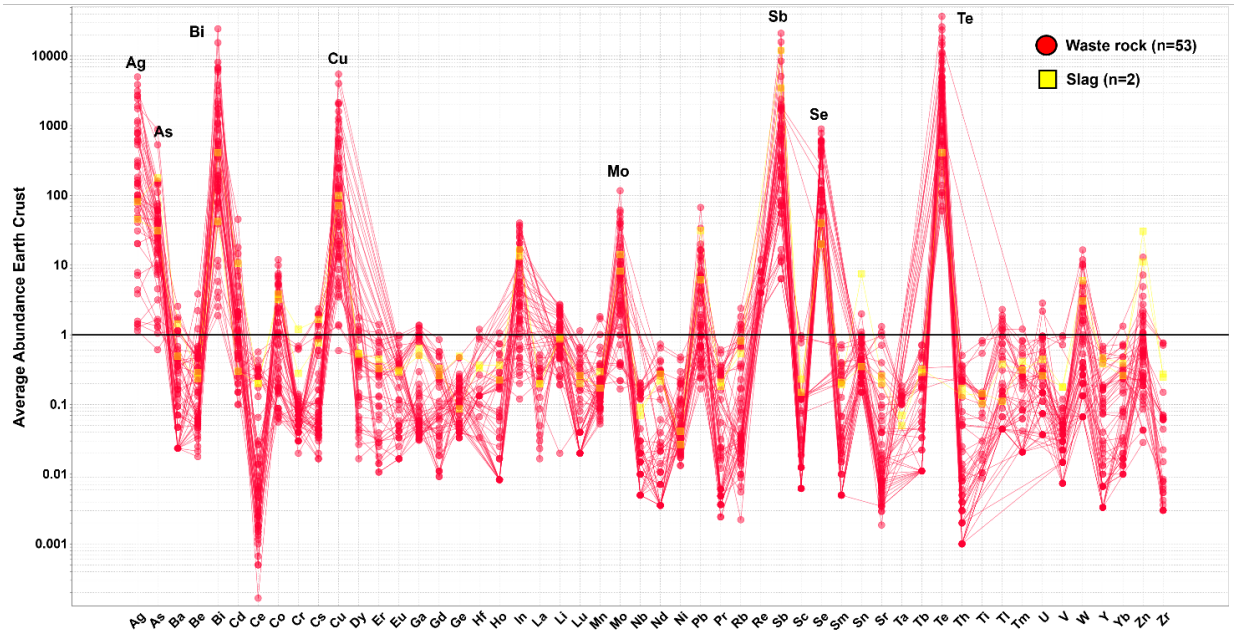

Fig. 3. **Bulk chemistry summary of the waste rock (red circle) and slag (yellow square) samples collected in Normanby compared to average crustal abundance values (Levinson, 1974)**

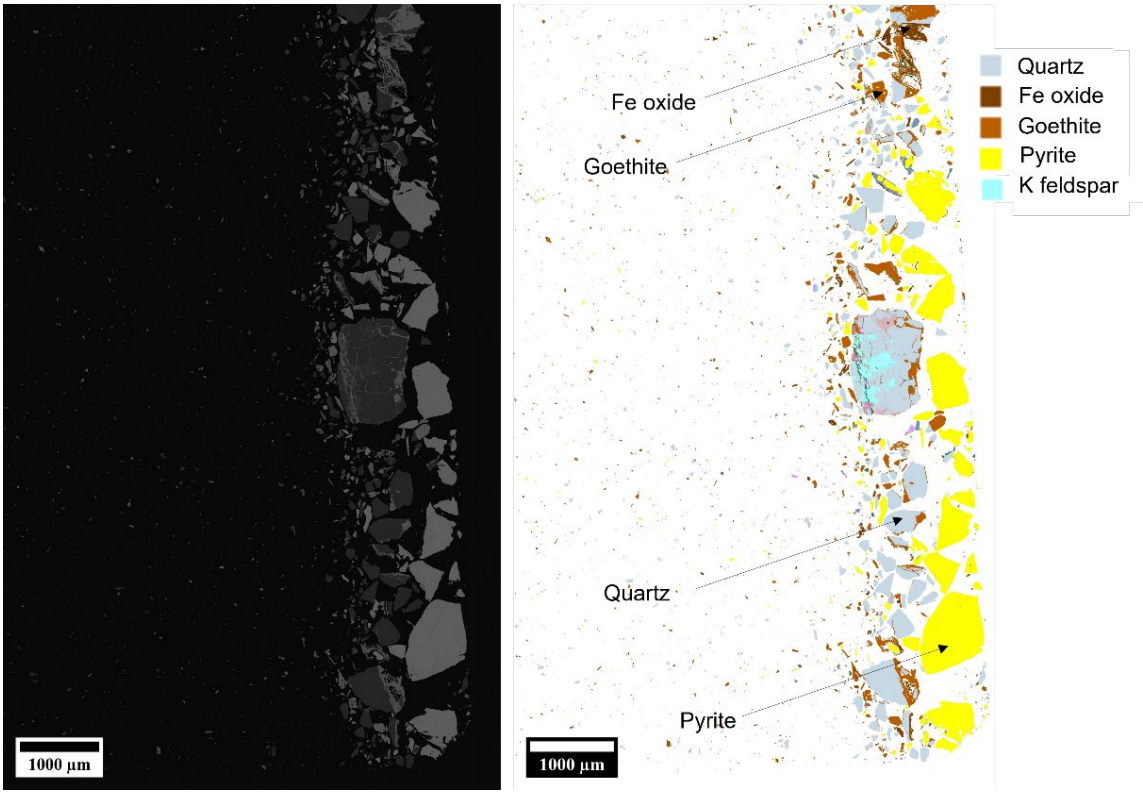

Fig. 4. **BSE and classified mineralogy image for sample N38 (waste rock) as determined by MLA. Major phases include quartz (44 wt. %), pyrite (24 wt. %) and goethite (22 wt. %). Minor phases include Fe oxide (4 wt. %) and schwertmannite (1.7 wt. %)**

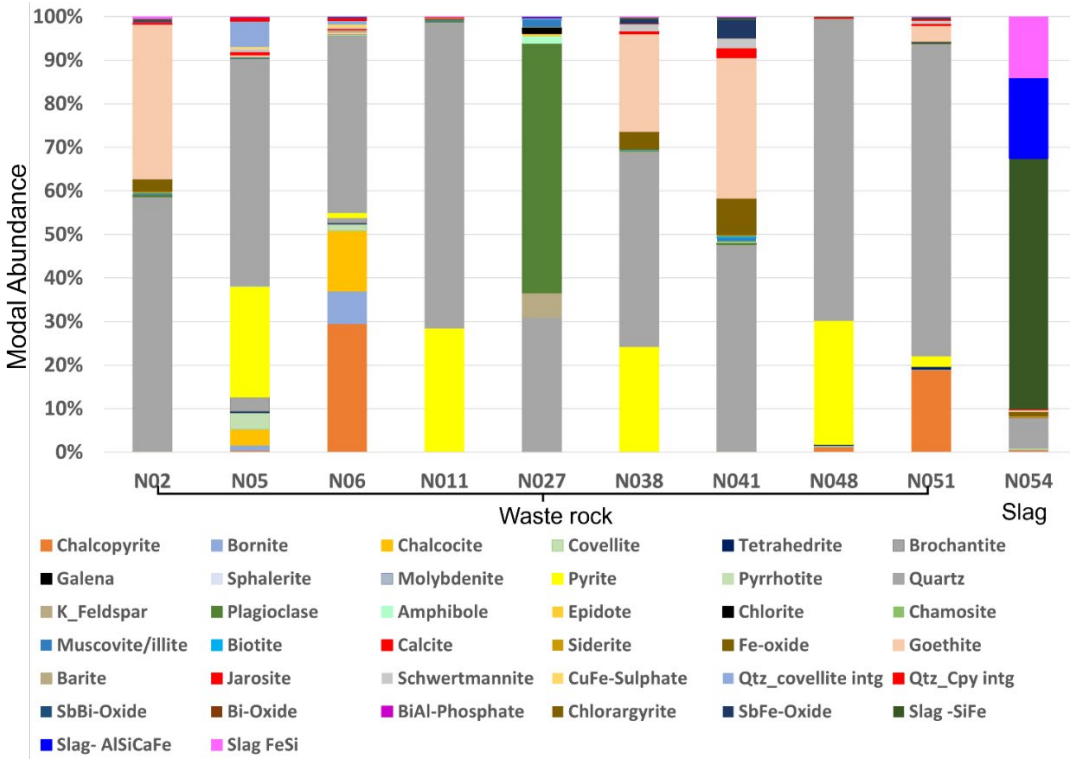

Fig. 5. **Modal mineralogy as determined by MLA for the Normanby waste rock (n=53) and slag (n=2)**

Table 2. **Statistical summary of concentrations for selected trace elements for LA-ICP-MS analyses: pyrite (n=200), chalcopyrite (n=55), bornite (n=7), chalcocite (n=11), covellite (n=10), Fe oxide (n=17) and goethite (n=40)**

	^{60}Ni	^{59}Co	^{107}Ag	^{75}As	^{65}Cu	^{77}Se	^{125}Te	^{66}Zn	^{208}Pb	^{121}Sb	^{209}Bi
					Pyrite (n=200)						
Min	0.04	0.01	0.01	0.32	0.13	0.6	1.1	0.3	0.01	0.05	0.01
Max	380	7,853	193	1,613	13,349	25	124	5,337	527	52	986
Mean	22	304	9	264	318	7	21.3	74	11	2.8	21
Median	0.7	24	0.5	159	4.9	5.3	14	0.6	0.2	0.4	1.4
					Chalcopyrite (n=55)						
Min	0.10	0.03	0.7	0.51	303,973	0.8	2.3	6.8	0.1	0.1	0.2
Max	2.4	14	965	206	571,166	26	31	11,882	849	119	552
Mean	0.7	1.4	81	11	347,827	5	9	359	30	12	39
Median	0.5	0.2	9	2.4	337,933	6	8	31	5	5	6
					Bornite (n=7)						
Min	0.1	0.03	458	2.4	639,637	1	1	1	2	17	31
Max	0.4	1.7	3,982	111	769,231	21	60	6	10	417	3,142
Mean	0.2	0.4	1,126	22	696,760	4	11	4	7	82	512
Median	0.1	0.1	629	6.3	690,872	1	3	5	7	25	83
					Chalcocite (n=11)						
Min	0.1	0.1	62	0.8	393,026	3	4	1.9	0.4	16	1.9

Max	5.3	4.3	1,679	68.4	747,255	10	119	43	13	975	1,488
Mean	1.3	0.7	782	14.3	682,156	7	21	13	5	134	210
Median	0.2	0.1	736	7.4	719,007	7	8	7	3	61	94
					Covellite (n=10)						
Min	0.1	0.04	623	1.7	474,847	3	11	1	3	5	19
Max	0.3	0.1	2,136	7.1	660,412	42	36	2	33	56	2,705
Mean	0.2	0.1	919	3.7	544,379	10	20	1	18	20	1,297
Median	0.1	0.1	839	3.2	535,991	5	18	1	18	14	1,401
					Fe oxide (n=17)						
Min	0.1	0.3	0.3	1.3	2.4	10	6	27	0.03	0.5	0.1
Max	5.0	9.2	4,335	2,962	24,579	55	87	789	1,562	26,058	35,749
Mean	1.1	2.2	556	1,021	12,211	31	36	193	487	6,708	7,615
Median	0.4	1.8	64	815	10,671	35	25	119	341	1,679	82
					Goethite (n=40)						
Min	0.1	0.3	0.6	141	4,402	1.6	1.1	14	127	3.9	0.4
Max	11	293	2,329	7,079	23,394	32	45	2,184	6,754	26,419	1,498
Mean	4	34	152	2,663	10,589	12	8	661	1,303	10,135	321
Median	1.3	10	22	1,687	9,900	10	4	152	578	7,384	165

Table 3. **Physico-chemical parameters of water samples (mg/L) from the Normanby water drainages (bdl = below detection limit). Livestock drinking water guidelines reported (ANZG, 2023)**

	pH	EC	$CaCO_3$	SO_4^{2-}	As	Cu	Ni	Zn	Ca	Na
ANZG	-	-	-	<500	<0.025	<0.5	<1	<20	<1,000	-
NW7	7.32	732.3	180	104	0	0.562	0.002	0.026	41	84
NW6.5	3.8	831.8	bdl	342	0.001	4.31	0.011	0.135	85	45
NW5.5	3.95	906	bdl	342	0	4.49	0.011	0.132	92	45
NW5	5.86	732.8	43	301	0.002	1.43	0.006	0.113	94	33
NW6	4.5	890	bdl	376	0.004	3.91	0.012	0.13	97	45
NWD1a	6.71	267	39	1	0.003	0.003	0	0.028	7	36
NWD4a	8.58	629.6	138	24	0.01	0.024	0	0.01	30	79
NWD3a	6.8	137.3	46	1	0.001	0.011	0	0.01	2	24
NWD2a	7.3	646.7	61	202	0.001	0.119	0.001	0.013	56	49
NWD8	1.91	3250	bdl	1200	0.007	20.8	0.033	0.207	74	34
NW1	4.76	1233	bdl	570	0.048	0.187	0.008	0.058	130	49
NW2	2.08	2940	bdl	960	0.02	17.5	0.043	0.312	143	59
NW3	2.37	2950	bdl	1330	0.002	31.1	0.058	0.437	153	63
NW4	2.22	2560	bdl	1170	0	27.1	0.059	0.444	148	66

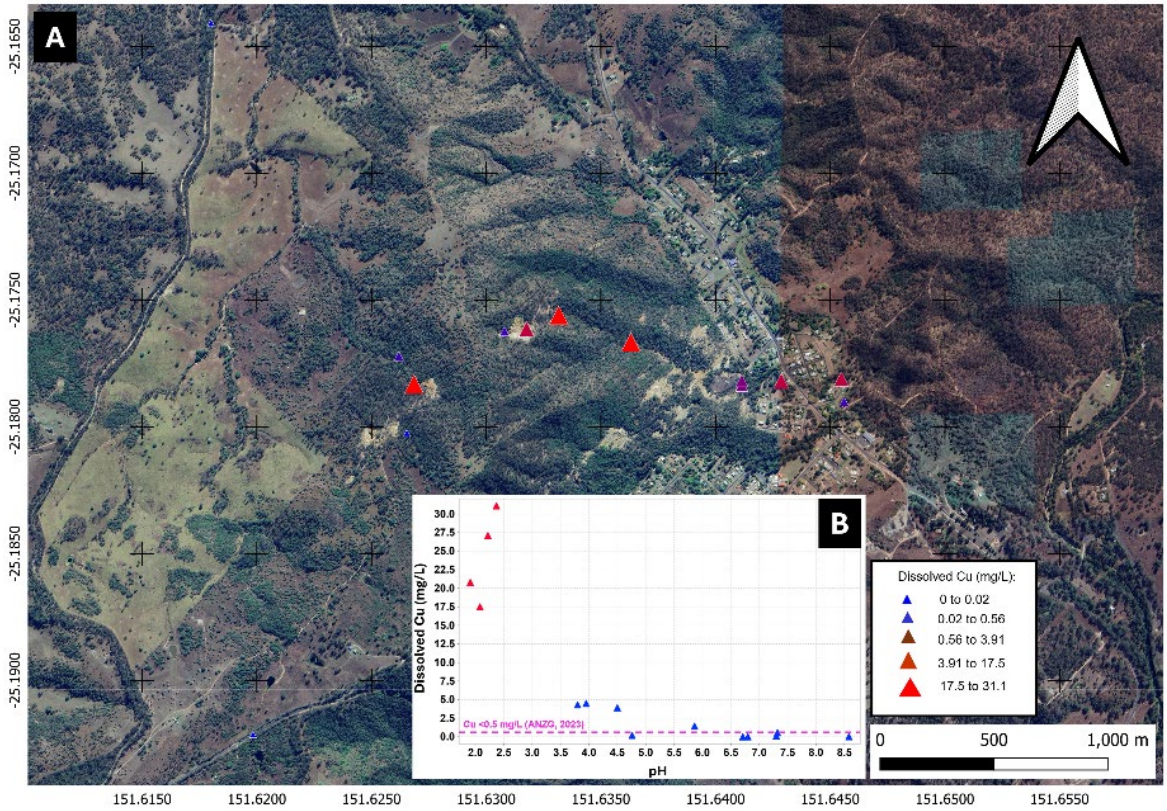

Fig. 6. **A) Spatial distribution of Cu contents (mg/L) in water samples from the Normanby water drainages. B) pH versus dissolved Cu concentrations (mg/L) for water samples. Pink dotted line: guideline value for Cu (ANZG, 2023)**

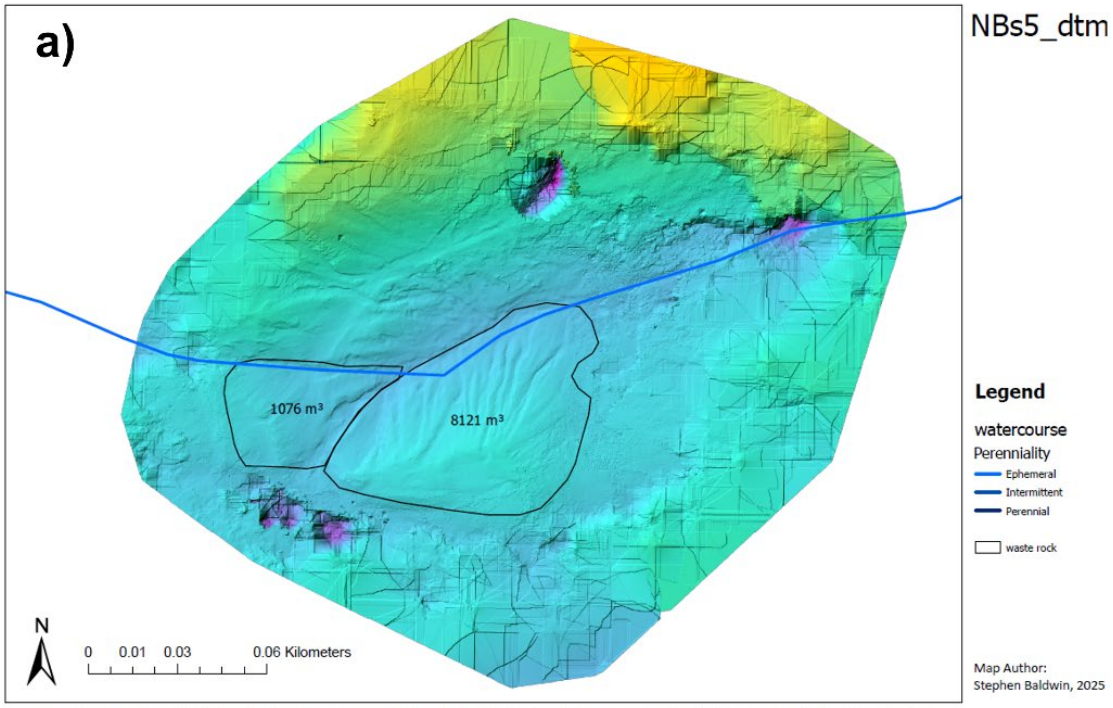

Figure : Digital terrain model of NBs5 from drone imagery using WebODM. The blue line shows the watercourse classified by perennity. Black outlines mark mine waste piles, with estimated volumes calculated in WebODM.

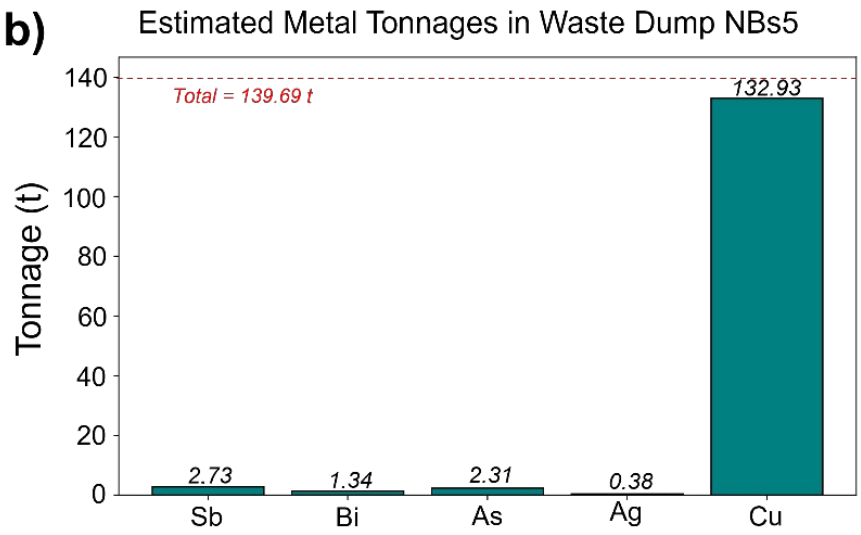

Fig. 7. **a) Digital terrain model of NBs5 from drone imagery using WebODM (refer to 2 location). The blue line shows the watercourse classified by perennity. Black outlines mark mine waste piles, with estimated volumes calculated in WebODM; b) estimated metal tonnages for NBs5 for selected metalloids. Red dotted horizontal line = total tonnages for NBs5**

Finding value in mining wastes: Towards development of an international standard

A. Golev[A], C. Unger[B], T. Laurençont[C], and K. Fogarty[A]

[A]Department of Natural Resources and Mines, Manufacturing and Regional and Rural Development, Brisbane, QLD 4002. artem.golev@resources.qld.gov.au

[B]Centre for Social Responsibility in Mining, Sustainable Minerals Institute, The University of Queensland, Brisbane, QLD 4067

[C]Chair Standards Australia, Mirror Committee TC82/SC7 Sustainable Mining and Mine Closure, Adelaide, SA 5250

1.0 INTRODUCTION

The global transition to clean energy is leading to a surge in demand for many minerals and commodities. Currently, mining is expected to expand to meet this growing demand. This increase in mining will result in a significant increase in mining waste, e.g. waste rock, tailings, sub-economic ores, etc. (Macklin et al., 2023; Owen & Kemp, 2019; Owen et al., 2024; Tang & Werner, 2023).

Mining waste is often presented as an environmental liability, particularly when the mining and placement methods for reactive waste allow for their exposure to the elements resulting in the generation of elevated concentrations of heavy metals in the acid and metalliferous drainage that can contaminate the receiving environment. However, they can also provide an opportunity for use as secondary resources whilst addressing environmental impacts as part of a secondary mining project (Cotrina-Teatino & Marquina-Araujo, 2025; Das et al., 2024; Lèbre et al., 2017; Tayebi-Khorami et al., 2019; Wade et al., 2022; Werner et al., 2018).

Data associated with mining waste is often lacking. In the basic sense, data on waste characterisation and waste volumes is either not maintained, or, when captured, is not available publicly, or lost if a site becomes abandoned. Without access to this data, decision making often contains assumptions and an acceptance of risk or becomes costly to infill the knowledge gaps. Ultimately, this can lead to limited opportunities to quantify the future potential of this material.

It is therefore necessary to have a systematic way for estimating potential economic value for current and/or historic mining waste. It is anticipated that this may incentivise segregation and/or separate handling for waste streams and sub-streams, presenting opportunities for their direct use or stockpiling for future use or reprocessing, consistent with the circular economy principles. A review of existing standards, government policy and codes for the classification of mineral exploration results, mineral resources and ore reserves has identified that this is not extensively covered and requires attention.

This abstract describes the process by which a Working Group within the International Organisation for Standardisation has responded to a call for an international standard on finding value in mining wastes.

2.0 ISO STANDARDS FOR SUSTAINABLE MINING

The International Organisation for Standardisation (ISO) is a non-governmental organization that develops and publishes international standards across various industries. It brings together experts to create voluntary standards ensuring quality, safety, efficiency of products, services, processes and systems, which in turn contribute to sharing and promoting knowledge and best practices worldwide.

The development of standards in the area of sustainable mining practices is coordinated by Subcommittee (SC) 7 'Sustainable Mining and Mine Closure', part of Technical Committee (TC) 82 'Mining' within ISO. Several new standards have been recently published by SC 7 and several more are in development, with 18 participating member countries and 14 observing member countries (ISO, 2025).

The process for ISO standards development includes several major steps, starting with a short proposal and the formation of a task force to allow for the development of a more detailed new work item proposal, which is then circulated to participating member countries for ballot. If this ballot is successful, a working group is formed comprised of global experts on the topic. The standard is developed through a series of drafts informed by review feedback within timelines set out by ISO. A committee draft is followed by a draft international standard (DIS), which then advances to a final draft international standard (FDIS), before final approval for publication. Annual international hybrid meetings of the working group are supplemented by virtual meetings through the year. The voluntary nature of ISO standards development means that working groups must operate efficiently while engaging widely.

3.0 NEW PROPOSAL FOR FINDING VALUE IN MINING WASTES

The Standards Australia's Mirror Committee of ISO/TC 82/SC 7 is currently leading the development of an ISO standard titled 'Finding value in mining wastes' (ISO/NP 25412, 2025).

The proposed standard will aim to provide a standardised method for determining economic value of mining wastes from historic, current and future mines. It is expected that the standard will also provide information on preventing unintended loss of material and/or resources value within processing and waste management operations. Thus, seeking to secure the highest economic value and/or best environmental outcome, encouraging the alignment of mining activities with the circular economy principles (Figure 1).

3.1 United Nations Sustainable Development Goals

The proposed standard aims to support the application of the following United Nations Sustainable Development Goals: 8 Decent work and economic growth, 9 Industry innovation and infrastructure, 10 Reduced inequality, 12 Responsible consumption and production, 13 Climate action, 14 Life below water, and 15 Life on land.

It will also be aligned with and compliment the recently published ISO 24419 'Mine closure and reclamation – Managing mining legacies' standard (ISO 24419-1:2023).

3.2 Standard structure and outline

The proposed standard consists of several sections focusing on:

- Material types and material characterisation, including the importance of keeping records through the life of mine;

- Evaluating principles and approaches, including distinguishing the value of minerals and materials versus the value of land, mixed versus segregated material streams, present value versus future value and opportunities, materials recoverability, processing options and available infrastructure;

- Evaluation methodology, starting with the inventory of materials and characterisation of material streams and sub-streams, but also considering waste management approach and objectives, discarded materials potential as a future asset, operational requirements and efficiency;

- Inclusion of the circular economy principles from exploration and mine design phase, followed by acknowledging changes and developments over the life of mine, integrating minerals and materials recovery, segregation, and mine closure and rehabilitation, and potential re-commercialisation of the site at the end of mine life, including opportunities for land reuse.

3.3 Other considerations

Accounting for economic value in mining wastes, while acknowledging the associated environmental liability, and understanding how these may change over the life of mine, presents a major opportunity for achieving better sustainability outcomes from mining operations. For example, in the case of a mine approaching mine closure the proposed standard may provide guidance to allow for the comparison of options by taking into account the potential value in mining wastes while also considering environmental liability. It is expected the standard may also drive policy changes which considers re-commercialisation as part of the risk mitigation strategy for historical or abandoned mining operations. The proposed standard should highlight the benefits of a life-cycle approach, especially for future mines. Essentially, leading to a paradigm shift from treating discarded materials as a waste and liability to focusing on their potential, including purposely creating secondary resources that can be (re)used now or in the future, increasing in value over time.

REFERENCES

Cotrina-Teatino, M. A., & Marquina-Araujo, J. J. (2025). Circular economy in the mining industry: A bibliometric and systematic literature review. Resources Policy, 102, 105513. https://doi.org/10.1016/j.resourpol.2025.105513.

Das, A. P., Hullebusch, E. D. v., & Akçil, A. (2024). Sustainable Management of Mining Waste and Tailings (1 ed.). CRC Press. https://doi.org/10.1201/9781003442455.

ISO 24419-1:2023. Mine closure and reclamation – Managing mining legacies. Part 1: Requirements and recommendations. https://www.iso.org/standard/83087.html.

ISO, 2025. International Organisation for Standardisation (ISO). ISO/TC 82/SC 7 Sustainable mining and mine closure. https://www.iso.org/committee/5052041.html.

ISO/NP 25412, 2025. New ISO standard proposal 'Finding value in mining wastes'. https://genorma.com/en/standards/iso-pwi-25412.

Lèbre, É., Corder, G., & Golev, A. (2017). The Role of the Mining Industry in a Circular Economy: A Framework for Resource Management at the Mine Site Level. Journal of Industrial Ecology, 21(3), 662-672. https://doi.org/10.1111/jiec.12596.

Macklin, M. G., Thomas, C. J., Mudbhatkal, A., Brewer, P. A., Hudson-Edwards, K. A., Lewin, J., Scussolini, P., Eilander, D., Lechner, A., Owen, J., Bird, G., Kemp, D., & Mangalaa, K. R. (2023). Impacts of metal mining on river systems: a global assessment. Science (American Association for the Advancement of Science), 381(6664), 1345-1350. https://doi.org/10.1126/science.adg6704.

Owen, J. R., & Kemp, D. (2019). Displaced by mine waste: The social consequences of industrial risk-taking. The Extractive Industries and Society, 6(2), 424-427. https://doi.org/10.1016/j.exis.2019.02.008.

Owen, J. R., Kemp, D., Lechner, A. M., Ang Li Ern, M., Lèbre, É., Mudd, G. M., Macklin, M. G., Saputra, M. R. U., Witra, T., & Bebbington, A. (2024). Increasing mine waste will induce land cover change that results in ecological degradation and human displacement. Journal of Environmental Management, 351, 119691. https://doi.org/10.1016/j.jenvman.2023.119691.

Tang, L., & Werner, T. T. (2023). Global mining footprint mapped from high-resolution satellite imagery. Communications earth & environment, 4(1), 134-112. https://doi.org/10.1038/s43247-023-00805-6.

Tayebi-Khorami, M., Edraki, M., Corder, G., & Golev, A. (2019). Re-Thinking Mining Waste Through an Integrative Approach Led by Circular Economy Aspirations. Minerals, 9 (5):286. https://doi.org/10.3390/min9050286.

Wade, B., Meath, C., & Griffiths, A. (2022). Capabilities for circularity: Overcoming challenges to turn waste into a resource. Business Strategy and the Environment, 31(6), 2658-2681. https://doi.org/10.1002/bse.2998.

Werner, T. T., Ciacci, L., Mudd, G. M., Reck, B. K., & Northey, S. A. (2018). Looking Down Under for a Circular Economy of Indium. Environ. Sci. Technol, 52(4), 2055-2062. https://doi.org/10.1021/acs.est.7b05022.

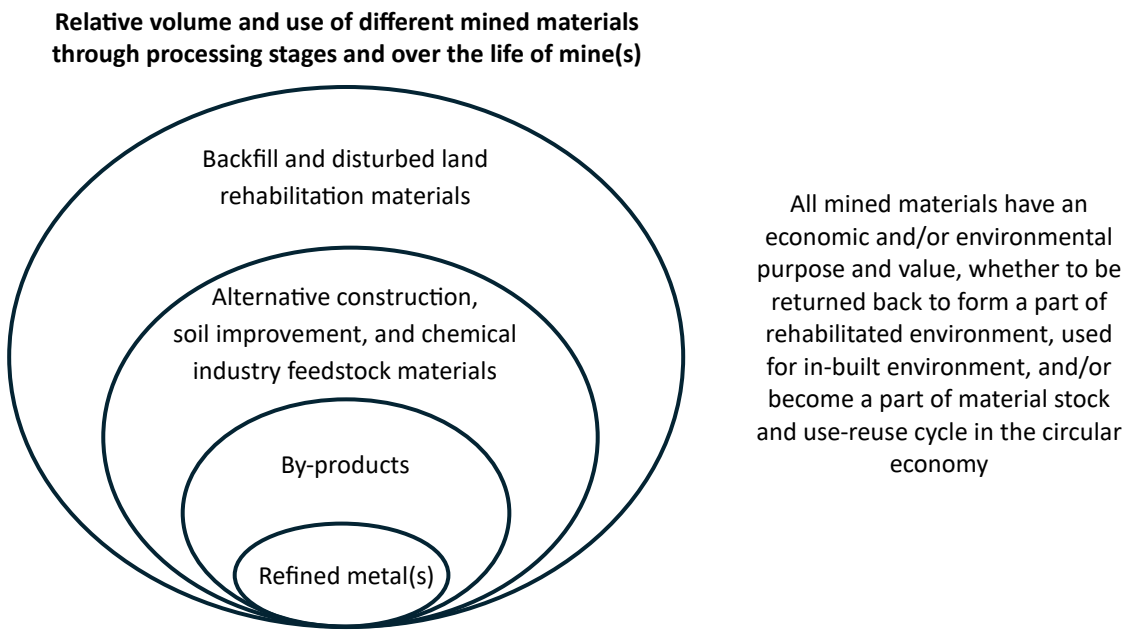

Fig. 1. A circular economy view for mined and processed materials, underlying the development of new ISO standard 'Finding value in mining wastes'.

Pyrite microencapsulation by composite inorganic coatings in acidic conditions for acid mine drainage mitigation: A one-year experimental study

Misbah Fatima Hussain[A,B], Fang Xia[A,*], Yuan Mei[B], Rong Fan[C]

[a] Sustainable Geochemistry and Mineral Sciences (GeMS), Murdoch University, Perth, WA 6150.

misbah.hussain@murdoch.edu.au

[b] CSIRO Mineral Resources, Perth, WA 6151

[c] CSIRO Mineral Resources, Urrbrae, SA 5064

Acid and metalliferous drainage (AMD), characterized by high acidity, elevated sulfate levels, and high heavy metal concentrations resulting from pyrite (FeS_2) oxidation, poses a significant environmental challenge (Kefeni *et al.,*2017; Park *et al.,* 2019). Microencapsulation offers a promising AMD prevention approach, particularly under neutral pH conditions (Fan *et al.,* 2017), yet its efficacy and long-term stability in acidic environments remain underexplored. This study develops phosphate/silica composite inorganic coatings to mitigate AMD under acidic conditions. Pyrite microencapsulation was achieved through either rapid coating formation in the presence of hydrogen peroxide or slow coating formation in air. Coating performance was evaluated over a one-year experimental period in batch and flow-through reactors. At pH 5, ICP-OES analysis of leachate revealed significantly reduced sulfate levels in treated samples compared to controls, indicating effective surface passivation. Moreover, low sulfate concentrations at pH 3 suggest slower AMD progression in highly acidic environments. SEM-EDS, FTIR and XRD analyses confirmed the formation of thin, compact passivation layers critical for halting oxidative processes. This microencapsulation approach minimizes reagent use, is potentially cost-effective, and enables solution recycling. This study underscores the potential of composite inorganic coatings as a sustainable and effective solution for AMD mitigation, paving the way for pilot trials and field studies.

References

Fan, R., et al. (2017). The formation of silicate-stabilized passivating layers on pyrite for reduced acid rock drainage. *Environmental*

Kefeni, K. K., et al. (2017). Acid mine drainage: Prevention, treatment options, and resource recovery: A review. *Journal of Cleaner Production*, *151*, 475-493.

Park, I., et al. (2019). A review of recent strategies for acid mine drainage prevention and mine tailings recycling. *Chemosphere*, *219*, 588-606.

Spatial and temporal (annual and decadal) trends of metal(loid) concentrations and loads in an AMD-affected river

E. Jennings[A,B*], P. Onnis[C], R. Crane[A,B], S.D.W. Comber[D], P. Byrne[E], A.L. Riley[F], W.M. Mayes[F], A.P. Jarvis[G], K.A. Hudson-Edwards[A,B]

[A]Camborne School of Mines, Department of Earth and Environmental Sciences, University of Exeter, Penryn TR10 9FE, UK

[B]Environment and Sustainability Institute, University of Exeter, Penryn TR10 9FE, UK

[C]Department of Chemical and Geological Sciences, University of Cagliari, Monserrato 09042, Italy

[D]School of Geography, Earth and Environmental Sciences, Plymouth University, Plymouth PL4 8AA, UK

[E]School of Biological and Environmental Sciences, Liverpool John Moores University, Liverpool L3 3AF, UK

[F]School of Environmental Sciences, University of Hull, Hull HU6 7RX, UK

[G]School of Engineering, Newcastle University, Newcastle upon Tyne NE1 7RU, UK

[*]Now at the WH Bryan Mining Geology Research Centre, Sustainable Minerals Institute, The University of Queensland, Brisbane, 4068, Australia. elin.jennings@uq.edu.au

1.0 Introduction

Acid and Metalliferous drainage (AMD) is a prevalent environmental problem resulting from the oxidation of sulfide minerals, such as pyrite, in mining-affected catchments (Akcil and Koldas, 2006; Crane and Sapsford, 2018). This process generates acidic waters enriched in sulfate, iron (Fe), and toxic metal(loid)s like arsenic (As), copper (Cu), and zinc (Zn), which pose ecological risks to river systems worldwide (Environment Agency, 2008; Nordstrom, Blowes and Ptacek, 2015). AMD treatment is challenging and expensive (Johnson and Hallberg, 2005; Akcil and Koldas, 2006). Estimates for total global AMD remediation cost are often in the order of US$100 bn, and as a result, AMD-affected rivers are frequently left untreated (Hudson-Edwards *et al.,* 2011; Lottermoser, 2015; Tremblay and Hogan, 2016). AMD-derived metal(loid)s accumulate in both the aqueous and sediment phases, posing spatial and temporal environmental hazards (Johnson and Thornton, 1987). River sediment-borne As, Cu, Zn and Fe, for example, can be remobilised due to both physical (e.g. enhanced erosion during a storm event) and/or geochemical processes (e.g. reductive dissolution of metal(loid)-bearing Fe (oxy)hydroxides) (Balistrieri *et al.*, 2007; Cánovas *et al.,* 2014; Lynch *et al.,* 2014).

Understanding the spatial and temporal dynamics of AMD-derived contaminants is essential for effective management and remediation. However, long-term and high-resolution monitoring data are often lacking, limiting insights into the seasonal and decadal variations of metal(loid) concentrations and loads in impacted rivers. This gap constrains the ability to predict contaminant behaviour under changing environmental conditions and to design targeted interventions.

The Carnon River in Cornwall, UK, represents a model AMD-affected system with a rich mining legacy documented since the Bronze Age (Embrey and Symes, 1987; Pirrie *et al.*, 2003; Rainbow, 2020). The Carnon River is 14 km long and drains a 31 km² catchment, discharging into the tidally affected Restronguet Creek (Environment Agency, 2020a, 2020b). The catchment's geology is underlain by silt and sandstones from the Mylor Slate Formation and hosts mineral veins rich in As-Cu-Fe-Pb-Zn sulfides, cassiterite (SnO_2) and wolframite ((Fe, Mn)WO_4) (Embrey and Symes, 1987; Pirrie *et al.*, 2002). It receives AMD inputs from multiple sources, including the heavily contaminated County Adit (input 2, 0.8 km), and has experienced episodic contamination events, such as the 1992 Wheal Jane Mine flooding (Pirrie *et al.*, 2002). Despite the Carnon River being investigated for many decades (e.g. Bryan and Gibbs, 1983; Pirrie *et al.*, 2003; Meyer *et al.,* 2019), a full understanding of the temporal and spatial

trends and sources of metal(loids) in the Carnon River has yet to be established. Additionally, discharge data have been recorded at very few sites along the river, and contaminant loads have been recorded only for Restronguet Creek and the County Adit (Mayes *et al.,* 2010, 2013). The limited discharge data means that source apportionment assessment is lacking, since mass input and export of metal(loid)s cannot be quantified by concentration data alone (Kimball *et al.*, 2002; Runkel *et al.*, 2018).

This study aims to address these knowledge gaps by investigating the temporal and spatial behaviour of several AMD-related metal(loid)s (As, Cu, Zn and Fe) along the Carnon River. This work combines the collection of instream concentration and discharge data collected over differing hydrological conditions and through monitoring data supplied by the Environment Agency (England) (EA) from 2000 to 2021. The outcomes of this study are intended to provide a fundamental mechanistic understanding of the dynamic behaviour and fate of these key AMD-generated metal(loid) contaminants within riverine systems as a function of changing hydrological conditions and time. Such detailed knowledge is essential for accurately informing river management policy in the future.

2.0 Methods and Materials

2.1 Water sampling, discharge measurement and geochemical analysis

Sampling was undertaken during four months (April, August, November 2021, and February 2022) representing low, medium, and high flow conditions based on the national river flow archive (NRFA) data. Twenty-one sites spanning main tributaries and AMD inputs were sampled, capturing both diffuse and point sources. The number of accessible sampling sites varied throughout the year, as some became either accessible or inaccessible due to seasonal or logistical constraints. During the sampling campaigns descriptions of water turbidity and embankment shape and colour data were collected. At each site (Figure 1), filtered (<0.45 µm) and unfiltered water samples were collected (n = 172) and acidified (5 M HNO_3) for laboratory analysis. In-situ measurements included pH, temperature, electrical conductivity (EC), and their coordinates. Discharge was measured at nine sites using the salt dilution gauging method, suitable for the river's morphology (Moore, 2004). Discharge from the County Adit was estimated by flow difference between upstream and downstream sites. For quality assurance, two sites (10 % of the sites) were selected randomly in each sampling campaign for field blanks and duplicates. Field blanks were used to assess potential atmospheric contamination and were made by exposing deionised water to environmental conditions at the site and prepared as aliquots of filtered and unfiltered samples. Field duplicates were taken to assess the precision of sampling and analysis.

Filtered aqueous samples were analysed for As, Cu, Zn by ICP-MS and Fe and sulfur (S) by ICP-OES. Unfiltered aqueous samples were analysed by ICP-OES. Certified reference materials for trace (QC1488_LRAC1572 Trace metals WS20mL) and major metal(loid)s (QC3041_LRAA8648 Mineral whole volume 500 mL) (1640a Trace metals in water) were analysed for data accuracy (calculated as co-efficient of variation), and duplicate and blank samples were analysed for precision and contamination.

The relationship between metal(loid) concentration (C) and discharge (Q) was analysed using the power-law model ($C = aQ^b$). Where a is a constant and b is the log-log slope. Statistical parameters distinguished chemostatic behaviour (concentration stable over discharge range (defined as slope b >±0.1 and CVC/CVQ is >0.5)) from chemodynamic (concentration varies with discharge (CVC/ CVQ < 0.5)) (Musolff *et al.*, 2015). Trends were defined as 'flushing' (concentration increases with discharge (slope b >0.1)) or 'dilution' (concentration decreases with discharge (slope b)) (Godsey *et al.,* 2009). Statistical analysis was performed using Origin Lab Pro (See Table 1 for p-values). Simple linear regression fits between discharge and concentration were completed to obtain the coefficient of variation (R^2). The standard error of the slope (Sb) was calculated to quantify the accuracy of the slope estimates based on the sample data.

2.2 Environment Agency Data Analysis

Historical water quality data (2000–2021) was supplied from the EA (Environment Agency, 2021) for As, Fe, Cu, and Zn at three sample points: upstream of the County Adit (50.234 N, − 5.139 W) (unaffected by the County Adit) (0.65 km), downstream of the confluence of the County Adit and the Carnon River (50.234 N, − 5.138 W) (directly affected by the County Adit) (0.94 km), and a downstream site which discharges into the estuary (50.214 N, − 5.10 W) (4.3 km) (Figure 1). Temporal trends were tested using the Mann-Kendall statistical method to identify significant changes over the two decades.

3.0 Results and Discussion

3.1 Annual and seasonal instream metal(loid) concentrations and loads, downstream trends, and sources in the Carnon River

During the sampling year, the Carnon River exhibited notable physical and geochemical changes influenced by seasonal hydrology and mining legacy inputs. Water clarity decreased downstream of the County Adit confluence due to abundant Fe (oxy)hydroxide (ochre) deposits, which accumulated on riverbanks and floodplains, especially near Bissoe (1.6 km) (Figure 2). These ochre deposits were observed periodically to be mobilised by rainfall and erosion, contributing to turbidity downstream.

In stream metal(loid) concentrations, pH and EC exhibited large ranges along the Carnon River (Table 2, Figure 3), supporting findings from earlier studies (Bryan and Gibbs, 1983; Environment Agency, 2021). EC increased markedly downstream of major AMD source; the County Adit (input 2, 0.8 km) and in addition the Wheal Jane Mine (input 4, 2.17 km), and EC reached elevated levels near the tidal estuary where seawater mixing occurred (Figure 3). Likewise, pH dropped downstream of the County Adit before rising toward the estuary (Figure 3). The concentrations of Cu and Zn increased after the County Adit input and generally increased or remained stable downstream, displaying chemodynamic (CV_C /CV_Q = 0.61–0.76) flushing (b = 0.57–0.79, R^2 = 0.03–0.1, S_b = $1.05E^{-04}$ -$3.88E^{-04}$) behaviour where concentrations rose with river discharge, likely reflecting erosion and remobilisation of metal-bearing Fe (oxy)hydroxide (ochre) deposits (Figure 3, 4, Table 1). In contrast, As, Fe and S concentrations tended to decrease downstream, suggesting precipitation of As-bearing Fe (oxy)hydroxides (Figure 3). Fluctuations in these concentrations downstream of this point may reflect dissolution, erosion and dispersion of these ochre (Figure 2B, D). Unfiltered and filtered Fe, S and As exhibited a chemodynamic (CV_C/CV_Q = 0.59–2.8) behaviour with very weak flushing (b = 0.04-0.30, R^2 = 0.002-0.41, S_b = $2.39E^{-05}$ -$6.10E^{-05}$) (Figure 4, Table 1). This suggests that although Fe, S and As concentrations vary with discharge, other factors may have more influence on their behaviour (Musolff *et al.*, 2015). These could include pH (Jarvis *et al.*, 2019), oxidation-reduction potential (ORP) (Lynch *et al.,* 2014), groundwater inflow and soil through flow (Byrne *et al.,* 2013).

The contribution of metal(loid) loads from the County Adit was substantial, with Cu, Zn, As, S and Fe loads increasing downstream of the confluence into the estuary and reaching peak unfiltered and filtered values of 742, 3,430, 354, 128,000 and 1,960 kg^{-1} month, respectively (Figure 5). These contaminants accumulate in sediments and floodplains, posing ongoing environmental risks through potential remobilisation during high flow events.

Seasonal patterns showed that metal(loid) concentrations and loads remained relatively consistent spatially but varied temporally, with peaks corresponding to low rainfall periods with limited dilution, as well as high rainfall events that enhanced flushing and sediment transport (Figure 3, 5). The highest contaminant loads were recorded in February, likely due to the high riverine discharge causing increased erosion of the river embankments (Figure 5). The highest metal(loid) concentrations were recorded in April 2021 (Figure 3), likely due to reduced rainfall in the sampling week that reduced dilution (Table 3), as observed in other AMD-affected catchments (e.g., Rio Odiel and Rio Tinto, Spain) (Braungardt *et al.*, 2003; Sarmiento *et al.*, 2009).

3.2 Decadal trends in metal(loid) concentrations

Long-term analysis of EA monitoring data from 2000 to 2021 revealed contrasting trends in metal(loid) behaviour. The upstream site (Twelveheads), which was not affected by AMD inputs exhibited minimal change (Figure 6). While at the County Adit confluence, Cu and Zn concentrations increased significantly (Mann Kendall (MK) 1220 to 2110, n 149, $p < 0.05$) over time while pH declined (MK -1766, n 149, $p < 0.05$) (Figure 6, Table 4). These trends differ from those in other AMD-affected systems, including the Afon Ystwyth (UK) (1919–2005) and Rookhope Burn (UK) (1977–2008) (Mayes *et al.,* 2010). The Carnon River's increasing Cu, Zn and acid generation over time could have been due to the continuous and perhaps increasing discharge of AMD from the County Adit and to a lack of buffering capacity in the underlying silts and sandstone (Embrey and Symes, 1987; Scrivener and Shepherd, 1998; Pirrie *et al.*, 2002). Conversely, As and Fe concentrations decreased (MK -2295 to 2932, n 149, $p < 0.001$), likely reflecting increased precipitation of As-bearing Fe (oxy) hydroxides from Fe (II) oxidation and hydrolysis (Dold, 2014) of the County Adit AMD over the 20 years of data collection (Figure 6, Table 4). Downstream at the estuary, As, Fe, and pH showed significant (MK 2892 to 8783, n 357, $p < 0.001$) increases over two decades, whereas Cu and Zn concentrations decreased (MK -18,078 to 21,028, n 357, $p < 0.001$), possibly due to sorption or ion exchange of Cu and Zn as a response to increased pH with time (Figure 6, 7, Table 4) (Dzombak and Francois, 1990; Wołowiec *et al.*, 2019).

4.0 Conclusions

This study has highlighted the importance of using both contemporary and historical data to investigate metal(loid) behaviour within an AMD-affected river catchment, considering spatial and temporal variability over the course of one year and across two decades. The annual (2021–2022) and decadal (+20 years) trends in metal(loid) concentrations, pH, and electrical conductivity from the Carnon River demonstrate that legacy underground mining adits continue to discharge contaminant metal(loid)s even decades after mining ceased. Over the 20-year study, metal(loid) concentrations changed significantly downstream toward the estuary, with Cu and Zn showing a slight downward trend, while As and Fe exhibited a slight increase. These trends may be attributed to the erosion and dissolution of As-bearing Fe (oxy)hydroxides, and the sorption or ion exchange of Cu and Zn. Such processes could be responding to increased pH over time. Metal(loid) loadings measured throughout the year increased downstream of the AMD input County Adit, with maximum loads recorded at 742 (Cu), 3,430 (Zn), 354 (As), 128,000 (S) and 1,960 (Fe) kg^{-1} month discharging into the estuary. The concentrations of As, Cu, Fe, S, and Zn exhibited chemodynamic and flushing behaviours, suggesting susceptibility to changes in river discharge and mobilisation from historically contaminated riverine sediments. However, Fe, S, and As showed only weak flushing behaviour, indicating that other factors such as pH, ORP, groundwater inflow, and soil throughflow may be more critical in controlling their behaviour.

This research reaffirms previous findings identifying the County Adit as a primary source of metal(loid) contamination in the Carnon River. Importantly, it also emphasises the role of diffuse sources contributing to metal(loid) loads in both the river and coastal zones, sources which may have been overlooked in other AMD-affected catchments. Overall, the study illustrates the necessity of sustained monitoring in AMD-affected rivers due to their highly variable behaviour in space and time, and their capacity to contaminate fluvial and coastal environments for decades or even centuries after mining activity has ceased. A multifaceted approach combining comprehensive water sampling that accounts for river discharge variability alongside historical trend data is essential to developing an understanding of the behaviour of these systems. Such knowledge is crucial for designing effective remediation strategies and anticipating how AMD-affected rivers might respond to future climate change impacts. Further details of the results and methods are discussed in Jennings *et al.,* 2025.

References

Akcil, A. and Koldas, S. (2006) 'Acid Mine Drainage (AMD): causes, treatment and case studies', *Journal of Cleaner Production*, 14(12–13), pp. 1139–1145. Available at: https://doi.org/10.1016/J.JCLEPRO.2004.09.006.

Balistrieri, L.S. *et al.* (2007) 'Assessing the concentration, speciation, and toxicity of dissolved metals during mixing of acid-mine drainage and ambient river water downstream of the Elizabeth Copper Mine, Vermont, USA', *Applied Geochemistry*, 22(5), pp. 930–952. Available at: https://doi.org/10.1016/J.APGEOCHEM.2007.02.005.

Braungardt, C.B. *et al.* (2003) 'Metal geochemistry in a mine-polluted estuarine system in Spain', *Applied Geochemistry*, 18(11), pp. 1757–1771. Available at: https://doi.org/10.1016/S0883-2927(03)00079-9.

Bryan, G. and Gibbs, P. (1983) 'Heavy metals in the Fal estuary, Cornwall: A study of long term contamination by mining waste and its effects on estuarine organisms.', *Marine Biological Association* [Preprint]. Available at: http://plymsea.ac.uk/275/ (Accessed: 17 February 2021).

Byrne, P., Reid, I. and Wood, P.J. (2013) 'Stormflow hydrochemistry of a river draining an abandoned metal mine: the Afon Twymyn, central Wales', *Environmental Monitoring and Assessment*, 185(3), pp. 2817–2832. Available at: https://doi.org/10.1007/s10661-012-2751-5.

Cánovas, C.R., Olías, M. and Nieto, J.M. (2014) 'Metal(loid) attenuation processes in an extremely acidic river: The rio tinto (sw spain)', *Water, Air, and Soil Pollution*, 225(1), pp. 1–16. Available at: https://doi.org/10.1007/S11270-013-1795-7/FIGURES/8.

Crane, R.A. and Sapsford, D.J. (2018) 'Selective formation of copper nanoparticles from acid mine drainage using nanoscale zerovalent iron particles', *Journal of Hazardous Materials*, 347, pp. 252–265. Available at: https://doi.org/10.1016/j.jhazmat.2017.12.014.

Dold, B. (2014) 'Evolution of Acid Mine Drainage Formation in Sulphidic Mine Tailings', *Minerals*, 4(3), pp. 621–641. Available at: https://doi.org/10.3390/min4030621.

Dzombak, D.A. and Francois, M.M. (1990) *Surface complexation modeling: hydrous ferric oxide*. John Wiley and Sons.

Embrey P.G and Symes R.F. (1987) *Minerals of Cornwall and Devon.*, *Minerals of Cornwall and Devon* . Tuscon, Arizona.: London: British Museum Natural History and the Mineralogical Record Inc. Available at: https://encore.exeter.ac.uk/iii/encore/plus/C__S Minerals of Cornwall and Devon embrey and symes__Orightresult__U__X0?lang=eng&link=https%3A%2F%2Fuoelibrary.idm.oclc.org%2Flogin%3Furl%3Dhttp%3A%2F%2Fsearch.ebscohost.com%2Flogin.aspx%3Fdirect%3Dtrue%26site%3Deds-live%26db%3Dcat07716a%26AN%3Dpclc.99697763405136&suite=cobalt (Accessed: 19 November 2020).

Environment Agency (2008) 'Abandoned mines and the water environment', *Environment Agency Science Report SC030136/SR41* [Preprint].

Environment Agency (2020a) *Lower River Carnon, Catchment Data Explorer*. Available at: https://environment.data.gov.uk/catchment-planning/WaterBody/GB108048001231 (Accessed: 15 March 2021).

Environment Agency (2020b) *Upper Carnon River, Catchment Data Explorer*. Available at: https://environment.data.gov.uk/catchment-planning/WaterBody/GB108048001160 (Accessed: 15 March 2021).

Environment Agency (2021) *Open WIMS data*. Available at: https://environment.data.gov.uk/water-quality/view/download (Accessed: 7 December 2022).

Godsey, S.E., Kirchner, J.W. and Clow, D.W. (2009) 'Concentration-discharge relationships reflect chemostatic characteristics of US catchments', *Hydrological Processes*, 23(13), pp. 1844–1864. Available at: https://doi.org/10.1002/hyp.7315.

Hudson-Edwards, K., Jamieson, H.E. and Lottermoser, B.G. (2011) 'Mine Wastes: Past, Present, Future', *Elements*, 7(6), pp. 375–380. Available at: https://vle.exeter.ac.uk/pluginfile.php/2418807/mod_resource/content/1/Hudson-Edwards et al 2011 Elements.pdf (Accessed: 6 January 2021).

Jarvis, A.P., Jane E. Davis, Patrick H. A. Orme, Hugh A. B. Potter and Catherine J. Gandy(2019) 'Predicting the Benefits of Mine Water Treatment under Varying Hydrological Conditions using a Synoptic Mass Balance Approach', *Environmental Science and Technology*, 53(2), pp. 702–709. Available at: https://doi.org/10.1021/ACS.EST.8B06047/ASSET/IMAGES/LARGE/ES-2018-06047C_0005.JPEG.

Jennings, E., Onnis, P., Crane, R., Comber, S.D., Byrne, P., Riley, A.L., Mayes, W.M., Jarvis, A.P. and Hudson-Edwards, K.A., 2025. Spatial and temporal (annual and decadal) trends of metal (loid) concentrations and loads in an acid mine drainage-affected river. *Science of the Total Environment*, *964*, p.178496.

Johnson, C.A. and Thornton, I. (1987) 'Hydrological and chemical factors controlling the concentrations of Fe, Cu, Zn and As in a river system contaminated by acid mine drainage', *Water Research*, 21(3), pp. 359–365. Available at: https://doi.org/10.1016/0043-1354(87)90216-8.

Johnson, D.B. and Hallberg, K.B. (2005) 'Acid mine drainage remediation options: a review', *Science of The Total Environment*, 338(1–2), pp. 3–14. Available at: https://doi.org/10.1016/J.SCITOTENV.2004.09.002.

Kimball, B.A., R.L. Runkel, K. Walton-Day, and K.E. Bencala (2002) 'Assessment of metal loads in watersheds affected by acid mine drainage by using tracer injection and synoptic sampling: Cement Creek, Colorado, USA', *Applied Geochemistry*, 17(9), pp. 1183–1207. Available at: https://doi.org/10.1016/S0883-2927(02)00017-3.

Lottermoser, B.G. (2015) 'Predicting acid mine drainage: past, present, future', *Mining Report* [Preprint].

Lynch, S.F.L., Batty, L.C. and Byrne, P. (2014) 'Environmental Risk of Metal Mining Contaminated River Bank Sediment at Redox-Transitional Zones', *Minerals 2014, Vol. 4, Pages 52-73*, 4(1), pp. 52–73. Available at: https://doi.org/10.3390/MIN4010052.

Mayes, W.M., Potter, H.A.B. and Jarvis, A.P. (2010) 'Inventory of aquatic contaminant flux arising from historical metal mining in England and Wales', *Science of the Total Environment*, 408(17), pp. 3576–3583. Available at: https://doi.org/10.1016/j.scitotenv.2010.04.021.

Mayes, W.M., Potter, H.A.B. and Jarvis, A.P. (2013) 'Riverine flux of metals from historically mined orefields in england and wales', *Water, Air, and Soil Pollution*, 224(2), pp. 1–14. Available at: https://doi.org/10.1007/S11270-012-1425-9/TABLES/5.

Meyer, N., Borg, G. and Kamradt, A. (2019) 'Mineralogical and geochemical aspects of vein-type ores from the Carnon River Mining District, Cornwall'. Available at: https://www.researchgate.net/publication/336461775 (Accessed: 23 August 2022).

Moore, D. (2004) *Introduction to salt dilution gauging for streamflow measurement: Part 1*. Available at: https://www.researchgate.net/publication/228822476_Introduction_to_salt_dilution_gauging_for_streamflow_measurement_Part_1 (Accessed: 18 November 2020).

Musolff, A., C. Schmidt, B. Selle, and J.H. Fleckenstein (2015) 'Catchment controls on solute export', *Advances in Water Resources*, 86, pp. 133–146. Available at: https://doi.org/10.1016/j.advwatres.2015.09.026.

Nordstrom, D.K., Blowes, D.W. and Ptacek, C.J. (2015) 'Hydrogeochemistry and microbiology of mine drainage: An update', *Applied Geochemistry*, 57, pp. 3–16. Available at: https://doi.org/10.1016/J.APGEOCHEM.2015.02.008.

Pirrie, D. *et al.* (2002) *Mapping and visualisation of historical mining contamination in the Fal Estuary, Cornwall*, *Camborne school of Mines*. Available at: https://projects.exeter.ac.uk/geomincentre/estuary/home.htm (Accessed: 11 March 2021).

Pirrie, D., M.R. Power, G. Rollinson, G.S. Camm, S.H. Hughes, A.R. Butcher, and P. Hughes *(2003) 'The spatial distribution and source of arsenic, copper, tin and zinc within the surface sediments of the Fal Estuary, Cornwall, UK', Sedimentology*, 50(3), pp. 579–595. Available at: https://doi.org/10.1046/j.1365-3091.2003.00566.x.

Rainbow, P.S. (2020) 'Mining-contaminated estuaries of Cornwall - Field research laboratories for trace metal ecotoxicology', *Journal of the Marine Biological Association of the United Kingdom*. Cambridge University Press, pp. 195–210. Available at: https://doi.org/10.1017/S002531541900122X.

Runkel, R.L., Verplanck, P.L., Kimball, B.A. and Walton-Day, K. (2018) 'Cinnamon Gulch revisited: Another look at separating natural and mining-impacted contributions to instream metal load', *Applied Geochemistry*, 95, pp. 206–217. Available at: https://doi.org/10.1016/j.apgeochem.2018.04.010.

Sarmiento, A.M., Nieto, J.M., Olías, M. and Cánovas, C.R., (2009) 'Hydrochemical characteristics and seasonal influence on the pollution by acid mine drainage in the Odiel river Basin (SW Spain)', *Applied Geochemistry*, 24(4), pp. 697–714. Available at: https://doi.org/10.1016/j.apgeochem.2008.12.025.

Scrivener, R.C. and Shepherd, T.J. (1998) 'Mineralisation', in E.M. Selwood (ed.) *The geology of Cornwall*. Exeter: University of Exeter press, pp. 136–157.

Tremblay, G. and Hogan, C. (2016) 'Mine environment neutral drainage (MEND) manual 5.4. 2d: prevention and control', *Canada Centre for Mineral and Energy Technology, Natural Resources, Canada, Ottawa.*, (5.4. 2d), pp. 1–23.

Wołowiec, M., Komorowska-Kaufman, M., Pruss, A., Rzepa, G. and Bajda, T., (2019) 'Removal of Heavy Metals and Metalloids from Water Using Drinking Water Treatment Residuals as Adsorbents: A Review', *Minerals*, 9(8), p. 487. Available at: https://doi.org/10.3390/min9080487.

Figures

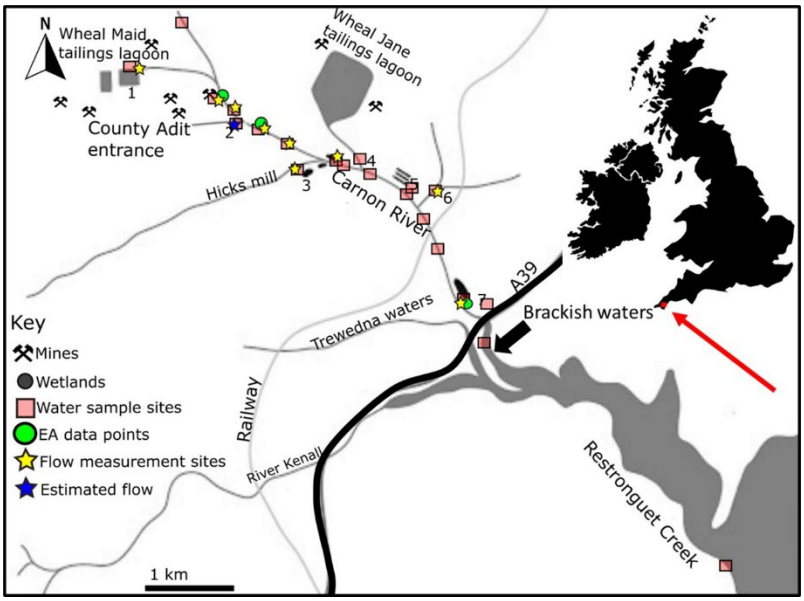

Fig. 1. **Location of the Carnon River and Restronguet Creek sample sites used in this study. Sample locations from the Environment Agency are indicated as circles. For this study, squares stars represent water samples and flow measurements. EA data points are monitoring sites. Numbered inputs refer to adit inputs and tributaries of the Carnon River. Input 1 – Wheal Maid sites. Input 2 – County Adit (Wellington and Nangiles Adit) (discharge estimate taken) Input 3 – Hicks Mill (historic As calciner) (discharge measured) Input 4 – Wheal Jane Adit (no discharge measured) Input – 5 Potential Adit (no discharge measured) Input 6 – Grenna Lane Bridge (discharge measured) Input 7 – Downstream Devoran Bridge wetland (no discharge measured). Downstream of the A39 road is the fresh- and seawater mixing zone (4.6 km).**

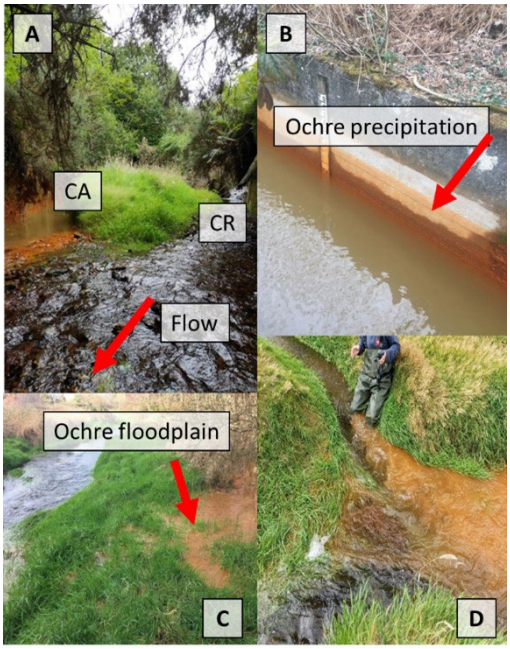

Fig. 2. **Photographs of the Carnon River and County Adit taken between April 2021 and February 2022. (A) The confluence of the County Adit (CA) and Carnon River (CR); (B) Iron (oxy)hydroxide (ochre) precipitation on the culvert wall downstream of the confluence of the CR and CA; (C) Iron (oxy)hydroxide (ochre) rich floodplain; (D) Physical release of floodplain Fe (oxy)hydroxides (ochres) downstream of Bissoe (1.6 km) by agitation.**

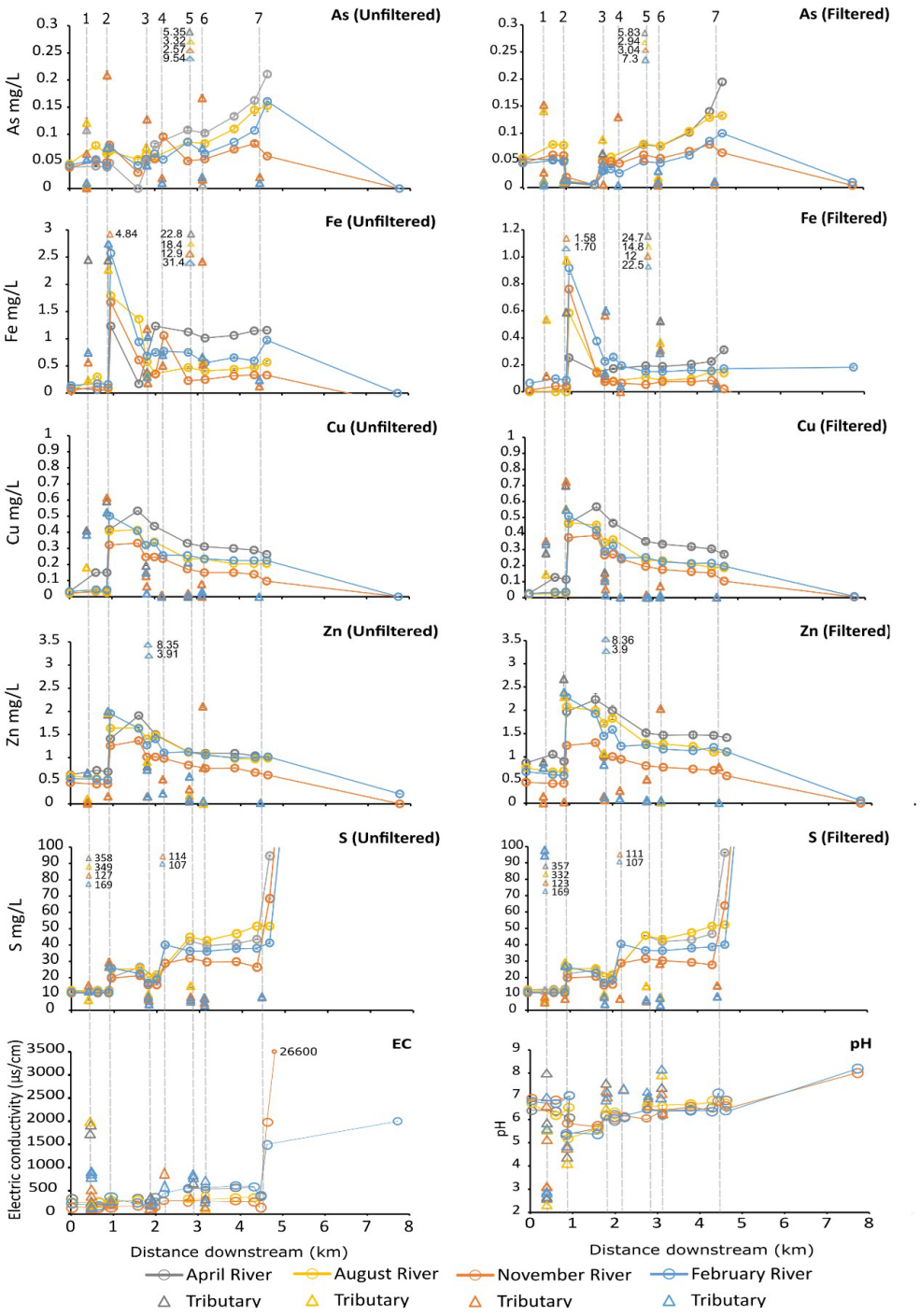

Fig. 3. **Filtered (<0.45 µm suspended particulate and dissolved phases) and unfiltered (suspended particulate (>0.45 µm) and dissolved phases) metal(loid) concentrations and water parameters (pH and EC) vs distance downstream in April, August, November (2021) and February (2022). Locations of numbered incoming tributary sites (numbered vertical lines in Figure 1) are as follows: input 1 is Wheal Maid (0.4 km), input 2 is the County Adit (0.88 km), input 3 is Hicks Mill stream (1.8 km), input 4 is Wheal Jane (2.17 km), input 5 is potential adit (2.79 km), input 6 is Grenna Lane Bridge tributary (3.12 km) and input 7 is the Devoran Bridge wetland (4.64 km)). 0 km is an unaffected site upstream of the County Adit – Carnon River**

confluence. Input 1 has been marked as 0.4 km to avoid confusion with the County Adit distance and placed in the correct position in the Carnon River.

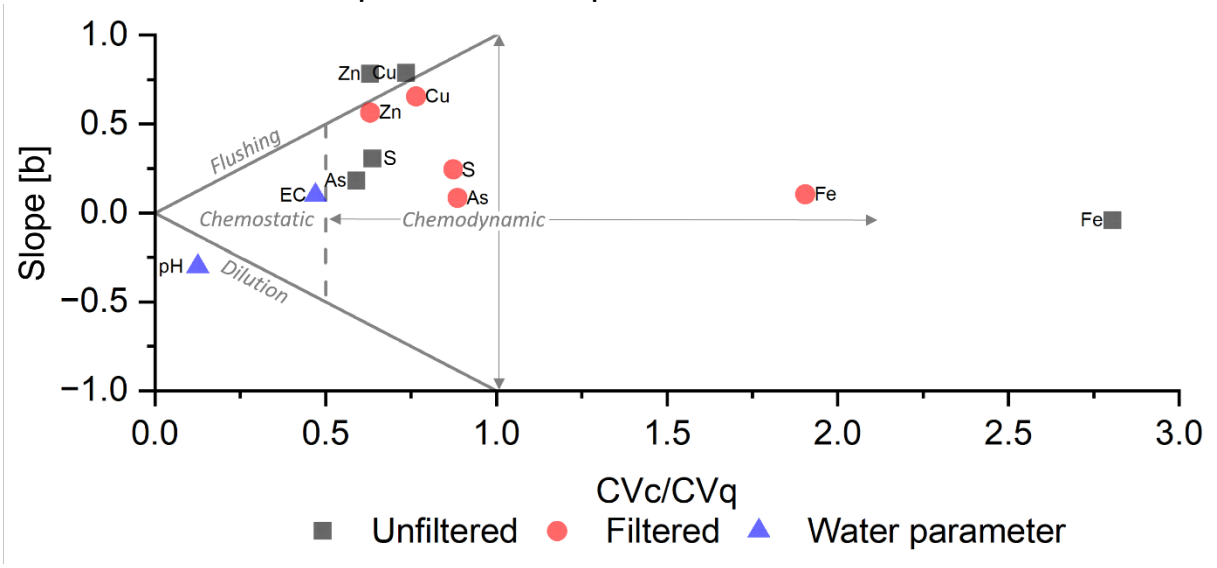

Fig. 4. **Power law relation (slope [b]) vs coefficient of variation of concentration divided by the coefficient of variation of discharge (CVC/CVQ). The dashed line shows the definition between chemostatic and chemodynamic behaviour. The 0 to +1 line defines the 'flushing' trend. The 0 to -1 line defines the 'dilution' trend.**

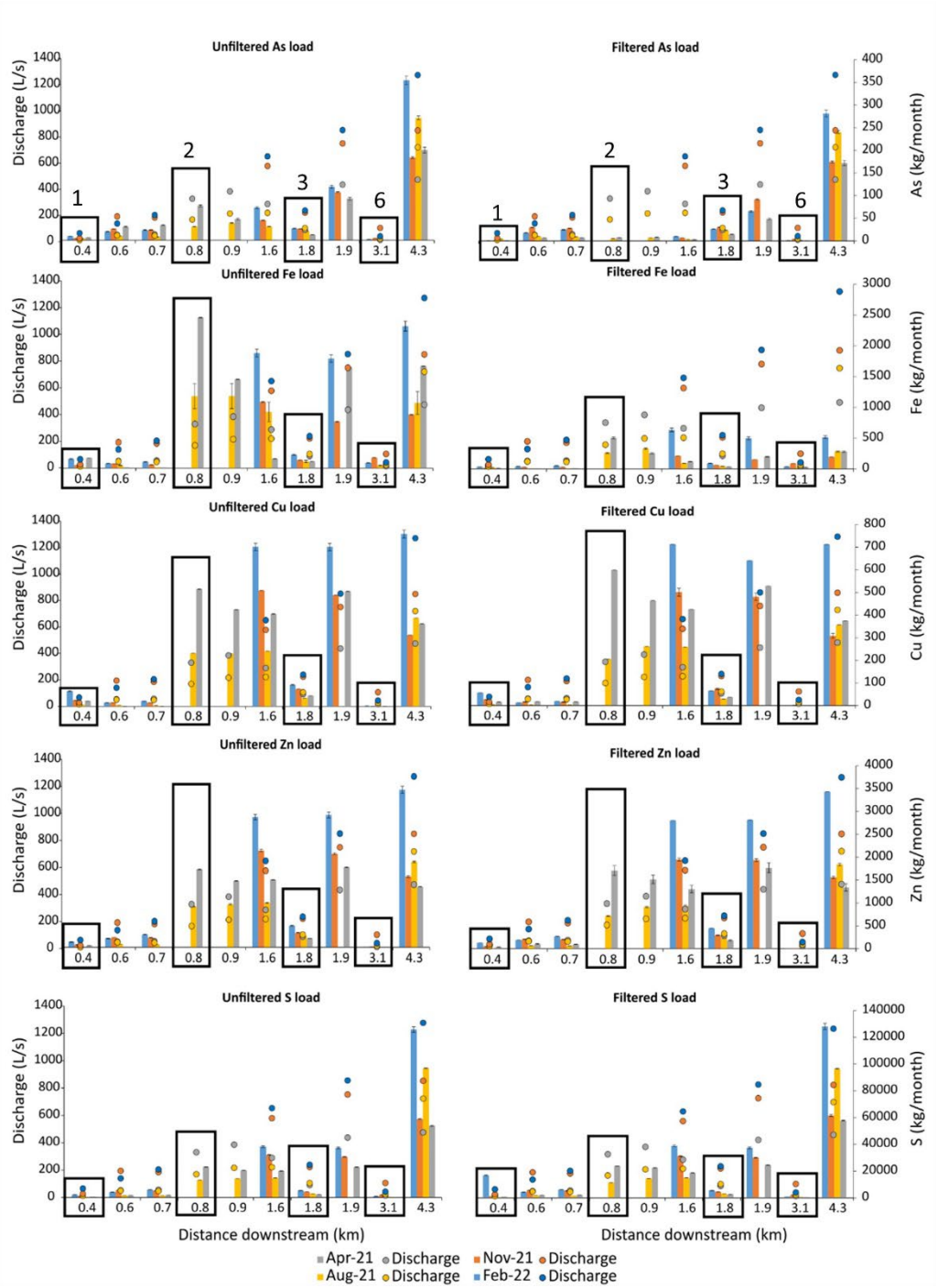

Fig. 5. **Unfiltered (comprising suspended particulate and the dissolved phases) and filtered (comprising <0.45 µm suspended particulate and dissolved phases) metal(loid) loads vs distance downstream between April, August, November (2021) and February (2022). Discharge values are shown as circular symbols. Rectangular boxes highlight tributary and adit inputs (Figure 1). Input 1 (Wheal Maid) has been marked as 0.4 km to avoid confusion with the County Adit distance and placed in the correct entry part of the Carnon River (0.8**

km). Input 2 represents the County Adit site (0.8 km). 0 km is an unaffected site upstream of the County Adit. Input 3 is Hicks Mill (1.8 km). Input 6 is the Grenna Lane Bridge tributary (3.1 km).

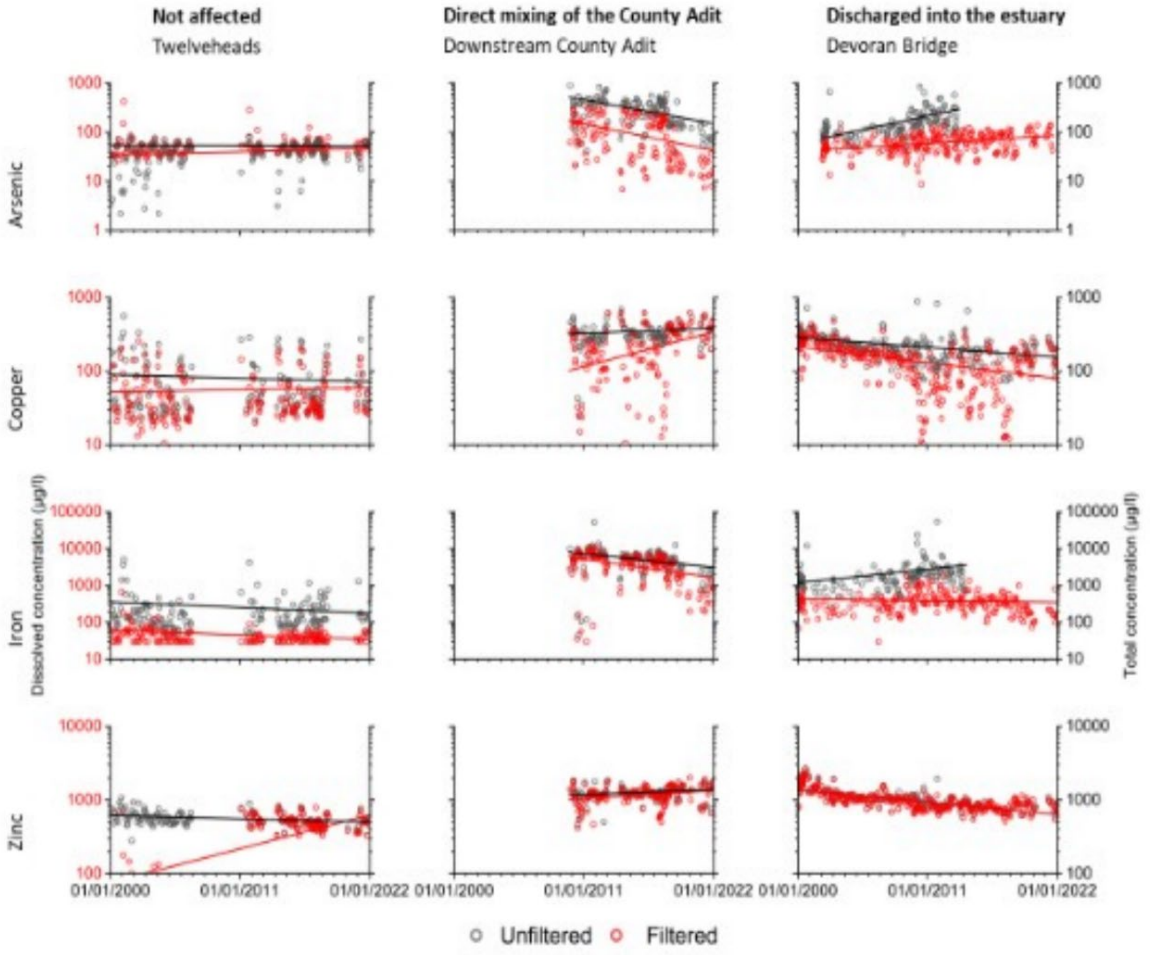

Fig. 6. **Unfiltered (black) (comprising suspended particulate and the dissolved phases) and filtered (red) (comprising <0.45 µm suspended particulate and dissolved phases) As, Cu, Fe and Zn concentrations between 01/01/2000 and 02/12/2021 at Twelveheads, Confluence of the County Adit (CA) and Carnon River (CR), and Devoran Bridge in the Carnon River (green circles on Figure 1). Data from Environment Agency monitoring sites (Environment Agency, 2021). Lines are linear curve fits extracted using Origin Lab Pro.**

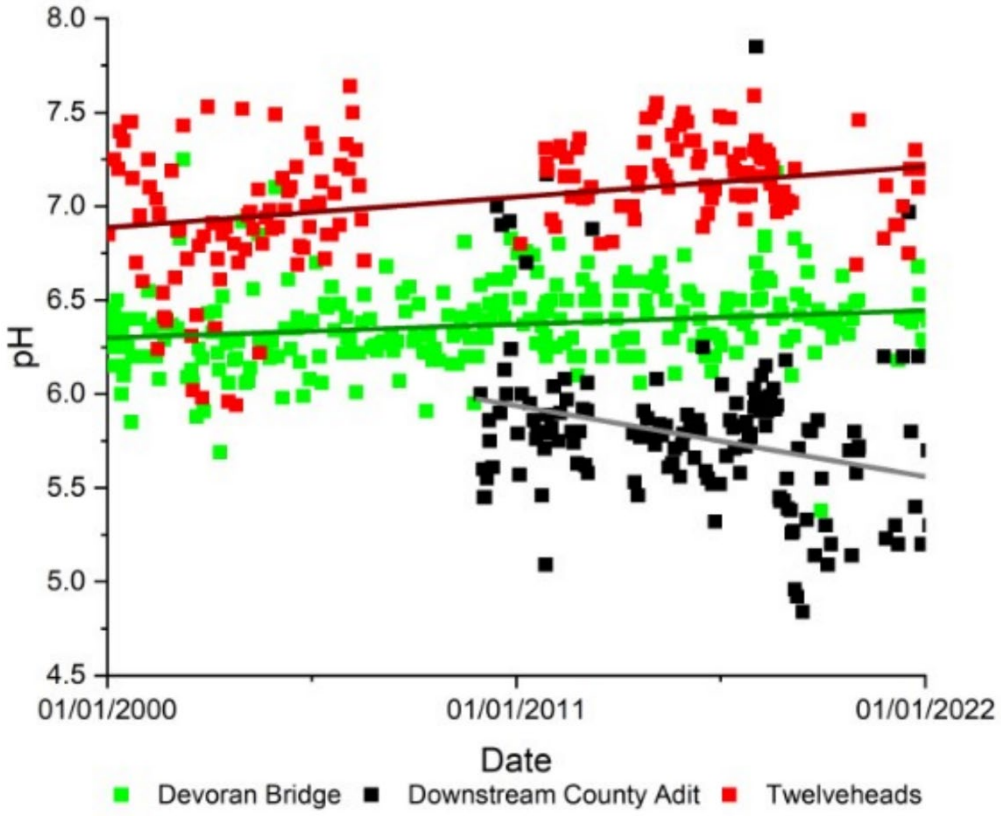

Fig. 7. **pH data collected between 01/01/2000 and 02/12/2021 at Twelveheads, immediately downstream of the County Adit – Carnon River confluence and Devoran Bridge in the Carnon River (green circles in Figure 1). Data from Environment Agency monitoring stations (Environment Agency, 2021).**

Tables

Table 1. **Coefficients of variation of metal(loid) concentrations (CVC) divided by the coefficients of variation for river discharge (CVQ), concentration-discharge power law slopes (b), coefficients of determination (R^2) and standard errors (Sb)**

Parameter	CV_C / CV_Q	Slope [b]	R^2	S_b	p-value
pH	0.125	-0.301	-0.012	4.45E-04	0.491
EC	0.468	0.099	0.111	0.067	0.029
Unfiltered					
As	0.587	0.184	0.023	2.39E-05	0.192
Cu	0.733	0.789	0.031	1.05E-04	0.415
Fe	2.792	-0.039	-0.002	0.003	0.343
Zn	0.628	0.784	0.105	3.27E-04	0.037
S	0.651	0.303	0.406	0.005	2.65E-05
Filtered					
As	0.882	0.085	0.002	0	0.296
Cu	0.761	0.656	0.065	1.06E-04	0.088
Fe	1.897	0.106	0.002	6.10E-04	0.309
Zn	0.612	0.565	0.074	3.88E-04	0.073
S	0.863	0.270	0.064	0.009	0.079

Table 2. **Unfiltered and filtered (<0.45 µm) concentrations of As, Cu, Fe, and Zn in the Carnon River from this study and earlier works. All concentrations are in mg/L.**

	Bryan and Gibbs (1983) (n = 3)		Environment Agency (2021) (2000-2021) (n = 695)		This study (n = 172)	
	Unfiltered	Filtered	Unfiltered	Filtered	Unfiltered	Filtered
As	0.03-0.2	0.031-0.082	0.01-0.67	0.01-0.15	≤0.0004-0.21	0.004-0.2
Cu	0.053-0.68	0.054-0.68	0.03-1.17	0.03-1.17	0.02-0.53	0.02-0.6
Fe	0.137-25	0.05-18.5	0.08-13	0.03-4.9	0.05-2.6	<0.003-0.9
Zn	0.93-12	0.95-12	0.29-3.4	0.78-2.6	0.42-1.95	0.4-2.2

Table 3. **Rainfall recordings during the water sampling campaign from April 2021 to February 2022 were from UKCEH et al. (2022).**

Sampling month	The week of (mm)	The week before (mm)	Average (mm)
April 2021 (27-30th)	5.1-8.6	2.8	8.6
August 2021 (16-18th)	38.6-38.8	37.9-38.6	42.3
November 2021 (9-12th)	18.6-25	11.1-17	68.3
February 2022 (1-3rd)	0.4-5	83.4-87.2	116.2

Table 4. **Mann Kendall (MK) results between contaminants/pH with increasing time. CA is the County Adit. CR is the Carnon River. n.r. = not recorded**

Response variable	Twelveheads (n=187)		The confluence of CA and CR (n=149)		Devoran Bridge (n=357)	
	MK Statistic	p-value (two-sided)	MK Statistic	p-value (two-sided)	MK Statistic	p-value (two-sided)
As unfiltered	2216	0.0046*	-2255	<0.001**	4083	<0.001**
As <0.45 µm	2170	0.0051*	-2672	<0.001**	5606	<0.001**
Cu unfiltered	-224	0.7744	1357	0.0107*	-12871	<0.001**
Cu <0.45 µm	636	0.4197	2110	<0.001**	-15929	<0.001**
Fe unfiltered	-576	0.4456	-2295	<0.001**	2892	<0.001**
Fe <0.45 µm	-1985	0.0077*	-2932	<0.001**	-1634	0.1613
Zn unfiltered	-4453	<0.001**	1220	0.0217*	-18078	<0.001**
Zn <0.45 µm	-1174	<0.001**	1417	0.0099*	-21028	<0.001**
pH	3482	<0.001**	-1766	0.0011*	8783	<0.001**
Cl unfiltered	1445	0.0381*	676	0.0322*	3815	0.0101*
Temperature	-68	0.9335	-271	0.4953	1579	0.3106
EC	-993	0.0020*	-1094	0.0059*	-608	0.4085
Discharge	686489	<0.001**	298217	0.0035*	n.r.	n.r.

Acid and metalliferous drainage prediction for cold and dry climates at two scales

S. Palomino-Ore, M. Edraki, and W. Zhang
Sustainable Minerals Institute, The University of Queensland, St Lucia, QLD 4072, Australia.
s.palominoore@uq.edu.au

1.0 INTRODUCTION

Accurate prediction of acid and metalliferous (AMD) generation is complicated by the need to upscale results from small-scale laboratory tests to field conditions (Morin & Hutt, 2001). Laboratory tests are conducted under controlled environments that often accelerate weathering and sulfide oxidation, whereas field conditions are characterised by heterogeneous waste rock, variable water infiltration, gas flow, and fluctuating temperatures (Morin & Hutt, 1997). Methodological limitations, such as the inability to account for spatial heterogeneity, dynamic hydrological processes, and extended temporal scales, undermine the reliability of AMD predictions. For example, previous studies (Vriens et al., 2019) in cold climates such as Alaska and Peru revealed that leaching occurs primarily during warming periods, rather than continuously as laboratory models suggest. In arid regions like northern Chile, episodic leaching and evaporation-driven suppression of drainage contradict steady-state laboratory assumptions (Tapia et al., 2018). Reliable AMD prediction requires integrated approaches that combine laboratory testing with site-specific field trials, adaptive monitoring, and waste classification schemes that consider both physical and chemical parameters. This project explores how upscaling laboratory-derived data from bench-top kinetic leaching columns to a mesoscale can improve understanding and prediction of AMD risk in waste rock dumps located in cold and dry climates.

2.0 METHODOLOGY

2.1 Site description

The mine experiences extreme continental climate with cold winters and hot summers. Summer brings 102 mm precipitation versus 5 mm in winter, with 70% of annual rainfall occurring in just 18 days, creating intense runoff events that complicate contaminant management. The mine supplied 4,000 kg of waste material (augite basalt and quartz monzodiorite) from a dump classified as 33% PAF risk, containing pyrite and chalcopyrite.

The methodology involves modifying standard kinetic lab tests to incorporate factors like temperature, precipitation, and oxygen availability. The experiments include columns with 8 kg of material and Intermediate Bulk Containers (IBC) containers with 1,582 and 1515 kg of waste rock to simulate field-scale processes using two distinct material groups: highly reactive and less reactive waste materials respectively. Each group was tested at two different particle sizes (less than 16 mm and less than 4 mm), each of them with a duplicate, to evaluate temporal behavior patterns (Table 1). The experiments are conducted in a temperature-controlled room to mimic field temperature conditions and water irrigation variation per climatic season; these values were quantified using real in situ weather data.

Geochemical characterization was performed to assess environmental risks such as Acid Mine Drainage (AMD) and trace element release. Techniques including Acid-Base Accounting (ABA), pH paste testing, and mineralogical analyses (XRD, XRF) were used to evaluate the acid-generating and neutralizing potential of the materials. The methodology is summarized in Figure 1.

2.3 Scaling-up experiments

Scaling-up experiments used columns and IBC containers (Figure 2) to simulate field conditions and predict long-term mine waste geochemical behavior. Columns tested two particle sizes (<16mm and <4mm) in twin replicates to assess their influence on leachate quality and acid generation. IBC containers replicated field-scale water flow and weathering processes for better AMD risk prediction.

All experiments were instrumented with sensors monitoring electrical conductivity, temperature, oxygen, and water saturation in real-time, enabling precise tracking of factors influencing leachate quality and mineral weathering.

Precipitation was scaled to match exposed surface areas, reflecting natural rainfall patterns. Time was accelerated: each week simulates three months (one year per month), enabling faster observation of long-term geochemical behavior and AMD risks.

3.0 RESULTS AND DISCUSSION

3.1 Mineralogy and chemical composition

Two rock types were identified: augite basalt (dominated by plagioclase, chlorite, hornblende, pyroxene; minimal quartz at 0.51%) and quartz monzodiorite (up to 45.94% quartz, illite/mica, pyrite 4-15%). Pyrite in quartz monzodiorite is the key acidity producer. Carbonates are minimal in both types. Both samples classify as intermediate acidity based on SiO_2, MgO, and CaO content. Augite basalt is more basic due to higher MgO and CaO (Figure 3) and shows higher Cu concentrations despite lower sulfur (~1%), while quartz monzodiorite contains higher sulfur due to pyrite content.

3.2 AMD Potential

In the acid generation capacity graph (Figure 4), the quartz monzodiorite samples are potentially acid forming, in contrast to the augite basalt samples. When selecting the samples to fill the IBCs, these two groups were considered: IBC-1 for the more reactive material and IBC-2 for the less reactive material.

3.3 Particle size distribution

The particle size distribution analysis of the samples revealed notable differences between the materials (Figure 5). Less reactive material was found to have the largest particle sizes, indicating coarser material composition. In contrast, most reactive material exhibited a much finer particle size distribution, suggesting a greater proportion of smaller particles within this sample. These variations in particle size can influence water movement, geochemical reactions, and the overall behavior of the materials during the experiments. The particle size for P80 is 36 mm. Two sizes were selected for the columns, size below 16mm and below 4 mm.

3.4 Sensors results

The sensors provide real-time data replicating experimental conditions. In IBC-1 (most reactive material,Figure 6), electrical conductivity increased with depth, indicating water accumulation where water and oxygen availability enhance geochemical reactions. Saturation levels consistently exceeded 0.2, confirming stored water's influence on geochemical behavior. Columns showed more pronounced saturation changes than IBCs, making them more sensitive for observing water distribution variations.

Reactive material columns exhibited distinct behaviors: C1 (<16mm) showed rapid surface flow (0.1 m^3/m^3) with accumulation at 25cm depth (0.35 m^3/m^3), while C2 (<4mm) maintained uniform water content at both depths. Less reactive columns differed - C5 (<16mm) retained more water at depth (~0.4 m^3/m^3) than surface (0.2 m^3/m^3), while C6 (<4mm) maintained consistent storage (~0.3 m^3/m^3) throughout. Smaller particle sizes promoted more uniform water distribution regardless of reactivity.

3.5 Hydrochemistry

This item examines the hydrogeochemical response of the two material types and two scales through three experimental configurations:

3.5.1 Experimental Setup 1: Precipitation vs Net Infiltration Effects

This experiment evaluated water input control on oxygen availability and acid generation: four months (July-October 2024) at 100 mm precipitation, then eight months (November 2024-June 2025) at 46 mm infiltration. Drainage valves remained closed except for monthly sampling.
Reducing irrigation demonstrated oxygen availability as the primary acid generation control. Coarse material (≤16 mm) liberated pore spaces, enabling oxygen infiltration and severe acidification (pH ~2). Fine material (≤4 mm) maintained stability through water retention, limiting oxygen penetration (Figure 7).

Water conditions reversed reactivity patterns. Under saturation (100 mm), fine particles showed higher conductivity, sulfate, and metals due to longer residence times and surface area. Under limited water (46 mm), coarse materials became most reactive with highest values, while fine materials showed lowest—reflecting oxygen infiltration through larger pores creating oxidation zones. Reactive materials: columns acidified (pH 3→2), IBCs stayed near-neutral (pH 7→6) due to preferential flow. Less reactive materials showed minimal response, maintaining stability from lower sulfide content and rapid drainage.

3.5.2 Experimental Setup 2: Closed vs Free Drainage Flow Regimes

This configuration assessed how drainage conditions influence oxidation processes through 12 months of closed drainage (July 2024-June 2025) with monthly valve opening, followed by six months of continuous free drainage (July-December 2025) under variable climatic conditions.
The transition to free drainage resulted in substantial increases in oxidation-reduction potential from 400 mV to 600 mV in columns and from 100 mV to 400 mV in IBCs. Moisture content decreased from 0.35 to 0.23 in column middle sections, while both sulfate concentrations and electrical conductivity showed increasing trends despite pH stabilization (Figure 8 and Figure 9).

Scale-dependent responses were evident between systems. Columns maintained consistently acidic pH throughout the experiment, reflecting homogeneous water-rock interaction. IBCs showed slight pH increases over time, attributed to preferential flow pathways where water reaches collection points without extensive geochemical interaction. More reactive materials in both systems showed similar pH evolution trends though with different absolute values, while less reactive materials maintained neutral pH with slight conductivity increases and ORP doubling from ~200 mV to 400 mV.

3.5.3 Experimental Setup 3: Leachate vs Pore Water Chemistry Comparison

This approach evaluated spatial heterogeneity through simultaneous monitoring of drainage leachate and in-situ pore water conditions using tube collectors located at the surface (5 cm) and middle depths (25 cm in IBCs). Vertical acidification gradients were revealed that were not apparent from leachate analysis alone (Figure 10 and Figure 11). Surface collector recorded the most acidic conditions due to enhanced oxygen availability, while middle collectors yielded results more comparable to bulk leachate values. The differences were particularly pronounced in IBC systems, where leachate remained neutral while pore water showed extreme acidification (pH ~2) at 25 cm depth, demonstrating active internal geochemical processes not reflected in drainage chemistry.

For more reactive materials, highly acidic pore water conditions developed that were not reflected in leachate chemistry, indicating aggressive internal processes occurring within the material matrix. Less reactive materials showed generally neutral pore water with slight variations, though some locations demonstrated acidification to pH 4, suggesting initial oxidation processes even in low-sulfide materials.

4.0 CONCLUSIONS

Oxygen availability emerges as the dominant control mechanism: The October 2024 shift from 100mm to 46mm irrigation created a critical turning point where drier conditions in larger particle size columns (≤16mm) led to severe acid generation (pH dropping to ~2). This demonstrates that oxygen availability becomes more critical than water availability for sustaining oxidation processes—a phenomenon that would be significantly amplified in arid mining environments where natural precipitation is minimal, and evaporation rates are high.

Particle size governs oxidation potential under water-limited conditions: Large-particle columns exhibited rapid water drainage with highly acidic, dry surfaces (pH ~2, conductivity up to 10,000 µS/cm), while fine-particle columns (≤4mm) retained water more uniformly with more stable geochemical conditions. In arid climates, this particle size effect would be magnified, as coarse waste rock would maintain air-filled pore spaces for extended periods, creating persistent oxidizing conditions.

Pore water monitoring reveals critical hidden processes: Even when leachate appeared neutral or stable, significant acid generation was detected within materials through pore water analysis, with surface sensors consistently showing more acidic conditions due to enhanced oxygen infiltration. This finding is particularly crucial for arid mine sites where minimal leachate generation may mask extensive internal acid production, potentially leading to severe underestimation of environmental risks when relying solely on drainage monitoring.

Water management strategies have limited effectiveness under arid conditions: The transition from water-limited to oxygen-enhanced reactivity after modest irrigation reduction (54% decrease) indicates that in naturally arid environments, traditional water management approaches may be insufficient. The persistent oxygen availability in arid climates suggests that oxygen exclusion strategies (covers, barriers) become more critical than water addition for preventing acid mine drainage in these environments.

Low-reactivity materials remain vulnerable: Even non-reactive materials showed oxidation potential when oxygen access was available, with IBC-2 pore water acidifying to pH ~4. In arid climates with enhanced oxygen availability and higher temperatures, materials currently classified as non-acid generating may develop acid production capacity over extended timeframes, requiring long-term monitoring and management strategies.

Type drainage influence oxidation: Free drainage consistently accelerated oxidation compared to closed systems, producing lower pH, higher electrical conductivity, elevated sulfate, and increased redox potential, particularly in reactive materials.

Conservative baseline for arid site predictions: These results, obtained under predominantly cold conditions (4°C with intermittent warming to 7-8°C and one week at 23°C simulating summer conditions) with reduced but still substantial moisture input, provide a conservative baseline for arid mine site behavior. Even the brief exposure to elevated temperatures (23°C) during the simulated summer week demonstrated accelerated geochemical processes within the overall cold-dominated system. This suggests that actual arid conditions with sporadical high temperatures would produce significantly more severe outcomes.

These findings provide valuable insights for predicting AMD generation at field scale and designing appropriate mitigation strategies for mine waste management in arid and cold environments.

REFERENCES

Morin, K.A., and N.M. Hutt. (1997) Environmental Geochemistry of Minesite Drainage: Practical Theory and Case Studies. MDAG Publishing, Vancouver, British Columbia. ISBN 0-9682039-0-6.

Morin, K.A., and N.M. Hutt. (2001) Environmental Geochemistry of Minesite Drainage: Practical Theory and Case Studies, Digital Edition. PDF Version, MDAG Publishing, Vancouver, Canada. ISBN 0-9682039-1-4

Tapia, J., Davenport, J., Townley, B., Dorador, C., Schneider, B., Tolorza, V., & von Tümpling, W. (2018). Sources, enrichment, and redistribution of As, Cd, Cu, Li, Mo, and Sb in the Northern Atacama Region, Chile: Implications for arid watersheds affected by mining. Journal of Geochemical Exploration, 185, 33-51.

Vriens B, Peterson H, Laurenzi L, Smith L, Aranda C, Mayer KU, Beckie RD (2019) Long-term monitoring of waste-rock weathering at the Antamina mine, Peru. Chemosphere. 2019 Jan;215:858-869. doi: 10.1016/j.chemosphere.2018.10.105. Epub 2018 Oct 17. PMID: 30408882.

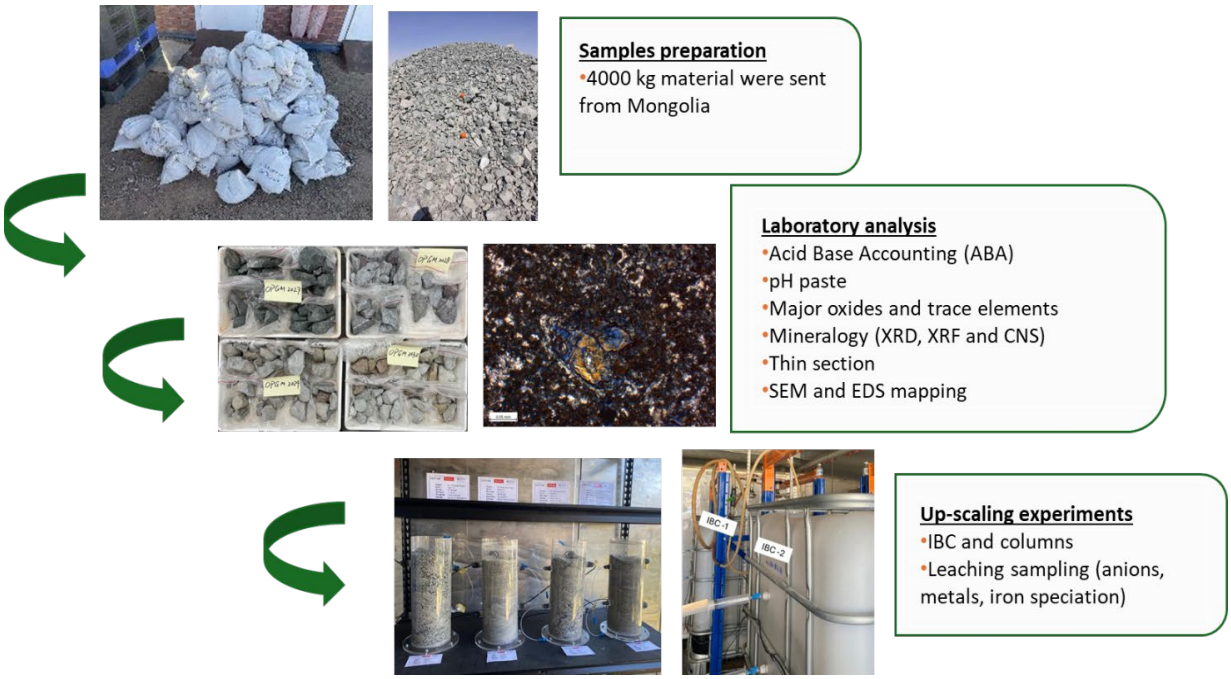

Fig. 8. **Summary of methodology**

Fig. 9. **Design of Columns and IBCs container**

Table 8. **Summary of materials used in the experimental set up**

Experiment	Type of rock		Size of particle		
	Augite Basalt	Quartz monzodiorite	<65 mm	< 16 mm	< 4 mm
C1		X		X	
C2		X			X
C3		X		X	
C4		X			X
IBC-1		X	X		
C5	X	X		X	
C6	X	X			X
C7	X	X		X	
C8	X	X			X
IBC-2	X	X	X		

Table 9. Water regime irrigation (Columns and IBCs)

Seasons	Precipitation			Evaporation	Potential infiltration		Water addition		Temperature
	mm	days	mm/day	mm/day	mm/day	mm/season	IBCs (L)	Columns (L)	°C
Winter	2	2	1	0.43	0.6	1	1	0	4
Spring	12	5	2.4	1.4	1.03	5	5	0.1	9
Summer	73	17	4.3	2.5	1.81	31	31	0.5	23
Autumn	16	5	3.2	1.3	1.91	10	10	0.2	8

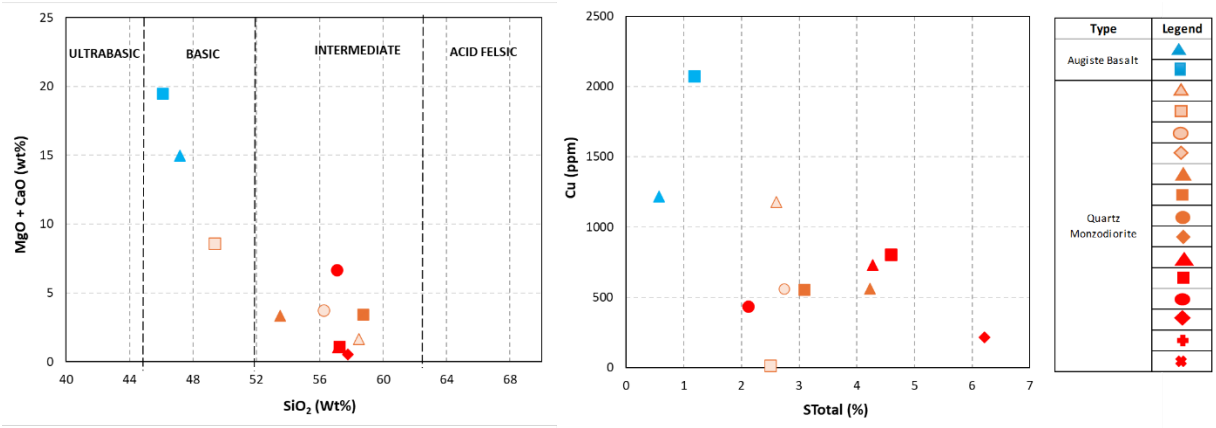

Fig. 10. **Rock classification a) Igneous and sedimentary rock b) Ultrabasic, basic, intermediate, and acid felsic rock.**

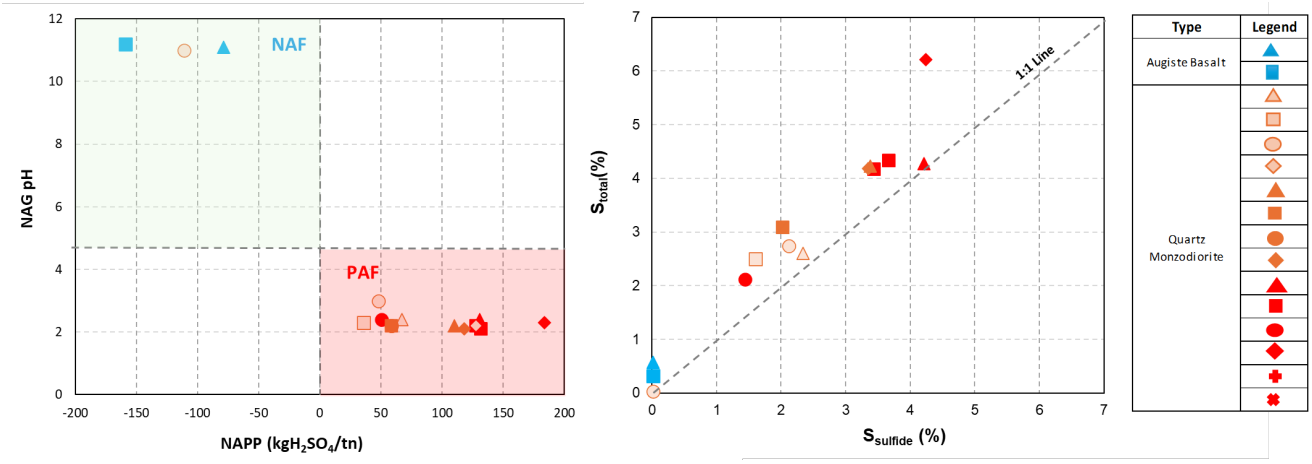

Fig. 11. **Acid mine drainage potential generation a) NPR vs NAG pH, b) Sulfide sulfur (%) vs total sulfur (%).**

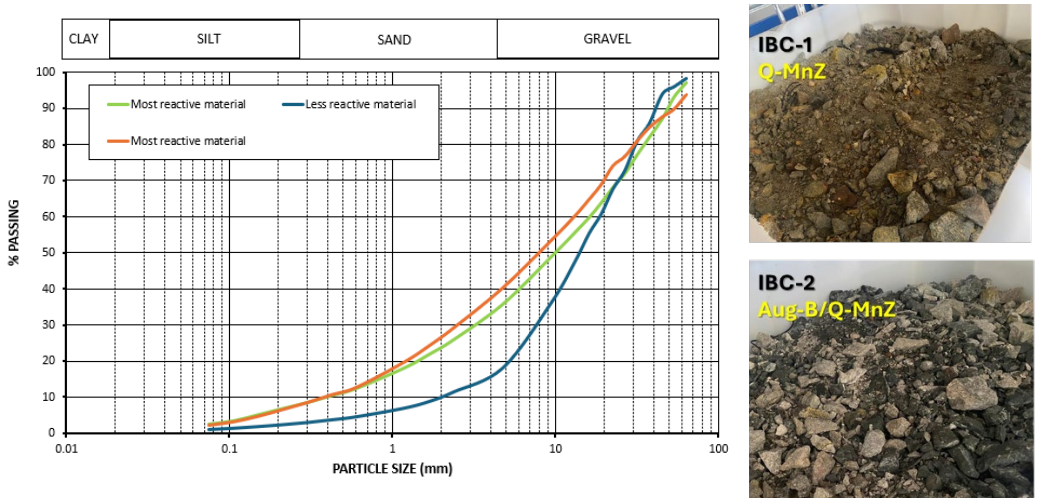

Fig. 12. **Particle size distribution of materials**

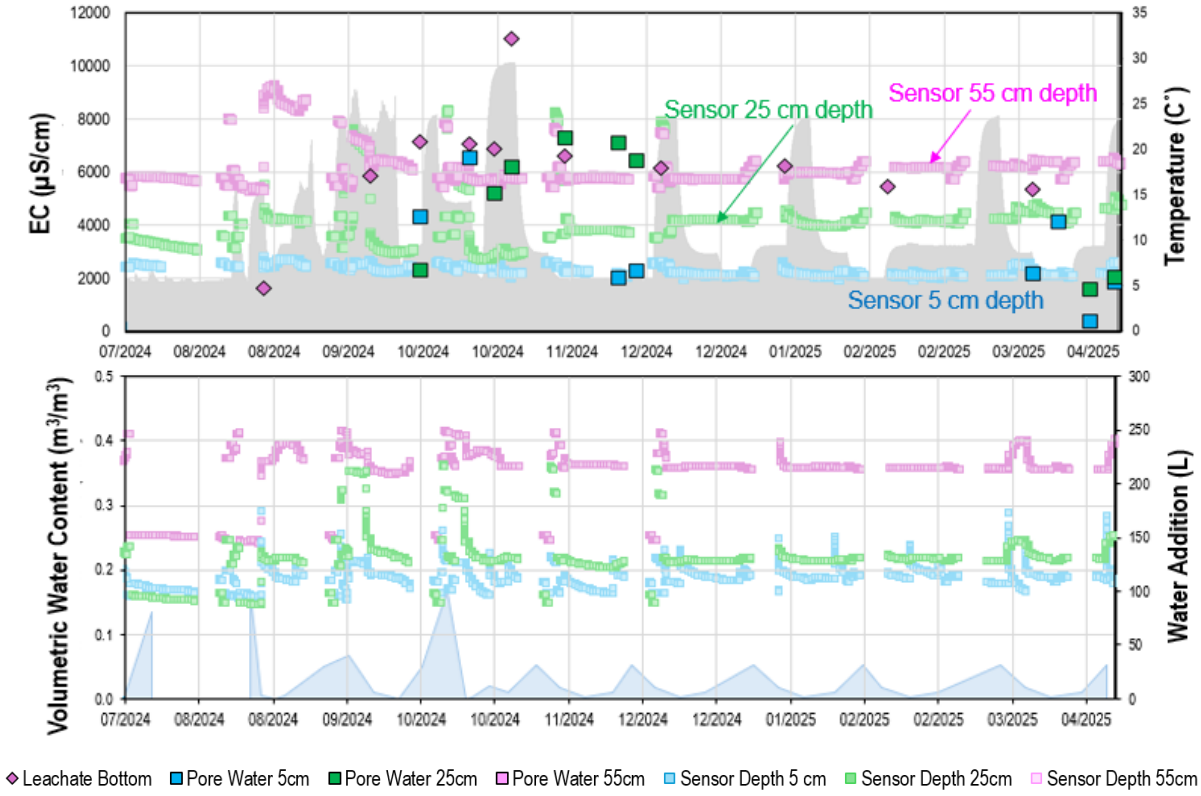

Fig. 13. **Graph results from sensors in IBC-1 (volumetric water and conductivity)**

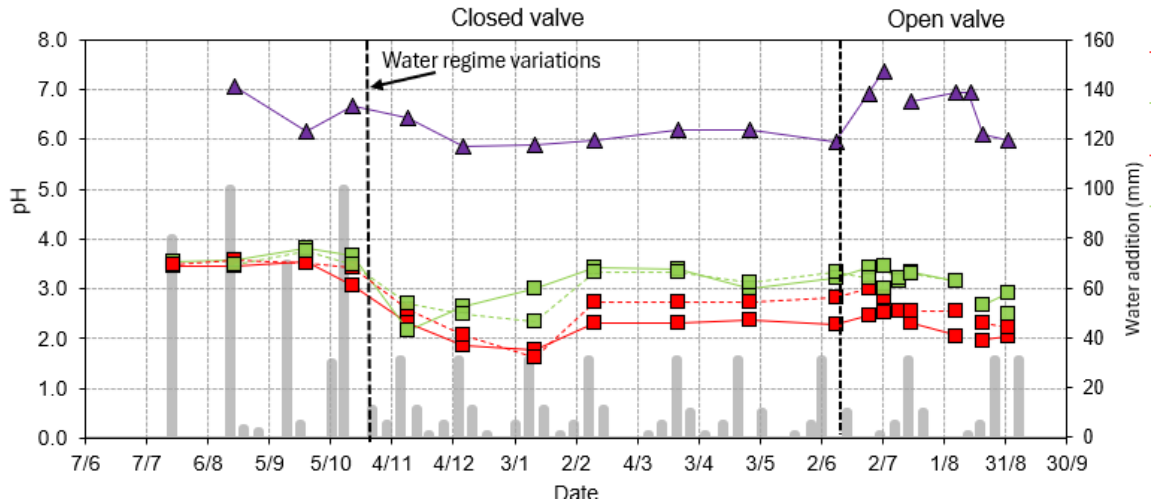

Fig. 14. **pH variation in most reactive materials**

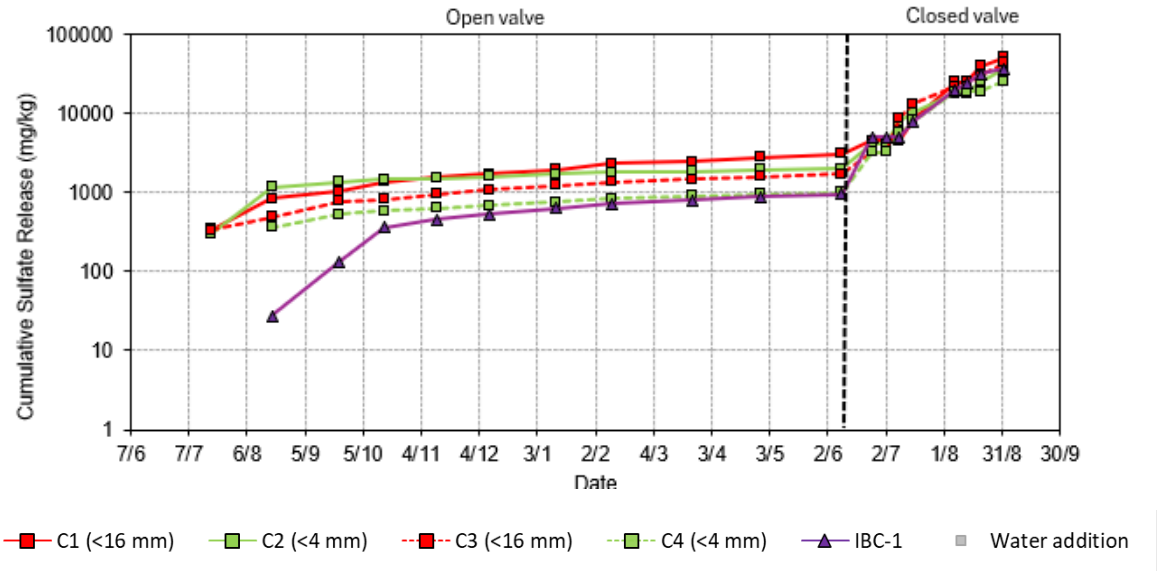

Fig. 15. **Cumulative sulfate release (mg/kg) in most reactive materials.**

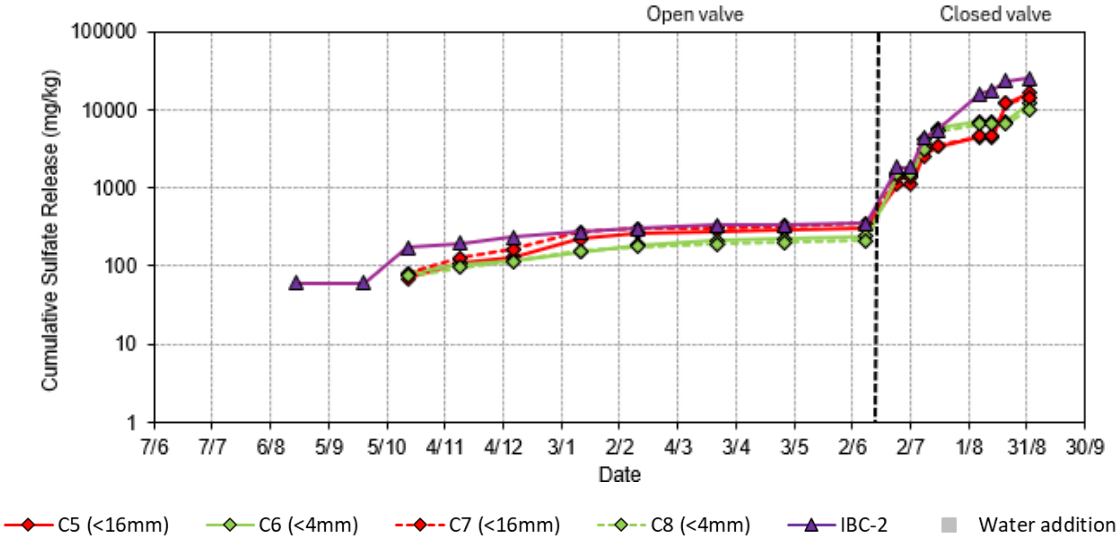

Fig. 16. **Cumulative sulfate release (mg/kg) in most reactive material (IBC-2).**

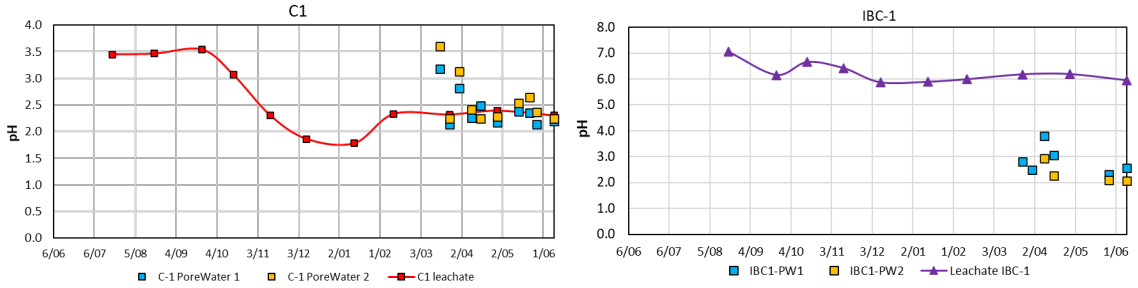

Fig. 17. **Pore water water quality for most reactive material (C1 (<16 mm), IBC-1)**

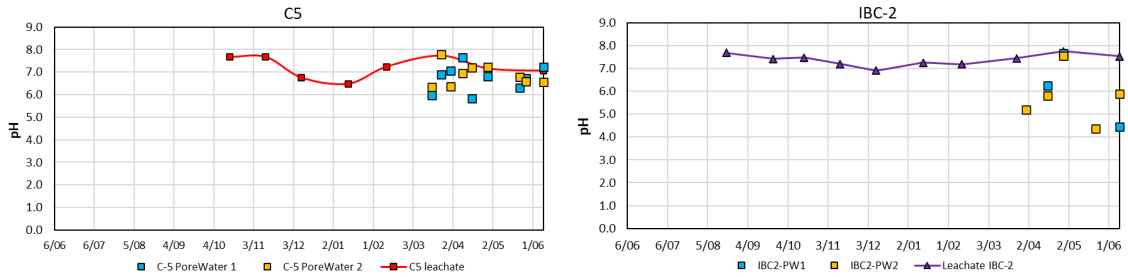

Fig. 18. Pore water water quality for less reactive material (C5 (<16 mm), IBC-2)

Mineral Carbonation for Acid and Metalliferous Drainage (AMD) Mitigation in Queensland Mine Wastes

E.O. Ansah, C. Adoko and A. Parbhakar-Fox
WH Bryan Mining Geology Research Centre, Sustainable Minerals Institute, 40 Isles Rd, Indooroopilly 4068, Queensland, Australia. e.oansah@uq.edu.au

Mining operations in Australia generate large volumes of waste, which increases the risk of acid and metalliferous drainage (AMD), contributing to environmental pollution and high carbon emissions. The challenge lies in managing this waste sustainably while reducing the carbon footprint, which is significant, as traditional methods for waste treatment (such as the addition of limestone – $CaCO_3$ for AMD treatment) can be carbon-intensive. Current research on mineral carbonation—a technique that locks CO_2 into stable minerals like carbonates—mainly targets ultramafic wastes from nickel, platinum, or diamond mines, which are scarce in Queensland. This leaves a gap for gold and copper operations, common in Queensland, where tailings from sites like Mt Isa, Ernest Henry, Baal Gammon, and Mt Morgan hold untapped potential for CO_2 sequestration. This study proposes utilizing brine solutions to convert reactive waste minerals into inert carbonates, enabling efficient CO_2 storage while reducing pollution. To assess viability, we created a quantitative metric that evaluates the theoretical CO_2 storage capacity based on magnesium (Mg) and calcium (Ca) minerals, their behaviour in real mine wastes (including tailings), and practical feasibility factors. First, we validated this metric using a 3D model generated from synthetic geochemical data. Next, we applied it to actual mineralogical and geochemical data from some Queensland mine wastes. The results offer valuable insights into how Ca- and Mg-carbonates can effectively mitigate AMD. Future work will investigate the kinetics of mineral carbonation in Australian copper and gold mine waste samples utilizing reactive transport models and laboratory analysis. This work paves the way for greener mining practices, turning waste into a resource for carbon-neutral closure.

Chemically engineered cementation of sulfidic waste rocks for preventing acid and metalliferous drainage pollution

N. Saha[A], S. Yang[B], and L, Huang[C]
[A]Sustainable Minerals Institute, The University of Queensland, QLD 4072, Australia.
n.saha@uq.edu.au
[B]Agnico Eagle Australia, Dorat Road, Hayes Creek, NT 0822, Australia
[C]Sustainable Minerals Institute, The University of Queensland, QLD 4072, Australia

Acid and metalliferous drainage (AMD) from sulfidic waste rock dumps remains one of the most persistent environmental challenges for the mining industry, driving long-term ecological risks and costly liabilities. This study presents a novel proof of concept for environmental geopolymer (EG) technology, which chemically activates sulfidic waste rock (WR) with Class F fly ash (FA) to form stable, cementitious structures under ambient conditions. The alkali-activated reaction generates sodium aluminosilicate hydrate (N-A-S-H) gels that encapsulate and passivate pyrite and other reactive minerals, thereby suppressing oxidation and AMD generation. Laboratory experiment demonstrated that WR–FA composites (with 60% WR) developed unconfined compressive strengths of 22 MPa in 4 weeks, increasing to 29 MPa after 24 weeks, exceeding benchmarks for monolithic waste stability. Advanced synchrotron-based NEXAFS spectroscopy confirmed the transformation of octahedral Al in WR into tetrahedral coordination, forming a three-dimensional Al-Si polymeric gel framework that immobilised up to 95% of toxic metal(loid)s during leaching tests.

This chemically engineered, cementation-driven stabilisation approach mimics natural sedimentary rock formation processes but accelerates them into practical, field-feasible timescales. By transforming polymineral wastes into pseudo-sedimentary horizons with extremely low permeability and toxic metal(oid)s leachability, the technology offers an innovative solution for encapsulation and passivation of WR facilities. Beyond reducing AMD pollution, the method valorises mine and energy byproducts, advancing circular economy pathways for mine closure. Overall, environmental geopolymerisation emerges as a scalable, cost-effective, and sustainable alternative to conventional systems, with strong potential for field application in mine waste rehabilitation.